

# Dynnikov Coordinates and pseudo-Anosov braids

Thesis submitted in accordance with the requirements of  
the University of Liverpool for the degree of Doctor in Philosophy

by  
Saadet Öykü Yurttaş

January, 2011

# Abstract

The aim of this thesis is to study dynamical properties of pseudo-Anosov braids on the  $n$ -times punctured disk  $D_n$  making use of a particular coordinate system called the *Dynnikov coordinate system*. The Dynnikov coordinate system gives a homeomorphism from the space of measured foliations  $\mathcal{MF}_n$  on  $D_n$  (up to a certain equivalence relation) to  $\mathcal{S}_n = \mathbb{R}^{2n-4} \setminus \{0\}$ , and restricts to a bijection from the set of *integral laminations* (disjoint unions of finitely many essential simple closed curves) on  $D_n$  to  $\mathcal{C}_n = \mathbb{Z}^{2n-4} \setminus \{0\}$ .

In the first part of the thesis, we introduce a new method for computing the topological entropy of each member of an infinite family of pseudo-Anosov braids making use of Dynnikov's coordinates. The method is developed using the results in Thurston's seminal paper on the geometry and dynamics of surface automorphisms and builds on, more recent work of Moussafir. To be more specific, the method gives a so-called *Dynnikov matrix* which describes the action of a given pseudo-Anosov braid  $\beta$  near its invariant unstable measured foliation  $[\mathcal{F}, \mu]$  on the projective space  $\mathcal{PS}_n$ , and the eigenvalue  $\lambda > 1$  of this matrix gives the topological entropy of  $\beta$ .

In the second part of the thesis, we compare the spectra of *Dynnikov matrices* with the spectra of the *train track transition matrices* of a given pseudo-Anosov braid, and show that these matrices are isospectral up to roots of unity and zeros under some particular conditions.

# Acknowledgements

First and foremost, I would heartily like to thank my supervisor Toby Hall for being a wonderful mentor. I consider myself very fortunate to get the opportunity to be supervised by my role model for the past four years. I deeply appreciate his friendly supervision, enthusiasm in teaching and critical reading which made this thesis possible.

I was very fortunate to be able to spend a month at the end of 2009 at the University of Florida in Gainesville working under the guidance of Philip Boyland. I deeply thank him for the many valuable and insightful discussions, particularly about the second part of the thesis, and his warm and friendly hospitality: he bought me ice-cream and showed me the alligators. He has continued to support me since then with his ideas on my work. I was hosted by Necibe Tuncer who made me feel completely at home with her kind and generous hospitality.

I also spent an enjoyable month at the University of Wisconsin-Madison, where I had the opportunity to discuss my work with Jean-Luc Thiffeault: he suggested several interesting problems related to my work, and in particular extensions to higher genus surfaces. I am thankful for all the discussions with him and his Ph.D student Sarah Matz.

I had the good fortune to meet Sara Maloni at the Cambridge University on ‘The Women in Mathematics Day’ meeting. I am grateful to her for showing such interest in my problem – I enjoyed my discussions with her which are still ongoing. She also invited me to give a talk in Warwick, where I had the opportunity to talk about my work with Caroline Series and Saul Schleimer.

The Department of Mathematical Sciences has provided a very friendly environment. I appreciate the presence of such experts in Dynamical Systems as Mary Rees, Lasse Rempe and Kit Nair, and their Ph.D. students, Freddie Exall and Helena Mihaljević-Brandt. There was a very happy atmosphere in my office, for which I am very grateful to Fawaz Alharbi, Joel Haddley, and Graham Reeves.

I am grateful to all of the other friends who have made my time in Liverpool enjoyable, in particular: Alana and Özgür Selsil and their lovely children Bláithín and Eibhleann for the warm family atmosphere, and for always being there whenever I needed them, Marie Binz, Ana De Castro Guimaraes, Stella Kung for being great flat mates and the stimulating discussions in the kitchen, Judith Carter, Bessy and Kate for the very friendly and the full of fun times we spent together. I will always remember our trip to Istanbul. I also would like to express my sincere gratitude to Professor Hasan İlhan Tutalar for all his encouragement and advice before and during my Ph.D.

I am grateful to all of those who provided financial support for my work. First and foremost the University of Dicle who sponsored me throughout my Ph.D. studies in Liverpool, and funded my trips to the US and Poland. I have also received travel and accommodation support from the Universities of Liverpool, Cambridge, and Warwick.

Lastly, my deepest gratitude goes to my family, for all their support and love. Thanks to my Mom and Dad for always believing in me more than I believed in myself, thanks to my brother Güney for always finding the right words to cheer me up on my difficult days and my niece Beren for bringing a lot of joy and smiles into our days.

# Contents

<b>Contents</b>	<b>v</b>
<b>1 Introduction</b>	<b>1</b>
<b>I On the topological entropy of families of braids</b>	<b>8</b>
<b>2 Background</b>	<b>11</b>
2.1 Dynamical Systems . . . . .	11
2.1.1 Symbolic Dynamics . . . . .	13
2.2 Automorphisms of Surfaces . . . . .	16
2.3 Tools from Thurston's theory on surface automorphisms . . . . .	19
2.4 Some results of Thurston's theory on surface automorphisms . . . . .	23
2.4.1 Some properties of pseudo-Anosov automorphisms . . . . .	26
2.5 Braids . . . . .	29
<b>3 Dynnikov Coordinates</b>	<b>36</b>
3.1 Dynnikov coordinates of integral laminations and measured foliations	37
3.2 Geometric intersection of integral laminations with relaxed curves	51
3.3 Aside: Addition on $\mathcal{L}_n$ . . . . .	56
3.4 Update rules for Dynnikov coordinates of integral laminations . . . . .	58
3.5 Update rules for sequences of contiguous generators . . . . .	70
3.6 Dynnikov coordinates of measured foliations . . . . .	79

<b>4</b>	<b>Computing topological entropy of families of braids</b>	<b>81</b>
4.1	Topological Entropy of pseudo-Anosov braids and Moussafir's iterative technique . . . . .	82
4.2	Computing Topological entropy of families of braids . . . . .	83
4.3	The braids $\beta_{m,n}$ . . . . .	90
4.4	The braids $\sigma_{m,n}$ . . . . .	93
4.4.1	The pseudo-Anosov case: $n \geq m + 2$ . . . . .	93
4.4.2	The reducible case: $\sigma_{m,m+1}$ . . . . .	95
4.5	Exposé of the method on the braid family $\beta_{n-2,1}$ . . . . .	97
 <b>II On Dynnikov matrices and train track transition matrices of pseudo-Anosov braids</b>		<b>105</b>
<b>5</b>	<b>Train Tracks</b>	<b>108</b>
5.1	Constructing integral laminations and measured foliations from a train track . . . . .	110
5.2	Train paths . . . . .	114
5.3	Train tracks and pseudo-Anosov automorphisms . . . . .	115
<b>6</b>	<b>Transition matrices and Dynnikov matrices</b>	<b>120</b>
6.1	Train track coordinates and Dynnikov coordinates . . . . .	120
6.2	The spectrum of a Dynnikov matrix when $\tau$ is complete . . . . .	125
6.3	The spectrum of a Dynnikov matrix when $\tau$ is not complete . . . . .	130
6.3.1	Pinching and diagonal extension . . . . .	130
6.3.2	The spectrum of the Dynnikov matrices when $\beta$ fixes the prongs of $\tau$ . . . . .	141
6.3.3	Future work: The spectrum of Dynnikov matrices when $\beta$ permutes the prongs of $\tau$ non-trivially . . . . .	153

# Chapter 1

## Introduction

In the 1970s, Thurston classified surface automorphisms up to isotopy and described his results in a preprint which was extensively studied. His preprint later appeared as [29] in which he also discussed many more recent developments and ramifications in the theory. As Thurston remarked in his preprint, the classification of surface automorphisms began with the work of Nielsen in the 1920s which is why the result is also known as the Nielsen-Thurston classification theorem. This famous theorem states that each automorphism of a surface is isotopic to either a *finite order* or a *pseudo-Anosov* or a *reducible* automorphism.

If some iterate of an automorphism is the identity, it is called *finite order*. If an automorphism preserves a transverse pair of measured foliations [29] on the surface, stretching one foliation uniformly by a real number  $\lambda > 1$  and contracting the other uniformly by  $1/\lambda$ , then it is called *pseudo-Anosov*. We say that  $\lambda$  is the dilatation or the growth rate of the pseudo-Anosov. If an automorphism preserves a collection of mutually disjoint essential simple closed curves (reducing curves), it is called *reducible*. The surface can then be cut along these curves into pieces which are permuted by the automorphism, and hence each piece is preserved by some iterate of the automorphism. When the surface has been cut as much as possible along such reducing curves, the action on each piece is isotopic either to a finite order or a pseudo-Anosov automorphism.

Each isotopy class is represented by an automorphism which is of one of these three types, and the isotopy class is named by the type of the automorphism it contains. The focus of this thesis is the study of pseudo-Anosov isotopy classes on the  $n$ -times punctured disk  $D_n$  making use of a particular coordinate system called the *Dynnikov coordinate system* [13]. The Dynnikov coordinate system gives a homeomorphism from the space of measured foliations  $\mathcal{MF}_n$  on  $D_n$  (up to a certain equivalence relation) to  $\mathbb{R}^{2n-4} \setminus \{0\}$ , and restricts to a bijection from the set of *integral laminations* (disjoint unions of finitely many essential simple closed curves) on  $D_n$  to  $\mathbb{Z}^{2n-4} \setminus \{0\}$ . We will use the Dynnikov coordinate system to study two main problems. In the first part of the thesis, we shall introduce a new method for computing the topological entropy of each member of an infinite family of pseudo-Anosov isotopy classes (or indeed an individual isotopy class) making use of Dynnikov's coordinates; and in the second part of the thesis, we shall compare the spectra of the so-called *Dynnikov matrices* with the spectra of the *train track transition matrices* of a given pseudo-Anosov isotopy class on  $D_n$ .

The topological entropy of an isotopy class is defined to be the minimum topological entropy of an automorphism contained in it. When the isotopy class is pseudo-Anosov, all pseudo-Anosovs in the class have the minimum topological entropy which is  $\log \lambda$ . Thus, the topological entropy of a pseudo-Anosov isotopy class equals  $\log \lambda$ .

The normal approach to compute the topological entropy of an isotopy class of surface automorphisms is to use train-track methods [5, 17, 22]. In [5], the algorithm starts with a graph  $G$  which is a spine of the surface and the isotopy class is represented by a graph map. The algorithm repeatedly modifies  $G$  and the associated graph map until it either finds an explicit reducing curve for the isotopy class, or a graph map which is the simplest possible. If the isotopy class is pseudo-Anosov, this simplest graph map can be used to construct a train track and train track map from which the growth rate of the isotopy class and the singularity structure of the invariant foliations are obtained. However, for



complicated isotopy classes (that is, ones with high topological entropy), the lengths of the image edge paths (represented by words whose letters label the edges) of the train track are so long such that even a computer cannot store them. Therefore, it is usually far from straightforward to describe an infinite family of train tracks, in order to verify that they are indeed invariant under the action of relevant isotopy classes.

On the other hand, the method developed here provides formulae which compute the topological entropy explicitly in a much more computationally efficient (such terms are used informally) way. The idea of our method lies in Thurston's seminal paper [29] and builds on more recent work of Moussafir [25]. Given a surface  $M$ , the Teichmüller space  $\mathcal{T}(M)$  of  $M$  is an open ball and the space of projective measured foliations  $\mathcal{PMF}(M)$  forms its boundary. Let  $\text{MCG}(M)$  denote the mapping class group of  $M$  (the group of isotopy classes of automorphisms of  $M$ ). The closure  $\overline{\mathcal{T}(M)}$  is a closed ball on which  $\text{MCG}(M)$  acts continuously. By Brouwer's Fixed Point Theorem each isotopy class  $[f]$  has a fixed point on  $\overline{\mathcal{T}(M)}$ , and the analysis of this fixed point yields the Nielsen-Thurston Classification Theorem.

When  $[f]$  is pseudo-Anosov, it has exactly two fixed points which both lie on  $\mathcal{PMF}(M)$ , the projective classes  $[\mathcal{F}^u, \mu^u]$  and  $[\mathcal{F}^s, \mu^s]$  of its invariant foliations; and every other point on  $\mathcal{PMF}(M)$  converges to  $[\mathcal{F}^u, \mu^u]$  rapidly under the action of  $[f]$ . The induced action of  $[f]$  on  $\mathcal{PMF}(M)$  is piecewise linear and is locally described by integer matrices. The matrix on any piece which contains  $[\mathcal{F}^u, \mu^u]$  on its closure has an eigenvalue  $\lambda > 1$  since  $[\mathcal{F}^u, \mu^u]$  is a fixed point on  $\mathcal{PMF}(M)$ . Therefore, if we can compute the action of  $[f]$  on  $\mathcal{PMF}(M)$  and find a matrix with an eigenvalue  $\lambda > 1$  with associated eigenvector contained in the relevant piece, the eigenvector corresponds to  $[\mathcal{F}^u, \mu^u]$  and  $\lambda$  gives the growth rate and hence the topological entropy. We realize this idea on  $D_n$  by coordinatizing  $\mathcal{PMF}_n$  using the *Dynnikov coordinates* and describe the action of  $\text{MCG}(D_n)$  on  $\mathcal{PMF}_n$  using the *update rules* [13].

Let us be more specific about some of the details of this procedure. We first

take a particular collection of  $3n - 5$  arcs embedded in  $D_n$  and describe each measured foliation by an element of  $\mathbb{R}^{3n-5}$ , the associated measures of these arcs (and similarly each integral lamination by an element of  $\mathbb{Z}^{3n-5}$ , its geometric intersection numbers with these arcs). *Dynnikov coordinates* [13] are certain linear combinations of these real numbers/integers which yield a one-to-one correspondence between the set of measured foliations (up to isotopy and Whitehead equivalence) on  $D_n$  and  $\mathcal{S}_n = \mathbb{R}^{2n-4} \setminus \{0\}$  (and between the set of integral laminations on  $D_n$  and  $\mathcal{C}_n = \mathbb{Z}^{2n-4} \setminus \{0\}$ ). The space of *projective Dynnikov coordinates*  $\mathcal{PS}_n$  is therefore a  $(2n - 5)$ -dimensional sphere and the action of the mapping class group on  $\mathcal{PS}_n$  is described by the update rules. The update rules induce a piecewise linear action on this space. Often  $[\mathcal{F}^u, \mu^u]$  lies on the boundary of several piecewise linear regions: in such cases, each region containing  $[\mathcal{F}^u, \mu^u]$  on its boundary is called a *Dynnikov region*, and the associated matrix is called a *Dynnikov matrix*. Each Dynnikov matrix has an eigenvalue  $\lambda > 1$  with corresponding eigenvector the Dynnikov coordinates  $[a^u, b^u]$  of  $[\mathcal{F}^u, \mu^u]$  which gives the topological entropy of the isotopy class from the discussion above. Therefore, the way to compute the topological entropy of a given isotopy class will be achieved by finding a Dynnikov region and then computing the growth rate using the associated Dynnikov matrix. This process will be described in detail in Chapter 4.

The main reasons that our method works much faster than the train track approach are: first, because of the simple way we put global coordinates on  $\mathcal{MF}_n$ ; and second, because it is easy to find the Dynnikov coordinates of  $[\mathcal{F}^u, \mu^u]$  on  $\mathcal{PMF}_n$  numerically since it is a globally attracting fixed point of the induced action. In addition, the method is more transparent since it relies on algebraic calculations rather than on understanding the image of a train track under the action of an isotopy class.

We note that since each isotopy class in  $\text{MCG}(D_n)$  is described by a braid in Artin's braid group  $B_n$  [3, 4], the isotopy classes in  $\text{MCG}(D_n)$  will be represented by sequences of Artin's braid generators.

Our goal in the second part of the thesis is to compare the spectrum of a Dynnikov matrix  $D$  with the spectrum of a train track transition matrix  $T$  of a given pseudo-Anosov braid  $\beta \in B_n$ . The spectrum of  $T$  is interpreted in a recent paper [6] by Birman, Brinkman and Kawamuro. Their paper investigates the spectrum of the transition matrix  $T$  of a given pseudo-Anosov automorphism  $f$  on an orientable surface and shows that the characteristic polynomial of  $T$  factors into three polynomials: the first has the dilatation  $\lambda$  of  $f$  as its largest root; the second relates to the action of  $f$  on the singularities of the invariant foliations  $(\mathcal{F}^u, \mu^u)$  and  $(\mathcal{F}^s, \mu^s)$ ; and the third relates to the degeneracies of a symplectic form introduced in [26]. Our aim is to prove that any Dynnikov matrix shares the same set of eigenvalues with any train track transition matrix up to roots of unity and zeros — this is proved in some cases but not in full generality. The properties of the spectrum of  $T$ , which is difficult to calculate, can therefore be studied using the spectrum of  $D$ , which is easy to calculate.

A *train track*  $\tau$  on  $D_n$  is a one dimensional CW complex made up of vertices (*switches*) and edges (*branches*) smoothly embedded on  $D_n$  such that at each switch there is a unique tangent vector, and every component of  $D_n - \tau$  is either a once-punctured  $p$ -gon with  $p \geq 1$  or an unpunctured  $k$ -gon with  $k \geq 3$  (where the boundary of  $D_n$  is regarded as a puncture). A transverse measure on  $\tau$  is a function which assigns a measure to each branch of  $\tau$  such that these measures satisfy the *switch conditions* (some particular linear equations) at each switch of  $\tau$ . Train tracks equipped with a transverse measure are called *measured train tracks*: they provide another way to coordinatize measured foliations and integral laminations [24, 26]. We write  $\mathcal{W}(\tau)$  for the space of transverse measures associated to  $\tau$  and say that a foliation  $(\mathcal{F}, \mu)$  is *carried* by  $\tau$  if it arises from some transverse measure in  $\mathcal{W}(\tau)$ . In particular, there is a homeomorphism from the space of non-negative transverse measures  $\mathcal{W}^+(\tau)$  on  $\tau$  to the space of measured foliations  $\mathcal{MF}(\tau)$  carried by  $\tau$ .

The action of a given pseudo-Anosov isotopy class  $[f]$  on  $\mathcal{W}(\tau)$  is given by the transition matrix associated to the (regular) invariant train track of  $[f]$ . Every

pseudo-Anosov automorphism  $f$  has an *invariant train track*: that is, a train track  $\tau$  whose image under  $[f]$  is another train track which can be collapsed onto  $\tau$  in a regular neighbourhood of  $\tau$  in a smooth way. The associated *train track transition matrix*  $T$  has entries  $T_{i,j}$  given by the number of occurrences of  $e_i$  in the edge path  $f(e_j)$  where  $e_1, \dots, e_k$  denote the branches of  $\tau$ . The largest eigenvalue of  $T$  equals the dilatation  $\lambda$  and the entries of the unique (up to scale) associated eigenvector  $v^u$  in  $\mathcal{W}(\tau)$  are strictly positive and correspond to  $(\mathcal{F}^u, \mu^u)$ . If  $(\mathcal{F}^u, \mu^u)$  has only unpunctured 3-pronged and punctured 1-pronged singularities (which is a generic property in  $\mathcal{PMF}_n$ ), it is carried by a *complete* train track  $\tau$ . That is,  $\tau$  has the property that each component of  $D_n - \tau$  is either a trigon or a once punctured monogon. In this case,  $\mathcal{MF}(\tau)$  defines a chart in  $\mathcal{MF}_n$  containing  $(\mathcal{F}^u, \mu^u)$  in its interior and hence there is a unique Dynnikov matrix  $D$ . We use the change of coordinate function  $L : \mathcal{W}^+(\tau) \rightarrow \mathcal{S}_n$  and show that  $D$  and  $T$  share the same spectrum. This part of the argument is relatively straightforward: the main work is to show that the change of coordinate function  $L$  is linear in some neighbourhood of  $v^u$  in  $\mathcal{W}^+(\tau)$ .

If  $(\mathcal{F}^u, \mu^u)$  has singularities other than unpunctured 3-pronged and punctured 1-pronged singularities, then  $\tau$  is not complete and therefore does not define a chart. There are two subcases to consider: first, when  $\beta$  fixes the prongs of  $(\mathcal{F}^u, \mu^u)$ ; and second, when it permutes them non-trivially. Whichever is the case, we construct a complete train track  $\tau_p$  from  $\tau$  so that  $(\mathcal{F}^u, \mu^u)$  is carried by  $\tau_p$  and is contained in the interior of  $\mathcal{MF}(\tau_p)$ . In order to do this, we make use of the *pinching move* [24, 26]. However,  $\tau_p$  is not an invariant train track unless relevant prongs of  $(\mathcal{F}^u, \mu^u)$  are fixed by  $\beta$ . Therefore, we use another move called the *diagonal extension move* [24, 26] which constructs several complete train tracks that give a set of charts which fit nicely in  $\mathcal{MF}(\tau_p)$ , with the property that the action in each of them is described explicitly. The results in Chapter 6 are mainly based on the interplay between the charts constructed from these two different moves. Lemma 6.18 explains how these charts fit together. Using this lemma, we shall prove that if  $\beta$  fixes the prongs of  $(\mathcal{F}^u, \mu^u)$  then every Dynnikov

matrix is isospectral to  $T$  up to some eigenvalues 1. Then, we shall discuss the case when  $\beta$  permutes the prongs of  $(\mathcal{F}^u, \mu^u)$  non-trivially. The claim, which has been confirmed with a wide range of examples, is that any Dynnikov matrix  $D$  is isospectral to  $T$  up to roots of unity and zeros. Using Lemma 6.18, we shall observe the problems which arise in this case and some approaches to their solution.

**Part I**

**On the topological entropy of  
families of braids**

The main aim of this first part of the thesis is to describe a new method for computing the topological entropy of each member of an infinite family of pseudo-Anosov elements of the mapping class group  $MCG(D_n)$  on the  $n$ -times punctured disk  $D_n$  making use of Dynnikov's coordinates on the boundary of Teichmüller space [19]. The method is illustrated in Chapter 4 by applying it to two families of braids considered in [20], which are of interest in the study of braids of low topological entropy. These families are  $\{\beta_{m,n} : m, n \geq 1\}$ , and  $\{\sigma_{m,n} : 1 \leq m \leq n\}$ , where (using the standard Artin braid generators  $\sigma_i$ )

$$\beta_{m,n} = \sigma_1 \sigma_2 \dots \sigma_{m-1} \sigma_m \sigma_{m+1}^{-1} \sigma_{m+2}^{-1} \dots \sigma_{m+n-1}^{-1} \sigma_{m+n}^{-1} \in B_{m+n+1}, \quad \text{and}$$

$$\sigma_{m,n} = \sigma_1 \sigma_2 \dots \sigma_{m-1} \sigma_m \sigma_m \sigma_{m-1} \dots \sigma_2 \sigma_1 \sigma_1 \sigma_2 \dots \sigma_{m+n-1} \sigma_{m+n} \in B_{m+n+1}.$$

The tools to prove our results will be Thurston's theory on surface automorphisms [29, 16], the Dynnikov coordinate system and the update rules defined for Artin braid generators [11, 12, 13, 25]. This background material is summarized in Chapter 2 and Chapter 3.

Chapter 2 serves as a background to the thesis and is divided into five sections. Section 2.1 and Section 2.2 review the relevant basic results and terminology of dynamical systems and surface automorphisms, Section 2.3 and Section 2.4 give some background and results of Thurston's theory on surface automorphisms which will be necessary in proving our results in Chapter 3 and Chapter 4, and Section 2.5 provides a brief introduction to braids.

The main tools on which the thesis is based are developed in Chapter 3. It gives a detailed study of the Dynnikov coordinate system and update rules for Artin braid generators [13, 11, 12] presenting new results and illustrative examples, and motivates the reader to study Chapter 4. It is divided into five sections. Section 3.1 describes the Dynnikov coordinate system [13] on  $D_n$  which provides an explicit bijection between the set of integral laminations  $\mathcal{L}_n$  on  $D_n$  and  $\mathcal{C}_n = \mathbb{Z}^{2n-4} \setminus \{0\}$ . An explicit formula is given for the inverse of the bijection  $\rho : \mathcal{L}_n \rightarrow \mathcal{C}_n$  which has not appeared in the literature before and has several useful applications. An interesting problem is solved in Section 3.2: a recipe is given to compute the geometric intersection number of an integral lamination  $\mathcal{L} \in \mathcal{L}_n$  with a particular type of integral lamination, known as a *relaxed integral lamination*, using the inverse of the Dynnikov coordinate function. This provides a way to find the geometric intersection number of two arbitrary integral laminations when combined with an algorithm of Dynnikov and Wiest [14]. Section 3.3 is also an aside: it discusses the interpretation of the group operation on  $\mathcal{L}_n \cup \{\emptyset\}$  using the bijection between  $\mathcal{L}_n \cup \{\emptyset\}$  (where  $\emptyset$  corresponds to the "empty lamination") and  $\mathbb{Z}^{2n-4}$ .

The action of Artin's braid group  $B_n$  on  $C_n$  is given by so-called *update rules*. Section 3.4 gives the derivation of the update rules for the Artin braid generators and Section 3.5 derives the update rules for some sequences of Artin braid generators which are used to prove our results in Chapter 4. Finally, Section 3.6 describes the Dynnikov coordinate function  $\rho : \mathcal{MF}_n \rightarrow \mathbb{R}^{2n-4} \setminus \{0\}$  which coordinatizes the space of measured foliations on  $D_n$ .

The main results of this part of the thesis are given in Chapter 4: a new method for computing the topological entropy of families of pseudo-Anosov braids is described. To be more specific, Section 4.1 gives the background and motivation of the method; and Section 4.2 describes the method, introducing Dynnikov regions and Dynnikov matrices of a given pseudo-Anosov braid with an illustrative example. In Section 4.3 and Section 4.4, the method is applied to the two families  $\beta_{m,n}$  and  $\sigma_{m,n}$  described above. In these sections, relevant formulae are quoted and then proved: for readers interested in how these formulae were derived, Section 4.5 provides a step by step guide for a simple family of braids.



## Chapter 2

# Background

### 2.1 Dynamical Systems

In this first section we begin with some basic terminology and definitions from dynamical systems.

**Definitions 2.1.** A *topological dynamical system* is a pair  $(X, f)$  where  $X$  is a topological space and  $f: X \rightarrow X$  is a continuous self map. We say that  $(X, f)$  is *invertible* if  $f$  is a homeomorphism.

For each  $n \in \mathbb{Z}$ , we define  $f^n$  as the  $n$ -fold iterate  $\underbrace{f \circ \cdots \circ f}_{n \text{ times}}$  if  $n \geq 0$  and  $\underbrace{f^{-1} \circ \cdots \circ f^{-1}}_{-n \text{ times}}$  if  $n < 0$ .

The *orbit*  $o(x, f)$  of a point  $x \in X$  is the sequence  $\{f^i(x) : i \in \mathbb{N}\}$  if  $(X, f)$  is non-invertible or the sequence  $\{f^i(x) : i \in \mathbb{Z}\}$  if  $(X, f)$  is invertible. We say that  $x$  is a fixed point of  $f$  if  $f(x) = x$ , and that  $x$  is a periodic point if  $f^n(x) = x$  for some  $n \geq 1$ . If  $n$  is the least positive integer for which  $f^n(x) = x$  then  $n$  is called the period of  $x$  and  $o(x, f) = \{x_j = f^j(x) : j = 0, \dots, n-1\}$  is called a *period  $n$  orbit* of  $f$ . We denote the set of fixed points with  $Fix(f)$  and the set of periodic points of period  $n$  with  $Per_n(f)$ .

**Definitions 2.2.** For a topological dynamical system  $(X, f)$  a fixed point  $x_0 \in X$  of  $f$  is *attracting* if there exists a neighborhood  $U$  of  $x_0$  such that for every  $x \in U$ ,  $f^n(x) \rightarrow x_0$  as  $n \rightarrow \infty$ . A fixed point  $x_0$  of  $X$  is *repelling* if there exists a neighborhood  $U$  of  $x_0$  such that if  $x \in U$  and  $x \neq x_0$ ,  $f^k(x) \notin U$  for some  $k > 0$ .

**Definitions 2.3.** Two dynamical systems  $(X, f)$  and  $(Y, g)$  are said to be *topologically semi conjugate* if there exists a continuous surjection  $h: X \rightarrow Y$  such that  $h \circ f = g \circ h$ . If  $h: X \rightarrow Y$  is a homeomorphism then we say  $f$  and  $g$  are *topologically conjugate* and that the homeomorphism  $h$  is a *topological conjugacy*.

Now suppose  $A \subseteq X$  and  $B \subseteq Y$  with  $f(A) = A$  and  $g(B) = B$ . We say  $f: X \rightarrow X$  and  $g: Y \rightarrow Y$  are *topologically conjugate relative to A and B* if there exists a homeomorphism  $h: X \rightarrow Y$  such that  $h(A) = B$  and  $h \circ f = g \circ h$ .

Topologically conjugate homeomorphisms are the same in terms of their dynamics since the conjugacy  $h: X \rightarrow Y$  maps the orbits of  $f: X \rightarrow X$  onto the orbits of  $g: Y \rightarrow Y$  homeomorphically. Clearly,  $x_0$  is a fixed point/periodic point of period  $n$  of  $f: X \rightarrow X$  if and only if  $h(x_0)$  is a fixed point/periodic point of period  $n$  of  $g: Y \rightarrow Y$  since  $h(f^n(x_0)) = g^n(h(x_0))$ . Therefore two topologically conjugate homeomorphisms have the same number of fixed points and the same number of periodic points of each period.

Now, we shall define the *topological entropy*  $h(f)$  of  $f: X \rightarrow X$ , which is a non-negative number (possibly infinite) that is a measure for the complexity of the system  $(X, f)$ . Topological entropy was first introduced in [1] for compact topological spaces. Later, Bowen [8] gave a different definition which is applicable for metric spaces:

**Definitions 2.4.** Let  $X$  be a compact topological space. Given an open cover  $\mathcal{C}$  of  $X$ , denote by  $N(\mathcal{C})$  the number of sets in a subcover of minimal cardinality. Define  $H(\mathcal{C}) = \log N(\mathcal{C})$  and the join of two covers  $\mathcal{C}_1$  and  $\mathcal{C}_2$  by

$$\mathcal{C}_1 \vee \mathcal{C}_2 = \{A \cap B \mid A \in \mathcal{C}_1 \text{ and } B \in \mathcal{C}_2\}.$$

Given a continuous self map  $f: X \rightarrow X$ , let  $f^{-1}(\mathcal{C}) = \{f^{-1}(A) : A \in \mathcal{C}\}$ .

**Definition 2.5** (Adler, Konheim, McAndrew). Let  $(X, f)$  be a topological dynamical system with  $X$  compact, and define

$$h(f, \mathcal{C}) = \lim_{n \rightarrow \infty} \frac{H(\mathcal{C} \vee f^{-1}(\mathcal{C}) \vee \dots \vee f^{-n+1}(\mathcal{C}))}{n}.$$

The *topological entropy*  $h(f)$  of  $f$  is given by  $\sup h(f, \mathcal{C})$  where the supremum is taken over all open covers  $\mathcal{C}$ .

We note that the limit above always exists. See [1].

**Definition 2.6** (Bowen, Dinaburg). Let  $(X, d)$  be a compact metric space with a continuous map  $f: X \rightarrow X$ . Define a new metric on  $X$ ,

$$d_n(x, y) = \max\{d(f^i(x), f^i(y)) : 0 \leq i < n\}$$

for every natural number  $n$ . A set  $E \subset X$  is said to be  $(n, \epsilon)$ -separated if for every  $x, y \in E$  with  $x \neq y$ ,  $d_n(x, y) \geq \epsilon$ .

Let  $S_d(n, \epsilon)$  be the maximum cardinality of an  $(n, \epsilon)$ -separated set. The *topological entropy* of  $f$  is defined as

$$h(f) = \lim_{\epsilon \rightarrow 0} (\limsup_{n \rightarrow \infty} \frac{1}{n} \log S_d(n, \epsilon)).$$

Thus, if we assume that two points can only be distinguished if they are at least  $\epsilon$  apart, then the *topological entropy* is the exponential growth rate of the number of  $\epsilon$  distinguishable  $n$  orbits as  $n$  goes to infinity.

**Remark 2.7.** When  $X$  is a compact metric space and  $f: X \rightarrow X$  is continuous, these two definitions coincide. See [9]. It is clear from Definition 2.5 that topological entropy is an invariant for topological conjugacy.

**Theorem 2.8.** *Let  $f: X \rightarrow X$  be a homeomorphism of a compact topological space. Then  $h(f^k) = |k|h(f)$  for any integer  $k$ .*

See [1]. Note that if  $f: X \rightarrow X$  is any function, then  $h(f^k) = kh(f)$  for  $k \geq 1$ . □

### 2.1.1 Symbolic Dynamics

Given a dynamical system  $(X, f)$ , a *symbolic dynamical system* serves as a model of  $(X, f)$  to describe its dynamics in the simplest way. To do this, we set up the so-called ‘shift map’ as the model map that acts on the space of infinite sequences of  $N$  symbols. Here we shall introduce basic terminology. For more details see for example [21] and [2].

**Definitions 2.9.** Take a finite set  $A = \{1, \dots, N\}$ . This is referred as the *alphabet* or *the state set* for the sequences. Consider the *two-sided sequence space*,

$$\Sigma_N = A^{\mathbb{Z}} = \{(\dots x_{-2}x_{-1} \cdot x_0x_1x_2 \dots) : x_i \in A\}.$$

$A$  is a discrete metric space with the metric  $d(j, k) = \delta_{jk}$ , where  $\delta_{jk}$  is 1 if  $j \neq k$  and 0 if  $j = k$ .  $\Sigma_N$  has the product topology and is compact since the product of any collection of compact topological spaces is compact. The topology on  $\Sigma_N$  is generated by

$$d(x, y) = \sum_{i=-\infty}^{\infty} \frac{\delta_{x_i y_i}}{2^{|i|}}.$$

The shift map on  $\Sigma_N$  is defined by  $\sigma(x)_i = x_{i+1}$  for all  $i$ . In other words  $\sigma$  shifts all entries in a sequence one place to the left. That is,

$$\sigma(\dots x_{-2}x_{-1} \cdot x_0x_1x_2 \dots) = (\dots x_{-2}x_{-1}x_0 \cdot x_1x_2 \dots).$$

The shift map on  $\Sigma_N$  is a homeomorphism and we call the dynamical system  $(\Sigma_N, \sigma)$ , *the full two-sided  $N$  shift*.

**Remark 2.10.** A fixed point in  $(\Sigma_N, \sigma)$  is of the form  $(\cdots x \cdot xx \cdots)$  while a period  $p$  point in  $(\Sigma_N, \sigma)$  looks like  $(\cdots x_0 x_1 \cdots x_{p-1} \cdot x_0 x_1 \cdots x_{p-1} \cdots)$ .

The letters of the alphabet  $A$  denote various states and one can construct certain  $\sigma$  invariant closed subsets of  $(\Sigma_N, \sigma)$  using a so-called *transition matrix* by prohibiting the transition of a given state to another. That is, if the  $(j, k)^{\text{th}}$  entry of the transition matrix is 1, then transition from state  $a_j$  to state  $a_k$  is permitted, if 0, then it is prohibited. This new subspace corresponding to the matrix  $T$  is called the *subshift of finite type* defined by  $T$ . More formally,

**Definitions 2.11.** Given a matrix  $T = (T_{ij})_{N \times N}$  with entries in  $\{0, 1\}$ ; the *subshift of finite type* defined by  $T$  is the restriction  $\sigma_T : \Sigma_T \rightarrow \Sigma_T$  of  $\sigma$ , where

$$\Sigma_T = \{x \in \Sigma_N : T_{x_i x_{i+1}} = 1, \forall i \in \mathbb{Z}\}.$$

We call  $T$  the *transition matrix* and  $\Sigma_T$  the space of all sequences for  $T$ .

**Definitions 2.12.** An *allowable sequence* of length  $k$  is a sequence  $s_0 s_1 \cdots s_{k-1}$  where  $T_{s_i s_{i+1}} = 1$  for  $i = 0, \dots, k-2$ .

We can determine the periodic orbit structure of the subshift from the transition matrix  $T$ :

**Lemma 2.13.** *Let  $N_{ij}^m$  denote the number of admissible sequences of length  $m+1$  that begin at  $i$  and end at  $j$ . Then  $N_{ij}^m$  is equal to the  $ij^{\text{th}}$  entry of  $T^m$ .*

*Proof.* The proof is standard, induction on  $m$  will be used. The first observation is that the number of sequences that begin with  $i$  and end with  $j$  of length  $m$  ( $N_{ij}^{m+1}$ ) is equal to the sum of  $N_{ik}^m$  over all  $k$  for which  $T_{kj} = 1$ . That is,

$$N_{ij}^{m+1} = \sum_{k=1}^N N_{ik}^m T_{kj}$$

Now by definition  $N_{ij}^1 = T_{ij}$ . Assume that  $N_{ij}^m = (T^m)_{ij}$  for all  $i, j$ . Then,

$$N_{ij}^{m+1} = \sum_{k=1}^N (T^m)_{ik} T_{kj} = (T^{m+1})_{ij}.$$

□

For example, let

$$T = \begin{bmatrix} 0 & 1 \\ 1 & 1 \end{bmatrix}$$

Thus there is no sequence of length 2 of the form (00) and there is 1 length 2 sequence of each of the forms (10), (01) and (11). Similarly, using the matrix

$$T^2 = \begin{bmatrix} 1 & 1 \\ 1 & 2 \end{bmatrix}$$

there is 1 length 3 sequence of the form (1 \* 0) that is (110); 1 length 3 sequence of the form (0 \* 1) that is (011); 1 length 3 sequence of the form (0 \* 0) that is (010); and 2 length 3 sequences of the form (1 \* 1) that is (111) and (101). The examples can be extended for  $T^m$  for allowable  $m + 1$  length sequences.

**Corollary 2.14.** *The number of fixed points of  $\sigma_T^m$  is equal to  $\text{tr}(T^m)$  for all  $m \geq 1$ .*

*Proof.* An element  $s$  of  $\Sigma_T$  is a fixed point of  $\sigma_T^m$  if and only if it is of the form  $(s_0 s_1 \dots s_{m-1})^\infty \cdot (s_0 s_1 \dots s_{m-1})^\infty$ . Each such element defines a sequence  $s_0 s_1 \dots s_{m-1} s_0$  of length  $m + 1$  that starts and ends with  $s_0$ . Conversely, given such a sequence, a fixed point of  $\sigma_T^m$  can be constructed. Hence the number of fixed points of  $\sigma_T^m$  is equal to the number of allowable sequences of length  $m + 1$  that start and end with the same symbol. Therefore the number of fixed points  $\sigma_T^m$  is equal to the trace of  $T^m$ .  $\square$

**Definition 2.15.** The *spectral radius*  $\rho$  of  $T$  is the smallest real number for which  $\rho \geq |r|$  for any eigenvalue  $r$  of  $T$ .

**Definitions 2.16.** An  $n \times n$  matrix  $T = (T_{ij})$  is *positive* if  $T_{ij} > 0$  for all  $1 \leq i, j \leq n$  and *eventually positive* if there exists  $k > 1$  such that  $T_{ij}^k > 0$  for all  $1 \leq i, j \leq n$ .

**Theorem 2.17** (Perron-Frobenius). *Let  $T = (T_{ij})$  be an  $n \times n$  matrix with  $T_{ij} \geq 0$  for all  $1 \leq i, j \leq n$ . If  $T$  is eventually positive, then the spectral radius  $\rho$  of  $T$  satisfies the following:*

- i.  $\rho$  is a simple root of the characteristic equation (i.e.  $\rho$  is an eigenvalue with multiplicity 1). Hence the right and left eigenspace associated to  $\rho$  are 1-dimensional.*

ii. The right and left eigenvectors,

$$x = (x_1, \dots, x_n) \quad \text{and} \quad y = (y_1, \dots, y_n) \in \mathbb{R}^n$$

associated with  $\rho$  can be chosen to have strictly positive entries

iii. For any other eigenvalue  $r$ ,  $|r| < \rho$ .

**Lemma 2.18.** *If  $T$  is eventually positive the topological entropy of  $\sigma_T$  is equal to  $h(\sigma_T) = \log \rho$ .*

*Proof.* See for example [16]. □

Hence if  $T$  is eventually positive, the spectral radius  $\rho$  is an eigenvalue of  $T$  which is strictly greater than one and it dominates the trace. That is,  $\text{tr}(T^n)$  grows like  $\rho^n$  and the topological entropy is positive.

The next two sections will present some of the basic terminology and results related to Thurston's theory for surface automorphisms.

## 2.2 Automorphisms of Surfaces

This section presents some ingredients for Section 2.3 which focuses on Thurston's theory of surface automorphisms. Namely, surface automorphisms, isotopy of automorphisms/paths/curves in surfaces and some essential theorems for isotopy relation will be introduced.

Let  $M$  be a surface (by a surface we shall always mean a compact orientable 2-manifold, perhaps with boundary). An *automorphism* of  $M$  is a homeomorphism from  $M$  to itself. Let  $(M, A)$  denote a surface together with a finite subset  $A$  where  $A$  is taken as a set of punctures/ distinguished points on  $M$ .

**Definition 2.19.** An *automorphism* of  $(M, A)$  is a homeomorphism  $f : M \rightarrow M$  with  $f(A) = A$ . The set of all automorphisms of  $(M, A)$  is denoted  $\text{Aut}(M, A)$ .

**Definitions 2.20.** A *path* in  $(M, A)$  is a continuous map  $\alpha : [0, 1] \rightarrow M$  with  $\alpha((0, 1)) \subseteq M \setminus A$ . A path has two end points, the initial point  $\alpha(0)$  and the terminal point  $\alpha(1)$ . If  $\alpha$  is an embedding then we refer to it as an *arc*.

A *closed curve* in  $(M, A)$  is a continuous map  $\alpha : S^1 \rightarrow M \setminus A$  where  $S^1$  is the unit circle. If  $\alpha$  is an embedding then its image will be called a *simple closed curve* in  $(M, A)$ .

Every path is equipped with an orientation. However, for the purposes of Thurston's theory it is convenient to regard simple closed curves as unoriented.

Therefore a simple closed curve is defined to be a subset of  $M$  rather than a map whose image is that subset.

A *homotopy* between two continuous maps deforms one map into the other in a continuous fashion:

**Definitions 2.21.** Two automorphisms  $f$  and  $g \in \text{Aut}(M, A)$  are *homotopic* if there is a continuous map  $F: M \times [0, 1] \rightarrow M$  such that the map  $F_t: M \rightarrow M$  defined for each  $t \in [0, 1]$  by  $F_t(x) = F(x, t)$  satisfies  $F_0 = f$  and  $F_1 = g$  and  $F_t|_A = f|_A = g|_A$ . We say that  $F$  is a *homotopy* from  $f$  to  $g$ . If for each  $t \in [0, 1]$   $F_t$  lies in  $\text{Aut}(M, A)$ , then  $f$  and  $g$  are *isotopic* and  $F_t$  is called an *isotopy* from  $f$  to  $g$ . We consider all homotopies/isotopies rel  $A$  when  $f, g \in \text{Aut}(M, A)$  unless otherwise stated.

We say that two paths  $\alpha$  and  $\beta$  in  $(M, A)$  are *homotopic* and write  $\alpha \simeq \beta$  if there is a continuous map  $F: [0, 1] \times [0, 1] \rightarrow M$  such that  $F(x, 0) = \alpha(x)$ ,  $F(x, 1) = \beta(x)$  for all  $x \in [0, 1]$  and  $F(0, t) = \alpha(0) = \beta(0)$ ,  $F(1, t) = \alpha(1) = \beta(1)$  for all  $t \in [0, 1]$ ; and  $F(x, t) \notin A$  for all  $x \in (0, 1)$  and  $t \in [0, 1]$ .

If  $\alpha$  and  $\beta$  are arcs, then they are isotopic if they are homotopic through arcs. That is,  $F$  can be chosen so that for all  $t$ ,  $x \mapsto F(x, t)$  is an arc.

Two simple closed curves  $C$  and  $D$  are *homotopic/isotopic* if there exist embeddings

$\alpha: S^1 \rightarrow M \setminus A$  and  $\beta: S^1 \rightarrow M \setminus A$  with  $\alpha(S^1) = C$  and  $\beta(S^1) = D$  that are *homotopic/isotopic* as maps into  $M \setminus A$ .

**Definitions 2.22.** We say that arcs  $\alpha$  and  $\beta$  in  $(M, A)$  are *ambient isotopic* if there exists an automorphism  $h \in \text{Aut}(M, A)$  isotopic to the identity such that  $\beta = h \circ \alpha$ . Similarly, two simple closed curves  $C_1$  and  $C_2$  in  $(M, A)$  are *ambient isotopic* if there is an automorphism  $h$  in  $\text{Aut}(M, A)$  isotopic to the identity such that  $h(C_1) = C_2$ .

We do not distinguish homotopy and isotopy for simple closed curves; and for arcs with common end points that lie in  $\partial M$  and  $A$ . The following two results are from [15].

**Theorem 2.23** (Epstein). *Let  $\alpha$  and  $\beta$  be two arcs in  $(M, A)$  with end points  $\partial\alpha$ ,  $\partial\beta$  such that  $\partial M \cap \alpha = \partial\alpha = \partial M \cap \beta = \partial\beta$  and which are homotopic keeping the end points fixed. Then they are ambient isotopic by an isotopy which is fixed on  $\partial M$  and outside a compact subset of  $M \setminus A$ .*

□

**Theorem 2.24** (Epstein). *Two homotopic simple closed curves in  $(M, A)$  are isotopic; if they lie in  $\text{Int } M$  then they are ambient isotopic by an isotopy which is fixed on the complement of a compact subset of  $\text{Int } M$ .*

□

Isotopy defines an equivalence relation on  $\text{Aut}(M, A)$  and the isotopy class containing  $f$  is denoted  $[f]$ . The set of isotopy classes of orientation preserving automorphisms of  $(M, A)$  forms a group where the group operation is induced by the composition of automorphisms,  $[f] * [g] = [f \circ g]$ :

**Definition 2.25.** The *Mapping Class Group* of  $(M, A)$  is the group of isotopy classes of orientation preserving automorphisms of  $(M, A)$ , denoted  $\text{MCG}(M, A)$ .

Throughout the thesis we shall work on a standard model of the  $n$ -times punctured disk  $(D^2, A_n)$ .

**Definition 2.26.**  $D_n$  denotes  $(D^2, A_n)$  where  $D^2 = \{x \in \mathbb{R}^2 : \|x\| \leq 1\}$  and  $A_n = \{a_r = (-1 + \frac{2r}{n+1}, 0) : 1 \leq r \leq n\}$ .

**Theorem 2.27** (Alexander Trick). *If  $n = 0$  or  $n = 1$  then  $\text{MCG}(D_n)$  is trivial.*

□

When  $n > 1$  then  $\text{MCG}(D_n)$  is isomorphic to the  $n$ -braid group modulo its center. This will be explained in Section 2.5.

**Definitions 2.28.** A simple closed curve in  $(M, A)$  is *inessential* if it bounds an unpunctured disk, once punctured disk or an unpunctured annulus. It is *essential* otherwise.  $\mathcal{E}(M, A)$  denotes the space of isotopy classes of essential simple closed curves in  $(M, A)$ .

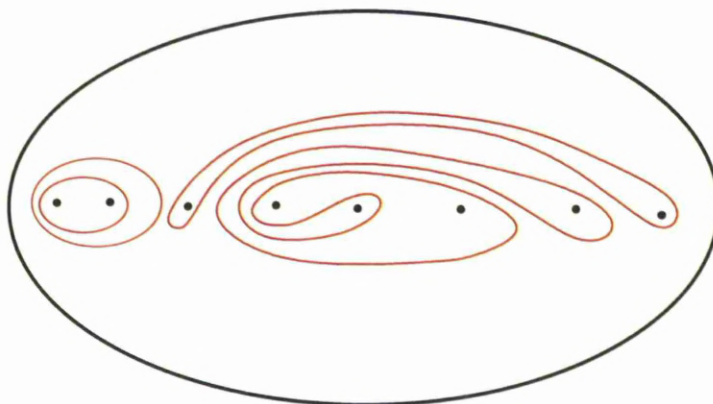


Figure 2.1: An integral lamination on  $D_8$



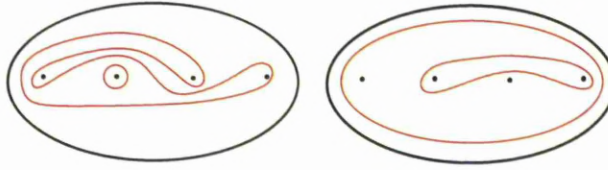


Figure 2.2: These curve systems are not integral laminations

**Definition 2.29.** An *integral lamination*  $\mathcal{L}$  on  $D_n$  is a disjoint union of finitely many essential simple closed curves in  $D_n$  modulo isotopy. The set of integral laminations on  $D_n$  is denoted  $\mathcal{L}_n$ .

We note that the curves of an integral lamination do not need to be mutually non-homotopic. Figure 2.1 and Figure 2.2 give examples of an integral lamination on  $D_8$  and disjoint unions of simple closed curves that do not form integral laminations on  $D_4$  respectively: notice the curves that bound a once punctured disk and an annulus on the left and right side of Figure 2.2 respectively.

Since  $f \in \text{Aut}(D_n)$  acts on  $\mathcal{L} \in \mathcal{L}_n$  by sending  $\mathcal{L}$  to its image  $f(\mathcal{L})$ , there is a well-defined action of  $\text{MCG}(D_n)$  on  $\mathcal{L}_n$ .

### 2.3 Tools from Thurston's theory on surface automorphisms

This section contains some results of Thurston's theory on surface automorphisms. We shall enumerate the principal theorems and results that are crucial for our purposes in Chapter 3 and Chapter 4, proofs of which can be found in [16]. We shall start with the basic terminology.

**Definitions 2.30.** A (*singular*) *foliation*  $\mathcal{F}$  on  $(M, A)$  is a decomposition of  $M$  as a disjoint union of pathwise-connected subsets, called *leaves*, such that

- any point  $x \in M \setminus \partial M$  outside of a finite set  $S$  of singularities is contained in a chart  $\phi : U \rightarrow \mathbf{R}^2$  carrying the components of  $U \cap \text{leaf}$  to horizontal lines.
- The singularities are classified with their number of *prongs*  $p \geq 1$ . A *prong* is a piece of a leaf beginning at a singularity. At a  $p$ -pronged singularity in  $\text{Int } M$  there is a local chart which looks like Figure 2.4.
- 1-pronged singularities only occur at points of  $A$  and the local chart looks like Figure 2.5.

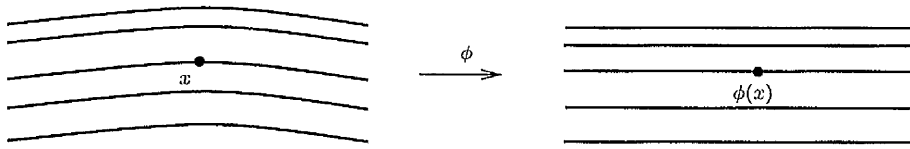


Figure 2.3: Leaves near  $x \in M \setminus \partial M$

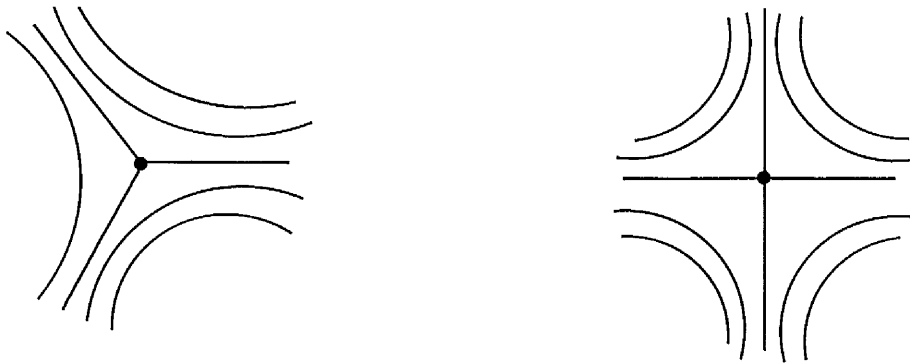


Figure 2.4: Leaves near 3-pronged and 4-pronged singularities in  $\text{Int } M$



Figure 2.5: Leaves near 1-pronged singularity  $x \in A$

- each boundary component has a  $p$ -pronged singularity where  $p \geq 1$  as shown in Figure 2.6. In this case, the boundary component and the  $p$  prongs which emanate from the singularity are all considered to lie in the same leaf.

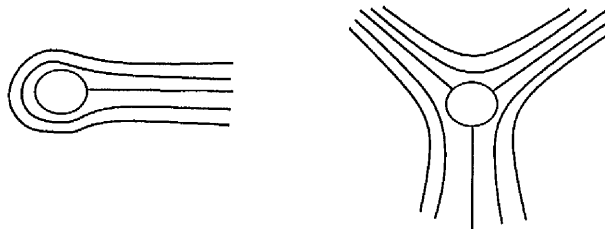


Figure 2.6: Leaves near a 1-pronged singularity and a 3-pronged singularity on  $\partial M$

Next, we define what it means for two foliations to be transverse.

**Definitions 2.31.** Two (singular) foliations are *transverse* if both foliations have  $p$ -pronged singularities at the same interior points and boundary components and in local charts the foliations are as depicted in Figure 2.7 and Figure 2.8.



Figure 2.7: Transverse foliations away from and near an interior singularity

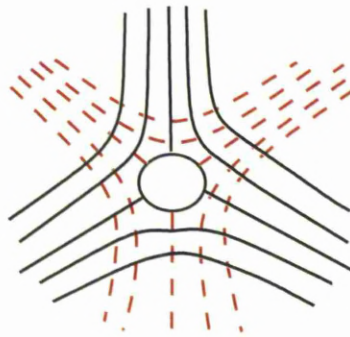


Figure 2.8: Transverse foliations near a 3-pronged boundary singularity

**Definition 2.32.** An arc  $\alpha$  in  $(M, A)$  is *transverse* to a singular foliation  $\mathcal{F}$  if it intersects the leaves of  $\mathcal{F}$  transversely and if whenever it passes through  $s \in S$  it enters and leaves through different sectors. See Figure 2.9.

**Definition 2.33.** Given a foliation  $\mathcal{F}$  on  $(M, A)$ , a *transverse measure*  $\mu$  on  $\mathcal{F}$  is a function which assigns a positive number  $\mu(\alpha) \in \mathbb{R}^+$  to every transverse arc  $\alpha$  such that the following hold:

- i. If  $\alpha_1$  and  $\alpha_2$  are two transverse arcs that are isotopic through other transverse arcs whose end points stay in the same leaf, then  $\mu(\alpha_1) = \mu(\alpha_2)$ .
- ii. If  $\alpha = \alpha_1 \cup \alpha_2$  with  $\alpha_1 \cap \alpha_2 = \partial\alpha_1 \cap \partial\alpha_2$ , then  $\mu(\alpha) = \mu(\alpha_1) + \mu(\alpha_2)$ .

See Figure 2.10.

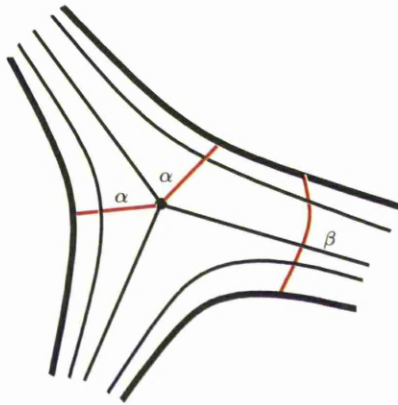


Figure 2.9: Transverse arcs

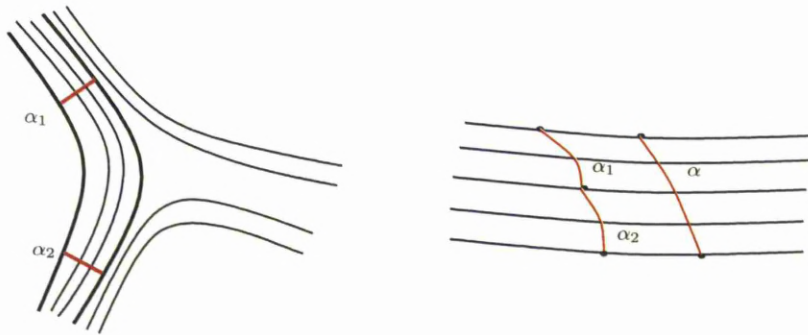


Figure 2.10:  $\mu(\alpha_1) = \mu(\alpha_2)$  and  $\mu(\alpha_1) + \mu(\alpha_2) = \mu(\alpha)$

**Definition 2.34.** A (full) measured foliation  $(\mathcal{F}, \mu)$  on  $(M, A)$  is a singular foliation  $\mathcal{F}$  on  $(M, A)$  equipped with a transverse measure  $\mu$ . A partial measured foliation  $(\mathcal{F}^*, \mu)$  on  $(M, A)$  is a full measured foliation on a subsurface of  $(M, A)$  which is not necessarily connected.

**Definitions 2.35.** Let  $(\mathcal{F}, \mu)$  be a measured foliation on  $(M, A)$  and  $\alpha$  be an arc in  $(M, A)$ . Using the measure  $\mu$  on the foliation we define the length  $\mu(\alpha)$  as,

$$\mu(\alpha) = \sup \sum_{i=1}^k \mu(\alpha_i)$$

where the supremum is taken over all finite collections  $\alpha_1, \dots, \alpha_k$  of mutually disjoint subarcs of  $\alpha$  that are transverse to  $\mathcal{F}$ . Let  $[\alpha]$  be the isotopy class of  $\alpha$  where the isotopies are relative to the end points of the arcs. We set

$$i(\mathcal{F}, [\alpha]) = \inf \mu(\beta)$$

where the infimum is over all arcs  $\beta$  isotopic to  $\alpha$  which are transverse to  $(\mathcal{F}, \mu)$  except at a set of measure zero. Similarly, we can define  $\mu(C)$  and  $i(\mathcal{F}, [C])$  for an essential simple closed curve  $C$  and its isotopy class  $[C]$ .

**Definitions 2.36.** A *Whitehead move* on a measured foliation contracts a compact leaf that joins two singularities or does the inverse. See Figure 2.11.

Two measured foliations are *Whitehead Equivalent* if one can be turned into the other after a finite number of Whitehead moves.

Observe from Figure 2.11 that if two foliations are related by a *Whitehead move*, then there is a natural one-to-one correspondence between their transverse measures.

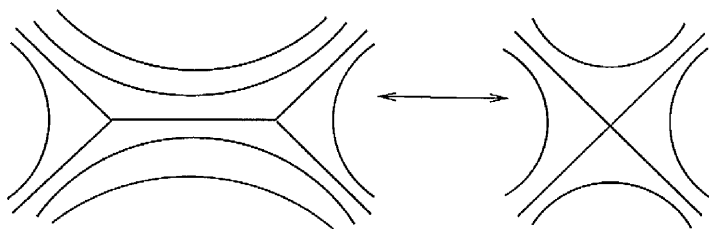


Figure 2.11: An example of a Whitehead Move

**Definition 2.37.** Let  $(\mathcal{F}, \mu)$  be a full or partial measured foliation on  $(M, A)$  and let  $k > 0$ .  $(\mathcal{F}, k\mu)$  is a measured foliation with the same leaves as those of  $(\mathcal{F}, \mu)$  such that any arc  $\alpha$  transverse to  $\mathcal{F}$  has measure  $k\mu(\alpha)$ .

Let  $\mathcal{MF}(M, A)$  be the set of measured foliations and partial measured foliations on  $(M, A)$  up to isotopy and Whitehead equivalence. Then by Definition 2.37 there is a natural action of the positive reals  $\mathbb{R}^+$  on  $\mathcal{MF}(M, A)$ .

**Definitions 2.38.** The space of *Projective Measured Foliations*,  $\mathcal{PMF}(M, A)$ , on  $(M, A)$  is the quotient space of  $\mathcal{MF}(M, A)$  modulo  $(\mathcal{F}, \mu) \sim (\mathcal{F}, k\mu)$ ,  $k > 0$ . That is,  $\mathcal{PMF}(M, A)$  is the space of equivalence classes  $[\mathcal{F}, \mu]$  where  $(\mathcal{F}, \mu)$  is identified with  $(\mathcal{F}, k\mu)$  for all  $k > 0$ .

## 2.4 Some results of Thurston's theory on surface automorphisms

In this section we present some known results of Thurston's theory on surface automorphisms which we shall refer to in Chapter 3 and Chapter 4. In particular, we shall see that each essential simple closed curve (or a union of them) is assigned

a non-negative number by the elements of three different spaces  $\mathcal{MF}(M, A)$ ,  $\mathcal{E}(M, A)$  and  $\mathcal{T}(M, A)$ . That is to say, there exist maps  $\mathcal{MF}(M, A) \rightarrow \mathbb{R}_{\geq 0}^{\mathcal{E}(M, A)}$ ,  $\mathcal{E}(M, A) \rightarrow \mathbb{R}_{\geq 0}^{\mathcal{E}(M, A)}$  and  $\mathcal{T}(M, A) \rightarrow \mathbb{R}_{\geq 0}^{\mathcal{E}(M, A)}$  which can be shown to be injective and therefore give embeddings of these spaces in  $\mathbb{R}_{\geq 0}^{\mathcal{E}(M, A)}$ .

Throughout this section  $(M, A)$  will denote a surface of genus  $g$  with  $b$  boundary components and  $s$  punctures, which has negative Euler characteristic  $\chi(M, A) = 2 - 2g - b - s$ .

**Definitions 2.39.** Given  $\alpha, \beta \in \mathcal{E}(M, A)$ , denote by  $i(\alpha, \beta) \geq 0$  the geometric intersection number of  $\alpha$  and  $\beta$ , which is the minimum number of intersections of  $a$  and  $b$  where  $a \in \alpha$  and  $b \in \beta$ . The function  $i: \mathcal{E}(M, A) \times \mathcal{E}(M, A) \rightarrow \mathbb{Z}_{\geq 0}$  is called the *geometric intersection function*.

Let  $\mathbb{R}_{\geq 0}^{\mathcal{E}(M, A)}$  be the set of functions from  $\mathcal{E}(M, A)$  to non-negative reals  $\mathbb{R}_{\geq 0}$  endowed with the product topology. There is an associated projective space  $P(\mathbb{R}_{\geq 0}^{\mathcal{E}(M, A)})$  given with a projection

$$\pi: \mathbb{R}_{\geq 0}^{\mathcal{E}(M, A)} \setminus 0 \rightarrow P(\mathbb{R}_{\geq 0}^{\mathcal{E}(M, A)}).$$

$P(\mathbb{R}_{\geq 0}^{\mathcal{E}(M, A)})$  is given the quotient topology.

The map  $i: \mathcal{E}(M, A) \times \mathcal{E}(M, A) \rightarrow \mathbb{R}_{\geq 0}$  gives a map  $i_*: \mathcal{E}(M, A) \rightarrow \mathbb{R}_{\geq 0}^{\mathcal{E}(M, A)}$  with  $i_*(\alpha)(\beta) = i(\alpha, \beta)$  which is known to be injective. We have,

$$\mathcal{E}(M, A) \xrightarrow{i_*} \mathbb{R}_{\geq 0}^{\mathcal{E}(M, A)} \xrightarrow{\pi} P(\mathbb{R}_{\geq 0}^{\mathcal{E}(M, A)})$$

and  $\pi \circ i_*(\mathcal{E}(M, A)) \subset P(\mathbb{R}_{\geq 0}^{\mathcal{E}(M, A)})$  is known to have a compact closure. Let  $\mathcal{PL}(M, A)$  denote this closure.

**Theorem 2.40.** ([29])  $\mathcal{PL}(M, A)$  is topologically a sphere which has dimension  $6g + 2s + 2b - 7$ .

See [16] for a proof.

Similarly  $i$  defines a map from  $\mathcal{MF}(M, A)$  to  $\mathbb{R}_{\geq 0}^{\mathcal{E}(M, A)}$  by Definition 2.35. That is,  $i: \mathcal{MF}(M, A) \times \mathcal{E}(M, A) \rightarrow \mathbb{R}_{\geq 0}$  gives a map  $i_*: \mathcal{MF}(M, A) \rightarrow \mathbb{R}_{\geq 0}^{\mathcal{E}(M, A)}$  with  $i_*(\mathcal{F})(\beta) = i(\mathcal{F}, \beta)$ . We have,

$$\mathcal{MF}(M, A) \xrightarrow{i_*} \mathbb{R}_{\geq 0}^{\mathcal{E}(M, A)} \xrightarrow{\pi} P(\mathbb{R}_{\geq 0}^{\mathcal{E}(M, A)})$$

**Theorem 2.41.** ([29]) The topological sphere  $\mathcal{PL}(M, A)$  is identified with

$$\{\pi \circ i_*(\mathcal{F}) : \mathcal{F} \in \mathcal{MF}(M, A)\}.$$

See [16] for a proof.

Therefore  $\mathcal{PMF}(M, A)$  can be identified with  $\mathcal{PL}(M, A)$  and it follows that  $\mathcal{PMF}(M, A)$  is homeomorphic to a sphere with dimension  $6g + 2s + 2b - 7$ .  $\mathcal{E}(M, A)$  is a dense set of *rational* points on this sphere. Using the coordinates of such a point the corresponding essential simple closed curve can be drawn. This can be done using Dehn-Thurston coordinates [26] or Dynnikov coordinates when  $M$  is the punctured disk  $D_n$  (Chapter 3).

**Definition 2.42.** A hyperbolic metric on  $(M, A)$  is a Riemannian metric on  $M \setminus A$  of constant curvature  $-1$ . The *Teichmüller space*  $\mathcal{T}(M, A)$  is the space of hyperbolic metrics on  $(M, A)$  modulo isotopy.

Let  $\rho \in \mathcal{T}(M, A)$  and  $\alpha \in \mathcal{E}(M, A)$ .  $i : \mathcal{T}(M, A) \times \mathcal{E}(M, A) \rightarrow \mathbb{R}_{\geq 0}$  given with  $i(\rho, \alpha) = \rho(\alpha)$  gives the length of a minimal geodesic in the isotopy class of  $\alpha$  and induces  $i_* : \mathcal{T}(M, A) \rightarrow \mathbb{R}_{\geq 0}^{\mathcal{E}(M, A)}$ .

$\mathcal{T}(M, A)$  is endowed with a minimum topology such that each function  $i(\rho, \alpha)$  is continuous from which a continuous map  $\pi \circ i_* : \mathcal{T}(M, A) \rightarrow \mathbb{R}_{\geq 0}^{\mathcal{E}(M, A)}$  is obtained.

The closure of  $\pi \circ i_*(\mathcal{T}(M, A))$  is  $\pi \circ i_*(\mathcal{T}(M, A)) \cup \mathcal{PMF}(M, A)$  from which  $\bar{\mathcal{T}} = \mathcal{T}(M, A) \cup \mathcal{PMF}(M, A)$  is endowed with a natural topology.

**Theorem 2.43.** ([29])  $\bar{\mathcal{T}} = \mathcal{T}(M, A) \cup \mathcal{PMF}(M, A)$  is homeomorphic to a disk of dimension  $6g - 6 + 2s + 2b$ . Therefore,  $\mathcal{T}(M, A)$  is an open ball of dimension  $6g - 6 + 2s + 2b$  and  $\mathcal{PMF}(M, A)$  forms its boundary.

If  $f \in \text{Aut}(M, A)$ , there is an induced action  $\tilde{f}$  on  $P(\mathbb{R}_{\geq 0}^{\mathcal{E}(M, A)})$  defined by  $\tilde{f}(\xi)(\alpha) = \xi(f^{-1}(\alpha))$ .  $\text{MCG}(M, A)$  acts continuously on  $\bar{\mathcal{T}}$  and  $\bar{\mathcal{T}}$  is invariant under  $\tilde{f}$ . Therefore by the *Brouwer Fixed Point Theorem*  $\tilde{f}$  has a fixed point in  $\bar{\mathcal{T}}$ . Analysis of this fixed point yields the famous Nielsen-Thurston classification theorem which says that any automorphism  $f$  in  $\text{Aut}(M, A)$  is isotopic to an automorphism  $g$  in  $\text{Aut}(M, A)$  which is either finite order or pseudo-Anosov or reducible [29, 16].

**Definition 2.44.** An automorphism  $f : (M, A) \rightarrow (M, A)$  is *reducible* if there exists a collection  $\mathcal{L} = \{\mathcal{L}_1, \dots, \mathcal{L}_k\}$  of mutually disjoint essential simple closed curves in  $(M, A)$  such that for all  $i$  there is some  $j$  with  $f(\mathcal{L}_i) = \mathcal{L}_j$ .

**Definition 2.45.** An automorphism  $f : (M, A) \rightarrow (M, A)$  is *finite order* if  $f^n = id$  for some integer  $n > 0$ .

Next, we define *pseudo-Anosov* automorphisms which are the main focus of this thesis. First we give the following preliminary definition.

**Definition 2.46.** Let  $f: (M, A) \rightarrow (M, A)$  be an automorphism, and  $(\mathcal{F}, \mu)$  be a measured foliation on  $(M, A)$ . Then,  $f((\mathcal{F}, \mu))$  is the measured foliation whose leaves are the images under  $f$  of the leaves of  $\mathcal{F}$  and which assigns the measure  $\mu(f^{-1}(\alpha))$  to an arc  $\alpha$  transverse to  $f(\mathcal{F})$ .

**Definition 2.47.** An automorphism  $f: (M, A) \rightarrow (M, A)$  is *pseudo-Anosov* if there exists a transverse pair of (full) measured foliations  $(\mathcal{F}^s, \mu^s)$  and  $(\mathcal{F}^u, \mu^u)$  and a number  $\lambda > 1$  (the dilatation) such that

$$f(\mathcal{F}^s, \mu^s) = (\mathcal{F}^s, (1/\lambda)\mu^s)$$

$$f(\mathcal{F}^u, \mu^u) = (\mathcal{F}^u, \lambda\mu^u).$$

We say that  $(\mathcal{F}^s, \mu^s)$  and  $(\mathcal{F}^u, \mu^u)$  are the *stable* and *unstable* invariant foliations of  $f$  respectively.

Before giving a list of properties of pseudo-Anosov automorphisms, we shall state the classification theorem [29] once more:

**Theorem 2.48** (Nielsen-Thurston). *Any automorphism  $f: (M, A) \rightarrow (M, A)$  is isotopic to an automorphism  $g: (M, A) \rightarrow (M, A)$  which is one of the following types:*

- i.  $g$  is finite order;*
- ii.  $g$  is pseudo-Anosov;*
- iii.  $g$  is reducible.*

*If  $f$  is isotopic to a pseudo-Anosov automorphism, then it is not isotopic to a reducible or finite order automorphism.*

**Definitions 2.49.** An isotopy class that contains a reducible automorphism is called a *reducible isotopy class*. It is *irreducible* otherwise. An irreducible isotopy class is called *finite order isotopy class* if it contains a finite order automorphism and *pseudo-Anosov isotopy class* if it contains a pseudo-Anosov automorphism.

**Remark 2.50.** Note that any iterate of a reducible, finite order or pseudo-Anosov automorphism is reducible, finite order or pseudo-Anosov respectively. Therefore the classification is invariant under powers, in  $\text{MCG}(M, A)$ .

### 2.4.1 Some properties of pseudo-Anosov automorphisms

Our goal in this section is to introduce some basic properties of pseudo-Anosov automorphisms which are essential in the remainder of the thesis. All the proofs can be found in [16].



Throughout this section  $f : (M, A) \rightarrow (M, A)$  will denote a pseudo-Anosov automorphism with invariant measured foliations  $(\mathcal{F}^s, \mu_s)$  and  $(\mathcal{F}^u, \mu_u)$  and dilatation  $\lambda > 1$ .

**Theorem 2.51.** *If  $g : (M, A) \rightarrow (M, A)$  is a pseudo-Anosov automorphism in the isotopy class of  $f$ , then  $f$  and  $g$  are topologically conjugate by a homeomorphism that is isotopic to the identity.*

See exposé 12 of [16] for a proof. This means that the pseudo-Anosov automorphism in a pseudo-Anosov isotopy class is essentially unique.

We go on with the following important theorem which gives the topological entropy of a pseudo-Anosov automorphism  $f : (M, A) \rightarrow (M, A)$ .

**Theorem 2.52.** *Let  $g : (M, A) \rightarrow (M, A)$  be in the isotopy class of  $f$ . Then  $h(f) \leq h(g)$ . Furthermore,  $h(f) = \log \lambda$ .*

See exposé 10 of [16] for a proof.

**Definition 2.53.** Let  $[\phi] \in \text{MCG}(M, A)$ . Then the topological entropy of  $[\phi]$  is defined as

$$h([\phi]) = \inf_{g \in [\phi]} h(g).$$

**Remark 2.54.** Theorem 2.52 tells that a pseudo-Anosov automorphism minimizes the topological entropy in its isotopy class. Therefore, the topological entropy of a pseudo-Anosov isotopy class equals  $\log \lambda$ .

**Theorem 2.55.** *Let  $\rho$  be a Riemannian metric on  $(M, A)$ ,  $\alpha \in \mathcal{E}(M, A)$  and  $l_\rho(\alpha)$  be the minimum length of a geodesic  $a \in \alpha$ . Then,*

$$\lim_{n \rightarrow \infty} \sqrt[n]{l_\rho(f^n(\alpha))} = \lambda.$$

See exposé 9 of [16].

There exists an  $f$ -invariant measure  $\mu$  which is given locally by the product  $\mu_u \otimes \mu_s$ . Since  $\mu$  is determined up to multiplication by positive constants, we can suppose that  $\mu_u \otimes \mu_s(M) = 1$ . If this is the case, we have the following theorem.

**Theorem 2.56.**

$$\lim_{n \rightarrow \infty} \frac{i(f^n([\alpha]), [\beta])}{\lambda^n} = \mu_u([\alpha])\mu_s([\beta])$$

for any two isotopy classes  $[\alpha], [\beta]$  in  $\mathcal{E}(M, A)$ .

See exposé 12 of [16] for a proof.

Therefore, the length of  $\alpha$  and its geometric intersection number  $i(\alpha, \beta)$  with a given essential simple closed curve  $\beta$  grows like  $\lambda^n$  as we repeatedly apply  $f$  to  $\alpha$ . Hence, Theorem 2.55 and Theorem 2.56 suggest a method to find an estimate for the dilatation  $\lambda$  of  $f$  and hence compute its topological entropy  $\log(\lambda)$  by Theorem 2.52. In fact Moussafir's technique on computing braid entropy is based on these two theorems. This will be elaborated in Section 4.1.

**Theorem 2.57.** *For any essential simple closed curve  $\alpha$ ,*

$$\lim_{n \rightarrow \infty} f^n[\alpha] = [\mathcal{F}^u, \mu^u], \quad \lim_{n \rightarrow \infty} f^{-n}[\alpha] = [\mathcal{F}^s, \mu^s],$$

and for any  $[\mathcal{F}, \mu] \in \mathcal{PMF}(M, A)$  with  $[\mathcal{F}, \mu] \neq [\mathcal{F}^u, \mu^u]$  and  $[\mathcal{F}, \mu] \neq [\mathcal{F}^s, \mu^s]$

$$\lim_{n \rightarrow \infty} f^n[\mathcal{F}, \mu] = [\mathcal{F}^u, \mu^u], \quad \lim_{n \rightarrow \infty} f^{-n}[\mathcal{F}, \mu] = [\mathcal{F}^s, \mu^s].$$

See exposé 12 of [16] for a proof.

Theorem 2.57 says that any essential simple closed curve  $[\alpha]$ , or measured foliation  $[\mathcal{F}, \mu]$  ( $[\mathcal{F}, \mu] \neq [\mathcal{F}^s, \mu^s]$ ) in  $\mathcal{PMF}(M, A)$  converges to the unstable foliation  $[\mathcal{F}^u, \mu^u]$  under iteration of the induced action of  $f$ .

**Theorem 2.58.** *The only fixed points of  $\tilde{f}$  in  $\overline{\mathcal{T}}$  are  $[\mathcal{F}^u, \mu^u]$  and  $[\mathcal{F}^s, \mu^s]$  on  $\mathcal{PMF}(M, A)$ .*

Theorems 2.57 and 2.58 will be extremely important for the methods developed in Chapter 4.

We give two more properties regarding the invariant measured foliations of a pseudo-Anosov automorphism  $f : (M, A) \rightarrow (M, A)$ .

- i.  $(\mathcal{F}^s, \mu^s)$  and  $(\mathcal{F}^u, \mu^u)$  are unique up to multiplication with positive constants and satisfy the following: No leaf connects two singularities and no leaf of  $(\mathcal{F}^s, \mu^s)$  or  $(\mathcal{F}^u, \mu^u)$  contains a simple closed curve except for the boundary components of  $M$ . See exposé 9 of [16].

Next, we give a formula which is known as ‘‘Euler-Poincaré formula’’ that reveals the strong connection between the singularity structure of the invariant foliations of  $f$  and the topology of the surface  $M$ . In particular, using this formula we can tell the possible singularity structures of the invariant foliations for  $D_n$ . See exposé 5 of [16] for a proof.

ii. We have

$$\sum_{p=1}^{\infty} n_p(2-p) = 4(1-g)$$

where  $n_p$  denotes the number of singular points (including boundary components) with  $p$  prongs.

Therefore for  $D_n$  we have that,

$$\sum_p n_p(2-p) = 4.$$

We first note that 1-prongs only occur at  $A$  and  $\partial D_n$ . Also, the summand is positive only when  $p = 1$ . Hence when  $n < 3$  there can be no pseudo-Anosov automorphisms of  $D_n$ .

When  $n = 3$ , the only possibility is to have a 1-pronged singularity on the boundary and 1-pronged singularities at each of the three punctures.

When  $n = 4$ , there are three possibilities:

- a 2-pronged singularity on the boundary and 1-pronged singularities at each of the four punctures or
- a 2-pronged singularity at one of the punctures and 1-pronged singularities at the other punctures and the boundary.
- a 1-pronged singularity on the boundary and 1-pronged singularities at each of the four punctures, and an interior 3-pronged singularity.

## 2.5 Braids

It is well known (see for example [7]) that isotopy classes of orientation preserving automorphisms on  $D_n$  are represented by *braids*. Since our principal goal in this thesis is to study isotopy classes of pseudo-Anosov automorphisms on  $D_n$ , we shall always work with braids.

We will start with some basic definitions and properties and explain the group structure of geometric braids, and finally explain briefly why the braid group modulo its center is naturally isomorphic to the mapping class group of  $D_n$ .

**Definition 2.59.** Let  $D_n = (D^2, A_n)$  be the standard  $n$ -punctured disk (see Definition 2.26). A *geometric braid*  $\beta \in B_n$  is a collection of  $n$  disjoint arcs  $\alpha_1, \dots, \alpha_n$  in  $D^2 \times [0, 1]$  connecting the points of  $A_n \times \{0\}$  to those of  $A_n \times \{1\}$

such that each level plane  $D^2 \times \{s\}$  for  $s \in [0, 1]$  intersects each arc at only one point. The arc with initial point  $(a_r, 0)$  and end point  $(a_{\pi_\beta(r)}, 1)$  is called the  $r^{\text{th}}$  string of  $\beta$  and  $\pi_\beta$  is called the permutation induced by the geometric braid  $\beta$ . Note that everything is taken up to isotopy.

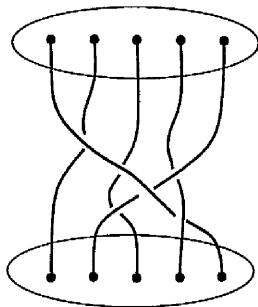


Figure 2.12: A braid on a 5-punctured disk

The set of geometric braids  $B_n$  forms a group with the following composition rule: Take two geometric  $n$ -braids  $\beta_1, \beta_2$  embedded in  $D^2 \times [0, 1]$  with the arcs  $\alpha_j^1 : [0, 1] \rightarrow D^2 \times [0, 1]$  and  $\alpha_j^2 : [0, 1] \rightarrow D^2 \times [0, 1]$  respectively. Writing  $\phi$  for the projection  $\phi : D^2 \times [0, 1] \rightarrow D^2$ , the arcs  $\alpha_j$  of  $\beta_1\beta_2$  are defined by

$$\alpha_j(t) = \begin{cases} (\phi(\alpha_j^1(2t)), t); & t \leq 1/2 \\ (\phi(\alpha_{\pi_1(j)}^2(2t-1)), t); & t \geq 1/2 \end{cases} \quad (2.1)$$

where  $\pi_1$  is the permutation induced by  $\beta_1$ . See Figure 2.13.

Informally speaking, this operation joins the bottoms of the strings of  $\beta_1$  to the tops of the strings of  $\beta_2$ , and then squashes the constructed braid in such a way that it is embedded in  $D^2 \times I$ . The set of geometric braids with this given operation forms a group: The arcs of the trivial braid are defined by

$$\alpha_j(t) = (a_j, t), \quad 0 \leq j \leq 1$$

and the arcs of the braid which is the inverse to the braid given with the arcs  $\alpha_j$  are defined by

$$\alpha'_j(t) = (\phi(\alpha_j(1-t)), t), \quad 0 \leq j \leq 1.$$

Observe that any geometric braid  $\beta \in B_n$  can be constructed as a composition of geometric braids  $\sigma_i$  and  $\sigma_i^{-1}$  as depicted in Figure 2.14 and satisfies the relations as depicted in Figure 2.15 and Figure 2.16.

In fact this group is canonically isomorphic to the *Artin Braid Group*:

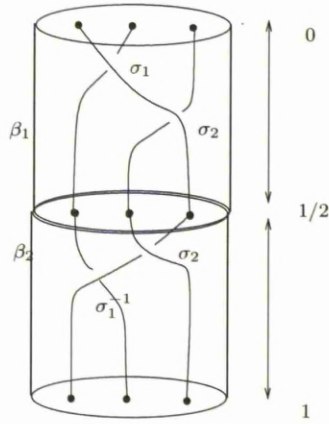


Figure 2.13: Constructing a braid  $\beta$  from two given braids  $\beta_1$  and  $\beta_2$

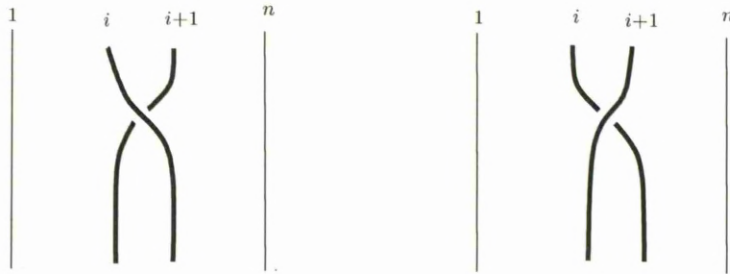


Figure 2.14:  $\sigma_i$  and  $\sigma_i^{-1}$



Figure 2.15:  $\sigma_i \sigma_{i+1} \sigma_i = \sigma_{i+1} \sigma_i \sigma_{i+1}$

**Definitions 2.60.** The *Artin braid group* is the finitely generated group with  $n - 1$  generators  $\sigma_1, \dots, \sigma_{n-1}$  and relations

$$\sigma_i \sigma_j = \sigma_j \sigma_i, \quad \text{if } 1 \leq i, j \leq n - 1, \quad |i - j| \geq 2,$$

$$\sigma_i \sigma_{i+1} \sigma_i = \sigma_{i+1} \sigma_i \sigma_{i+1}, \quad \text{if } 1 \leq i \leq n - 2.$$

Rotating the strings through  $\pi$  and  $2\pi$  around the center of the disk defines two important braids in  $B_n$ ; the *half twist* and the *full twist*.

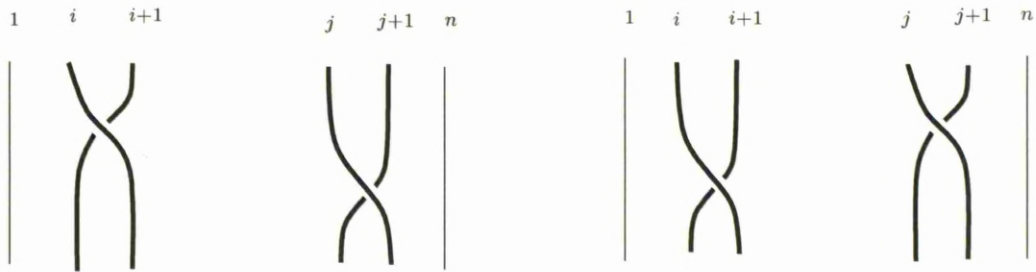


Figure 2.16:  $\sigma_i \sigma_j = \sigma_j \sigma_i$  when  $|i - j| \geq 2$

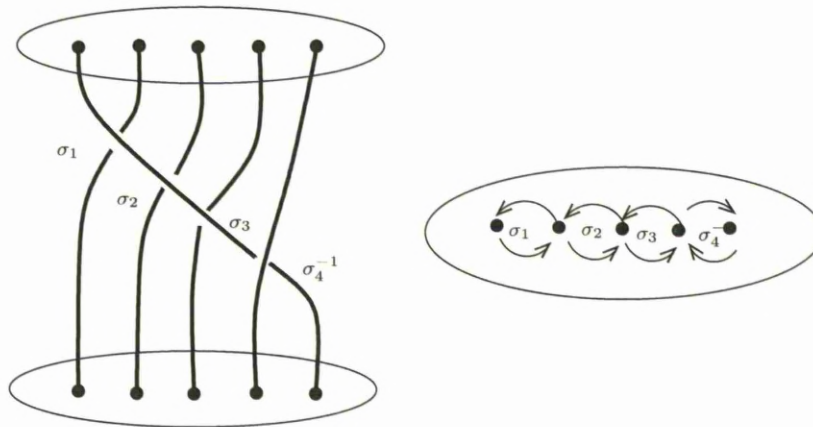


Figure 2.17: Moving punctures

**Definitions 2.61.** The *half twist* in  $B_n$  is given by,

$$\Delta_n = (\sigma_1 \dots \sigma_{n-1})(\sigma_1 \dots \sigma_{n-2}) \dots (\sigma_1 \sigma_2)(\sigma_1)$$

and the *full twist* in  $B_n$  is given by

$$\theta_n = \Delta_n^2 = (\sigma_1 \sigma_2 \dots \sigma_{n-1})^n.$$

**Theorem 2.62** (Chow [10]). For  $n \geq 3$ , the center  $Z(B_n)$  of  $B_n$  is the infinite cyclic subgroup generated by the full twist; that is,  $Z(B_n) = \langle \theta_n \rangle$ .

**Theorem 2.63.**  $\text{MCG}(D_n)$  is isomorphic to the quotient of Artin's braid group  $B_n$  by its center. That is,  $\text{MCG}(D_n) \cong B_n / Z(B_n)$ .

We shall give a brief explanation of how the correspondence between the two groups works.

First, we explain how to construct a braid from a given mapping class  $\delta \in \text{MCG}(D_n)$ :

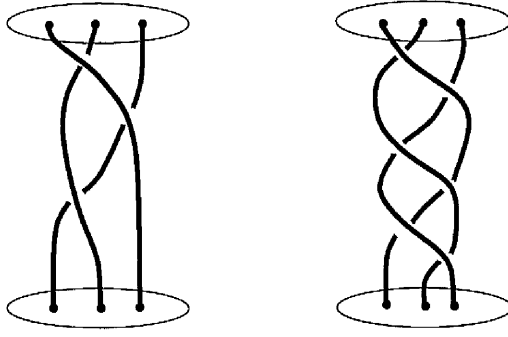


Figure 2.18: A half and full twist on a 3-punctured disk.

Let  $f \in \delta$ . Regard  $f: D^2 \rightarrow D^2$ . Then by Theorem 2.27 there exists an isotopy  $\{\gamma_t\}: D^2 \rightarrow D^2$  so that  $\gamma_0 = id: D^2 \rightarrow D^2$  and  $\gamma_1 = f: D^2 \rightarrow D^2$ . One can construct a geometric braid by taking the union,  $\bigcup_{t \in [0,1]} \gamma_t(A_n) \times \{t\}$ . Note that this construction has been made taking a particular  $\{\gamma_t\}$ . If we picked another isotopy  $\{\gamma'_t\}$ , we would obtain a different braid. However, choosing different isotopies yields braids which differ by powers of  $\theta_n$ .

Therefore, we take the quotient  $B_n / \langle \theta_n \rangle$  to get a homomorphism from  $MCG(D_n)$  to  $B_n / \langle \theta_n \rangle = B_n / Z(B_n)$ .

Now we shall explain the inverse construction of a homeomorphism from a braid.

Let  $\mathcal{B}(0, r)$  denote the ball of radius  $r$  centred on the origin in  $\mathbb{R}^2$ . Define  $f: \mathcal{B}(0, 2) \rightarrow \mathcal{B}(0, 2)$  in polar coordinates by

$$f(r, \theta) = \begin{cases} (r, \theta + \pi); & r \leq 1 \\ (r, \theta + \pi(2 - r)); & 1 \leq r \leq 2 \end{cases} \quad (2.2)$$

For  $1 \leq i \leq n - 1$  choose disks  $B_1^i \subseteq B_2^i \subseteq D_n$  which contain punctures  $i$  and  $i + 1$  and no others.

Choose a homeomorphism  $\phi_i: B_2^i \rightarrow \mathcal{B}(0, 2)$  such that  $\phi_i(B_1^i) = \mathcal{B}(0, 1)$ ,  $\phi_i(a_i) = (-1/2, 0)$  and  $\phi_i(a_{i+1}) = (1/2, 0)$ . Define  $f_i: D_n \rightarrow D_n$  by

$$f_i = \begin{cases} \phi_i^{-1} \circ f \circ \phi_i; & x \in B_2^i \\ id & x \notin B_2^i \end{cases} \quad (2.3)$$

Given  $\beta = \prod \sigma_{i_k}^{\epsilon_k}$ , the corresponding mapping class  $[f] \in MCG(D_n)$  contains the composition  $f = \bigcirc f_{i_k}^{\epsilon_k}$ . See Figure 2.19.

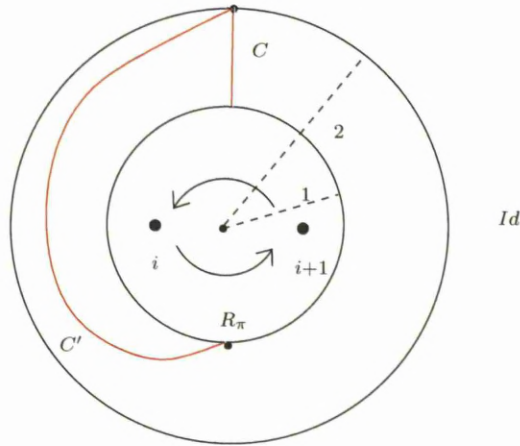


Figure 2.19:  $\sigma_i$  as a homeomorphism

**Remark 2.64.** Theorem 2.63 implies that the action of  $MCG(D_n)$  on  $\mathcal{L}_n$  defines an action of  $B_n$  on  $\mathcal{L}_n$ . However, we note the unfortunate convention for the composition of braid actions. The composition is from left to right, that is, if  $C$  is a curve and  $\beta_1, \beta_2 \in B_n$ , then  $(\beta_1\beta_2)(C) = \beta_2(\beta_1(C))$ .

Given a braid  $\beta \in B_n$ , write  $\xi(\beta)$  for the element of  $MCG(D_n)$  corresponding to  $\beta Z(B_n)$ . By Theorem 2.63, the Nielsen-Thurston classification also applies to braids:

**Definition 2.65.** A braid  $\beta \in B_n$  is *finite order*, *reducible* or *pseudo-Anosov* if  $\xi(\beta)$  is finite order, reducible or pseudo-Anosov respectively.

**Definition 2.66.** The topological entropy of  $\beta \in B_n$  is given by

$$h(\beta) = \inf_{g \in \xi(\beta)} h(g).$$

In the pseudo-Anosov case the dilatation of  $\beta$  is the dilatation of a pseudo-Anosov homeomorphism in  $\xi(\beta)$ . Hence if  $\lambda$  is the dilatation of a pseudo-Anosov braid  $\beta \in B_n$ , the topological entropy of  $\beta$  is  $\log \lambda$ .

Braids provide a convenient way to visualize the action of  $MCG(D_n)$  on  $\mathcal{L}_n$ .

**Example 2.67.** Take a simple closed curve  $C$  as depicted in Figure 2.20 and observe the action of the finite order braid  $\beta = \sigma_1\sigma_2$  (Figure 2.21) and the pseudo-Anosov braid  $\gamma = \sigma_1\sigma_2^{-1}$  (Figure 2.22 to Figure 2.25).

In the pseudo-Anosov case the iterated curve converges to the unstable measured foliation of the pseudo-Anosov automorphism in the isotopy class as described in Theorem 2.57. Naturally, it becomes increasingly difficult in time to





Figure 2.20: A simple closed curve  $C$  on  $D_3$

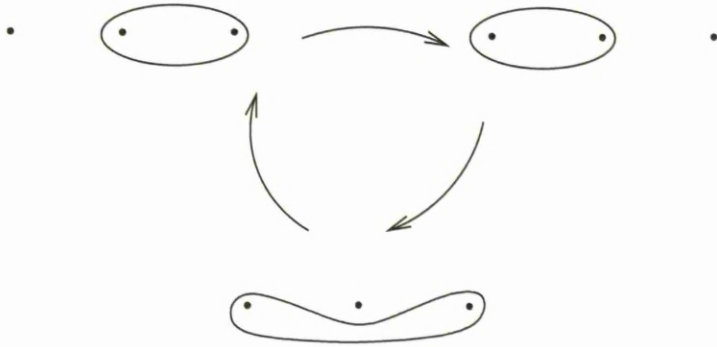


Figure 2.21:  $\beta^3(C) = C$

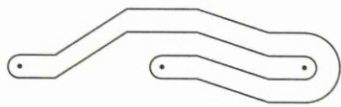


Figure 2.22:  $\gamma(C)$

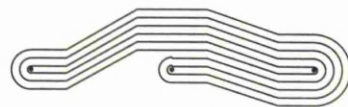


Figure 2.23:  $\gamma^2(C)$



Figure 2.24:  $\gamma^3(C)$



Figure 2.25:  $\gamma^4(C)$

track the iterations of curves under the action of pseudo-Anosov braids. The next chapter solves this problem by coordinatizing  $\mathcal{L}_n$  and giving explicit formulae for the action of the generators of  $B_n$  on  $\mathcal{L}_n$ .

## Chapter 3

# Dynnikov Coordinates

Given a surface  $M$  of genus  $g$  with  $s$  boundary components, a well known way of giving coordinates to integral laminations and measured foliations is to use either the Dehn-Thurston coordinates or train track coordinates. See [26] for details.

An alternative way to coordinatize integral laminations and measured foliations on a standard punctured disk  $D_n$  is achieved by the *Dynnikov coordinate system*. That is, Dynnikov's coordinate system provides an explicit bijection between the set of integral laminations on  $D_n$  and  $\mathbb{Z}^{2n-4} \setminus \{0\}$ ; and the set of measured foliations up to isotopy and Whitehead equivalence on  $D_n$  and  $\mathbb{R}^{2n-4} \setminus \{0\}$ . The Dynnikov coordinate system together with the Dynnikov formulae (update rules) which give the action of Artin's braid group  $B_n$  on  $\mathcal{L}_n$  in terms of Dynnikov coordinates, was introduced in [13]. Then, it was studied in [11, 12] as an efficient method for a solution of the word problem of  $B_n$ , that is, the problem of determining whether a given braid  $\beta \in B_n$ , given in terms of the Artin generators, is the identity. (Here, and throughout the thesis, we use *efficient* in an informal sense and do not carry out any formal efficiency analysis.)

Later, Moussafer used Dynnikov coordinates in [25] and introduced a method which gives an estimate for the topological entropy of braids. We shall explain his method briefly in Chapter 4.

Our method to compute the topological entropy of families of pseudo-Anosov braids which we shall introduce in Chapter 4 also uses Dynnikov coordinates and is inspired by Moussafer's technique.

This chapter provides background material for Chapter 4 and contains a detailed study of triangle coordinates, the Dynnikov coordinate system and update rules for Artin braid generators [13, 11, 12]. One difference when discussing update rules will be that, in the cited papers  $B_n$  acts on  $D_{n+2}$  whereas here,  $B_n$  acts on  $D_n$ . The reason for this is the following:

For the solution of the word problem using the Dynnikov coordinates, one chooses an integral lamination which is changed under the action of any non-identity braid. There is no such lamination on  $D_n$  as if we take any “innermost curve”, it bounds a punctured disk, and any action on that disk doesn’t affect the lamination.

Theorem 3.19 gives the inverse of the Dynnikov coordinate function. That is, it gives a formula that describes integral laminations from given Dynnikov coordinates. We shall prove this theorem and therefore show that the Dynnikov coordinates coordinatize integral laminations. We note that this theorem has not appeared in the literature before. We shall then give an identical theorem for measured foliations.

In Section 3.2 we shall use this theorem to give a recipe which gives the geometric intersection number of an integral lamination  $\mathcal{L} \in \mathcal{L}_n$  with a particular type of integral lamination, known as a *relaxed integral lamination*. This provides a way to find the geometric intersection number of two arbitrary integral laminations when combined with an algorithm of Dynnikov and Wiest [14]. This algorithm takes an arbitrary integral lamination  $\mathcal{L}$  and finds an  $n$ -braid  $\beta$  such that  $\beta(\mathcal{L})$  is relaxed. That is the algorithm *relaxes* integral laminations.

Because Dynnikov coordinates give a bijection between  $\mathcal{L}_n \cup \{\emptyset\}$  (where  $\emptyset$  corresponds to the “empty lamination”) and  $\mathbb{Z}^{2n-4}$ , they endow  $\mathcal{L}_n \cup \{\emptyset\}$  with an abelian group structure. In Section 3.3 we shall introduce and discuss the interpretation of the group operation on  $\mathcal{L}_n \cup \{\emptyset\}$ .

In Section 3.4 update rules for Artin braid generators are derived and in Section 3.5 update rules for some sequences of Artin braid generators are given which are also new and will be used in the proof of the results in Chapter 4.

Finally, in Section 3.6 Dynnikov coordinates will be extended to measured foliations.

### 3.1 Dynnikov coordinates of integral laminations and measured foliations

The aim of this section is to describe the Dynnikov coordinate system for the set of integral laminations  $\mathcal{L}_n$  and prove that there is an explicit bijection between  $\mathcal{L}_n$  and  $\mathbb{Z}^{2n-4} \setminus \{0\}$ . We shall begin with the triangle coordinates which describe each integral lamination by an element of  $\mathbb{Z}^{3n-5}$  using its geometric intersection number with given  $3n - 5$  embedded arcs in  $D_n$ . *Dynnikov coordinates* [13] are certain linear combinations of these integers and yield a one-to-one correspondence between  $\mathcal{L}_n$  and  $\mathcal{C}_n = \mathbb{Z}^{2n-4} \setminus \{0\}$ . This will be proved by Theorem 3.19

which gives the inversion of Dynnikov coordinates. The results of this section will then be extended naturally to measured foliations in Section 3.6.

Let  $\mathcal{A}_n$  be the set of arcs in  $D_n$  which have each endpoint either on the boundary or at a puncture. Consider the arcs  $\alpha_i \in \mathcal{A}_n$  ( $1 \leq i \leq 2n - 4$ ) and  $\beta_i \in \mathcal{A}_n$  ( $1 \leq i \leq n - 1$ ) as depicted in Figure 3.1: the arcs  $\alpha_{2i-3}$  and  $\alpha_{2i-2}$  (for  $2 \leq i \leq n - 1$ ) join the  $i^{\text{th}}$  puncture to the boundary, while the arc  $\beta_i$  has both endpoints on the boundary and passes between the  $i^{\text{th}}$  and  $i + 1^{\text{th}}$  punctures.

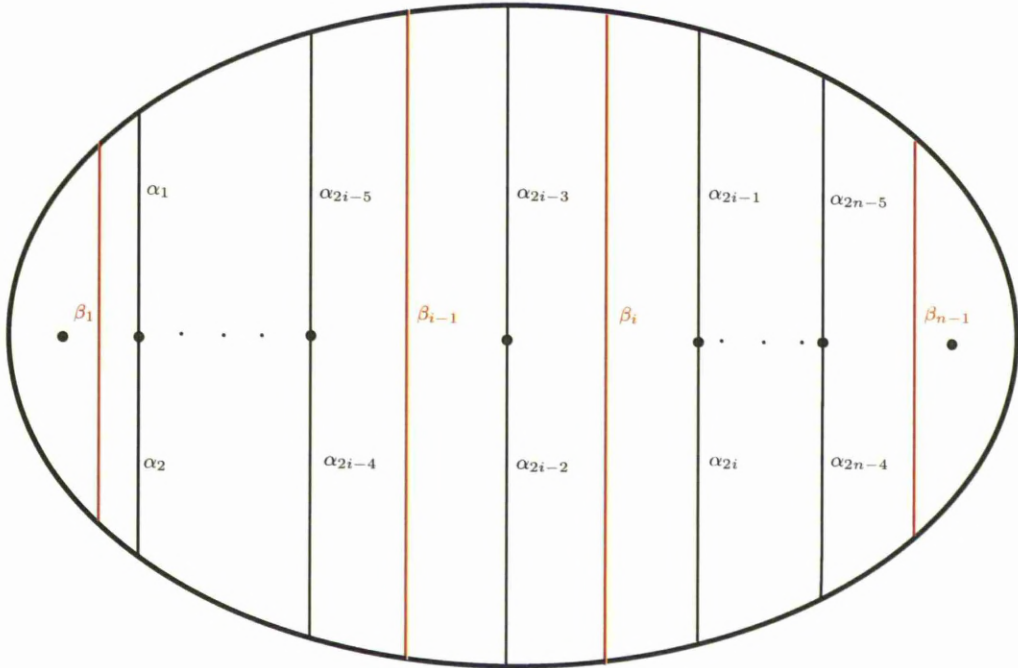


Figure 3.1: The arcs  $\alpha_i$  and  $\beta_i$

Observe that the arcs divide the disk into  $2n - 2$  (closed) regions and  $2n - 4$  of these are *triangular*: Identifying the outer boundary of the disk with a point, each region on the left and right side of the  $i^{\text{th}}$  puncture for  $2 \leq i \leq n - 1$  is a triangle since it is bounded by three arcs.

The two triangles  $\Delta_{2i-3}$  and  $\Delta_{2i-2}$  on the left and right side of the  $i^{\text{th}}$  puncture are defined by the arcs  $\alpha_{2i-3}$ ,  $\alpha_{2i-2}$ ,  $\beta_{i-1}$  and  $\alpha_{2i-3}$ ,  $\alpha_{2i-2}$ ,  $\beta_i$  respectively. The two end regions  $\Delta_0$  and  $\Delta_{2n-3}$  are bounded by  $\beta_1$  and  $\beta_{n-1}$  respectively. See Figure 3.2.

A naive way to describe integral laminations is achieved by triangle coordinates: Given  $[\alpha]$  (the isotopy class of an arc  $\alpha \in \mathcal{A}_n$  under isotopies through  $\mathcal{A}_n$ ) and an integral lamination  $\mathcal{L}$ , we write  $S(\mathcal{L}, [\alpha])$  for the geometric intersection number of  $\mathcal{L} \in \mathcal{L}_n$  with the arc  $\alpha \in \mathcal{A}_n$ .

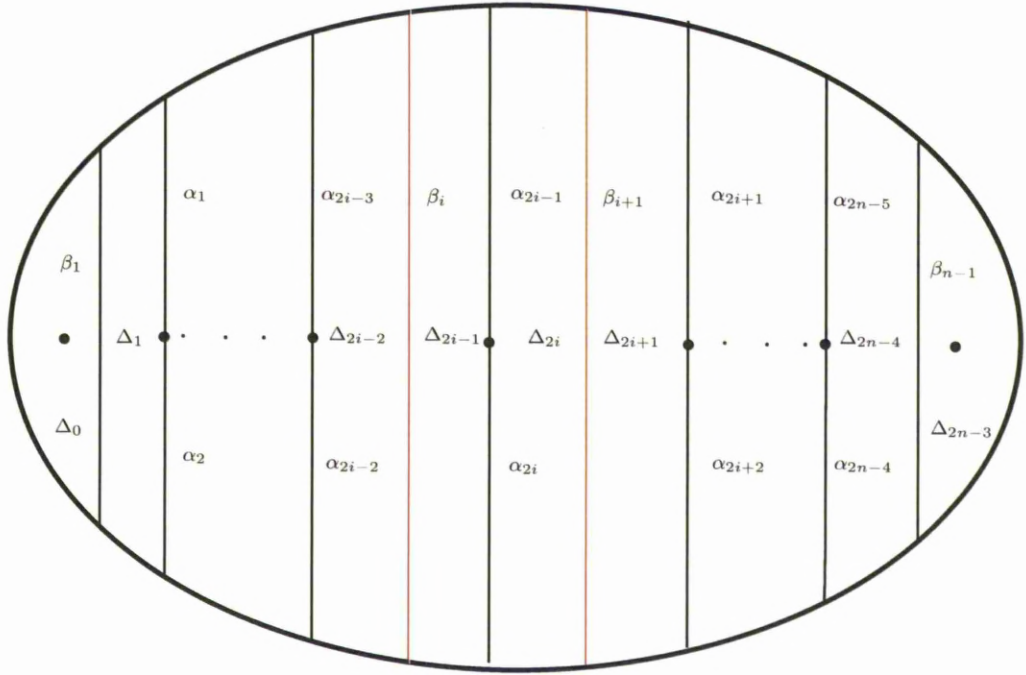


Figure 3.2:  $\beta_i$  and  $\beta_{i+1}$  bound  $S_i = \Delta_{2i-1} \cup \Delta_{2i}$

**Remark 3.1.** We note that if  $\mathcal{L} \in \mathcal{L}_n$  there is some curve system  $L \in \mathcal{L}$  which is *taut* (has minimum number of intersections in its homotopy class with each  $\alpha_i$  and  $\beta_i$ ). We fix a taut representative  $L$  of a given integral lamination  $\mathcal{L} \in \mathcal{L}_n$  throughout.

**Definition 3.2.** The triangle coordinate function  $\tau : \mathcal{L}_n \rightarrow \mathbb{Z}_{\geq 0}^{3n-5}$  is defined by

$$\tau(\mathcal{L}) = (S(\mathcal{L}, [\alpha_1]), \dots, S(\mathcal{L}, [\alpha_{2n-4}]), S(\mathcal{L}, [\beta_1]), \dots, S(\mathcal{L}, [\beta_{n-1}])).$$

From now on we shall simply write  $\alpha$  for  $S(\mathcal{L}, [\alpha])$ . It will always be clear from the context whether we mean the arc or the geometric intersection number assigned on the arc.

**Example 3.3.** The triangle coordinates of the integral lamination  $\mathcal{L}$  in Figure 3.3 are given by  $\tau(\mathcal{L}) = (\alpha_1, \alpha_2, \alpha_3, \alpha_4, \alpha_5, \alpha_6; \beta_1, \beta_2, \beta_3, \beta_4) = (2, 6, 3, 5, 4, 4; 4, 8, 8, 4)$ .

**Definitions 3.4.** For each  $i$  with  $1 \leq i \leq n-2$ , define  $S_i = \Delta_{2i-1} \cup \Delta_{2i}$  (see Figure 3.2). A *path component* of  $L$  in  $S_i$  is a component of  $L \cap S_i$ . There are four types of path components in  $S_i$ . An *above component* has end points on  $\beta_i$  and  $\beta_{i+1}$  and passes across  $\alpha_{2i-1}$ . A *below component* has end points on  $\beta_i$  and  $\beta_{i+1}$  and passes across  $\alpha_{2i}$ . A *left loop component* has both end points on  $\beta_{i+1}$  and a *right loop component* has both end points on  $\beta_i$ .

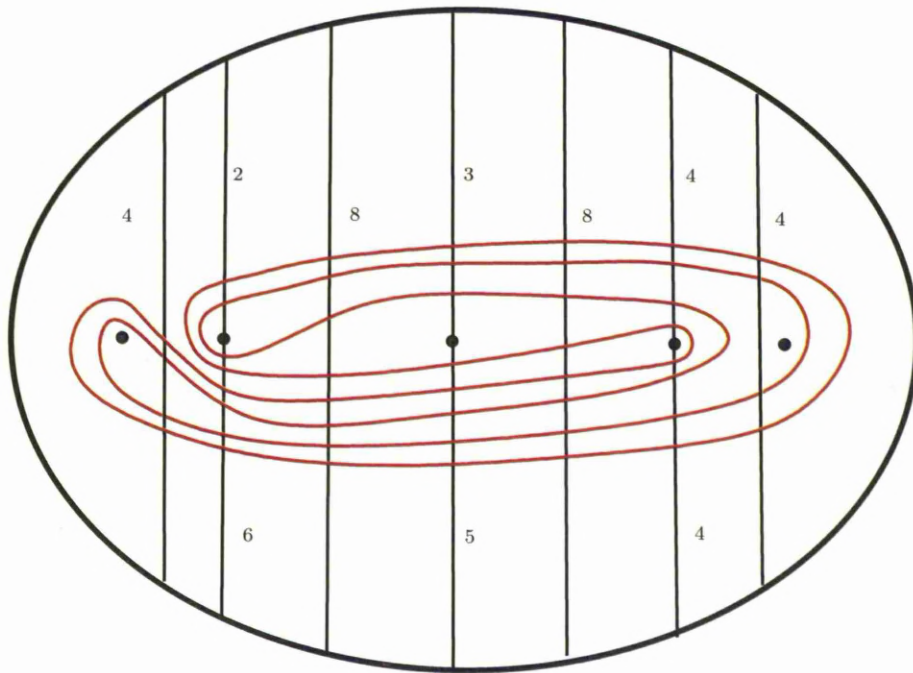


Figure 3.3: Triangle coordinates of an integral lamination

The green lines in Figure 3.4 depict the above and below components. Left and right loop components are depicted blue. Note that there is one type of path component in the end regions: *left loop components* in region  $\Delta_0$  and *right loop components* in region  $\Delta_{2n-3}$ .

**Remark 3.5.** We note that there could only be one of the two types of loop components (i.e. right or left) in each  $S_i$  since the curves in  $L$  are mutually disjoint.

**Definitions 3.6.** For each  $1 \leq i \leq n - 2$  we define

$$b_i = \frac{\beta_i - \beta_{i+1}}{2}. \quad (3.1)$$

Then  $|b_i|$  gives the number of loop components in  $S_i$  and  $\epsilon_i = \text{sgn}(b_i)$  tells whether the loop components are left or right. That is, when  $b_i > 0$  the loop components are right and when  $b_i < 0$  the loop components are left.

See Figure 3.4. On the left,  $\beta_{i+1} = \beta_i + 2$  (so  $b_i = -1$ ) and the additional two intersections of  $L$  with  $\beta_{i+1}$  yield one left loop component. Similarly, on the right  $\beta_i = \beta_{i+1} + 4$  (so  $b_i = 2$ ) and the additional four intersections of  $L$  with  $\beta_i$  yield two right loop components.

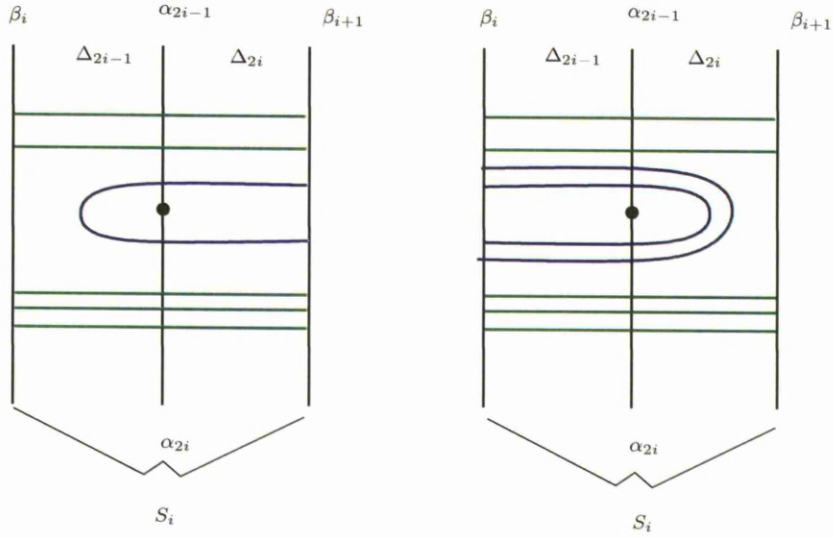


Figure 3.4: Above, below, left loop and right loop components

The following Lemma is obvious since each above and below component intersects  $\alpha_{2i-1}$  and  $\alpha_{2i}$  respectively.

**Lemma 3.7.** *The numbers of above and below components in region  $S_i$  are given by  $\alpha_{2i-1} - |b_i|$  and  $\alpha_{2i} - |b_i|$  respectively.*

Similarly, the next Lemma is obvious from Figure 3.5 and Figure 3.6.

**Lemma 3.8.** *There are equalities for each  $S_i$ :*

*When there are left loop components ( $b_i < 0$ ),*

$$\alpha_{2i} + \alpha_{2i-1} = \beta_{i+1} \quad (3.2)$$

$$\alpha_{2i} + \alpha_{2i-1} - \beta_i = 2|b_i|, \quad (3.3)$$

*when there are right loop components ( $b_i > 0$ ),*

$$\alpha_{2i} + \alpha_{2i-1} = \beta_i \quad (3.4)$$

$$\alpha_{2i} + \alpha_{2i-1} - \beta_{i+1} = 2|b_i|, \quad (3.5)$$

*and when there are no loop components ( $b_i = 0$ ),*

$$\alpha_{2i} + \alpha_{2i-1} = \beta_i = \beta_{i+1}. \quad (3.6)$$

Note that Lemma 3.8 implies that some coordinates are redundant.

**Example 3.9.** Let  $(4, 6, 4, 6, 3, 7, 2, 6, 1, 3; 10, 10, 10, 8, 4, 2)$  be the triangle coordinates of an integral lamination  $\mathcal{L} \in \mathcal{L}_7$  as depicted in Figure 3.7. We shall show

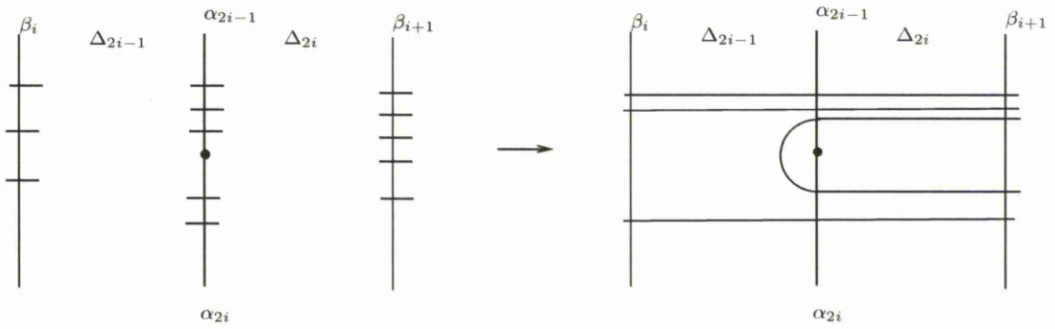


Figure 3.5: Left loop components and the case is  $b_i \leq 0$

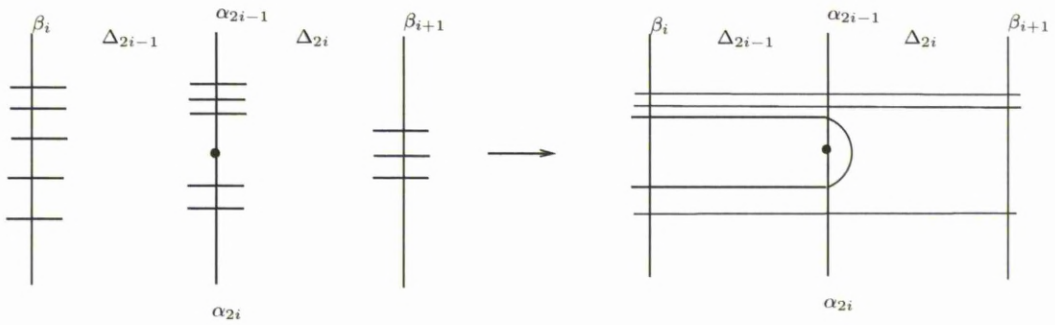


Figure 3.6: Right loop components and the case is  $b_i \geq 0$

how we draw  $\mathcal{L}$  from the given triangle coordinates. First, we find the loop components and then the number of above and below components using Lemma 3.7 in each region  $S_i = \Delta_{2i-1} \cup \Delta_{2i}$ .

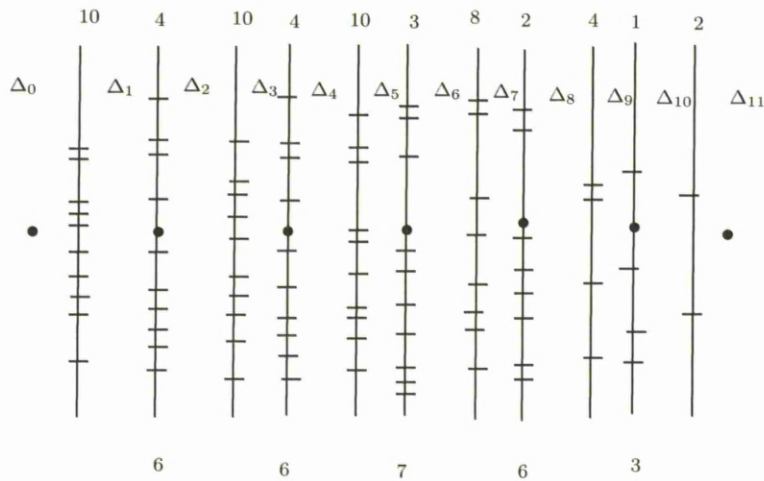


Figure 3.7: Triangle Coordinates of  $\mathcal{L}$

In  $\Delta_0$  there are clearly 5 loop components, and in  $\Delta_{11}$  there is 1 loop com-



ponent.

Since  $\beta_1 = \beta_2$  and  $\beta_2 = \beta_3$  ( $b_1 = 0, b_2 = 0$ ) there are no loop components in region  $S_1$  and  $S_2$ .

We have

$$b_3 = \frac{\beta_3 - \beta_4}{2} = \frac{10 - 8}{2} = 1.$$

Since  $|b_3| = 1$  and  $\text{sgn}(b_3) = +1$ , there is one right loop in region  $S_3$ .

We have,

$$b_4 = \frac{\beta_4 - \beta_5}{2} = \frac{8 - 4}{2} = 2.$$

Since,  $|b_4| = 2$  and  $\text{sgn}(b_4) = +1$ , there are two right loop components in region  $S_4$ .

We have

$$b_5 = \frac{\beta_5 - \beta_6}{2} = \frac{4 - 2}{2} = 1.$$

Since,  $|b_5| = 1$  and  $\text{sgn}(b_4) = +1$ , there is one right loop in region  $S_5$  (Figure 3.8).

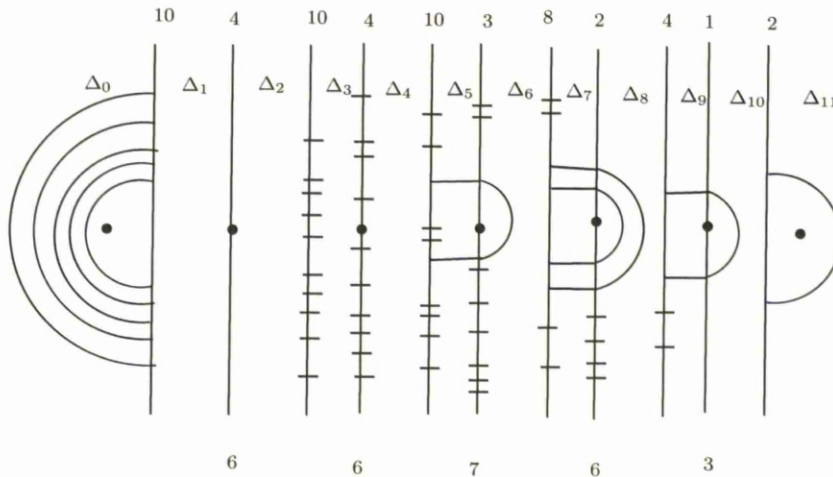


Figure 3.8: Determining loop components

Now we can find the above and below components in each region  $S_i$  by Lemma 3.7. We have  $\alpha_1 - b_1 = 4 - 0 = 4$ ,  $\alpha_2 - b_1 = 6 - 0 = 6$ . Then the number of above and below components in  $S_1$  is 4 and 6 respectively. We have  $\alpha_3 - b_2 = 4 - 0 = 4$ ,  $\alpha_4 - b_2 = 6 - 0 = 6$ . Then the number of above and below components in  $S_2$  is 4 and 6 respectively. Since  $\alpha_5 - b_3 = 3 - 1 = 2$ ,  $\alpha_6 - b_3 = 7 - 1 = 6$ , the number of above and below components in  $S_3$  is 2 and 6 respectively. Similarly, we find that there is no above component and four below components in  $S_4$ . Finally, there is no above component and two below components in  $S_5$ . We get Figure 3.9 which yields Figure 3.10.

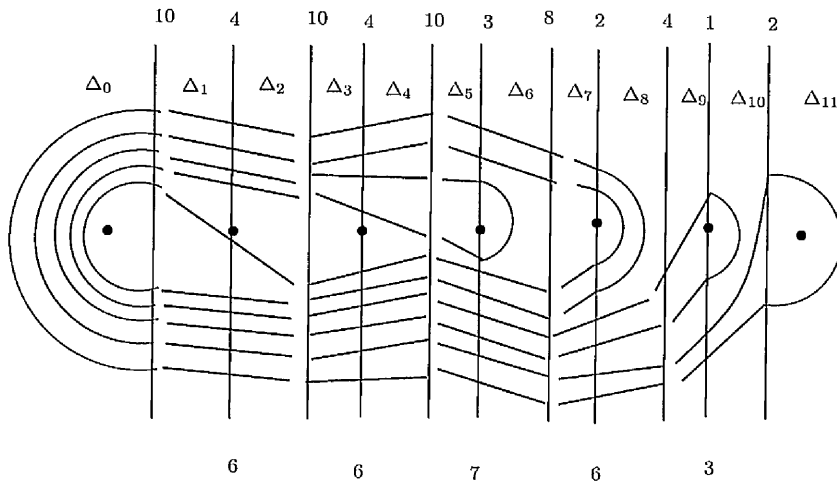


Figure 3.9: Connecting path components in each  $S_i$

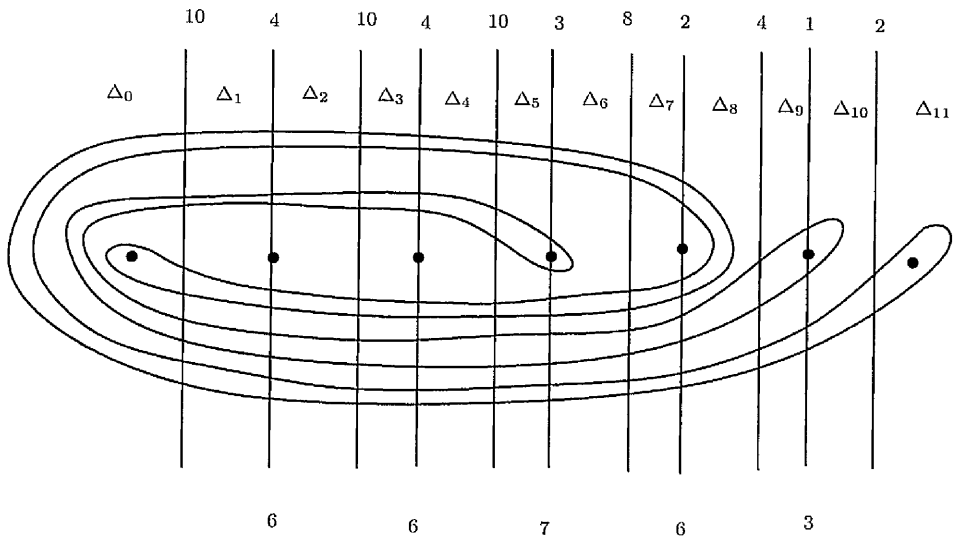


Figure 3.10:  $(4, 6, 4, 6, 3, 7, 2, 6, 1, 3; 10, 10, 10, 8, 4, 2)$  gives  $\mathcal{L} \in \mathcal{L}_n$

**Lemma 3.10.** *The triangle coordinate function  $\tau : \mathcal{L}_n \rightarrow \mathbb{Z}_{\geq 0}^{3n-5}$  is injective.*

*Proof.* Working in each region  $S_i$  as in Example 3.9 we can determine the number of above, below and right/left loop components. Therefore, the path components in each  $S_i$  are connected in a unique way up to isotopy and hence  $\mathcal{L}$  is determined uniquely.  $\square$

We have seen that the triangle coordinate function  $\tau : \mathcal{L}_n \rightarrow \mathbb{Z}_{\geq 0}^{3n-5}$  is injective. However, is it always possible to construct an integral lamination from given triangle coordinates? Namely, is  $\tau : \mathcal{L}_n \rightarrow \mathbb{Z}_{\geq 0}^{3n-5}$  surjective?

The answer to this question is “no” since  $\tau(\mathcal{L})$  must satisfy the triangle inequality in each of the strips of Figure 3.1, as well as additional conditions such as the equalities in Lemma 3.8. The next few examples will illustrate some cases where an element of  $\mathbb{Z}_{\geq 0}^{3n-5}$  is not the triangle coordinates of any element of  $\mathcal{L}_n$ .

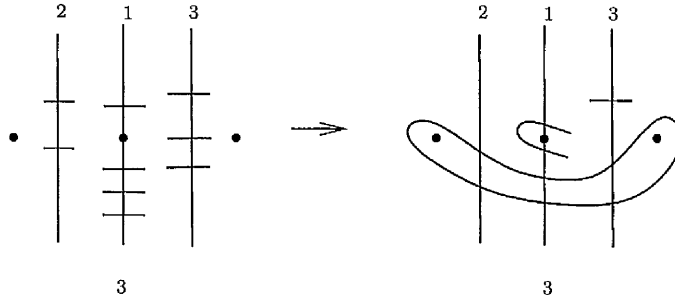


Figure 3.11:  $\beta_2$  is odd

**Example 3.11.** Is it possible to construct an integral lamination  $\mathcal{L} \in \mathcal{L}_3$  with  $(\alpha_1, \alpha_2, \beta_1, \beta_2) = (1, 3, 2, 3)$ ?

No, it isn't. Observe that  $\beta_2$  is odd and every taut simple closed curve must intersect  $\beta_2$  an even number of times (Figure 3.11).

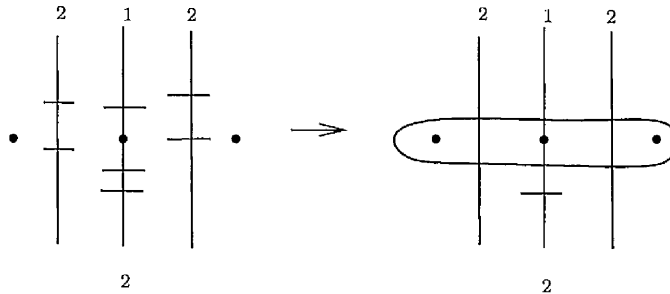


Figure 3.12:  $\alpha_1 + \alpha_2$  is odd

**Example 3.12.** Is it possible to construct an integral lamination  $\mathcal{L} \in \mathcal{L}_3$  with  $(\alpha_1, \alpha_2, \beta_1, \beta_2) = (1, 2, 2, 2)$ ?

No, it isn't.  $\alpha_2 + \alpha_1$  is odd: Observe that every taut simple closed curve must intersect  $\alpha_1 \cup \alpha_2$  an even number of times (Figure 3.12).

**Example 3.13.** Is it possible to construct an integral lamination  $\mathcal{L} \in \mathcal{L}_3$  with  $(\alpha_1, \alpha_2, \beta_1, \beta_2) = (1, 1, 2, 4)$ ?

No, it isn't. The triangle inequality is not satisfied in  $\Delta_2$ :  $\beta_2 > \alpha_1 + \alpha_2$  (Figure 3.13).

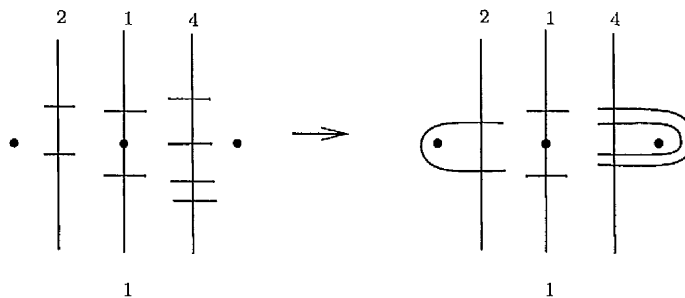


Figure 3.13:  $\alpha_1 + \alpha_2 < \beta_2$

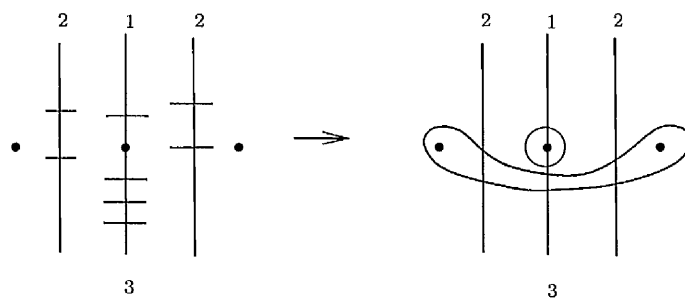


Figure 3.14:  $\beta_1 = \beta_2$  and  $\alpha_2 + \alpha_1 > \beta_1$

If a set of coordinates is not incompatible in any of the ways shown in examples 3.11, 3.12 and 3.13 — that is, if each  $\beta_i$  is even, each  $\alpha_{2i} + \alpha_{2i-1}$  is even, and the triangle inequalities are satisfied in each region — then it is possible to construct a curve system with these triangle coordinates. However, this system of curves may not necessarily be an integral lamination as the following examples illustrate.

**Example 3.14.** Is it possible to construct an integral lamination  $\mathcal{L} \in \mathcal{L}_3$  with  $(\alpha_1, \alpha_2, \beta_1, \beta_2) = (1, 3, 2, 2)$ ?

No, it isn't. Since  $\beta_1 = \beta_2$  and  $\alpha_2 + \alpha_1 > \beta_1$ , Lemma 3.8 isn't satisfied (Figure 3.14).

In fact it is possible to draw a curve system whose minimal intersection with the arcs is given by these coordinates, but it contains a curve that bounds a puncture and therefore is not a representative of an integral lamination.

**Example 3.15.** Is it possible to construct an integral lamination  $\mathcal{L} \in \mathcal{L}_3$  with  $(\alpha_1, \alpha_2, \beta_1, \beta_2) = (1, 1, 2, 2)$ ?

No, it isn't. Even though Lemma 3.8 is satisfied, the resulting simple closed curve is not essential. Observe that connecting the path components in  $S_1$  and the two end regions yields a curve parallel to  $\partial D_n$  (Figure 3.15).

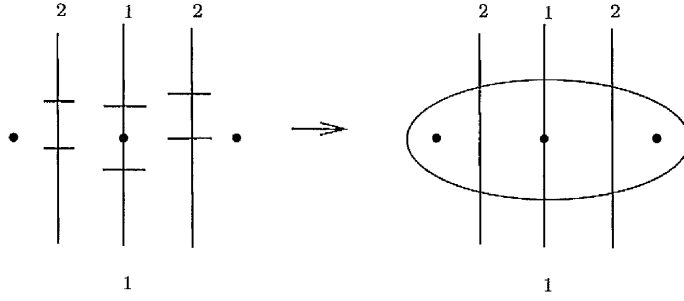


Figure 3.15:  $\beta_1 = \beta_2$  and  $\alpha_2 + \alpha_1 = \beta_1$

Next, we shall discuss what properties an integral lamination  $\mathcal{L} \in \mathcal{L}_n$  satisfies in terms of its triangle coordinates and construct a new coordinate system from the triangle coordinates which describes integral laminations in a unique way. Namely, we shall describe the *Dynnikov coordinate system*.

Given a taut representative  $L$  of  $\mathcal{L} \in \mathcal{L}_n$  one can initially observe the following:

- Remarks 3.16.**
- i. Every component of  $L$  intersects each  $\beta_i$  an even number of times. Also recall that the number of loop components in  $S_i$  is given as in Definitions 3.6. That is,  $b_i = \frac{\beta_i - \beta_{i+1}}{2}$  and  $|b_i|$  gives the number of loop components in  $S_i$ . When  $b_i > 0$  the loop components are right and when  $b_i < 0$  the loop components are left (Figure 3.16).
  - ii. Set  $x_i = |\alpha_{2i} - \alpha_{2i-1}|$  and  $m_i = \min\{\alpha_{2i-1} - |b_i|, \alpha_{2i} - |b_i|\}$ ;  $1 \leq i \leq n-2$ . Then  $x_i$  gives the difference between the number of above and below components in  $S_i$ , and  $m_i$  gives the smaller of these two numbers by Lemma 3.7 (Figure 3.16). We note that  $x_i$  is even since each simple closed curve in  $L$  intersects  $\alpha_{2i} \cup \alpha_{2i-1}$  an even number of times.
  - iii. Set  $2a_i = \alpha_{2i} - \alpha_{2i-1}$ ;  $1 \leq i \leq n-2$ , ( $a_i$  is an integer since  $|a_i| = \frac{x_i}{2}$ ). Assume that  $b_i \geq 0$ . Then,  $\beta_i = \alpha_{2i} + \alpha_{2i-1}$  by Lemma 3.8. Since  $2a_i = \alpha_{2i} - \alpha_{2i-1}$  it follows that

$$\alpha_{2i} = a_i + \frac{\beta_i}{2}; \quad \text{and} \quad \alpha_{2i-1} = -a_i + \frac{\beta_i}{2}.$$

A similar calculation for  $b_i \leq 0$  gives

$$\alpha_{2i} = a_i + \frac{\beta_{i+1}}{2}; \quad \text{and} \quad \alpha_{2i-1} = -a_i + \frac{\beta_{i+1}}{2}.$$

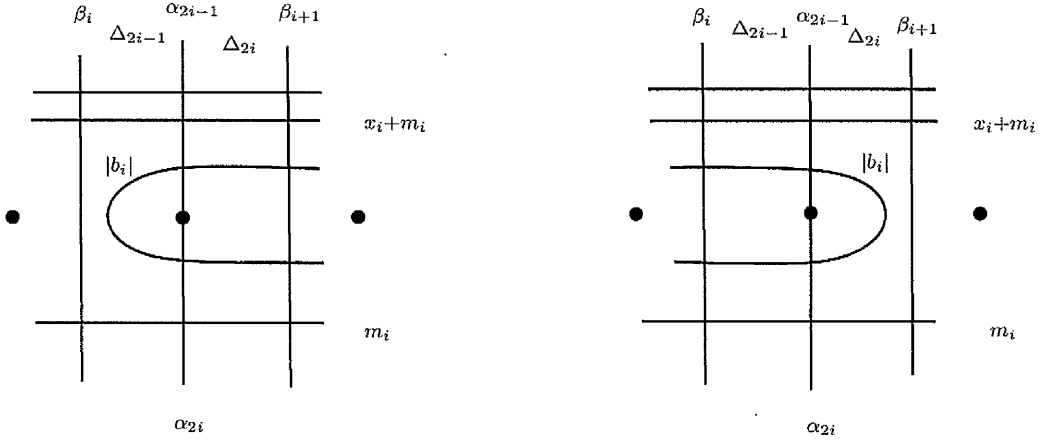


Figure 3.16: Number of above and below components in  $S_i$

That is to say:

$$\alpha_i = \begin{cases} (-1)^i a_{\lceil i/2 \rceil} + \frac{\beta_{\lceil i/2 \rceil}}{2} & \text{if } b_{\lceil i/2 \rceil} \geq 0; \\ (-1)^i a_{\lceil i/2 \rceil} + \frac{\beta_{1+\lceil i/2 \rceil}}{2} & \text{if } b_{\lceil i/2 \rceil} \leq 0 \end{cases}$$

where  $\lceil x \rceil$  denotes the smallest integer which is not less than  $x$ .

iv. From item ii. and item iii., it is straightforward to compute  $\beta_i$ ;  $1 \leq i \leq n-1$ .

$$\beta_i = \begin{cases} 2m_i + 2|a_i| & \text{if } b_i \leq 0; \\ 2m_i + 2|a_i| + 2b_i & \text{if } b_i \geq 0. \end{cases} \quad (3.7)$$

That is,

$$\beta_i = 2[|a_i| + \max(b_i, 0) + m_i].$$

Since  $\beta_i = \beta_1 - 2 \sum_{j=1}^{i-1} b_j$  by (3.1),

$$\beta_1 = 2 \left[ |a_i| + \max(b_i, 0) + m_i + \sum_{j=1}^{i-1} b_j \right] \quad \text{for } 1 \leq i \leq n-2.$$

v. A crucial observation is that  $m_i = 0$  for some  $1 \leq i \leq n-1$  since otherwise there would be both above and below components in each  $S_i$  and hence the integral lamination would have a curve parallel to  $\partial D_n$ . Then,

When  $m_i = 0$ ;

$$\beta_1 = 2 \left[ |a_i| + \max(b_i, 0) + \sum_{j=1}^{i-1} b_j \right].$$

When  $m_i > 0$ ;

$$\beta_1 > 2 \left[ |a_i| + \max(b_i, 0) + \sum_{j=1}^{i-1} b_j \right].$$

Therefore,

$$\beta_1 = \max_{1 \leq k \leq n-2} 2 \left[ |a_k| + \max(b_k, 0) + \sum_{j=1}^{k-1} b_j \right].$$

We have seen that  $\alpha_i$  and  $\beta_i$  have been recovered from  $a_i$  and  $b_i$  where

$$a_i = \frac{\alpha_{2i} - \alpha_{2i-1}}{2} \quad \text{and} \quad b_i = \frac{\beta_i - \beta_{i+1}}{2}.$$

Now, we are ready to define the *Dynnikov coordinate system* which has the advantage to coordinatize  $\mathcal{L}_n$  bijectively and with the least number of coordinates.

**Definition 3.17.** The *Dynnikov coordinate function*  $\rho : \mathcal{L}_n \rightarrow \mathbb{Z}^{2n-4} \setminus \{0\}$  is defined by

$$\rho(\mathcal{L}) = (a, b) = (a_1, \dots, a_{n-2}, b_1, \dots, b_{n-2}),$$

where for  $1 \leq i \leq n-2$

$$a_i = \frac{\alpha_{2i} - \alpha_{2i-1}}{2} \quad \text{and} \quad b_i = \frac{\beta_i - \beta_{i+1}}{2} \quad (3.8)$$

Let  $\mathcal{C}_n = \mathbb{Z}^{2n-4} \setminus \{0\}$  denote the space of Dynnikov coordinates of integral laminations on  $D_n$ .

**Example 3.18.** The Dynnikov coordinates of the integral lamination  $\mathcal{L}$  in Figure 3.3 are given by  $\rho(\mathcal{L}) = (2, 1, 0, -2, 0, 2)$ . We have,

$$\begin{aligned}
\alpha_1 &= 2, & \beta_1 &= 2, & a_1 &= \frac{\alpha_2 - \alpha_1}{2} = \frac{6 - 2}{2} = 2 \\
\alpha_2 &= 6, & \beta_2 &= 8, & a_2 &= \frac{\alpha_4 - \alpha_3}{2} = \frac{5 - 3}{2} = 1 \\
\alpha_3 &= 3, & \beta_3 &= 8, & a_3 &= \frac{\alpha_5 - \alpha_6}{2} = \frac{4 - 4}{2} = 0 \\
\alpha_4 &= 5, & \beta_4 &= 4, & b_1 &= \frac{\beta_1 - \beta_2}{2} = \frac{4 - 8}{2} = -2 \\
\alpha_5 &= 4, & & & b_2 &= \frac{\beta_2 - \beta_3}{2} = \frac{8 - 8}{2} = 0 \\
\alpha_6 &= 4, & & & b_3 &= \frac{\beta_3 - \beta_4}{2} = \frac{8 - 4}{2} = 2.
\end{aligned}$$

Note that  $b_i$  can easily be read off from a picture of the lamination by counting the number of loop components and checking whether they are left or right. For example, there are two left loop components in  $S_1$ , therefore  $b_1$  should be  $-2$ .

**Theorem 3.19** (Inversion of Dynnikov coordinates). *Let  $(a, b) \in \mathcal{C}_n$ . Then  $(a, b)$  is the Dynnikov coordinate of exactly one element  $\mathcal{L}$  of  $\mathcal{L}_n$ , which has*

$$\beta_i = 2 \max_{1 \leq k \leq n-2} \left[ |a_k| + \max(b_k, 0) + \sum_{j=1}^{k-1} b_j \right] - 2 \sum_{j=1}^{i-1} b_j \quad (3.9)$$

$$\alpha_i = \begin{cases} (-1)^i a_{\lceil i/2 \rceil} + \frac{\beta_{\lceil i/2 \rceil}}{2} & \text{if } b_{\lceil i/2 \rceil} \geq 0; \\ (-1)^i a_{\lceil i/2 \rceil} + \frac{\beta_{1+\lceil i/2 \rceil}}{2} & \text{if } b_{\lceil i/2 \rceil} \leq 0 \end{cases} \quad (3.10)$$

where  $\lceil x \rceil$  denotes the smallest integer which is not less than  $x$ .

*Proof.*  $\rho$  is injective: Let  $\mathcal{L} \in \mathcal{L}_n$ , with  $\tau(\mathcal{L}) = (\alpha, \beta)$  and  $\rho(\mathcal{L}) = (a, b)$ . We showed in Remarks 3.16 that  $(\alpha, \beta)$  must be given by (3.9) and (3.10). Hence there is no other  $\mathcal{L}' \in \mathcal{L}_n$  with  $\rho(\mathcal{L}') = (a, b)$  by Lemma 3.10.

$\rho$  is surjective: Let  $(a, b) \in \mathcal{C}_n$ . We will show that  $(\alpha, \beta)$  defined by (3.9) and (3.10) are the triangle coordinates of some  $\mathcal{L} \in \mathcal{L}_n$  which has  $\rho(\mathcal{L}) = (a, b)$ . It is clear that if there is some  $\mathcal{L}$  with  $\tau(\mathcal{L}) = (\alpha, \beta)$ , then  $\rho(\mathcal{L}) = (a, b)$ . By the construction in Remarks 3.16, it is possible to draw in each  $S_i$ ,  $1 \leq i \leq n-2$  some non-intersecting path components which intersect  $\beta_i, \alpha_{2i-1}, \alpha_{2i}$ , and  $\beta_{i+1}$  the number of times given by  $(\alpha, \beta)$ . Joining these components (and completing in the only way in the two end regions) gives a system of mutually disjoint simple closed curves in  $D_n$ . There are no curves that bound punctures as every path



component of a curve system has the property that its intersection with each  $S_i$  is of one of the four types by construction, so in particular there can't be a curve that bounds a puncture. There are no curves parallel to  $\partial D_n$  as some  $m_i$  is equal to zero. Hence this is an integral lamination which has triangle coordinates  $(\alpha, \beta)$  as required.  $\square$

In the next section we shall give a formula to compute the geometric intersection number of a given integral lamination  $\mathcal{L} \in \mathcal{L}_n$  with a given *relaxed curve* [14]  $C_{ij}$  in  $D_n$  in terms of triangle coordinates. Furthermore, the formula can be given in terms of Dynnikov coordinates by Theorem 3.19.

### 3.2 Geometric intersection of integral laminations with relaxed curves

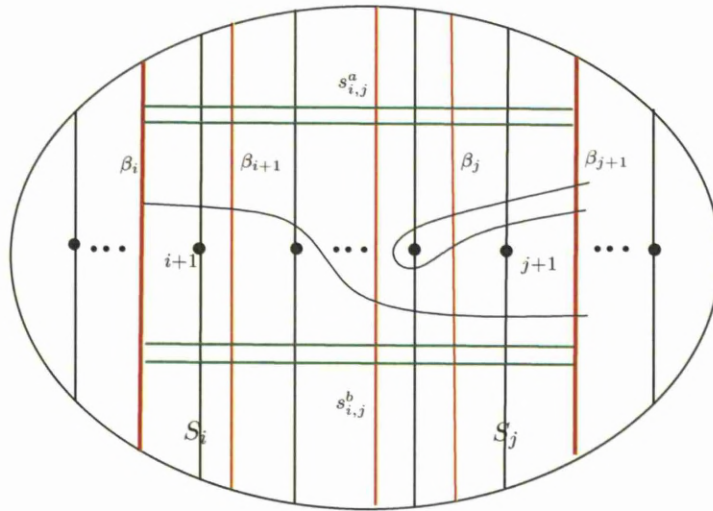


Figure 3.17:  $s_{i,j}^a$  and  $s_{i,j}^b$

**Definition 3.20.** Let  $S_{i,j} = \bigcup_{i \leq k \leq j} S_k$ . A *path component* of  $L$  in  $S_{i,j}$  is a component of  $L \cap S_{i,j}$ . An *above component* in  $S_{i,j}$  has end points on  $\beta_i$  and  $\beta_{j+1}$  and does not intersect any  $\alpha_{2k}$  with  $i \leq k \leq j$ . A *below component* in  $S_{i,j}$  has end points on  $\beta_i$  and  $\beta_{j+1}$  and does not intersect any  $\alpha_{2k-1}$  with  $i \leq k \leq j$  (Figure 3.17).

Using Lemma 3.7 one can compute the number of above and below components in  $S_{i,j}$ .

**Lemma 3.21.** *The number of above and below components in  $S_{i,j}$  is given by*

$$s_{i,j}^a = \min_{i \leq k \leq j} \{\alpha_{2k-1} - |b_k|\} \quad \text{and} \quad s_{i,j}^b = \min_{i \leq k \leq j} \{\alpha_{2k} - |b_k|\}$$

*respectively. Therefore the sum  $s_{i,j} = s_{i,j}^a + s_{i,j}^b$  gives the number of above and below components in  $S_{i,j}$ .*

*Proof.* For each  $1 \leq k \leq n-2$ ,  $s_k^a = \alpha_{2k-1} - |b_k|$  and  $s_k^b = \alpha_{2k} - |b_k|$  by Lemma 3.7.

Then  $s_{i,j}^b = \min_{i \leq k \leq j} \{s_k^b\}$  and  $s_{i,j}^a = \min_{i \leq k \leq j} \{s_k^a\}$ . Hence,

$$s_{i,j} = \min_{i \leq k \leq j} \{s_k^a\} + \min_{i \leq k \leq j} \{s_k^b\}.$$

□

**Remark 3.22.** Notice that the number of path components in  $S_{i,j}$  which are not simple closed curves is given by  $\frac{\beta_i + \beta_{j+1}}{2}$  (Figure 3.17).

**Definitions 3.23** (Dynnikov and Wiest [14]). Given an essential simple closed curve  $C$  in  $D_n$ ,  $\|C\|$  denotes the minimum number of intersections of  $C$  with the  $x$ -axis. Then, given  $\mathcal{L} \in \mathcal{L}_n$ , the *norm* of  $\mathcal{L}$  is defined as

$$\|\mathcal{L}\| = \sum \|C_i\|$$

where  $\{C_i\}$  are connected components of  $\mathcal{L}$ . We say that  $C_i$  is *relaxed* if  $\|C_i\| = 2$ . Then,  $\mathcal{L}$  is *relaxed* if each of its connected components  $C_i$  is relaxed [14].

It is always possible to turn a non-relaxed integral lamination  $\mathcal{L} \in \mathcal{L}_n$  into one which is relaxed. That is to say, for any  $\mathcal{L} \in \mathcal{L}_n$  there exists a braid  $\beta \in B_n$  such that  $\beta(\mathcal{L})$  is relaxed. This is known as *relaxing an integral lamination* and an algorithm to accomplish this is given in [14].

Given  $\mathcal{L}_1 \in \mathcal{L}_n$  and  $\mathcal{L}_2 \in \mathcal{L}_n$  which are not relaxed, the geometric intersection number  $i(\mathcal{L}_1, \mathcal{L}_2)$  can be computed by first relaxing one of the integral laminations with an  $n$ -braid  $\beta$  by the algorithm described in [14] and then computing  $i(\beta(\mathcal{L}_1), \mathcal{L}_2)$  (note that  $i(\mathcal{L}_1, \mathcal{L}_2) = i(\beta(\mathcal{L}_1), \mathcal{L}_2)$  since geometric intersection number is preserved under homeomorphisms). Now two questions arise: First, how do we compute  $\beta(\mathcal{L})$  in terms of Dynnikov coordinates? Second, how do we find the geometric intersection number of an integral lamination with one which is relaxed? This section presents a formula in terms of Dynnikov coordinates that gives the geometric intersection number of an integral lamination  $\mathcal{L}$  with a relaxed curve and hence answers the second question; and Section 3.4 describes update rules which gives  $\beta(\mathcal{L})$  in terms of Dynnikov coordinates.

Definition 3.24 describes a relaxed curve in  $D_n$  in terms of its Dynnikov coordinates.

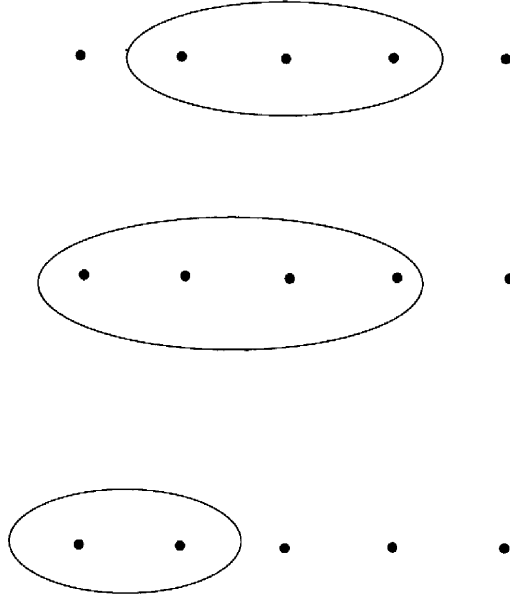


Figure 3.18: Relaxed curves  $C_{24}$ ,  $C_{14}$ ,  $C_{12}$  in  $D_5$  from top to bottom

**Definition 3.24.** For  $1 \leq i < j < n$  or  $1 < i < j \leq n$ ,  $C_{ij} \in \mathcal{L}_n$  denotes the isotopy class of relaxed curves in  $D_n$  which bound a disk containing the set of punctures  $\{i, i+1, \dots, j\}$ .

Hence, we observe that

$$\rho(C_{ij}) = (0, \dots, 0, b_1, \dots, b_{n-2})$$

where  $b_{i-1} = -1$  if  $i > 1$ ,  $b_{j-1} = 1$  if  $j < n$  and  $b_k = 0$  for all other cases.

Figure 3.18 shows some examples of relaxed curves.

**Theorem 3.25.** Given an integral lamination  $\mathcal{L} \in \mathcal{L}_n$  with triangle coordinates  $(\alpha, \beta)$  and  $C_{ij} \in \mathcal{L}_n$ ,  $i(\mathcal{L}, C_{ij})$  is given by,

$$i(\mathcal{L}, C_{ij}) = \beta_{i-1} + \beta_j - 2s_{i-1, j-1}. \quad (3.11)$$

where  $s_{i,j}$  is defined as in Lemma 3.21.

*Proof.* Take a taut representative  $L \in \mathcal{L}$  and a representative  $\gamma_{ij}$  of  $C_{ij}$  which is composed of subarcs of  $\beta_{i-1}$  and  $\beta_j$  and horizontal arcs which are such that the disk bounded by  $\gamma_{ij}$  contains all of the path components of  $L$  in  $S_{i-1, j-1}$ . The number of intersections of  $\gamma_{ij}$  with the path components of  $L$  in  $S_{i-1, j-1}$  is given by  $\beta_{i-1} + \beta_j$  (See Remark 3.22). This number can be minimized by subtracting

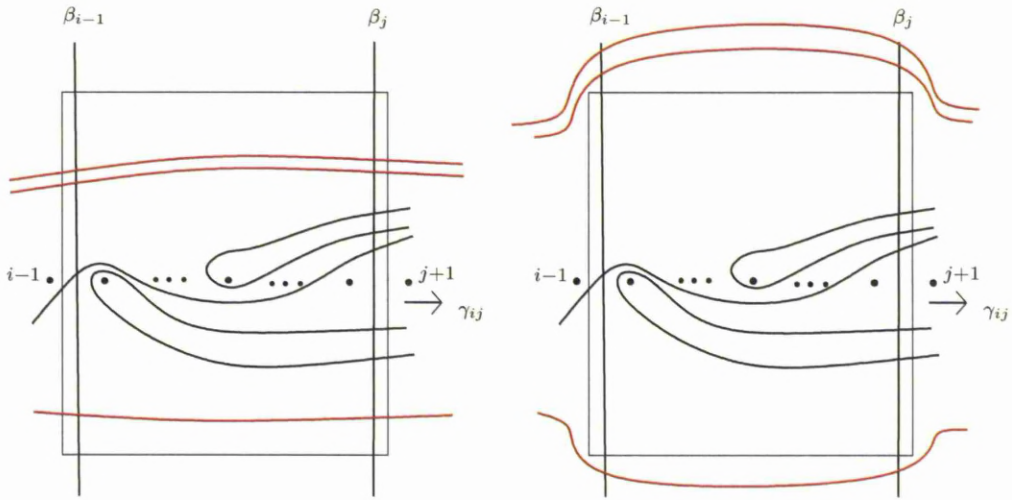


Figure 3.19: Proof of Theorem 3.25

from it the number of path components which can be isotoped so that they do not intersect  $\gamma_{ij}$  any more. Such path components can only be above and below components in  $S_{i-1, j-1}$  (Figure 3.19). Since, each above and below component intersects  $\gamma_{ij}$  twice, we have that

$$i(\mathcal{L}, C_{ij}) = \beta_{i-1} + \beta_j - 2s_{i-1, j-1}.$$

□

Notice that the formulae given above can be written using Dynnikov coordinates since one can write each  $\alpha_i$  and  $\beta_i$  in terms of  $a_i$  and  $b_i$  by Theorem 3.19.

**Example 3.26.** Let  $\rho(\mathcal{L}) = (2, 1, 0, -2, 0, 2)$  (Figure 3.3). We want to find  $i(C_{24}, \mathcal{L})$ . Using the formula (3.11) we get,

$$i(\mathcal{L}, C_{24}) = \beta_1 + \beta_4 - 2s_{1,3}.$$

From Theorem 3.19, we know that

$$(\alpha_1, \alpha_2, \alpha_3, \alpha_4, \alpha_5, \alpha_6; \beta_1, \beta_2, \beta_3, \beta_4) = (2, 6, 3, 5, 4, 4; 4, 8, 8, 4).$$

From Lemma 3.21 we have,

$$s_{1,3}^a = \min_{1 \leq k \leq 3} \{\alpha_{2k-1} - |b_k|\} \quad \text{and} \quad s_{1,3}^b = \min_{1 \leq k \leq 3} \{\alpha_{2k} - |b_k|\}$$

Therefore,

$$\begin{aligned} s_{1,3}^a &= \min\{\alpha_1 - |b_1|, \alpha_3 - |b_2|, \alpha_5 - |b_3|\} \\ &= \min\{2 - |-2|, 3 - 0, 4 - 2\} = 0 \end{aligned}$$

and

$$\begin{aligned} s_{1,3}^b &= \min\{\alpha_2 - |b_1|, \alpha_4 - |b_2|, \alpha_6 - |b_3|\} \\ &= \min\{6 - |-2|, 5 - 0, 4 - 2\} = 2 \end{aligned}$$

So the number of above and below components in  $S_{1,3}$  equals  $s_{1,3}^a + s_{1,3}^b = 2$ .

Therefore,

$$i(\mathcal{L}, C_{24}) = \beta_1 + \beta_4 - 2s_{1,3} = 4 + 4 - 2 \times 2 = 4$$

See Figure 3.20 and Figure 3.21.

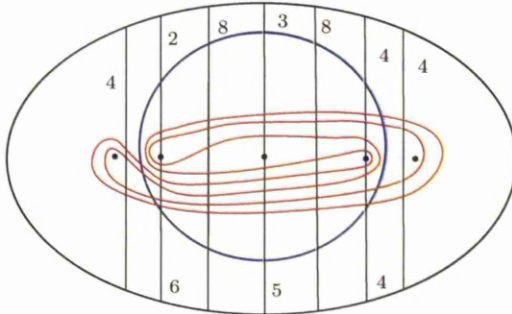


Figure 3.20:  $i(\mathcal{L}, C_{ij}) = 4$

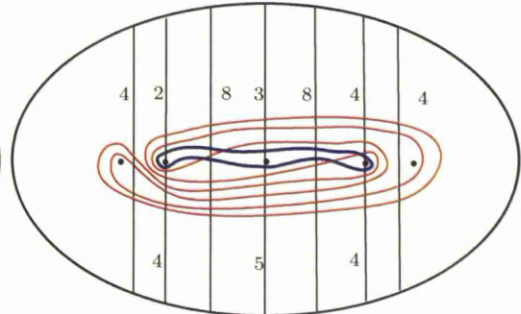


Figure 3.21:  $i(\mathcal{L}, C_{ij}) = 4$

**Remark 3.27.** Observe that if  $\mathcal{L}_1 = \bigcup C_{ij} \in \mathcal{L}_n$  and  $\mathcal{L}_2 \in \mathcal{L}_n$ , then

$$i(\mathcal{L}_1, \mathcal{L}_2) = \sum i(C_{ij}, \mathcal{L}_2)$$

since the above construction can be carried out for each  $C_{ij}$  in turn, working from the inside out.

### 3.3 Aside: Addition on $\mathcal{L}_n$

For the sake of this section set  $\mathcal{C}_n = \mathbb{Z}^{2n-4}$ . This adds the *empty lamination*  $\emptyset$  to  $\mathcal{L}_n$ . Then by Theorem 3.19 there exists an operation  $\oplus$  on  $\mathcal{L}_n$  such that the diagram in (3.12) commutes.

$$\begin{array}{ccc} \mathcal{L}_n \cup \{\emptyset\} \times \mathcal{L}_n \cup \{\emptyset\} & \xrightarrow{\oplus} & \mathcal{L}_n \cup \{\emptyset\} \\ \rho \times \rho \downarrow & & \rho \downarrow \\ \mathbb{Z}^{2n-4} \times \mathbb{Z}^{2n-4} & \xrightarrow{+} & \mathbb{Z}^{2n-4} \end{array} \quad (3.12)$$

In this section, we shall describe the operation  $\oplus$  on  $\mathcal{L}_n$  and concretely see what addition of two integral laminations looks like.

**Theorem 3.28.** *Let  $\mathcal{L}_1 \in \mathcal{L}_n$  and  $\mathcal{L}_2 \in \mathcal{L}_n$  have triangle coordinates  $(\alpha^1, \beta^1)$  and  $(\alpha^2, \beta^2)$ . Then the integral lamination  $\mathcal{L}$  with  $\rho(\mathcal{L}) = \rho(\mathcal{L}_1) + \rho(\mathcal{L}_2)$  has triangle coordinates  $(\alpha, \beta)$  given by*

$$\begin{cases} \alpha_{2i} & = \alpha'_{2i} - P_i - B; \quad 1 \leq i \leq n-2 \\ \alpha_{2i-1} & = \alpha'_{2i-1} - P_i - B; \quad 1 \leq i \leq n-2 \\ \beta_i & = \beta'_i - 2B; \quad \text{for } 1 \leq i \leq n-1 \end{cases} \quad (3.13)$$

where,

$$\alpha'_{2i} = \alpha_{2i}^1 + \alpha_{2i}^2, \quad \alpha'_{2i-1} = \alpha_{2i-1}^1 + \alpha_{2i-1}^2, \quad \beta'_i = \beta_i^1 + \beta_i^2$$

and

$$P_i = \frac{\alpha'_{2i} + \alpha'_{2i-1} - \max(\beta'_i, \beta'_{i+1})}{2}; \quad 1 \leq i \leq n-2$$

$$B = \min(s_{1,n-2}^a, s_{1,n-2}^b)$$

where  $s_{1,n-2}^a$  and  $s_{1,n-2}^b$  are given by the formulae in Lemma 3.21, except that  $b_i = \frac{\beta'_i - \beta'_{i+1}}{2}$  and  $\alpha_i = \alpha'_i$ .

*Proof.* Let  $L'$  denote a curve system which intersects each arc  $\alpha_i$   $\alpha'_i$  times and each arc  $\beta_i$   $\beta'_i$  times. This can be drawn piecing together arcs in each triangle since  $\alpha'_i$  and  $\beta'_i$  satisfy the triangle inequalities in each triangle (note that since  $\alpha_i^1, \beta_i^1$  and  $\alpha_i^2, \beta_i^2$  satisfy the triangle inequalities so do  $\alpha'_i$  and  $\beta'_i$ ).

Let  $s_{1,n-2}^a$  and  $s_{1,n-2}^b$  denote the number of above and below components of  $L'$  in  $S_{1,n-2}$  respectively as given in Lemma 3.21. If  $s_{1,n-2}^a \neq 0$  and  $s_{1,n-2}^b \neq 0$ ,

then some curves of  $L'$  are parallel to  $\partial D_n$ . Observe that the number of such curves is given by  $B = \min(s_{1,n-2}^a, s_{1,n-2}^b)$  (see Figure 3.22) and intersects each  $\alpha'_i$  once and  $\beta'_i$  twice.

Hence one can construct from  $L'$  a new curve system  $L$  which does not contain any curve that bounds a puncture by subtracting  $P_i$  from the  $\alpha'_i$  coordinates; and which has no curves that are parallel to  $\partial D_n$  by subtracting  $B$  from the  $\alpha'_i$  coordinates and  $2B$  from the  $\beta'_i$  coordinates (observe that if  $\mathcal{L}_1$  and  $\mathcal{L}_2$  are disjoint,  $\mathcal{L}$  is just their union).

Hence the formula in 3.13 realizes the triangle coordinates of an integral lamination  $\mathcal{L}$  (See Figure 3.22) and  $\mathcal{L}_n \cup \{\emptyset\}$  becomes an abelian group. Let

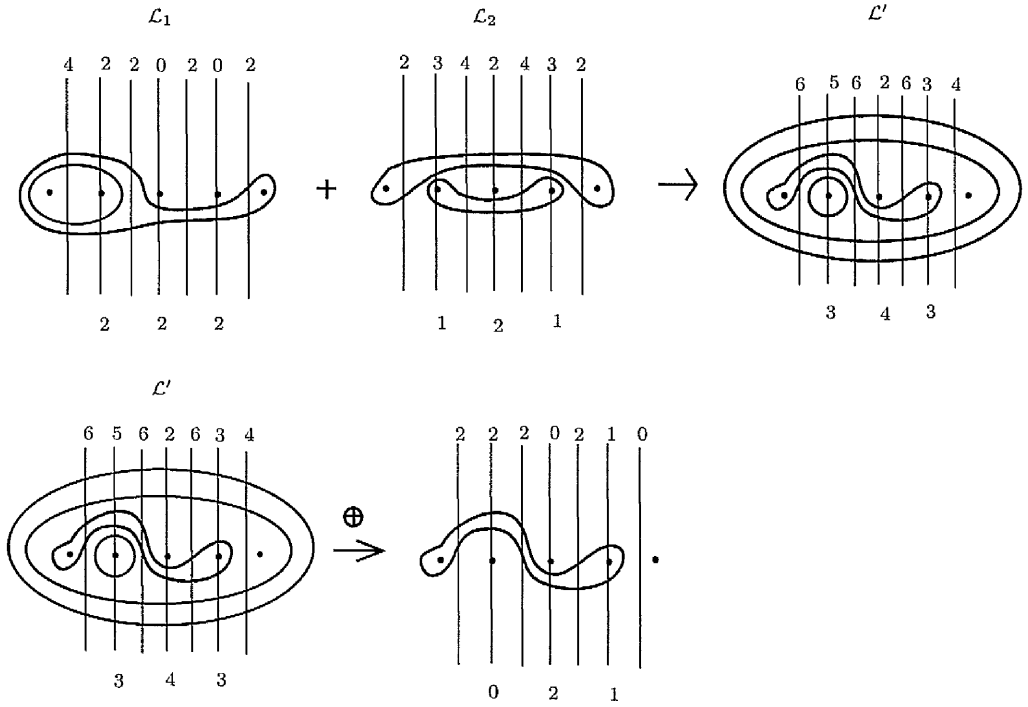


Figure 3.22: Addition of integral laminations

$(a_i^1, b_i^1)$ ,  $(a_i^2, b_i^2)$  and  $(a, b)$  denote the Dynnikov coordinates of  $\mathcal{L}_1$ ,  $\mathcal{L}_2$  and  $\mathcal{L}$  respectively. Then  $\rho(\mathcal{L}_1 \oplus \mathcal{L}_2) = \rho(\mathcal{L}_1) + \rho(\mathcal{L}_2)$  since

$$\begin{aligned}
 a_i &= \frac{\alpha_{2i} - \alpha_{2i-1}}{2} = \frac{\alpha_{2i}^1 + \alpha_{2i}^2 - P_i - B - \alpha_{2i-1}^1 - \alpha_{2i-1}^2 + P_i + B}{2} \\
 &= \frac{\alpha_{2i}^1 - \alpha_{2i-1}^1 + \alpha_{2i}^2 - \alpha_{2i-1}^2}{2} \\
 &= a_i^1 + a_i^2
 \end{aligned}$$

and,

$$\begin{aligned}
 b_i &= \frac{\beta_i - \beta_{i+1}}{2} = \frac{\beta_i^1 + \beta_i^2 - 2B - \beta_{i+1}^1 - \beta_{i+1}^2 + 2B}{2} \\
 &= \frac{\beta_i^1 - \beta_{i+1}^1 + \beta_i^2 - \beta_{i+1}^2}{2} \\
 &= b_i^1 + b_i^2.
 \end{aligned}$$

so that  $\mathcal{L} = \mathcal{L}_1 \oplus \mathcal{L}_2$ .

□

### 3.4 Update rules for Dynnikov coordinates of integral laminations

Given  $f \in \text{Aut}(D_n)$ ,  $f$  acts on  $\mathcal{L} \in \mathcal{L}_n$  by sending  $\mathcal{L}$  to its image  $f(\mathcal{L})$  which gives a well-defined action of  $\text{MCG}(D_n)$  on  $\mathcal{L}_n$ . Since  $\text{MCG}(D_n)$  is isomorphic to Artin's braid group modulo its center (Theorem 2.63), there is a well defined action of  $B_n$  on  $\mathcal{L}_n$ .

In this section we shall explain how to compute the action of  $B_n$  on  $\mathcal{C}_n$ . That is for each  $\beta \in B_n$ , we shall compute  $\beta : \mathcal{C}_n \rightarrow \mathcal{C}_n$  given by,

$$\beta(a, b) = \rho \circ \beta \circ \rho^{-1}(a, b).$$

To do this, we shall describe the action of Artin's braid generators  $\sigma_i, \sigma_i^{-1}$ , ( $1 \leq i \leq n-1$ ) on  $\mathcal{L}_n$  using the *Update rules* [13]. Update rules tell us  $\rho(\sigma_i(\mathcal{L}))$  and  $\rho(\sigma_i^{-1}(\mathcal{L}))$  in terms of  $\rho(\mathcal{L})$ : that is, they describe the action of the Artin braid generators in terms of Dynnikov coordinates. The integral lamination  $\mathcal{L}$  in Figure 3.23 has Dynnikov coordinates  $\rho(\mathcal{L}) = (1, 2, 1, -1, 1, 2)$ . Using the update rules we get the Dynnikov coordinates  $\rho(\sigma_1\sigma_2(\mathcal{L})) = (1, 0, 1, 1, -1, 2)$  of  $\sigma_1\sigma_2(\mathcal{L})$  depicted in Figure 3.24.

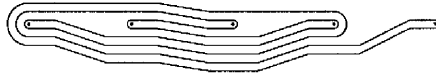


Figure 3.23:  $\rho(\mathcal{L}) = (1, 2, 1, -1, 1, 2)$

The difference between the update rules given here and those that appeared in [13, 25] will be that here  $B_n$  acts on  $D_n$  whereas in the cited papers  $B_n$  acts on the central  $n$  punctures in  $D_{n+2}$ . Thus we have special formulae for the



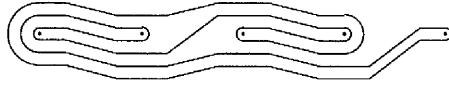


Figure 3.24:  $\rho(\sigma_1\sigma_2(\mathcal{L})) = (1, 0, 1, 1, -1, 2)$

action of  $\sigma_1, \sigma_{n-1}$  and their inverses. Also, for computational and notational convenience, we shall work in the max-plus semiring  $(\mathbb{R}, \max, +)$ . We also note that the derivation of the update rules has not appeared in the literature before.

The following lemma [28, 11] will be used to obtain the update rules.

**Lemma 3.29.** (Quadrilateral Trick) *Let  $Q$  be a quadrilateral in  $D_n$  with all of its vertices at punctures (where  $\partial D_n$  is regarded as a puncture at  $\infty$ ) and containing no punctures in its interior. Let the four edges of  $Q$  be denoted  $X_1, X_2, X_3, X_4$  and its diagonals  $X_5$  and  $X_6$  as shown in Figure 3.25. Let  $\mathcal{L}$  be an integral lamination on  $D_n$  and for each  $i$  let  $\tilde{X}_i$  denote the geometric intersection number between  $\mathcal{L}$  and  $X_i$ . Then,*

$$\tilde{X}_5 + \tilde{X}_6 = \max\{\tilde{X}_1 + \tilde{X}_2, \tilde{X}_3 + \tilde{X}_4\}$$

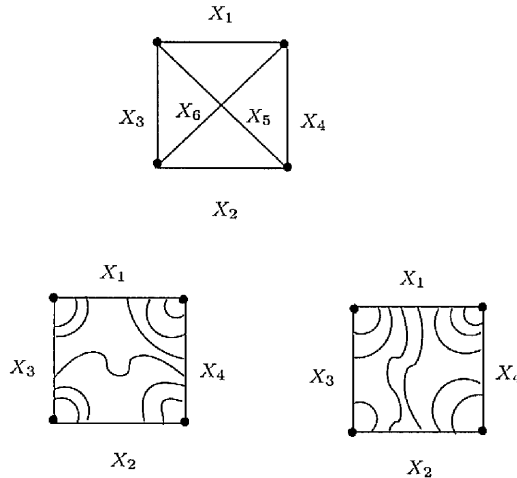


Figure 3.25: Components of  $L$  in  $Q$

*Proof.* Let  $L$  be a representative of  $\mathcal{L}$  which is taut with respect to the edges  $X_i$ . For  $1 \leq i < j \leq 4$ , let  $X_{ij}$  denote the number of components of  $L \cap K$  with endpoints on  $X_i$  and  $X_j$  where  $K$  is the interior of  $Q$  (note that no component

can have both endpoints on the same edge since there are no punctures in  $K$ ). Either  $X_{12}$  or  $X_{34}$  is zero since the components of  $L \cap K$  are disjoint. First suppose  $X_{12} = 0$ . Then,  $\tilde{X}_3 + \tilde{X}_4 \geq \tilde{X}_1 + \tilde{X}_2$  and

$$\begin{aligned}\tilde{X}_1 &= X_{13} + X_{14} \\ \tilde{X}_2 &= X_{23} + X_{24} \\ \tilde{X}_3 &= X_{13} + X_{23} + X_{34} \\ \tilde{X}_4 &= X_{14} + X_{24} + X_{34} \\ \tilde{X}_5 &= X_{13} + X_{24} + X_{34} \\ \tilde{X}_6 &= X_{14} + X_{23} + X_{34}.\end{aligned}$$

Therefore,

$$\begin{aligned}\tilde{X}_5 + \tilde{X}_6 &= X_{13} + X_{23} + X_{14} + X_{24} + 2X_{34} \\ &= \tilde{X}_3 + \tilde{X}_4.\end{aligned}$$

The argument when  $X_{34} = 0$  is identical and we have  $\tilde{X}_1 + \tilde{X}_2 \geq \tilde{X}_3 + \tilde{X}_4$ . Hence,

$$\begin{aligned}\tilde{X}_5 + \tilde{X}_6 &= 2X_{12} + X_{13} + X_{14} + X_{23} + X_{24} \\ &= \tilde{X}_1 + \tilde{X}_2\end{aligned}$$

which yields

$$\tilde{X}_5 + \tilde{X}_6 = \max\{\tilde{X}_1 + \tilde{X}_2, \tilde{X}_3 + \tilde{X}_4\}$$

as required. □

**Definitions 3.30.** For computational and notational convenience, we will work in the *max-plus semiring*  $(\mathbb{R}, \oplus, \otimes)$ , in which the additive and multiplicative operations are given by  $a \oplus b = \max(a, b)$  and  $a \otimes b = a + b$  (so the multiplicative identity is 0). It will be convenient to use normal additive and multiplicative notation, and to indicate that these are to be interpreted in the max-plus sense by enclosing the formulae in square brackets. Thus

$$\begin{aligned}
[a + b] &= \max(a, b) \\
[ab] &= a + b \\
[a/b] &= a - b \\
[1] &= 0
\end{aligned}$$

For example, the formula  $a'_i = \left[ \frac{a_{i-1}a_i b_i}{a_{i-1}(1+b_i)+a_i} \right]$  will be just another way of writing  $a'_i = a_{i-1} + a_i + b_i - \max(a_{i-1} + \max(0, b_i), a_i)$ . Note that both addition and multiplication are commutative and multiplication is distributive over addition:

$$\begin{aligned}
[a + b] &= \max(a, b) = \max(b, a) = [b + a], \\
[ab] &= a + b = b + a = [ba], \\
[a(b + c)] &= a + \max(b, c) = \max(a + b, a + c) = [ab + ac].
\end{aligned}$$

The symmetries described in the next two remarks will be useful for reducing the amount of computations which we have to do.

**Remark 3.31.** Rotation through  $\pi$  about the center of  $D_n$  conjugates each braid generator  $\sigma_i$  to  $\sigma_{n-i}$  and the corresponding transformation of Dynnikov coordinates is given by

$$(a_1, \dots, a_{n-2}, b_1, \dots, b_{n-2}) \mapsto (-a_{n-2}, \dots, -a_1, -b_{n-2}, \dots, -b_1),$$

or, in max-plus notation,

$$(a_1, \dots, a_{n-2}, b_1, \dots, b_{n-2}) \mapsto [(1/a_{n-2}, \dots, 1/a_1, 1/b_{n-2}, \dots, 1/b_1)].$$

**Remark 3.32.** Reflection in the horizontal diameter of  $D_n$  conjugates each braid generator  $\sigma_i$  to  $\sigma_i^{-1}$  and the corresponding transformation of Dynnikov coordinates is given by

$$(a_1, \dots, a_{n-2}, b_1, \dots, b_{n-2}) \mapsto (-a_1, \dots, -a_{n-2}, b_1, \dots, b_{n-2}),$$

or, in max-plus notation,

$$(a_1, \dots, a_{n-2}, b_1, \dots, b_{n-2}) \mapsto [(1/a_1, \dots, 1/a_{n-2}, b_1, \dots, b_{n-2})].$$

The following theorem gives the update rules for the generators  $\sigma_i$ . We note that while the rules have a complicated form, they are ideally suited for computer implementation.

**Theorem 3.33.** Let  $(a, b) \in \mathcal{C}_n$  and  $1 \leq i \leq n - 1$ , and write  $\sigma_i(a, b) = (a', b')$ . Then  $a'_j = a_j$  and  $b'_j = b_j$  except when  $j = i - 1$  or  $j = i$ , and:

- if  $i = 1$  then

$$a'_1 = \left[ \frac{a_1 b_1}{a_1 + 1 + b_1} \right], \quad b'_1 = \left[ \frac{1 + b_1}{a_1} \right];$$

- if  $2 \leq i \leq n - 2$  then

$$a'_{i-1} = [a_{i-1}(1 + b_{i-1}) + a_i b_{i-1}], \quad b'_{i-1} = \left[ \frac{a_i b_{i-1} b_i}{a_{i-1}(1 + b_{i-1})(1 + b_i) + a_i b_{i-1}} \right]$$

$$a'_i = \left[ \frac{a_{i-1} a_i b_i}{a_{i-1}(1 + b_i) + a_i} \right], \quad b'_i = \left[ \frac{a_{i-1}(1 + b_{i-1})(1 + b_i) + a_i b_{i-1}}{a_i} \right];$$

- if  $i = n - 1$  then

$$a'_{n-2} = [a_{n-2}(1 + b_{n-2}) + b_{n-2}], \quad b'_{n-2} = \left[ \frac{b_{n-2}}{a_{n-2}(1 + b_{n-2})} \right].$$

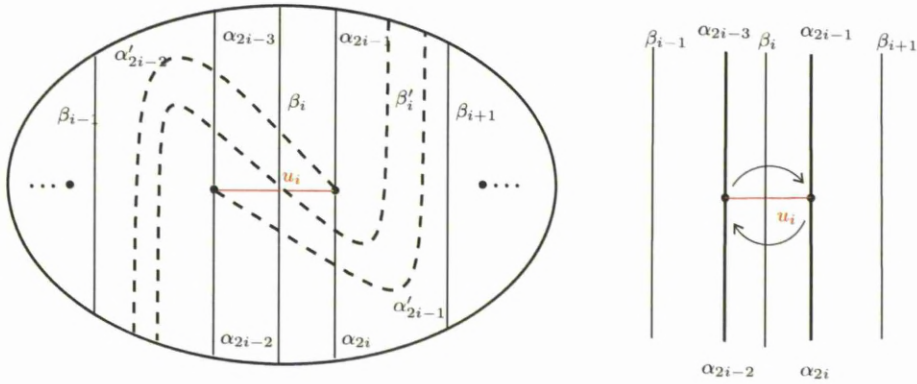


Figure 3.26: The action of  $\sigma_i^{-1}$  on the arcs

*Proof.* Observe that,  $\text{MCG}(D_n)$  acts on both  $\mathcal{A}_n$  (the set of arcs in  $D_n$  which have each endpoint either on the boundary or at a puncture) and  $\mathcal{L}_n$  and the minimum intersection function  $i: \mathcal{L}_n \times \mathcal{A}_n \rightarrow \mathbb{Z}^+$  is equivariant under this action. Namely, given  $\gamma \in \text{MCG}(D_n)$  and  $[\alpha] \in \mathcal{A}_n$ ,  $i(\mathcal{L}, [\alpha]) = i(\gamma(\mathcal{L}), \gamma([\alpha]))$ . Therefore, for the Artin braid generator  $\sigma_i$ ,

$$i(\sigma_i(\mathcal{L}), [\alpha]) = i(\mathcal{L}, \sigma_i^{-1}([\alpha])).$$

Therefore, instead of computing the number of intersections of  $\sigma_i(\mathcal{L})$  with  $\alpha_j$  ( $1 \leq j \leq 2n-4$ ) and  $\beta_j$  ( $1 \leq j \leq n-1$ ) we compute the number of intersections of  $\alpha'_j = \sigma_i^{-1}(\alpha_j)$  and  $\beta'_j = \sigma_i^{-1}(\beta_j)$  with  $\mathcal{L}$ . Then we have,

$$\alpha'_j = \frac{\alpha'_{2j} - \alpha'_{2j-1}}{2} \quad \text{and} \quad \beta'_j = \frac{\beta'_j - \beta'_{j+1}}{2}.$$

Throughout the computations we shall make use of an additional arc  $u_i$  which connects the  $i^{\text{th}}$  and  $i+1^{\text{th}}$  punctures as depicted in Figure 3.26. By Lemma 3.29 we have

$$u_i + \beta_i = \max\{\alpha_{2i-3} + \alpha_{2i}, \alpha_{2i-2} + \alpha_{2i-1}\},$$

that is,

$$u_i = \left\lfloor \frac{\alpha_{2i-3}\alpha_{2i} + \alpha_{2i-2}\alpha_{2i-1}}{\beta_i} \right\rfloor.$$

Before we start our computations we set  $A_j = 2a_j$  ( $1 \leq j \leq n-2$ ) and  $B_j = 2b_j$  ( $1 \leq j \leq n-2$ ). Therefore,

$$A_j = \left\lfloor \frac{\alpha_{2j}}{\alpha_{2j-1}} \right\rfloor \quad \text{and} \quad B_j = \left\lfloor \frac{\beta_j}{\beta_{j+1}} \right\rfloor.$$

We now consider the three separate cases of the statement.

- Suppose that  $2 \leq i \leq n-2$ . Observe first (Figure 3.26) that  $\beta'_j = \beta_j$  for  $j \neq i$  and  $\alpha'_j = \alpha_j$  for  $j < 2i-3$  and  $j > 2i$ . Therefore,  $A'_j = A_j$  and  $B'_j = B_j$  for except  $j = i-1$  and  $j = i$ . Next we shall compute  $A'_i, A'_{i-1}, B'_i$  and  $B'_{i-1}$ .

- i. We shall first compute  $A'_i = \left\lfloor \frac{\alpha'_{2i}}{\alpha'_{2i-1}} \right\rfloor$ . We have  $\alpha'_{2i} = \alpha_{2i-2}$ . To compute  $\alpha'_{2i-1}$ , we choose a quadrilateral in which  $\alpha'_{2i-1}$  is a diagonal as depicted in Figure 3.27. Then by Lemma 3.29,

$$\alpha'_{2i-1} + \alpha_{2i} = \max\{u_i + \beta_{i+1}, \alpha_{2i-2} + \alpha_{2i-1}\}.$$

That is,

$$\alpha'_{2i-1} = \left\lfloor \frac{u_i\beta_{i+1} + \alpha_{2i-2}\alpha_{2i-1}}{\alpha_{2i}} \right\rfloor.$$

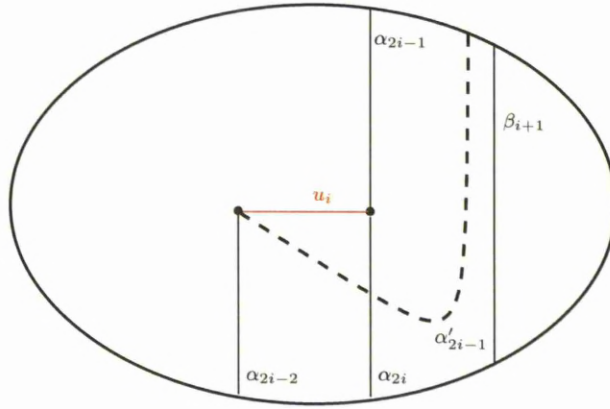


Figure 3.27: The first quadrilateral

Then,

$$\begin{aligned} \left[ \frac{1}{A'_i} \right] &= \left[ \frac{\alpha_{2i-3}\alpha_{2i}\beta_{i+1}}{\alpha_{2i-2}\alpha_{2i}\beta_i} + \frac{\alpha_{2i-2}\alpha_{2i-1}\beta_{i+1}}{\alpha_{2i-2}\alpha_{2i}\beta_i} + \frac{\alpha_{2i-2}\alpha_{2i-1}\beta_i}{\alpha_{2i-2}\alpha_{2i}\beta_i} \right] \\ &= \left[ \frac{1}{A_{i-1}B_i} + \frac{1}{A_iB_i} + \frac{1}{A_i} \right] \end{aligned}$$

and hence,

$$A'_i = \left[ \frac{A_{i-1}A_iB_i}{A_{i-1}(1+B_i) + A_i} \right]$$

as required.

- ii. We shall now compute  $A'_{i-1} = \left[ \frac{\alpha'_{2i-2}}{\alpha'_{2i-3}} \right]$ . We have  $\alpha'_{2i-3} = \alpha_{2i-1}$ . For  $\alpha'_{2i-2}$ , we choose a quadrilateral in which  $\alpha'_{2i-2}$  is a diagonal as depicted in Figure 3.28. Then,

$$\alpha'_{2i-2} = \left[ \frac{\alpha_{2i-2}\alpha_{2i-1} + u_i\beta_{i-1}}{\alpha_{2i-3}} \right].$$

Hence,

$$\begin{aligned} A'_{i-1} &= \left[ \frac{\alpha_{2i-3}\alpha_{2i}\beta_{i-1}}{\alpha_{2i-3}\alpha_{2i-1}\beta_i} + \frac{\alpha_{2i-2}\alpha_{2i-1}\beta_{i-1}}{\alpha_{2i-3}\alpha_{2i-1}\beta_i} + \frac{\alpha_{2i-2}\alpha_{2i-1}\beta_i}{\alpha_{2i-3}\alpha_{2i-1}\beta_i} \right] \\ &= [A_iB_{i-1} + A_{i-1}B_{i-1} + A_{i-1}] \end{aligned}$$

and hence,

$$A'_{i-1} = [A_{i-1}(1+B_{i-1}) + A_iB_{i-1}]$$

as required.

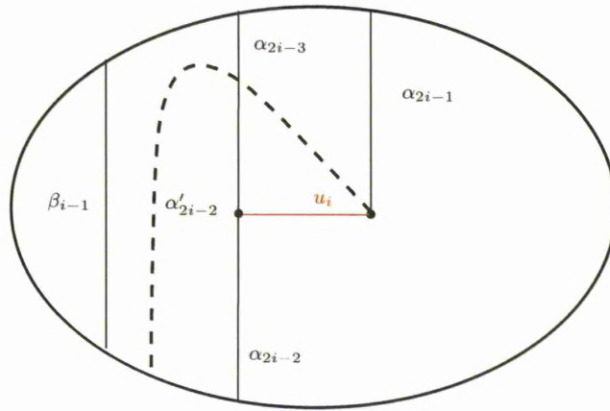


Figure 3.28: The second quadrilateral

iii. To compute  $B'_i = \left[ \frac{\beta'_i}{\beta'_{i+1}} \right]$ , we observe from Figure 3.29 that,

$$\beta'_i = \left[ \frac{\alpha'_{2i-2}\alpha'_{2i-1} + \alpha_{2i-2}\alpha_{2i-1}}{u_i} \right].$$

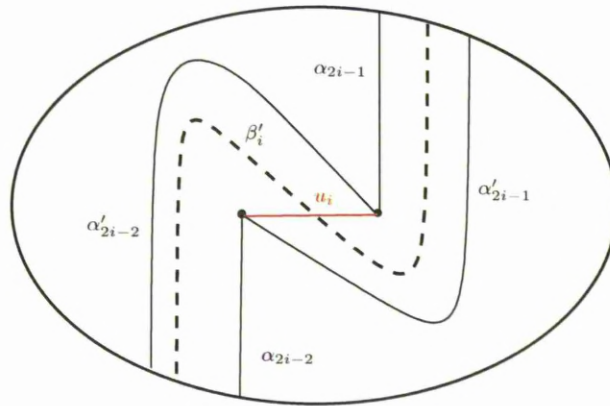


Figure 3.29: The third quadrilateral

Since  $\beta'_{i+1} = \beta_{i+1}$  we get

$$B'_i = \left[ \frac{\alpha'_{2i-2}\alpha'_{2i-1} + \alpha_{2i-2}\alpha_{2i-1}}{u_i\beta_{i+1}} \right].$$

Since  $\alpha'_{2i-3} = \alpha_{2i-1}$  and  $\alpha'_{2i} = \alpha_{2i-2}$

$$\alpha'_{2i-2} = [A'_{i-1}\alpha_{2i-1}] \quad \text{and} \quad \alpha'_{2i-1} = \left[ \frac{\alpha_{2i-2}}{A'_i} \right].$$

Recalling that

$$u_i = \left[ \frac{\alpha_{2i-3}\alpha_{2i} + \alpha_{2i-2}\alpha_{2i-1}}{\beta_i} \right]$$

we obtain,

$$\begin{aligned} B'_i &= \left[ \frac{\frac{A'_{i-1}}{A'_i}\alpha_{2i-2}\alpha_{2i-1} + \alpha_{2i-2}\alpha_{2i-1}}{u_i\beta_{i+1}} \right] = \left[ \frac{\alpha_{2i-2}\alpha_{2i-1}\left(\frac{A'_{i-1}}{A'_i} + 1\right)}{\frac{\beta_{i+1}}{\beta_i}(\alpha_{2i-3}\alpha_{2i} + \alpha_{2i-2}\alpha_{2i-1})} \right] \\ &= \left[ B_i\left(\frac{A'_{i-1} + A'_i}{A'_i}\right)\frac{1}{\frac{\alpha_{2i-3}\alpha_{2i} + \alpha_{2i-2}\alpha_{2i-1}}{\alpha_{2i-2}\alpha_{2i-1}}} \right] = \left[ B_i\left(\frac{A'_{i-1} + A'_i}{A'_i}\right)\frac{A_{i-1}}{A_{i-1} + A_i} \right] \\ &= \left[ \frac{A_{i-1}(1 + B_{i-1})(1 + B_i) + A_i B_{i-1}}{A_i} \right] \end{aligned}$$

as required.

iv. Now we shall compute  $B'_{i-1} = \left[ \frac{\beta'_{i-1}}{\beta'_i} \right]$ . We have

$$\beta'_{i-1} = \beta_{i-1}, \beta'_{i+1} = \beta_{i+1} \text{ and } B'_i = \left[ \frac{\beta'_i}{\beta'_{i+1}} \right].$$

Therefore,

$$B'_{i-1} = \left[ \frac{\beta_{i-1}}{B'_i\beta_{i+1}} \right].$$

Multiplying the numerator and denominator by  $\beta_i$  gives

$$\begin{aligned} B'_{i-1} &= \left[ \frac{B_i B_{i-1}}{B'_i} \right] \\ &= \left[ \frac{A_i B_{i-1} B_i}{A_{i-1}(1 + B_{i-1})(1 + B_i) + A_i B_{i-1}} \right] \end{aligned}$$

as required.

- Suppose that  $i = 1$ . Observe as before that  $A'_j = A_j$  and  $B'_j = B_j$  for all  $j > 1$ . Since there are no arcs joining the first puncture to the boundary, our approach to compute  $A'_1$  and  $B'_1$  is to add new arcs  $\alpha_{-1}$ ,  $\alpha_0$  and  $\beta_0$  as depicted in Figure 3.30, which enables us to use the formulae for  $A'_i$  and  $B'_i$  in the previous statement. Then we have

$$A'_1 = \left[ \frac{A_0 A_1 B_1}{A_0(1 + B_0) + A_1} \right] \text{ and } B'_1 = \left[ \frac{A_0(1 + B_0)(1 + B_1) + A_1 B_0}{A_1} \right].$$

We observe that  $\alpha_{-1} = \alpha_0 = \frac{\beta_1}{2}$  and  $\beta_0 = 0$ . Hence  $A_0 = 0$  and  $B_0 = -\beta_1$ .



i. We shall compute  $A'_1$  first. We have,

$$\begin{aligned} A'_1 &= \left[ \frac{A_0 A_1 B_1}{A_0(1+B_1) + A_1} \right] = A_0 + A_1 + B_1 - \max(A_0 + \max(B_1, 0), A_1) \\ &= A_1 + B_1 - \max(\max(B_1, 0), A_1) = \left[ \frac{A_1 B_1}{A_1 + 1 + B_1} \right] \end{aligned}$$

as required.

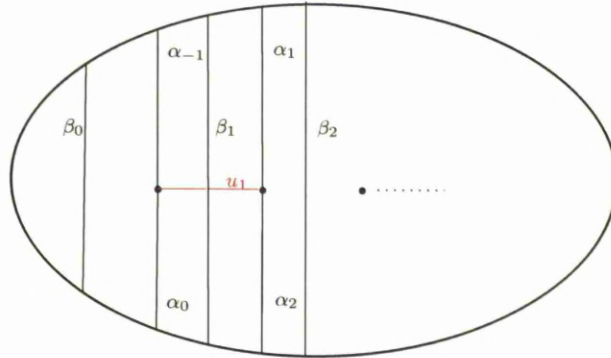


Figure 3.30: The arcs  $\alpha_{-1}$ ,  $\alpha_0$  and  $\beta_0$

ii. Now we shall compute  $B'_1$ . We have,

$$\begin{aligned} B'_1 &= \left[ \frac{A_0(1+B_0)(1+B_1) + A_1 B_0}{A_1} \right] \\ &= \max(A_0 + \max(0, B_0) + \max(B_1, 0), A_1 + B_0) - A_1 \\ &= \max(\max(B_1, 0), A_1 + B_0) - A_1 = \max(B_1, 0) - A_1 = \left[ \frac{1+B_1}{A_1} \right]. \end{aligned}$$

In the above calculation we have used  $\max(B_1, 0) \geq A_1 + B_0$ . This is true since  $\alpha_2 - \alpha_1 - \beta_1 \leq 0$ . In other words,

$$\max(\beta_1 - \beta_2, 0) \geq \alpha_2 - \alpha_1 - \beta_1.$$

We have  $\alpha_2 - \alpha_1 - \beta_1 \leq 0$  from the following observation. If  $\beta_1 \geq \beta_2$ , we have  $\alpha_1 + \alpha_2 = \beta_1$  and if  $\beta_1 \leq \beta_2$ ,  $|\alpha_2 - \alpha_1| \leq \beta_1$ .

- Suppose that  $i = n - 1$ . The rules for  $A'_{n-2}$  and  $B'_{n-2}$  will be obtained by symmetry, conjugating the rules for  $A'_1$  and  $B'_1$  by the involution

$$(A_1, \dots, A_{n-2}, B_1, \dots, B_{n-2}) \mapsto [(1/A_{n-2}, \dots, 1/A_1, 1/B_{n-2}, \dots, 1/B_1)]$$

of Remark 3.31. Then we get,

$$\left[ \frac{1}{A'_{n-2}} \right] = \left[ \frac{\frac{1}{A_{n-2}} \frac{1}{B_{n-2}}}{\frac{1}{A_{n-2}} + \frac{1}{B_{n-2}} + 1} \right] = \left[ \frac{1}{B_{n-2} + A_{n-2} + A_{n-2}B_{n-2}} \right],$$

Hence

$$A'_{n-2} = [A_{n-2}(1 + B_{n-2}) + B_{n-2}].$$

And,

$$\left[ \frac{1}{B'_{n-2}} \right] = \left[ \frac{1 + \frac{1}{B_{n-2}}}{\frac{1}{A_{n-2}}} \right] = \left[ \frac{A_{n-2}(1 + B_{n-2})}{B_{n-2}} \right],$$

Hence

$$B'_{n-2} = \left[ \frac{B_{n-2}}{A_{n-2}(1 + B_{n-2})} \right].$$

□

**Example 3.34.** Given  $\mathcal{L}$  as depicted in Figure 3.23 with  $\rho(\mathcal{L}) = (1, 2, 1, -1, 1, 2)$ , we can compute the Dynnikov coordinates  $(a', b') = \rho(\sigma_1\sigma_2(\mathcal{L}))$  of  $\sigma_1\sigma_2(\mathcal{L})$  depicted in Figure 3.24 using the formulae in Theorem 3.33. We shall only compute  $a'_1$  here. The rest is done similarly. First write  $(a'', b'') = \sigma_1(a, b)$ . Then

$$\begin{aligned} a''_1 &= \left[ \frac{a_1 b_1}{a_1 + 1 + b_1} \right] = a_1 + b_1 - \max(a_1, b_1, 0) \\ &= 1 - 1 - \max(1, -1, 0) = -1 \quad \text{and,} \\ b''_1 &= \left[ \frac{1 + b_1}{a_1} \right] = \max(b_1, 0) - a_1 = 0 - 1 = -1. \end{aligned}$$

Hence, applying the update rules for  $\sigma_2$  to  $(a'', b'')$  we get

$$\begin{aligned} a'_1 &= \max(a''_1 + \max(b''_1, 0), a''_2 + b''_1) \\ &= \max(-1 + \max(-1, 0), 2 - 1) = 1 \end{aligned}$$

**Theorem 3.35** (Update rules for inverse Artin generators). *Let  $(a, b) \in C_n$  and  $1 \leq i \leq n - 1$ , and write  $\sigma_i^{-1}(a, b) = (a'', b'')$ . Then  $a''_j = a_j$  and  $b''_j = b_j$  except when  $j = i - 1$  or  $j = i$ , and:*

- if  $i = 1$  then

$$a''_1 = \left[ \frac{1 + a_1(1 + b_1)}{b_1} \right], \quad b''_1 = [a_1(1 + b_1)];$$

- if  $2 \leq i \leq n-2$  then

$$a''_{i-1} = \left[ \frac{a_{i-1}a_i}{a_{i-1}b_{i-1} + a_i(1+b_{i-1})} \right], \quad b''_{i-1} = \left[ \frac{a_{i-1}b_{i-1}b_i}{a_{i-1}b_{i-1} + a_i(1+b_{i-1})(1+b_i)} \right],$$

$$a''_i = \left[ \frac{a_{i-1} + a_i(1+b_i)}{b_i} \right], \quad b''_i = \left[ \frac{a_{i-1}b_{i-1} + a_i(1+b_{i-1})(1+b_i)}{a_{i-1}} \right];$$

- if  $i = n-1$  then

$$a''_{n-2} = \left[ \frac{a_{n-2}}{a_{n-2}b_{n-2} + 1 + b_{n-2}} \right], \quad b''_{n-2} = \left[ \frac{a_{n-2}b_{n-2}}{1 + b_{n-2}} \right].$$

*Proof.* We shall obtain the update rules for  $\sigma_i^{-1}$  by conjugating the rules of Theorem 3.33 by the involution

$$(a_1, \dots, a_{n-2}, b_1, \dots, b_{n-2}) \mapsto [(1/a_1, \dots, 1/a_{n-2}, b_1, \dots, b_{n-2})]$$

of Remark 3.32. Take for example  $a''_i$ . Since  $a'_i = \left[ \frac{a_{i-1}a_i b_i}{a_{i-1}(1+b_i) + a_i} \right]$  we get,

$$\left[ \frac{1}{a''_i} \right] = \left[ \frac{\frac{1}{a_{i-1}} \frac{1}{a_i} b_i}{\frac{1}{a_{i-1}}(1+b_i) + \frac{1}{a_i}} \right] = \left[ \frac{b_i}{a_i(1+b_i) + a_{i-1}} \right],$$

hence

$$a''_i = \left[ \frac{a_i(1+b_i) + a_{i-1}}{b_i} \right].$$

□

Working in the max-plus semiring, one can obtain the update rules for a general  $n$ -braid using the usual composition of the functions in Theorem 3.33 and Theorem 3.35. We remark that the resulting rational functions correspond to piecewise linear functions. We also note that these functions can be extremely complicated. However, this is not the case for the families of braids with a contiguous sequence of generators given in Section 3.5. These braid families will be important to prove our results in Chapter 4.

### 3.5 Update rules for sequences of contiguous generators

In this section the update rules for the  $n$ -braids

$$\begin{aligned}\gamma_n^{k,l} &= \sigma_k \sigma_{k+1} \cdots \sigma_{l-1} \sigma_l, \\ \delta_n^{k,l} &= \sigma_l \sigma_{l-1} \cdots \sigma_{k+1} \sigma_k, \\ \epsilon_n^{k,l} &= \left( \delta_n^{k,l} \right)^{-1} = \sigma_k^{-1} \sigma_{k+1}^{-1} \cdots \sigma_{l-1}^{-1} \sigma_l^{-1}, \quad \text{and} \\ \zeta_n^{k,l} &= \left( \gamma_n^{k,l} \right)^{-1} = \sigma_l^{-1} \sigma_{l-1}^{-1} \cdots \sigma_{k+1}^{-1} \sigma_k^{-1},\end{aligned}$$

will be given where  $1 \leq k \leq l \leq n-1$ . These update rules have a relatively simple form. Their description is, however, complicated by the need to consider separately the “end” cases  $k=1$  and  $l=n-1$ . Only the update rules for  $\gamma_n^{k,l}$  will be derived directly. Those for the other families of braids will then follow using the symmetries of Remark 3.31 and Remark 3.32.

**Lemma 3.36** (Update rules for  $\gamma_n^{k,l}$ ). *Let  $n \geq 3$ , and for  $1 \leq k \leq l \leq n-1$  let  $\gamma_n^{k,l}$  denote the braid  $\sigma_k \sigma_{k+1} \cdots \sigma_{l-1} \sigma_l \in B_n$ .*

*Given  $(a, b) \in \mathcal{C}_n$  and an integer  $j$  with  $k-1 \leq j \leq n-2$ , write*

$$P_j = P_j(b, k) = \left[ (1 + b_{k-1}) \prod_{i=k}^j b_i \right].$$

*(Note the interpretation of this formula in special cases:  $P_j(b, k) = \left[ \prod_{i=k}^j b_i \right]$  if  $k=1$ ,  $P_j(b, k) = [(1 + b_{k-1})]$  if  $j=k-1$ , and  $P_j(b, k) = [1]$  if  $k=1$  and  $j=0$ .) Similarly, for  $k \leq j \leq n-2$ , write*

$$S_j = S_j(a, b, k) = \left[ \sum_{i=k}^j \frac{(1 + b_i) P_{i-1}}{a_i} \right].$$

*Let  $(a', b') = \gamma_n^{k,l}(a, b)$ . Then  $a'_j = a_j$  and  $b'_j = b_j$  for  $j < k-1$  and for  $j > l$ .*

*Moreover,*

*1. If  $k > 1$  and  $l < n-1$  then*

$$\begin{aligned}a'_{k-1} &= [a_{k-1}(1 + b_{k-1}) + a_k b_{k-1}], & b'_{k-1} &= \left[ \frac{a_k b_{k-1} b_k}{a_{k-1}(1 + b_{k-1})(1 + b_k) + a_k b_{k-1}} \right], \\ a'_j &= [a_{j+1} b_{k-1} + a_{k-1}(a_{j+1} S_j + P_j)], & b'_j &= \left[ b_{j+1} \left( \frac{b_{k-1} + a_{k-1} S_j}{b_{k-1} + a_{k-1} S_{j+1}} \right) \right] \quad (k \leq j < l), \\ a'_l &= \left[ \frac{a_{k-1} P_l}{1 + b_{k-1} + a_{k-1} S_l} \right], & b'_l &= [b_{k-1} + a_{k-1} S_l].\end{aligned}$$

2. If  $k > 1$  and  $l = n - 1$  then the formulae in case 1 hold for  $k - 1 \leq j < n - 2$ , while

$$a'_{n-2} = [b_{k-1} + a_{k-1}(S_{n-2} + P_{n-2})], \quad b'_{n-2} = \left[ \frac{1}{P_{n-2}} \left( \frac{b_{k-1}}{a_{k-1}} + S_{n-2} \right) \right].$$

3. If  $k = 1$  and  $l < n - 1$  then

$$\begin{aligned} a'_j &= [P_j + a_{j+1}S_j], & b'_j &= [b_{j+1}S_j/S_{j+1}] \quad (1 \leq j < l), \\ a'_l &= [P_l/(1 + S_l)], & b'_l &= [S_l]. \end{aligned}$$

4. If  $k = 1$  and  $l = n - 1$  then the formulae in case 3 hold for  $1 \leq j < n - 2$ , while

$$a'_{n-2} = [P_{n-2} + S_{n-2}], \quad b'_{n-2} = [S_{n-2}/P_{n-2}].$$

*Proof.* The proof is a straightforward induction on  $l \geq k$  for each  $k$ , with the base case  $l = k$  given by the update rules for single braid generators (Theorem 3.33).

1. Consider the case  $1 < k < n - 1$  (cases 1 and 2). Putting  $l = k$  gives  $P_l = [(1 + b_{k-1})b_k]$  and  $S_l = [(1 + b_{k-1})(1 + b_k)/a_k]$ . The rules for  $a'_{k-1}$  and  $b'_{k-1}$  given in case 1 of the lemma are identical to those of Theorem 3.33, while

$$\begin{aligned} a'_k &= a'_l = \left[ \frac{a_{k-1}a_k b_k}{a_{k-1}(1 + b_k) + a_k} \right] = \left[ \frac{a_{k-1}(1 + b_{k-1})b_k}{1 + b_{k-1} + a_{k-1}(1 + b_{k-1})(1 + b_k)/a_k} \right] \\ &= \left[ \frac{a_{k-1}P_l}{1 + b_{k-1} + a_{k-1}S_l} \right], \quad \text{and,} \\ b'_k &= b'_l = \left[ \frac{a_{k-1}(1 + b_{k-1})(1 + b_k) + a_k b_{k-1}}{a_k} \right] = [b_{k-1} + a_{k-1}(1 + b_{k-1})(1 + b_k)/a_k] \\ &= [b_{k-1} + a_{k-1}S_l], \end{aligned}$$

in agreement with Theorem 3.33.

Now assume the result is true for some  $l$  with  $k \leq l < n - 1$ , so that  $\gamma_n^{k,l}(a, b) = (a', b')$  as given by case 1 of the Lemma. Let  $(a'', b'') = \gamma_n^{k,l+1}(a, b)$ , so that  $(a'', b'') = \sigma_{l+1}(a', b')$ . In particular,  $a''_j = a'_j$  and  $b''_j = b'_j$  for all  $j$  except  $l$  and  $l + 1$ . Consider  $a''_{l+1}$  and  $b''_{l+1}$  for  $l + 1 < n - 1$  and  $a''_l, b''_l$  for  $l + 1 = n - 1$ :

If  $l + 1 < n - 1$ , then Theorem 3.33 gives

$$\begin{aligned}
a''_{l+1} &= \left[ \frac{a'_l a'_{l+1} b'_{l+1}}{a'_l(1 + b'_{l+1}) + a'_{l+1}} \right] \\
&= \left[ \frac{a_{l+1} b_{l+1} a_{k-1} P_l / (1 + b_{k-1} + a_{k-1} S_l)}{a_{l+1} + (1 + b_{l+1}) a_{k-1} P_l / (1 + b_{k-1} + a_{k-1} S_l)} \right] \\
&= \left[ \frac{a_{k-1} P_{l+1}}{1 + b_{k-1} + a_{k-1} (S_l + (1 + b_{l+1}) P_l / a_{l+1})} \right] \\
&= \left[ \frac{a_{k-1} P_{l+1}}{1 + b_{k-1} + a_{k-1} S_{l+1}} \right]
\end{aligned}$$

and

$$\begin{aligned}
b''_{l+1} &= \left[ \frac{a'_l(1 + b'_l)(1 + b'_{l+1}) + a'_{l+1} b'_l}{a'_{l+1}} \right] \\
&= \left[ \frac{a_{k-1} P_l (1 + b_{l+1}) + a_{l+1} (b_{k-1} + a_{k-1} S_l)}{a_{l+1}} \right] \\
&= \left[ a_{k-1} \left( P_l \frac{1 + b_{l+1}}{a_{l+1}} + S_l \right) + b_{k-1} \right] \\
&= [a_{k-1} S_{l+1} + b_{k-1}].
\end{aligned}$$

Similarly if  $l + 1 = n - 1$ , then Theorem 3.33 gives

$$\begin{aligned}
a''_l &= [a'_l(1 + b'_l) + b'_l] = \left[ \frac{a_{k-1} P_l}{1 + b_{k-1} + a_{k-1} S_l} (1 + b_{k-1} + a_{k-1} S_l) + b_{k-1} + a_{k-1} S_l \right] \\
&= [b_{k-1} + a_{k-1} (S_{n-2} + P_{n-2})],
\end{aligned}$$

$$\begin{aligned}
b''_l &= [b'_l / a'_l (1 + b'_l)] = \left[ \frac{b_{k-1} + a_{k-1} S_l}{a_{k-1} P_l} \right] \\
&= \left[ \frac{1}{P_{n-2}} \left( \frac{b_{k-1}}{a_{k-1}} + S_{n-2} \right) \right].
\end{aligned}$$

For  $k \leq j < l$  observe that

$$P_{j+1} = [b_{j+1} P_j] \quad \text{and} \quad S_{j+1} = \left[ S_j + \frac{1 + b_{j+1}}{a_{j+1}} P_j \right].$$

From Theorem 3.33 and using the inductive hypothesis,

$$\begin{aligned}
a''_{j+1} &= [a'_{j+1}(1 + b'_{j+1}) + a'_{j+2}b'_{j+1}] \\
&= \left[ \frac{a_{k-1}P_{j+1}}{1 + b_{k-1} + a_{k-1}S_{j+1}}(1 + b_{k-1} + a_{k-1}S_{j+1}) + a_{j+2}(b_{k-1} + a_{k-1}S_{j+1}) \right] \\
&= [a_{j+2}b_{k-1} + a_{k-1}(a_{j+2}S_{j+1} + P_{j+1})], \\
b''_{j+1} &= \left[ \frac{a'_{j+2}b'_{j+1}b'_{j+2}}{a'_{j+1}(1 + b'_{j+1})(1 + b'_{j+2}) + a'_{j+2}b'_{j+1}} \right] \\
&= \left[ \frac{a_{j+2}(b_{k-1} + a_{k-1}S_{j+1})b_{j+2}}{\frac{a_{k-1}P_{j+1}}{1 + b_{k-1} + a_{k-1}S_{j+1}}(1 + b_{k-1} + a_{k-1}S_{j+1})(1 + b_{j+2}) + a_{j+2}(b_{k-1} + a_{k-1}S_{j+1})} \right] \\
&= \left[ \frac{b_{j+2}(b_{k-1} + a_{k-1}S_{j+1})}{b_{k-1} + a_{k-1}S_{j+1} + (a_{k-1}P_{j+1}(1 + b_{j+2})/a_{j+2})} \right] \\
&= \left[ \frac{b_{j+2}(b_{k-1} + a_{k-1}S_{j+1})}{a_{k-1}S_{j+2} + b_{k-1}} \right].
\end{aligned}$$

2. Now consider the case  $k = 1$  (cases 3 and 4). If  $l + 1 < n - 1$  we have

$$\begin{aligned}
a''_{l+1} &= \left[ \frac{a_{l+1}b_{l+1}P_l/1 + S_l}{a_{l+1} + (1 + b_{l+1})P_l/1 + S_l} \right] = \left[ \frac{P_l b_{l+1}}{(P_l(1 + b_{l+1}) + a_{l+1} + a_{l+1}S_l)/a_{l+1}} \right] \\
&= \left[ \frac{P_{l+1}}{1 + S_{l+1}} \right], \\
b''_{l+1} &= \left[ \frac{(1 + b_{l+1})(1 + S_l)P_l/(1 + S_l) + a_{l+1}S_l}{a_{l+1}} \right] = \left[ \frac{P_l(1 + b_{l+1}) + S_l a_{l+1}}{a_{l+1}} \right] \\
&= [S_{l+1}].
\end{aligned}$$

And if  $l + 1 = n - 1$  we have

$$\begin{aligned}
a''_l &= [a'_l(1 + b'_l) + b'_l], & b''_l &= \left[ \frac{b'_l}{a'_l(1 + b'_l)} \right] \\
&= [(1 + S_l)P_l/(1 + S_l) + S_l], & &= \left[ \frac{S_l}{(1 + S_l)P_l/(1 + S_l)} \right] \\
&= [P_l + S_l], & &= \left[ \frac{S_l}{P_l} \right].
\end{aligned}$$

Similarly for  $1 \leq j < l$ , from Theorem 3.33 and using the inductive hypothesis,

$$\begin{aligned}
a''_{j+1} &= [a'_{j+1}(1 + b'_{j+1}) + a'_{j+2}b'_{j+1}] = \left[ a_{j+2}S_{j+1} + (1 + S_{j+1})\frac{P_{j+1}}{1 + S_{j+1}} \right] \\
&= [P_{j+1} + a_{j+2}S_{j+1}], \\
b''_{j+1} &= \left[ \frac{a'_{j+2}b'_{j+2}b'_{j+1}}{a'_{j+1}(1 + b'_{j+1})(1 + b'_{j+2}) + a'_{j+2}b'_{j+1}} \right] \\
&= \left[ \frac{a_{j+2}S_{j+1}b_{j+2}}{(1 + S_{j+1})(1 + S_{j+2})P_{j+1}/1 + S_{j+1}} + a_{j+2}S_{j+1} \right] = \left[ \frac{a_{j+2}S_{j+1}b_{j+2}}{P_{j+1}(1 + S_{j+2}) + a_{j+2}S_{j+1}} \right] \\
&= \left[ \frac{b_{j+2}S_{j+1}}{S_{j+1} + P_{j+1}(1 + S_{j+2})/a_{j+2}} \right] = [b_{j+2}S_{j+1}/S_{j+2}].
\end{aligned}$$

□

We shall derive the update rules for  $\delta_n^{k,l}$  from those of Lemma 3.36 for  $\gamma_n^{n-l,n-k}$  which will be used later. To do this we shall conjugate the rules for  $\gamma_n^{n-l,n-k}$  by the involution

$$(a_1, \dots, a_{n-2}, b_1, \dots, b_{n-2}) \mapsto [(1/a_{n-2}, \dots, 1/a_1, 1/b_{n-2}, \dots, 1/b_1)]$$

in Remark 3.31.

**Lemma 3.37** (Update rules for  $\delta_n^{k,l}$ ). *Let  $n \geq 3$ , and for  $1 \leq k \leq l \leq n - 1$  let  $\delta_n^{k,l}$  denote the braid  $\sigma_l \sigma_{l-1} \dots \sigma_{k+1} \sigma_k \in B_n$ .*

*Given  $(a, b) \in C_n$  and an integer  $j$  with  $\max(k - 1, 1) \leq j \leq l$  write*

$$\tilde{P}_j = \tilde{P}_j(b, l) = \left[ (1 + b_l) \prod_{i=j}^l \frac{1}{b_i} \right].$$

*(In the special case  $l = n - 1$ ,  $\tilde{P}_j(b, n - 1) = \left[ \prod_{i=j}^{n-2} \frac{1}{b_i} \right]$  for  $j < l$ , while  $\tilde{P}_{n-1}(b, n - 1) = [1]$ .) Similarly, for  $\max(k - 1, 1) \leq j \leq l - 1$  write*

$$\tilde{S}_j = \tilde{S}_j(a, b, l) = \left[ \sum_{i=j}^{l-1} \frac{a_i(1 + b_i)\tilde{P}_{i+1}}{b_i} \right].$$

*Let  $(a', b') = \delta_n^{k,l}(a, b)$ . Then  $a'_j = a_j$  and  $b'_j = b_j$  for  $j < k - 1$  and for  $j > l$ . Moreover,*



1. If  $k > 1$  and  $l < n - 1$  then

$$\begin{aligned} a'_{k-1} &= \left[ \frac{a_l(1+b_l) + b_l \tilde{S}_{k-1}}{b_l \tilde{P}_{k-1}} \right], & b'_{k-1} &= \left[ \frac{a_l b_l}{a_l + b_l \tilde{S}_{k-1}} \right], \\ a'_j &= \left[ \frac{a_{j-1} a_l b_l}{a_l + b_l (\tilde{S}_j + a_{j-1} \tilde{P}_j)} \right], & b'_j &= \left[ b_{j-1} \left( \frac{a_l + b_l \tilde{S}_{j-1}}{a_l + b_l \tilde{S}_j} \right) \right] \quad (k \leq j < l), \\ a'_l &= \left[ \frac{a_{l-1} a_l b_l}{a_{l-1} (1+b_l) + a_l} \right], & b'_l &= \left[ \frac{a_{l-1} (1+b_{l-1}) (1+b_l) + a_l b_{l-1}}{a_l} \right]. \end{aligned}$$

2. If  $k = 1$  and  $l < n - 1$  then the formulae in case 1 hold for  $2 \leq j \leq l$ , while

$$a'_1 = \left[ \frac{a_l b_l}{a_l + b_l (\tilde{S}_1 + \tilde{P}_1)} \right], \quad b'_1 = \left[ \frac{b_l \tilde{P}_1}{a_l + b_l \tilde{S}_1} \right].$$

3. If  $k > 1$  and  $l = n - 1$  then

$$\begin{aligned} a'_j &= \left[ \frac{a_{j-1}}{a_{j-1} \tilde{P}_j + \tilde{S}_j} \right], & b'_j &= \left[ b_{j-1} \tilde{S}_{j-1} / \tilde{S}_j \right] \quad (k \leq j \leq n-2), \\ a'_{k-1} &= \left[ (1 + \tilde{S}_{k-1}) / \tilde{P}_{k-1} \right], & b'_{k-1} &= \left[ 1 / \tilde{S}_{k-1} \right]. \end{aligned}$$

4. If  $k = 1$  and  $l = n - 1$  then the formulae in case 3 hold for  $2 \leq j \leq n - 2$ , while

$$a'_1 = \left[ 1 / (\tilde{P}_1 + \tilde{S}_1) \right], \quad b'_1 = \left[ \tilde{P}_1 / \tilde{S}_1 \right].$$

**Sketch of Proof.** Let  $R_\pi$  denote the rotation through  $\pi$  about the center of  $D_n$ . Then,

$$\delta_n^{k,l} = R_\pi \gamma_n^{n-l, n-k} R_\pi$$

and hence the update rules of  $\delta_n^{k,l}$  can be obtained by conjugating the rules of  $\gamma_n^{n-l, n-k}$  by the transformation  $a_i \leftrightarrow \left[ \frac{1}{a_{n-1-i}} \right]$ ,  $b_i \leftrightarrow \left[ \frac{1}{b_{n-1-i}} \right]$  as stated in Remark 3.31. We shall prove the lemma for  $k \leq j < l$  for the “central” case  $k > 1$  and  $l < n - 1$  ( $n - l > 1$  and  $n - k < n - 1$ ) and only doing  $a'_j$ . The other cases can be checked similarly. Write  $(a^\gamma, b^\gamma) = \gamma_n^{n-l, n-k}(R_\pi(a), R_\pi(b))$  and  $(a', b') = \delta_n^{k,l}(a, b)$ . Define

$$P'_j(b, k) = P_j(R_\pi(b), k) = \left[ \left( 1 + \frac{1}{b_{n-k}} \right) \prod_{i=n-1-j}^{n-1-k} \frac{1}{b_i} \right]$$

and

$$S'_j(a, b, k) = S'_j(R_\pi(a), R_\pi(b), k) = \left[ \sum_{i=n-1-j}^{n-1-k} a_i \left(1 + \frac{1}{b_i}\right) P'_{n-2-i}(b, k) \right]$$

If  $k \leq j < l$  (that is,  $n-l < j < n-k$ ) we have

$$a'_j = \left[ \frac{1}{a_{n-2-j}} \frac{1}{b_l} + \frac{1}{a_l} \left( \frac{1}{a_{n-2-j}} S'_j(a, b, n-l) + P'_j(b, n-l) \right) \right].$$

Then  $n-l \leq n-1-j < n-k$  and

$$a'_j = \left[ \frac{1}{a'_{n-1-j}} \right] = \left[ \frac{1}{\frac{1}{a_{j-1}} \frac{1}{b_l} + \frac{1}{a_l} \left( \frac{1}{a_{j-1}} S'_{n-1-j}(a, b, n-l) + P'_{n-1-j}(b, n-l) \right)} \right]$$

Write

$$\tilde{P}_j(b, l) = P'_{n-1-j}(b, n-l) \quad \text{and} \quad \tilde{S}_j(a, b, l) = S'_{n-1-j}(a, b, n-l).$$

Then we get

$$\begin{aligned} a'_j &= \left[ \frac{1}{\frac{1}{a_{j-1}} \frac{1}{b_l} + \frac{1}{a_l} \left( \frac{1}{a_{j-1}} \tilde{S}_j(a, b, l) + \tilde{P}_j(b, l) \right)} \right] \\ &= \left[ \frac{a_{j-1} a_l b_l}{a_l + b_l \left( \tilde{S}_j(a, b, l) + a_{j-1} \tilde{P}_j(b, l) \right)} \right] \end{aligned}$$

where

$$\tilde{P}_j(b, l) = P'_{n-1-j}(b, n-l) = \left[ \left(1 + \frac{1}{b_l}\right) \prod_{i=j}^{l-1} \frac{1}{b_i} \right] = \left[ (1 + b_l) \prod_{i=j}^l \frac{1}{b_i} \right]$$

and

$$\tilde{S}_j(a, b, l) = S'_{n-1-j}(a, b, n-l) = \left[ \sum_{i=j}^{l-1} a_i \left(1 + \frac{1}{b_i}\right) \tilde{P}_{i+1}(b, l) \right] = \left[ \sum_{i=j}^{l-1} \frac{a_i (1 + b_i) \tilde{P}_{i+1}(b, l)}{b_i} \right].$$

The update rules for the other two families  $\epsilon_n^{k,l}$  and  $\zeta_n^{k,l}$  will be given without proof. The rules in Lemma 3.38 and Lemma 3.39 are obtained by conjugating the rules in Lemma 3.36 and Lemma 3.37 respectively by the transformation

$$(a_1, \dots, a_{n-2}, b_1, \dots, b_{n-2}) \mapsto [(1/a_1, \dots, 1/a_{n-2}, b_1, \dots, b_{n-2})].$$

**Lemma 3.38** (Update rules for  $\epsilon_n^{k,l}$ ). Let  $n \geq 3$ , and for  $1 \leq k \leq l \leq n-1$  let  $\epsilon_n^{k,l}$  denote the braid  $\sigma_k^{-1}\sigma_{k+1}^{-1}\dots\sigma_{l-1}^{-1}\sigma_l^{-1}$ . Given  $(a, b) \in \mathcal{C}_n$  and an integer  $j$  with  $k-1 \leq j \leq n-2$ , write

$$\check{P}_j = \check{P}_j(b, k) = \left[ (1 + b_{k-1}) \prod_{i=k}^j b_i \right].$$

(Note the interpretation of this formula in special cases:  $\check{P}_j(b, k) = \left[ \prod_{i=k}^j b_i \right]$  if  $k = 1$ ,  $\check{P}_j(b, k) = [(1 + b_{k-1})]$  if  $j = k-1$ , and  $\check{P}_j(b, k) = [1]$  if  $k = 1$  and  $j = 0$ .) Similarly, for  $k \leq j \leq n-2$ , write

$$\check{S}_j = \check{S}_j(a, b, k) = \left[ \sum_{i=k}^j a_i (1 + b_i) \check{P}_{i-1} \right].$$

Let  $(a', b') = \epsilon_n^{k,l}(a, b)$ . Then  $a'_j = a_j$  and  $b'_j = b_j$  for  $j < k-1$  and for  $j > l$ . Moreover,

1. If  $k > 1$  and  $l < n-1$  then

$$\begin{aligned} a'_{k-1} &= \left[ \frac{a_k a_{k-1}}{a_k(1 + b_{k-1}) + a_{k-1} b_{k-1}} \right], & b'_{k-1} &= \left[ \frac{a_{k-1} b_{k-1} b_k}{a_k(1 + b_{k-1})(1 + b_k) + a_{k-1} b_{k-1}} \right], \\ a'_j &= \left[ \frac{a_{k-1} a_{j+1}}{a_{k-1} b_{k-1} + \check{S}_j + a_{j+1} \check{P}_j} \right], & b'_j &= \left[ b_{j+1} \left( \frac{a_{k-1} b_{k-1} + \check{S}_j}{a_{k-1} b_{k-1} + \check{S}_{j+1}} \right) \right] \quad (k \leq j < l), \\ a'_l &= \left[ \frac{a_{k-1}(1 + b_{k-1}) + \check{S}_l}{\check{P}_l} \right], & b'_l &= \left[ \frac{a_{k-1} b_{k-1} + \check{S}_l}{a_{k-1}} \right]. \end{aligned}$$

2. If  $k > 1$  and  $l = n-1$  then the formulae in case 1 hold for  $k-1 \leq j < n-2$ , while

$$a'_{n-2} = \left[ \frac{a_{k-1}}{a_{k-1} b_{k-1} + \check{S}_{n-2} + \check{P}_{n-2}} \right], \quad b'_{n-2} = \left[ \frac{1}{\check{P}_{n-2}} (a_{k-1} b_{k-1} + \check{S}_{n-2}) \right].$$

3. If  $k = 1$  and  $l < n-1$  then

$$\begin{aligned} a'_j &= \left[ \frac{a_{j+1}}{a_{j+1} \check{P}_j + \check{S}_j} \right], & b'_j &= \left[ \frac{b_{j+1} \check{S}_j}{\check{S}_{j+1}} \right] \quad (1 \leq j < l), \\ a'_l &= \left[ \frac{1 + \check{S}_l}{\check{P}_l} \right], & b'_l &= [\check{S}_l]. \end{aligned}$$

4. If  $k = 1$  and  $l = n - 1$  then the formulae in case 3 hold for  $1 \leq j < n - 2$ , while

$$a'_{n-2} = \left[ \frac{1}{\check{P}_{n-2} + \check{S}_{n-2}} \right], \quad b'_{n-2} = \left[ \check{S}_{n-2} / \check{P}_{n-2} \right].$$

**Lemma 3.39** (Update rules for  $\zeta_n^{k,l}$ ). Let  $n \geq 3$ , and for  $1 \leq k \leq l \leq n - 1$  let  $\zeta_n^{k,l}$  denote the braid  $\sigma_l^{-1} \sigma_{l-1}^{-1} \dots \sigma_{k+1}^{-1} \sigma_k^{-1} \in B_n$ .

Given  $(a, b) \in \mathcal{C}_n$  and an integer  $j$  with  $\max(k - 1, 1) \leq j \leq l$  write

$$\hat{P}_j = \hat{P}_j(b, l) = \left[ (1 + b_l) \prod_{i=j}^l \frac{1}{b_i} \right].$$

(In the special case  $l = n - 1$ ,  $\hat{P}_j(b, n - 1) = \left[ \prod_{i=j}^{n-2} \frac{1}{b_i} \right]$  for  $j < l$ , while  $\hat{P}_{n-1}(b, n - 1) = [1]$ .) Similarly, for  $\max(k - 1, 1) \leq j \leq l - 1$  write

$$\hat{S}_j = \hat{S}_j(a, b, l) = \left[ \sum_{i=j}^{l-1} \frac{(1 + b_i) \hat{P}_{i+1}}{a_i b_i} \right].$$

Let  $(a', b') = \zeta_n^{k,l}(a, b)$ . Then  $a'_j = a_j$  and  $b'_j = b_j$  for  $j < k - 1$  and for  $j > l$ . Moreover,

1. If  $k > 1$  and  $l < n - 1$  then

$$\begin{aligned} a'_{k-1} &= \left[ \frac{a_l b_l \hat{P}_{k-1}}{(1 + b_l) + a_l b_l \hat{S}_{k-1}} \right], & b'_{k-1} &= \left[ \frac{b_l}{a_l b_l \hat{S}_{k-1} + 1} \right], \\ a'_j &= \left[ \frac{a_l b_l (a_{j-1} \hat{S}_j + \hat{P}_j) + a_{j-1}}{b_l} \right], & b'_j &= \left[ b_{j-1} \left( \frac{a_l b_l \hat{S}_{j-1} + 1}{a_l b_l \hat{S}_j + 1} \right) \right] \quad (k \leq j < l), \\ a'_l &= \left[ \frac{a_{l-1} + a_l (1 + b_l)}{b_l} \right], & b'_l &= \left[ \frac{a_l (1 + b_{l-1}) (1 + b_l) + a_{l-1} b_{l-1}}{a_{l-1}} \right]. \end{aligned}$$

2. If  $k = 1$  and  $l < n - 1$  then the formulae in case 1 hold for  $2 \leq j \leq l$ , while

$$a'_1 = \left[ \frac{a_l b_l (\hat{P}_1 + \hat{S}_1) + 1}{b_l} \right], \quad b'_1 = \left[ \frac{a_l b_l \hat{P}_1}{1 + a_l b_l \hat{S}_1} \right].$$

3. If  $k > 1$  and  $l = n - 1$  then

$$\begin{aligned} a'_j &= \left[ \hat{P}_j + a_{j-1} \hat{S}_j \right], & b'_j &= \left[ b_{j-1} \hat{S}_{j-1} / \hat{S}_j \right] \quad (k \leq j \leq n - 2), \\ a'_{k-1} &= \left[ \hat{P}_{k-1} / (1 + \hat{S}_{k-1}) \right], & b'_{k-1} &= \left[ 1 / \hat{S}_{k-1} \right]. \end{aligned}$$

4. If  $k = 1$  and  $l = n - 1$  then the formulae in case 3 hold for  $2 \leq j \leq n - 2$ , while

$$a'_1 = [\hat{P}_1 + \hat{S}_1], \quad b'_1 = [\hat{P}_1/\hat{S}_1].$$

### 3.6 Dynnikov coordinates of measured foliations

The Dynnikov coordinates for integral laminations can be extended in a natural way to Dynnikov coordinates of measured foliations. We first recall from Definitions 2.35 that if  $\alpha \in \mathcal{A}_n$ , then its measure  $\mu(\alpha)$  is defined to be

$$\mu(\alpha) = \sup \sum_{i=1}^k \mu(\alpha_i),$$

where the supremum is taken over all finite collections  $\alpha_1, \dots, \alpha_k$  of mutually disjoint subarcs of  $\alpha$  which are transverse to  $\mathcal{F}$  and the isotopy class  $[\alpha]$  (under isotopies through  $\mathcal{A}_n$ ), has measure

$$\mu([\alpha]) = i(\mathcal{F}, [\alpha]) = \inf_{\beta \in [\alpha]} \mu(\beta),$$

which is well defined on  $\mathcal{MF}_n$ .

**Definition 3.40.** The *Dynnikov coordinate function*  $\rho : \mathcal{MF}_n \rightarrow \mathbb{R}^{2n-4} \setminus \{0\}$  is defined by

$$\rho(\mathcal{L}) = (a, b) = (a_1, \dots, a_{n-2}, b_1, \dots, b_{n-2}),$$

where for  $1 \leq i \leq n - 2$

$$a_i = \frac{\mu([\alpha_{2i}]) - \mu([\alpha_{2i-1}])}{2} \quad \text{and} \quad b_i = \frac{\mu([\beta_i]) - \mu([\beta_{i+1}])}{2} \quad (3.14)$$

$\mathcal{S}_n = \mathbb{R}^{2n-4} \setminus \{0\}$  denotes the space of Dynnikov coordinates of measured foliations on  $D_n$ .

Dynnikov's coordinate system provides an explicit bijection  $\rho : \mathcal{MF}_n \rightarrow \mathcal{S}_n$  that is, a global coordinate system on  $\mathcal{MF}_n$ .

**Theorem 3.41.** *Let  $(a, b) = (a_1, a_2, \dots, a_{n-2}, b_1, b_2, \dots, b_{n-2}) \in \mathbb{R}^{2n-4} \setminus \{0\}$ . Then  $(a, b)$  is the Dynnikov coordinate of exactly one element  $(\mathcal{F}, \mu) \in \mathcal{MF}_n$ ,*

which has

$$\mu([\beta_i]) = 2 \max_{1 \leq k \leq n-2} \left[ |a_k| + \max(b_k, 0) + \sum_{j=1}^{k-1} b_j \right] - 2 \sum_{j=1}^{i-1} b_j$$

$$\mu([\alpha_i]) = \begin{cases} (-1)^i a_{\lceil i/2 \rceil} + \frac{\mu([\beta_{\lceil i/2 \rceil}])}{2} & \text{if } b_i \geq 0; \\ (-1)^i a_{\lceil i/2 \rceil} + \frac{\mu([\beta_{1+\lceil i/2 \rceil}])}{2} & \text{if } b_i \leq 0 \end{cases}$$

*Proof.* The proof is identical to the proof of Theorem 3.19 □

Projectivizing Dynnikov coordinates yields an explicit bijection between  $\mathcal{S}_n/\mathbb{R}^+$  and  $S^{2n-5} \cong \mathcal{PMF}_n$ . Let  $\mathcal{PS}_n$  denote the space of projective Dynnikov coordinates and  $\rho(\mathcal{F}, \mu) = (a, b)$ . We shall write  $[a, b] \in \mathcal{PS}_n$  to denote the Dynnikov coordinates of the projective class  $[\mathcal{F}, \mu]$  on  $\mathcal{PMF}_n$ . Given a braid  $\beta \in B_n$ , the update rules describe the action of  $\beta$  on  $\mathcal{PS}_n$  and the various maxima in the update rules induce a piecewise linear action of  $\beta$  on  $\mathcal{PS}_n$ . This will be illustrated with an example in the next chapter.

## Chapter 4

# Computing topological entropy of families of braids

In this chapter we shall describe a new method for computing the topological entropy of families of pseudo-Anosov braids, making use of Dynnikov's coordinates on the boundary of Teichmüller space. The method will be illustrated with two families of braids considered in [20], which are of interest in the study of braids of low topological entropy. These families are  $\{\beta_{m,n} : m, n \geq 1\}$ , and  $\{\sigma_{m,n} : 1 \leq m \leq n\}$ , where

$$\beta_{m,n} = \sigma_1 \dots \sigma_m \sigma_{m+1}^{-1} \dots \sigma_{m+n}^{-1} = \gamma_{m+n+1}^{1,m} \epsilon_{m+n+1}^{m+1,m+n} \in B_{m+n+1}, \quad \text{and}$$

$$\sigma_{m,n} = \sigma_1 \dots \sigma_m \sigma_m \dots \sigma_1 \sigma_1 \dots \sigma_{m+n} = \gamma_{m+n+1}^{1,m} \delta_{m+n+1}^{1,m} \gamma_{m+n+1}^{1,m+n} \in B_{m+n+1}.$$

The normal approach to compute the topological entropy of an isotopy class is to use train-track methods [5, 17, 22]. In [5], the algorithm starts with a graph  $G$  which is a spine of the surface and the isotopy class is represented by a graph map. The algorithm repeatedly modifies  $G$  until it either finds an explicit reducing curve for the isotopy class, or a graph map which is the simplest possible (that is, one with minimum growth rate). If the isotopy class is pseudo-Anosov, this simplest graph map can be used to construct a train track and train track map from which the invariant foliations are obtained.

However, for complicated isotopy classes (that is, ones with high topological entropy), the lengths of the image edge paths (represented by words whose letters label the edges) of the train track are so long that even a computer cannot store them (note that the image edge paths grow like  $\lambda$ ). Therefore, it is usually far from straightforward to describe an infinite family of train tracks and to verify that they are indeed invariant under the action of relevant isotopy classes. Nevertheless, until now computing the topological entropy of family of braids has

been established only through train tracks. In 2006 Moussafir [25] approached the problem making use of Dynnikov coordinates and update rules [14]. The major advantage of his method which is described in Section 4.1 below, is that it works much faster and is more direct than the train-track approach. However, the method is numerical and only gives an estimate for braid entropy. The method which we shall introduce in this chapter provides the exact topological entropy.

## 4.1 Topological Entropy of pseudo-Anosov braids and Moussafir's iterative technique

Our aim in this section is to explain briefly why the topological entropy  $h(f)$  of a given pseudo-Anosov map  $f \in \text{Aut}(D_n)$  is  $\log \lambda$ , where  $\lambda$  is the dilatation of  $f$ ; and then Moussafir's method [25] for estimating the topological entropy of braids making use of Dynnikov coordinates and update rules [14], which is the motivation for our method.

Let  $M$  be a compact manifold and  $f : M \rightarrow M$  be a continuous map. There is an important relationship between the topological entropy of  $f$  and the induced action  $f_* : \pi_1(M) \rightarrow \pi_1(M)$  on the fundamental group  $\pi_1(M)$  of  $M$ . If  $\lambda$  is the growth rate of  $f_*$ , then  $h(f) \geq \log \lambda$  [9, 16]. This follows from Manning's theorem [23] which states that  $h(f) \geq \log |\lambda|$  for all eigenvalues  $\lambda$  of the induced action  $f_{*1} : H_1(M; \mathbb{R}) \rightarrow H_1(M; \mathbb{R})$  on the first homology group. If  $f \in \text{Aut}(M)$  is pseudo-Anosov we can obtain the reverse inequality,  $h(f) \leq \log \lambda$ , by constructing a subshift of finite type as described in [16]. Every pseudo-Anosov map has a Markov partition [16] and one way to construct it is by means of its invariant train track.

In [25] Moussafir introduced an alternative method for computing the topological entropy of braids making use of Dynnikov coordinates and update rules [14]. The main idea of his approach lies in Theorem 2.56. That is, if  $\lambda$  is the dilatation of a given pseudo-Anosov braid  $\beta \in B_n$ , then for any essential simple closed curves  $\alpha$  and  $\beta$ , the geometric intersection number  $i(f^n(\alpha), \beta)$  grows like  $C \times \lambda^n$  as  $n \rightarrow \infty$ . The method starts with a relaxed integral lamination which is denoted  $\mathcal{L}_0^n$  given with its Dynnikov coordinates  $\rho(\mathcal{L}_0^n) = (a, b)$ , and assigns to it a sequence

$$c_m = \frac{1}{m} \log c(\beta^m \mathcal{L}_0^n)$$

where  $\rho(\beta^m \mathcal{L}_0^n)$  is obtained from the update rules and  $c(\beta^m \mathcal{L}_0^n)$  denotes the minimum number of intersections of  $\beta^m \mathcal{L}_0^n$  with the  $x$ -axis. Given  $\mathcal{L} \in \mathcal{L}_n$  with



$\rho(\mathcal{L}) = (a, b)$ ,  $c(\mathcal{L})$  is given by the formula

$$c(\mathcal{L}) = \sum_{i=1}^n |b_i| + \sum_{i=1}^{n-1} |a_{i+1} - a_i| + |a_1| + |a_n| + \frac{\beta_1}{2} + \frac{\beta_{n-1}}{2}.$$

(we note that  $B_n$  acts on  $D_{n+2}$  in Moussafir's paper and hence each integral lamination is assigned a point from  $\mathbb{R}^{2n}$ ).

Then, the method ends when  $|c_m - c_{m+1}| < \epsilon$  for a chosen  $\epsilon > 0$ . Therefore an estimate for the topological entropy of  $\beta$  is obtained.

## 4.2 Computing Topological entropy of families of braids

In this section we shall introduce a new method for computing the topological entropy of each braid in an infinite family, making use of Dynnikov's coordinates on the boundary of Teichmüller space. The method will be illustrated on the following two-parameter families of braids [20]

$$\beta_{m,n} = \sigma_1 \dots \sigma_m \sigma_{m+1}^{-1} \dots \sigma_{m+n}^{-1} = \gamma_{m+n+1}^{1,m} \epsilon_{m+n+1}^{m+1,m+n} \in B_{m+n+1}, \quad \text{and}$$

$$\sigma_{m,n} = \sigma_1 \dots \sigma_m \sigma_m \dots \sigma_1 \sigma_1 \dots \sigma_{m+n} = \gamma_{m+n+1}^{1,m} \delta_{m+n+1}^{1,m} \gamma_{m+n+1}^{1,m+n} \in B_{m+n+1}.$$

The method, and in particular the transparency of the calculations, can be contrasted with the train track methods in [20]. First, we shall reinterpret some of the results of Thurston theory in Section 2.4.1 in terms of Dynnikov coordinates. We begin with the following lemma restating Nielsen-Thurston's Theorem in terms of Dynnikov coordinates.

**Lemma 4.1.** *Let  $\beta \in B_n$ . Then*

- i.  $\beta$  is reducible if and only if there is some  $(a, b) \in \mathcal{C}_n$  with  $\beta(a, b) = (a, b)$ .
- ii. If  $\beta$  is not reducible, then
  - $\beta$  is finite order if and only if there is some  $N > 1$  such that  $\beta^N(a, b) = (a, b)$  for all  $(a, b) \in \mathcal{S}_n$ .
  - $\beta$  is pseudo-Anosov if and only if there is some  $(a^u, b^u) \in \mathcal{S}_n$  and a number  $\lambda > 1$  (the dilatation) such that  $\beta(a^u, b^u) = \lambda(a^u, b^u)$ . In this case there is also some  $(a^s, b^s) \in \mathcal{S}_n$  such that  $\beta(a^s, b^s) = \frac{1}{\lambda}(a^s, b^s)$ .

*Proof.* The first statement i. is immediate from Definition 2.44. Suppose i. does not hold. Then  $\beta$  is not reducible. Hence, by Theorem 2.48  $\beta$  is either finite-order or pseudo-Anosov. Assume that  $\beta$  is pseudo-Anosov. Then, by Definition 2.47,

there exists  $(a^u, b^u)$  and  $(a^s, b^s)$  and  $\lambda > 1$  with  $\beta(a^u, b^u) = \lambda(a^u, b^u)$  and  $\beta(a^s, b^s) = \frac{1}{\lambda}(a^s, b^s)$ . Now assume that there exists  $(a^u, b^u) \in \mathcal{S}_n$  and  $\lambda > 1$  with  $\beta(a^u, b^u) = \lambda(a^u, b^u)$ . Since  $\beta(a^u, b^u) = \lambda(a^u, b^u)$  then  $\beta^N(a^u, b^u) = \lambda^N(a^u, b^u)$ . Thus  $\beta$  is not finite order and hence is pseudo-Anosov.

Similarly, assume that  $\beta$  is finite-order with  $\beta^N = Id$ . Then  $\beta^N(a, b) = (a, b)$  for all  $(a, b) \in \mathcal{S}_n$ . Conversely, if there is some  $N > 1$  such that  $\beta^N(a, b) = (a, b)$  for all  $(a, b) \in \mathcal{S}_n$ , then  $f$  can't be pseudo-Anosov since  $\beta^N(a^u, b^u) = \lambda^N(a^u, b^u)$  for some  $(a^u, b^u) \in \mathcal{S}_n$ . Therefore,  $f$  is finite-order.  $\square$

Let  $\beta \in B_n$  be a pseudo-Anosov braid with unstable and stable invariant foliations having Dynnikov coordinates  $(a^u, b^u)$  and  $(a^s, b^s)$ . Let  $[a^u, b^u]$  and  $[a^s, b^s]$  denote the projective classes of  $(a^u, b^u)$  and  $(a^s, b^s)$  on  $\mathcal{PS}_n$  respectively. By Theorem 2.58 and Theorem 2.57, we get the following two lemmas.

**Lemma 4.2.** *The only fixed points of  $\beta$  on  $\mathcal{PS}_n$  are  $[a^u, b^u]$  and  $[a^s, b^s]$ .*

Therefore, any  $(a, b) \in \mathcal{S}_n$  satisfying  $\beta(a, b) = k(a, b)$  for some  $k > 0$  is a multiple either of  $(a^u, b^u)$  or of  $(a^s, b^s)$ .

**Lemma 4.3.** *For any  $[a, b] \in \mathcal{PS}_n$ , with  $[a, b] \neq [a^s, b^s]$ ,*

$$\lim_{n \rightarrow \infty} \beta^n([a, b]) = [a^u, b^u].$$

In the previous chapter we stated that the update rules define piecewise linear action of braids on  $\mathcal{PMF}_n$  since one obtains linear maps with integer coefficients when the various maxima in the formulae in Theorem 3.33 and Theorem 3.35 are resolved. Now, we shall illustrate this with an example. That is, we shall compute the action of  $\sigma_1\sigma_2^{-1} \in B_3$  on  $\mathcal{PMF}_3$ .

**Example 4.4.** Let  $\mathcal{PMF}_3 \cong S^1$  be the space of projective measured foliations on  $D_3$ . In this example, we shall work out the update rules for  $\sigma_1\sigma_2^{-1}$  on  $\mathcal{PMF}_3$ . That is, we shall explicitly compute the  $2 \times 2$  integer matrices which describe the piecewise linear action of  $\sigma_1\sigma_2^{-1}$  on  $\mathcal{PMF}_3$ . This example is important since it concretely illustrates the action of a pseudo-Anosov braid (which is the simplest possible) on the whole space  $\mathcal{PMF}_3$ . Let  $(a, b) \in \mathcal{S}_3$ ,  $\sigma_1(a, b) = (a', b')$  and  $\sigma_2^{-1}(a', b') = (a'', b'')$ . From Theorem 3.33,

$$a' = \left[ \frac{ab}{1+a+b} \right] \quad b' = \left[ \frac{1+b}{a} \right]$$

that is

$$a' = a + b - \max\{0, a, b\} \quad b' = \max\{b, 0\} - a$$

From Theorem 3.35 acting by  $\sigma_2^{-1}$  yields

$$a'' = a' - \max\{a' + b', b', 0\}, \quad b'' = a' + b' - \max\{b', 0\}.$$

There are four main cases to consider.

i.  $a \leq 0, b \leq 0$  :

$$a' = a + b \quad \text{and} \quad b' = -a$$

$$\begin{aligned} a'' &= a + b - \max\{a + b - a, -a, 0\} & b'' &= a + b - a - \max\{-a, 0\} \\ &= 2a + b & &= a + b \end{aligned}$$

Hence the action is given by the matrix;

$$\begin{bmatrix} 2 & 1 \\ 1 & 1 \end{bmatrix}.$$

ii.  $a \geq 0, b \leq 0$  :

$$a' = a + b - a = b \quad \text{and} \quad b' = -a.$$

$$\begin{aligned} a'' &= b - \max\{b - a, -a, 0\} & b'' &= b - a - \max\{-a, 0\} \\ &= b & &= b - a \end{aligned}$$

The action is given by the matrix;

$$\begin{bmatrix} 0 & 1 \\ -1 & 1 \end{bmatrix}.$$

iii.  $a \leq 0, b \geq 0$  :

$$a' = a + b - b = a \quad \text{and} \quad b' = b - a.$$

$$\begin{aligned} a'' &= a - \max\{a + b - a, b - a, 0\} & b'' &= a + b - a - \max\{b - a, 0\} \\ &= 2a - b & &= a. \end{aligned}$$

The action is given by the matrix;

$$\begin{bmatrix} 2 & -1 \\ 1 & 0 \end{bmatrix}.$$

iv.  $a \geq 0, b \geq 0$  :

$$a' = a + b - \max(a, b) \quad \text{and} \quad b' = \max\{b, 0\} - a = b - a.$$

Therefore, we distinguish two cases:  $a \geq b$  and  $b \geq a$ .

- If  $a \geq b$ , we have  $a' = b$  and  $b' = b - a$ . Then,

$$a'' = a' - \max\{a' + b', b', 0\} = b - \max\{2b - a, b - a, 0\}$$

and,

$$b'' = a' + b' - \max(b', 0) = 2b - a.$$

We distinguish two subcases:  $2b \geq a$  and  $2b \leq a$ .

– If  $2b \geq a$  we have

$$a'' = a - b \quad \text{and} \quad b'' = 2b - a$$

and the corresponding matrix is

$$\begin{bmatrix} 1 & -1 \\ -1 & 2 \end{bmatrix}.$$

– If  $2b \leq a$  we have

$$a'' = a \quad \text{and} \quad b'' = 2b - a$$

and the corresponding matrix is

$$\begin{bmatrix} 1 & 0 \\ -1 & 2 \end{bmatrix}.$$

- If  $a \leq b$ , we have  $a' = a$  and  $b' = b - a$ . Then,

$$a'' = b - a \quad \text{and} \quad b'' = a$$

and the corresponding matrix is

$$\begin{bmatrix} -1 & 1 \\ 1 & 0 \end{bmatrix}.$$

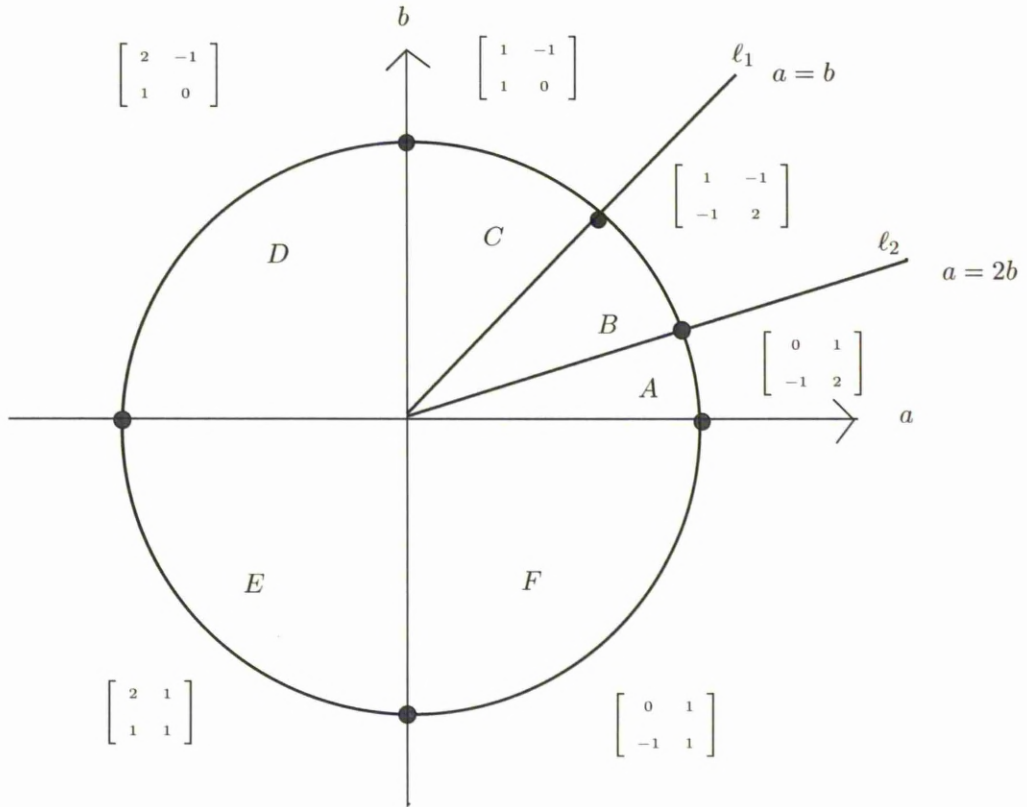


Figure 4.1: The action of  $\sigma_1\sigma_2^{-1}$  on the boundary of the Teichmüller Space,  $S^1$

The piecewise linear action of  $\sigma_1\sigma_2^{-1}$  is illustrated in Figure 4.1. Let  $\ell_1$  and  $\ell_2$  denote the lines  $a = b$  and  $a = 2b$  in the first quadrant. Let  $+a$  ( $-a$ ) and  $+b$  ( $-b$ ) denote the positive (negative)  $a$ -axis and  $b$ -axis respectively. Write  $x \rightarrow y$  if  $x$  is sent onto  $y$  by the action of  $\sigma_1\sigma_2^{-1}$ . Then we have  $\ell_1 \rightarrow +b \rightarrow -a$ ,  $\ell_2 \rightarrow +a \rightarrow -b$  and then  $-a$  and  $-b$  are sent into the interior of  $E$ . Hence  $A \rightarrow F \rightarrow E$  and  $C \rightarrow D \rightarrow E$ . Therefore, we can see that  $p^u = [a^u, b^u]$  lies in region  $E$  and  $p^s = [a^s, b^s]$  lies in region  $B$ .

Indeed the matrix

$$D = \begin{bmatrix} 2 & 1 \\ 1 & 1 \end{bmatrix}$$

has an eigenvalue  $\lambda > 1$  and the eigenvector  $p^u = [a^u, b^u]$  corresponding to it belongs to  $E$ . That is,  $a^u \leq 0$  and  $b^u \leq 0$ . Hence  $p^u$  is a fixed point for  $\sigma_1\sigma_2^{-1}$  on  $\mathcal{PS}_3$ . Hence, by Lemma 4.2  $p^u = [a^u, b^u]$  corresponds to the invariant unstable

foliation  $[\mathcal{F}^u, \mu^u]$ . Similarly, the matrix

$$\begin{bmatrix} 1 & -1 \\ -1 & 2 \end{bmatrix}$$

has an eigenvalue  $1/\lambda$  and the associated eigenvector  $p^s$  belongs to the region  $a \geq 0$ ,  $b \geq 0$ ,  $b \leq a \leq 2b$ . Hence  $p^s$  is a fixed point and corresponds to the invariant stable foliation  $[\mathcal{F}^s, \mu^s]$ .

In this example,  $p^u = -(\frac{1+\sqrt{5}}{2}, 1)$  and  $\lambda = \frac{3+\sqrt{5}}{2}$ . Therefore, the topological entropy is  $\log(\frac{3+\sqrt{5}}{2})$ .

The collection of linear equations (not necessarily independent) in various maxima in update rules give each region on  $\mathcal{PS}_n$  the structure of a polyhedron. One can see this in Figure 4.1 by observing that each region is a solution set for a system of linear inequalities induced by these equations. Let  $p^u = (a^u, b^u)$  and  $p^s = (a^s, b^s)$  denote the Dynnikov coordinates of  $(\mathcal{F}^u, \mu^u)$  and  $(\mathcal{F}^s, \mu^s)$  respectively. Next we define the *Dynnikov matrices* which describe the action of  $\beta$  near  $p^u$ .

**Definition 4.5.** Let  $\beta \in B_n$  be a pseudo-Anosov braid with invariant unstable measured foliation  $(\mathcal{F}^u, \mu^u)$  given by the Dynnikov coordinates  $p^u = (a^u, b^u)$ . The action of  $\beta$  on  $\mathcal{S}_n$  is piecewise linear and each closed piece  $\mathcal{R}_i \subset \mathcal{S}_n$  containing  $(a^u, b^u)$  is called a *Dynnikov region*. Then a *Dynnikov matrix*  $D_i : \mathcal{R}_i \rightarrow \mathcal{S}_n$ , ( $1 \leq i \leq k$ ) is a  $(2n-4) \times (2n-4)$  integer matrix which describes the behaviour of the braid on a Dynnikov region  $\mathcal{R}_i$ . That is,

$$\rho(\beta(\mathcal{F}, \mu)) = D_i(a, b) \text{ for } (a, b) \in \mathcal{R}_i.$$

**Example 4.6.** There is one Dynnikov region for  $\sigma_1\sigma_2^{-1}$  which is

$$\mathcal{R} = \{[a, b] \in S^1 : a \leq 0, b \leq 0\}.$$

Hence, the Dynnikov matrix is

$$\begin{bmatrix} 2 & 1 \\ 1 & 1 \end{bmatrix}$$

as computed in Example 4.4.

**Remark 4.7.** There can be more than one Dynnikov region for a given pseudo-Anosov braid  $\beta$ . This happens when  $(a^u, b^u)$  is on the boundary of several regions on  $\mathcal{S}_n$ .

We shall illustrate this case with the following example:

**Example 4.8.** Take  $\beta = \sigma_1\sigma_2\sigma_3\sigma_4^{-1} \in B_5$ . By Theorem 3.33 and Theorem 3.35 we can compute the action of  $\sigma_1\sigma_2\sigma_3\sigma_4^{-1}$  on  $\mathcal{S}_5$ . We restrict to the case in which  $a_i \leq 0$  and  $b_i \leq 0$  for all  $i$  (it will be seen shortly that all of the coordinates of the unstable foliation of  $\beta$  are negative). Let  $(a, b) \in \mathcal{S}_5$ , and write  $(a', b') = \sigma_1(a, b)$ ,  $(a'', b'') = \sigma_2(a', b')$ ,  $(a''', b''') = \sigma_3(a'', b'')$  and  $(a''', b''') = \sigma_4^{-1}(a''', b''')$ .

$$\begin{aligned} a'_1 &= a_1 + b_1, & b'_1 &= -a_1 \\ a''_1 &= \max(a'_1 + b'_1, a'_2 + b'_1) = \max(b_1, a_2 - a_1) \\ b''_1 &= a'_2 + b'_1 + b'_2 - \max(a'_1 + b'_1, a'_2 + b'_1) \\ &= a_2 - a_1 + b_2 - \max(b_1, a_2 - a_1) \end{aligned}$$

We distinguish two cases:  $b_1 \leq a_2 - a_1$  and  $b_1 \geq a_2 - a_1$ .

- $b_1 \leq a_2 - a_1$ . We have,

$$\begin{aligned} a''_1 &= \max(b_1, a_2 - a_1) = a_2 - a_1 \\ b''_1 &= a'_2 + b'_1 + b'_2 - \max(a'_1 + b'_1, a'_2 + b'_1) = b_2 \\ a''_2 &= a'_1 + a'_2 + b'_2 - \max(a'_1, a'_2) = a_1 + b_1 + b_2 \\ b''_2 &= \max(a'_1 + b'_1, a'_2 + b'_1) - a'_2 = -a_1 \\ a''_2 &= \max(a''_2 + \max(b''_2, 0), a''_3 + b''_2) = b_1 + b_2 \\ b''_2 &= a''_3 + b''_2 + b''_3 - \max(a''_2 + \max(b''_2, 0), a''_3 + b''_2) = a_3 - a_1 + b_3 - b_1 - b_2 \\ a''_3 &= a''_2 + a''_3 + b''_3 - \max(a''_2 + \max(b''_3, 0), a''_3) = a_3 + b_3 \\ b''_3 &= \max(a''_2 + \max(b''_2, 0) + \max(b''_3, 0), a''_3 + b''_2) = b_1 + b_2 - a_3 \end{aligned}$$

Finally,

$$\begin{aligned} a'''_3 &= a''_3 - \max(a''_3 + b''_3, 0, b''_3) = 2a_3 - b_1 - b_2 + b_3 \\ b'''_3 &= a''_3 + b''_3 - \max(0, b''_3) = a_3 + b_3. \end{aligned}$$

Therefore the matrix induced by this action is

$$D_1 = \begin{bmatrix} -1 & 1 & 0 & 0 & 0 & 0 \\ 0 & 0 & 0 & 1 & 1 & 0 \\ 0 & 0 & 2 & -1 & -1 & 1 \\ 0 & 0 & 0 & 0 & 1 & 0 \\ -1 & 0 & 1 & -1 & -1 & 1 \\ 0 & 0 & 1 & 0 & 0 & 1 \end{bmatrix}$$

- Similar calculations for the latter case  $b_1 \geq a_2 - a_1$  give

$$D_2 = \begin{bmatrix} 0 & 0 & 0 & 1 & 0 & 0 \\ 0 & 0 & 0 & 1 & 1 & 0 \\ 0 & 0 & 2 & -1 & -1 & 1 \\ -1 & 1 & 0 & -1 & 1 & 0 \\ 0 & -1 & 1 & 0 & -1 & 1 \\ 0 & 0 & 1 & 0 & 0 & 1 \end{bmatrix}$$

Both of these matrices have eigenvalue  $\frac{3+\sqrt{5}+\sqrt{6\sqrt{5}-2}}{4}$ , with the corresponding eigenvector  $p^u$  having all negative entries and satisfying the equality  $a_2 = a_1 + b_1$ . Therefore, both  $D_1$  and  $D_2$  are Dynnikov matrices. In fact  $D_1$  and  $D_2$  are isospectral, we shall return to this issue in Chapter 6.

Example 4.4 gives the idea of our method to find the dilatation of a given braid  $\beta \in B_n$ : Compute the action of  $\beta \in B_n$  on  $\mathcal{S}_n$  using the update rules, find a matrix with an eigenvalue  $\lambda > 1$  and check whether the associated eigenvector is contained in the corresponding region or not. In other words, find a Dynnikov matrix for  $\beta$  and compute its dilatation  $\lambda > 1$ .

### 4.3 The braids $\beta_{m,n}$

The following results establish that  $\beta_{m,n}$ ;  $m, n \geq 1$  and  $\sigma_{m,n}$ ;  $n \geq m + 2$  as defined on page 83 are pseudo-Anosov and give formulae for the topological entropies  $h(\beta_{m,n})$  and  $h(\sigma_{m,n})$ .



**Theorem 4.9.** *Let  $m, n \geq 1$ . Then  $\beta_{m,n} \in B_{m+n+1}$  is a pseudo-Anosov braid, whose dilatation  $r$  is the unique root in  $(1, \infty)$  of the polynomial*

$$f_{m,n}(r) = (r-1)(r^{m+n+1} - 1) - 2r(r^m + r^n).$$

*The Dynnikov coordinates  $(a^u, b^u) \in \mathcal{S}_{m+n+1}$  of the unstable invariant measured foliation of  $\beta_{m,n}$  are given by*

$$a_i = \begin{cases} -r(r^n + 1)(r^i - 1) & \text{if } 1 \leq i \leq m-1 \\ -(r^{m+1} - 1)(r^{n+1} - 1) & \text{if } i = m \\ -(r^{m+1} - 1)(r^{m+n+1-i} - 1)r^{i-m} & \text{if } m+1 \leq i \leq m+n-1, \end{cases}$$

$$b_i = \begin{cases} -(r-1)(r^n + 1)r^{i+1} & \text{if } 1 \leq i \leq m-1 \\ -(r+1)(r^{m+1} - 1) & \text{if } i = m \\ -(r-1)(r^{m+1} - 1)r^{i-m} & \text{if } m+1 \leq i \leq m+n-1. \end{cases}$$

*Proof.*  $f_{m,n}$  has a root  $r > 1$  since  $f_{m,n}(1) = -4$ . It will be shown that  $\beta_{m,n}(a, b) = r(a, b)$ , from which the result (and the uniqueness of  $r$ ) follows.

Write  $N = m + n + 1$  and recall that  $\beta_{m,n} = \gamma_N^{1,m} \epsilon_N^{m+1, N-1}$ . Thus to show that  $\beta_{m,n}(a, b) = r(a, b)$  it suffices to show that  $\gamma_N^{1,m}(a, b) = r\delta_N^{m+1, N-1}(a, b)$ . It will be shown that each side of this equation is equal to  $(a', b')$ , where

$$(a'_j, b'_j) = \begin{cases} (ra_j, rb_j) & 1 \leq j < m \\ (a_m + b_m, r(r^n + 1)(r + 1)) & j = m \\ (a_j, b_j) & m < j \leq m + n - 1. \end{cases}$$

Observe that

$$ra_{m-1} - a_m + a_1 = f_{m,n}(r) + 2r(1 + r^n) = 2r(1 + r^n) > 0. \quad (4.1)$$

Consider first  $(a', b') = \gamma_N^{1,m}(a, b)$ , which is given by Lemma 3.36. The first step is to calculate the quantities  $P_j$  and  $S_j$  from the statement of Lemma 3.36 for  $1 \leq j \leq m$ .

Now  $P_j = \sum_{i=1}^j b_i$ , giving  $P_j = -r^2(r^n + 1)(r^j - 1) = ra_j$  for  $1 \leq j < m$ ; and hence  $P_m = P_{m-1} + b_m = ra_{m-1} + b_m$ . On the other hand,

$$S_j = \max_{1 \leq i \leq j} (\max(0, b_i) + P_{i-1} - a_i) = \max_{1 \leq i \leq j} (ra_{i-1} - a_i)$$

(setting  $a_0 = 0$ ), since  $b_i < 0$  for all  $i$ . Now  $ra_{i-1} - a_i = -a_1$  for all  $i < m$ , so  $S_j = -a_1$  for  $1 \leq j < m$ . Finally by (4.1)

$$S_m = \max(-a_1, ra_{m-1} - a_m) = ra_{m-1} - a_m.$$

Let  $1 \leq j \leq m-2$ . Then (using case 3 of Lemma 3.36)

$$a'_j = \max(P_j, a_{j+1} + S_j) = \max(ra_j, a_{j+1} - a_1) = \max(ra_j, ra_j) = ra_j \quad \text{and}$$

$$b'_j = b_{j+1} + S_j - S_{j+1} = b_{j+1} = rb_j$$

as required. Let  $j = m-1$ . Then

$$a'_{m-1} = \max(P_{m-1}, a_m + S_{m-1}) = \max(ra_{m-1}, a_m - a_1) = ra_{m-1}$$

by (4.1), and

$$b'_{m-1} = b_m + S_{m-1} - S_m = b_m - a_1 - (ra_{m-1} - a_m) = rb_{m-1}$$

as required.

Let  $j = m$ . Then

$$a'_m = P_m - \max(0, S_m) = ra_{m-1} + b_m - (ra_{m-1} - a_m) = a_m + b_m$$

as required, while

$$b'_m = S_m = ra_{m-1} - a_m = 2r(1 + r^n) - a_1$$

by (4.1), giving  $b'_m = r(r^n + 1)(r + 1)$  as required.

Now let  $(a'', b'') = \delta_N^{m+1, N-1}(a, b)$ . Showing that  $(a'', b'') = (a', b')/r$ , will complete the proof. The argument, using Lemma 3.37, is similar to the first part of the proof. Calculating the quantities  $\tilde{P}_j$  and  $\tilde{S}_j$  from the statement of Lemma 3.37 gives

$$\tilde{P}_j = r^{j-m}(r^{m+1} - 1)(r^{m+n-j} - 1), \quad \tilde{S}_j = -r^n(r-1)(r^{m+1} - 1) \quad (j > m),$$

$$\tilde{P}_m = (r^{m+1} - 1)(r^n + 1), \quad \tilde{S}_m = -(r+1)(r^n + 1).$$

Then, by case 3 of Lemma 3.37,

$$a''_m = \max(0, \tilde{S}_m) - \tilde{P}_m = -\tilde{P}_m = (a_m + b_m)/r,$$

$$b''_m = -\tilde{S}_m = (r^n + 1)(r + 1),$$

$$a''_{m+1} = a_m - \max(a_m + \tilde{P}_{m+1}, \tilde{S}_{m+1}) = a_m - \tilde{S}_{m+1} = a_{m+1}/r,$$

$$b''_{m+1} = b_m + \tilde{S}_m - \tilde{S}_{m+1} = b_{m+1}/r + f_{m,n}(r) = b_{m+1}/r,$$

$$a''_j = a_{j-1} - \max(a_{j-1} + \tilde{P}_j, \tilde{S}_j) = a_{j-1} - \tilde{S}_j = a_j/r \quad (j > m+1), \quad \text{and}$$

$$b''_j = b_{j-1} + \tilde{S}_{j-1} - \tilde{S}_j = b_{j-1} = b_j/r \quad (j > m+1)$$

as required. □

**Remark 4.10.** The singularity structure of the invariant foliation  $[\mathcal{F}_{m,n}^u, \mu_{m,n}^u]$  can be seen in its Dynnikov coordinates. The equations

$$\begin{aligned} a_{i+1} &= a_i + b_i & \text{if } 1 \leq i \leq m-2 \\ a_{i+1} &= a_i - b_i & \text{if } m+1 \leq i \leq m+n-2 \end{aligned}$$

correspond to the existence of an  $(m+1)$ -pronged and an  $(n+1)$ -pronged singularities respectively. This will be clarified in Section 4.5.

#### 4.4 The braids $\sigma_{m,n}$

In this section we study the braids  $\sigma_{m,n} = \sigma_1 \dots \sigma_m \sigma_m \dots \sigma_1 \sigma_1 \dots \sigma_{m+n} \in B_{m+n+1}$ . For  $1 \leq m \leq n$ ,  $\sigma_{m,n}$  is pseudo-Anosov if  $n \geq m+2$  and reducible if  $n = m+1$ . The statement that  $\sigma_{m,n}$  is pseudo-Anosov if  $n \geq m+2$  can be proven analogously to Theorem 4.9.

##### 4.4.1 The pseudo-Anosov case: $n \geq m+2$

**Theorem 4.11** (The braids  $\sigma_{m,n}$  for  $n \geq m+2$ ). *Let  $1 \leq m \leq n-2$ . Then  $\sigma_{m,n} \in B_{m+n+1}$  is a pseudo-Anosov braid, whose dilatation  $r$  is the unique root in  $(1, \infty)$  of the polynomial*

$$g_{m,n}(r) = (r-1)(r^{m+n+1} + 1) + 2r(r^m - r^n).$$

The Dynnikov coordinates  $(a^u, b^u) \in \mathcal{S}_{m+n+1}$  of the unstable invariant measured foliation of  $\sigma_{m,n}$  are given by

$$\begin{aligned} a_i &= \begin{cases} (r^n - 1)(r^{i+1} - 1)r & \text{if } 1 \leq i \leq m-1 \\ (r^{m+1} - 1)(r^{m+n-i} - 1)r^{i+1-m} & \text{if } m \leq i \leq m+n-1, \end{cases} \\ b_i &= \begin{cases} (r-1)(r^n - 1)r^{i+1} & \text{if } 1 \leq i \leq m-1 \\ (r-1)(r^{m+1} - 1)r^{i-m} & \text{if } m \leq i \leq m+n-1. \end{cases} \end{aligned}$$

*Proof.* Rewrite the polynomial  $g_{m,n}(r)$  as

$$(r-1)(r^{m+n+1} + 1 - 2r^{m+1}(1 + r + \dots + r^{n-m-1}))$$

and write  $\hat{g}_{m,n}(r)$  for the second factor of  $g_{m,n}(r)$  so that  $g_{m,n}(r) = (r-1)\hat{g}_{m,n}(r)$ . Then,  $\hat{g}_{m,n}(1) = 2 - 2(n-m)$  and hence  $\hat{g}_{m,n}(1) < 0$  since  $n-m \geq 2$ . There-

fore,  $\hat{g}_{m,n}$  must have a root  $r > 1$ . Now, assume that the following hold:

$$\begin{aligned}
a_i &\geq 0 & b_i &\geq 0 \\
b_i &\leq b_{i+1}, & 1 \leq i \leq m-2, & \quad m \leq i \leq m+n-2, \\
a_i &\geq b_i & 1 \leq i \leq m+n-1, \\
b_{i+1} &= a_{i+1} - a_i, & 1 \leq i \leq m-2 \\
b_{i+1} &= a_i - a_{i+1}, & m \leq i \leq m+n-2 \\
b_{m+n-1} &\leq b_{m-1}
\end{aligned}$$

(these conditions can easily be verified for  $(a, b)$  as given above).

Since  $\sigma_{m,n} = \gamma_{m+n+1}^{1,m} \delta_{m+n+1}^{1,m} \gamma_{m+n+1}^{1,m+n} \in B_{m+n+1}$ , the update rules for  $\sigma_{m,n}$  can be obtained by composing the rules for  $\gamma_{m+n+1}^{1,m}$ ,  $\delta_{m+n+1}^{1,m}$  and  $\gamma_{m+n+1}^{1,m+n}$  by letting  $(a', b') = \gamma_{m+n+1}^{1,m}(a, b)$ ,  $(a'', b'') = \delta_{m+n+1}^{1,m}(a, b)$  and  $(a''', b''') = \gamma_{m+n+1}^{1,m+n}(a'', b'')$ . Then, under the assumptions given above,  $(a''', b''')$  are given by

$$\begin{aligned}
a_i''' &= \begin{cases} a_{i+1} - a_1 + b_1 & 1 \leq i \leq m-1; \\ a_{i+1} + a_m - \sum_{j=1}^m b_j & m \leq i < m+n-2; \\ a_m - \sum_{j=1}^m b_j & i = m+n-1 \end{cases} \\
b_i''' &= \begin{cases} b_{i+1} & 1 \leq i \leq m-2, \quad m \leq i \leq m+n-2; \\ a_m - a_1 - \sum_{j=2}^{m-1} b_j & i = m-1; \\ a_m - \sum_{j=m+1}^{m+n-1} b_j & i = m+n-1 \end{cases}
\end{aligned}$$

It is easy to check that if  $(a''', b''') = \sigma_{m,n}(a, b)$  where  $(a, b)$  are as in the statement of the theorem, then  $(a''', b''') = r(a, b)$ .

Compute for example  $a_i'''$  for  $1 \leq i \leq m-1$ .

- When  $1 \leq i \leq m-2$

$$\begin{aligned}
a_i''' &= a_{i+1} - a_1 + b_1 = (r^n - 1)(r^{i+2} - 1)r - (r^n - 1)(r^2 - 1)r + (r - 1)(r^n - 1)r^2 \\
&= (r^n - 1)(r^{i+1} - 1)r^2 = ra_i.
\end{aligned}$$

- When  $i = m-1$ ,

$$\begin{aligned}
a_{m-1}''' &= a_m - a_1 + b_1 = (r^{m+1} - 1)(r^n - 1)r - (r^n - 1)(r^2 - 1)r + (r - 1)(r^n - 1)r^2 \\
&= r^2(r^n - 1)(r^m - 1) = ra_{m-1}.
\end{aligned}$$

□

#### 4.4.2 The reducible case: $\sigma_{m,m+1}$

The focus in this section is on the case  $n = m + 1$ , when  $\sigma_{m,n}$  is a reducible braid. Again, the emphasis in the next result is on the transparent computational nature of the proof, when compared with a more direct approach such as conjugating the braids in some suitable way and then appealing to the reader to observe that the resulting braids leave a certain system of curves invariant.

**Theorem 4.12.** *Let  $m \geq 1$ . Then the braid  $\sigma_{m,m+1} \in B_{2m+2}$  is reducible, having a system of reducing curves (see Figure 4.2)  $S_m$  with  $\rho(S_m) = (a, b) \in \mathbb{Z}^{4m} \setminus \{0\}$  given by*

$$(a_i, b_i) = \begin{cases} (i + 1, 1) & 1 \leq i \leq m \\ (2m + 1 - i, 1) & m + 1 \leq i \leq 2m \end{cases}$$

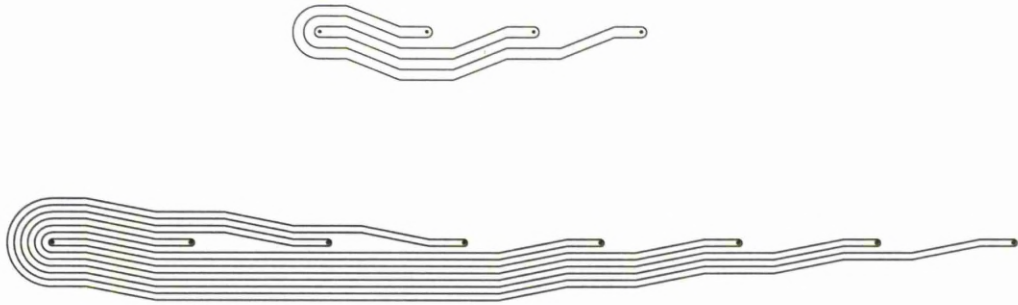


Figure 4.2: Reducing curves of  $\sigma_{m,m+1}$  in the cases  $m = 1, m = 3$

*Proof.* Recall that  $\sigma_{m,m+1} = \gamma_{2m+2}^{1,m} \delta_{2m+2}^{1,m} \gamma_{2m+2}^{1,2m+1}$ . The method of proof is to compute successively  $(a^{(1)}, b^{(1)}) = \gamma_{2m+2}^{1,m}(a, b)$ ,  $(a^{(2)}, b^{(2)}) = \delta_{2m+2}^{1,m}(a^{(1)}, b^{(1)})$ , and  $(a^{(3)}, b^{(3)}) = \gamma_{2m+2}^{1,2m+1}(a^{(2)}, b^{(2)})$ , and then to observe that  $(a^{(3)}, b^{(3)}) = (a, b)$ . The calculations are straightforward using Lemmas 3.36 and 3.37.

1.  $(a^{(1)}, b^{(1)})$  is computed using case 3 of Lemma 3.36. The quantities  $P_j$  and  $S_j$  are given for  $j \leq m$  by  $P_j = \sum_{i=1}^j b_i = j$  and

$$S_j = \max_{1 \leq i \leq j} (\max(b_i, 0) + P_{i-1} - a_i) = \max_{1 \leq i \leq j} (1 + (i - 1) - (i + 1)) = -1.$$

Then for  $1 \leq j < m$

$$a_j^{(1)} = \max(P_j, a_{j+1} + S_j) = \max(j, j + 2 - 1) = j + 1,$$

$$b_j^{(1)} = b_{j+1} + S_j - S_{j+1} = 1 - 1 + 1 = 1.$$

Finally  $a_m^{(1)} = P_m - \max(S_m, 0) = m - \max(-1, 0) = m$ , and  $b_m^{(1)} = S_m = -1$ .

Thus

$$(a_i^{(1)}, b_i^{(1)}) = \begin{cases} (i+1, 1) & 1 \leq i < m \\ (m, -1) & i = m \\ (2m+1-i, 1) & m+1 \leq i \leq 2m. \end{cases}$$

2.  $(a^{(2)}, b^{(2)})$  is computed using case 2 of Lemma 3.37. The quantities  $\tilde{P}_j$  and  $\tilde{S}_j$  are given for  $j \leq m$  by

$$\tilde{P}_j = \max(b_m^{(1)}, 0) - \sum_{i=j}^m b_i^{(1)} = 1 + j - m$$

and  $\tilde{S}_j = \max_{j \leq i \leq m-1} (a_i^{(1)} + \max(b_i^{(1)}, 0) + \tilde{P}_{i+1} - b_i^{(1)}) = m+1$ . Hence

$$\begin{aligned} a_1^{(2)} &= a_m^{(1)} + b_m^{(1)} - \max(a_m^{(1)}, b_m^{(1)} + \max(\tilde{S}_1, \tilde{P}_1)) \\ &= m - 1 - \max(m, -1 + \max(m+1, 2-m)) = -1, \end{aligned}$$

$$\begin{aligned} b_1^{(2)} &= b_m^{(1)} + \tilde{P}_1 - \max(a_m^{(1)}, b_m^{(1)} + \tilde{S}_1) \\ &= -1 + (2-m) - \max(m, -1 + m+1) = 1 - 2m, \end{aligned}$$

$$\begin{aligned} a_m^{(2)} &= a_{m-1}^{(1)} + a_m^{(1)} + b_m^{(1)} - \max(a_{m-1}^{(1)} + \max(b_m^{(1)}, 0), a_m^{(1)}) \\ &= m + m - 1 - \max(m, m) = m - 1, \end{aligned}$$

$$\begin{aligned} b_m^{(2)} &= \max(a_{m-1}^{(1)} + \max(b_{m-1}^{(1)}, 0) + \max(b_m^{(1)}, 0), a_m^{(1)} + b_{m-1}^{(1)}) - a_m^{(1)} \\ &= \max(m+1+0, m+1) - m = 1, \end{aligned}$$

and for  $2 \leq j < m$

$$\begin{aligned} a_j^{(2)} &= a_{j-1}^{(1)} + a_m^{(1)} + b_m^{(1)} - \max(a_m^{(1)}, b_m^{(1)} + \max(\tilde{S}_j, a_{j-1}^{(1)} + \tilde{P}_j)) \\ &= j + m - 1 - \max(m, -1 + \max(m+1, 2j+1-m)) = j + m - 1 - m = j - 1, \end{aligned}$$

$$b_j^{(2)} = b_{j-1}^{(1)} + \max(a_m^{(1)}, b_m^{(1)} + \tilde{S}_{j-1}) - \max(a_m^{(1)}, b_m^{(1)} + \tilde{S}_j) = b_{j-1}^{(1)} = 1.$$

Thus

$$(a_i^{(2)}, b_i^{(2)}) = \begin{cases} (-1, 1-2m) & i = 1 \\ (i-1, 1) & 2 \leq i \leq m \\ (2m+1-i, 1) & m+1 \leq i \leq 2m. \end{cases}$$

3.  $(a^{(3)}, b^{(3)})$  is computed using case 4 of Lemma 3.36. The quantities  $P_j$  and  $S_j$  are given by  $P_j = \sum_{i=1}^j b_i^{(2)} = j - 2m$  (and  $P_0 = 0$ ); and

$$S_j = \max_{1 \leq i \leq j} (\max(b_i^{(2)}, 0) + P_{i-1} - a_i^{(2)}).$$

Now  $\max(b_i^{(2)}, 0) + P_{i-1} - a_i^{(2)}$  is equal to 1 when  $i = 1$  and is negative for  $i > 1$ , and hence  $S_j = 1$  for all  $j$ . Thus  $a_{2m}^{(3)} = \max(P_{2m}, S_{2m}) = 1$ ,  $b_{2m}^{(3)} = S_{2m} - P_{2m} = 1$ , and for  $1 \leq j < 2m$

$$\begin{aligned} a_j^{(3)} &= \max(P_j, a_{j+1}^{(2)} + S_j) = \max(j - 2m, a_{j+1}^{(2)} + 1) = a_{j+1}^{(2)} + 1 \\ &= \begin{cases} j + 1 & 1 \leq j \leq m - 1 \\ 2m + 1 - (j + 1) + 1 & m \leq j \leq 2m - 1, \end{cases} \\ b_j^{(3)} &= b_{j+1}^{(2)} + S_j - S_{j+1} = b_{j+1}^{(2)} = 1. \end{aligned}$$

Hence  $(a^{(3)}, b^{(3)}) = (a, b)$  as required.  $\square$

The proofs of Theorem 4.9 and Theorem 4.11 are self-contained. However, we haven't explained how we computed the Dynnikov coordinates of the unstable foliations, and the polynomials  $f_{m,n}$  and  $g_{m,n}$ . To find the train tracks for an infinite family of braids, the usual method would be to compute train tracks [5, 20] for enough examples to spot a general pattern, and then to prove that the conjectured pattern does indeed hold for all braids in the family. The method here is similar. Since  $[\mathcal{F}, \mu]$  is a globally attracting fixed point for the action of  $\beta_{m,n}$  on  $\mathcal{PMF}_n$ , it is easy to find the Dynnikov coordinates numerically (similarly for  $\sigma_{m,n}; n \geq m + 2$ ).

Having done this for several cases of  $m$  and  $n$ , we can guess how the various maxima in the statements of Lemma 3.36 and Lemma 3.37 are resolved. That is, we compute the Dynnikov regions and matrices for enough braids in the family until we spot a general pattern, and conjecture that the pattern holds for all braids in the family. Then the conjecture is proved. The next section describes this process in more detail, illustrating the method on the family  $\tau_n = \sigma_1 \sigma_2 \dots \sigma_{n-1}^{-1} \in B_n$ .

## 4.5 Exposé of the method on the braid family $\beta_{n-2,1}$

This section is a guide to those who want to compute the topological entropy of each braid in various infinite braid families making use of Dynnikov's coordinates on the boundary of Teichmüller space. The method will be illustrated

on the pseudo-Anosov braids  $\beta_{n-2,1} = \sigma_1 \sigma_2 \dots \sigma_{n-2} \sigma_{n-1}^{-1} \in B_n$ . Throughout the section  $\beta_{n-2,1}$  will be denoted  $\tau_n$ . We shall explain how we obtain the Dynnikov coordinates of the unstable foliation, and hence a Dynnikov region with associated Dynnikov matrix and characteristic polynomial for each braid  $\tau_n$ .

The simplest braid in the family is  $\tau_3 = \sigma_1 \sigma_2^{-1} \in B_3$  which has one Dynnikov matrix as computed in Example 4.4. That is,

$$D = \begin{bmatrix} 2 & 1 \\ 1 & 1 \end{bmatrix}$$

and  $(a^u, b^u)$  has approximate Dynnikov coordinates  $(-0.850, -0.525)$ . The following steps give a recipe to find the Dynnikov coordinates of the invariant foliation and a Dynnikov matrix for each braid  $\tau_n$ .

1. **Step 1:** (Experiment) Since  $[\mathcal{F}^u, \mu^u]$  is a globally attracting fixed point for the action of  $\tau_n \in B_n$  on  $\mathcal{PMF}_n$ , it is easy to find its Dynnikov coordinates numerically. We use the Dynn.exe [18] program for this. The program picks a random point  $(a, b) \in \mathbb{R}^{2n-4} \setminus \{0\}$  and iterates it with the given braid  $\tau_n$  until it arrives in a region  $\mathcal{R}$  in which there exists a point  $(a^u, b^u)$  with  $D[a^u, b^u] = [a^u, b^u]$ , where  $D$  describes the action of  $\tau_n$  in  $\mathcal{R}$ . Thus,  $(a^u, b^u)$  corresponds to the Dynnikov coordinates of  $[\mathcal{F}, \mu]$  and  $D$  is a Dynnikov matrix. We note that there can be more than one Dynnikov matrix if  $[\mathcal{F}, \mu]$  is on the boundary of several Dynnikov regions (see Example 4.8). We first obtained Dynnikov matrices of  $\tau_n$  for different values of  $n$ . Below are some of them, that is for  $n = 4, 5$  and  $6$ .

- For  $\tau_4 = \sigma_1 \sigma_2 \sigma_3^{-1} \in B_4$  the program gives the following matrix

$$D = \begin{bmatrix} 0 & 0 & 1 & 0 \\ 0 & 2 & -1 & 1 \\ -1 & 1 & -1 & 1 \\ 0 & 1 & 0 & 1 \end{bmatrix}.$$

and  $(a^u, b^u)$  has approximate Dynnikov coordinates

$$a_1 = -0.151, \quad a_2 = -0.732, \quad b_1 = -0.347, \quad b_2 = -0.565.$$



- For  $\tau_5 = \sigma_1\sigma_2\sigma_3\sigma_4^{-1} \in B_5$  the program gives the following matrix

$$D = \begin{bmatrix} 0 & 0 & 0 & 1 & 0 & 0 \\ 0 & 0 & 0 & 1 & 1 & 0 \\ 0 & 0 & 2 & -1 & -1 & 1 \\ -1 & 1 & 0 & -1 & 1 & 0 \\ 0 & -1 & 1 & 0 & -1 & 1 \\ 0 & 0 & 1 & 0 & 0 & 1 \end{bmatrix}.$$

and  $(a^u, b^u)$  has approximate Dynnikov coordinates

$$a_1 = -0.071, \quad a_2 = -0.225, \quad a_3 = -0.680,$$

$$b_1 = -0.153, \quad b_2 = -0.331, \quad b_3 = -0.589.$$

- For  $\tau_6 = \sigma_1\sigma_2\sigma_3\sigma_4\sigma_5^{-1} \in B_6$  the program gives the following matrix

$$D = \begin{bmatrix} -1 & 1 & 0 & 0 & 0 & 0 & 0 & 0 \\ 0 & 0 & 0 & 0 & 1 & 1 & 0 & 0 \\ 0 & 0 & 0 & 0 & 1 & 1 & 1 & 0 \\ 0 & 0 & 0 & 2 & -1 & -1 & -1 & 1 \\ 0 & 0 & 0 & 0 & 0 & 1 & 0 & 0 \\ -1 & 0 & 1 & 0 & -1 & -1 & 1 & 0 \\ 0 & 0 & -1 & 1 & 0 & 0 & -1 & 1 \\ 0 & 0 & 0 & 1 & 0 & 0 & 0 & 1 \end{bmatrix}.$$

and  $(a^u, b^u)$  has approximate Dynnikov coordinates

$$a_1 = -0.035, \quad a_2 = -0.109, \quad a_3 = -0.263, \quad a_4 = -0.650,$$

$$b_1 = -0.074, \quad b_2 = -0.154, \quad b_3 = -0.320, \quad b_4 = -0.601.$$

We observe that the Dynnikov coordinates of  $(a^u, b^u)$  are all negative and hence decide to compute the update rules under the assumption that  $a_j \leq 0$  and  $b_j \leq 0$  for all  $1 \leq j \leq n-2$  as the second step.

- Step 2:** The aim of this step is to compute the update rules for  $\tau_n$  when  $a_j \leq 0$  and  $b_j \leq 0$  for  $1 \leq j \leq n-2$ . Let  $(a', b') = \sigma_1\sigma_2 \dots \sigma_{n-2}(a, b)$  and  $(a'', b'') = \sigma_{n-1}^{-1}(a', b')$ . Using Lemma 3.36 case 3 we shall compute  $(a', b')$ . The update rules are given by

$$a'_j = [P_j + a_{j+1}S_j], \quad b'_j = [b_{j+1}S_j/S_{j+1}] \quad (1 \leq j < n-2),$$

$$a'_{n-2} = [P_{n-2}/(1 + S_{n-2})], \quad b'_{n-2} = [S_{n-2}],$$

where

$$P_j(b, 1) = \left[ \prod_{i=1}^j b_i \right] \text{ and } S_j(a, b, 1) = \left[ \sum_{i=1}^j \frac{(1+b_i)P_{i-1}}{a_i} \right]; \quad 1 \leq j \leq n-2.$$

Since  $a_j \leq 0, b_j \leq 0$  for  $1 \leq j \leq n-2$  we have

$$P_j = \left[ \prod_{i=1}^j b_i \right] = b_1 + b_2 + \cdots + b_j, \quad \text{and}$$

$$S_j = \left[ \sum_{i=1}^j \frac{P_{i-1}}{a_i} \right] = \max(-a_1, b_1 - a_2, b_1 + b_2 - a_3, \dots, b_1 + b_2 + \cdots + b_{j-1} - a_j).$$

To resolve  $S_j$  we need to decide which is biggest of

$$-a_1, \quad b_1 - a_2, \quad b_1 + b_2 - a_3, \quad \dots, \quad b_1 + b_2 + \cdots + b_{j-1} - a_j.$$

We go back to the examples in Step 1 and check the Dynnikov coordinates  $(a^u, b^u)$  for each  $\tau_n$ . We observe that in each of these examples  $(a^u, b^u)$  satisfy  $b_{n-3} \geq a_{n-2} - a_{n-3}$  and  $b_j = a_{j+1} - a_j$  for  $1 \leq j \leq n-4$ . Hence, it follows that

$$-a_1 = b_1 - a_2 = b_1 + b_2 - a_3 = \cdots = b_1 + b_2 + \cdots + b_{n-4} - a_{n-3} \leq b_1 + b_2 + \cdots + b_{n-3} - a_{n-2}.$$

It follows that there are  $2^{n-4}$  Dynnikov regions adjacent to  $(a^u, b^u)$  since for each  $1 \leq j \leq n-4$  the update rules can be calculated either under the assumption that  $a_{j+1} - a_j \leq b_j$  or under the assumption that  $a_{j+1} - a_j \geq b_j$ . We choose a region where  $a_{j+1} - a_j \leq b_j$  for  $1 \leq j \leq n-3$  and write  $\mathcal{R}^{(n)}$  to denote this region. In this region, we therefore have

$$S_j = \max(-a_1, b_1 - a_2, b_1 + b_2 - a_3, \dots, b_1 + b_2 + \cdots + b_{j-1} - a_j) = \sum_{i=1}^{j-1} b_i - a_j.$$

Therefore,

$$\begin{aligned} a'_j &= \max(P_j, a_{j+1} + S_j) = \max\left(\sum_{i=1}^j b_i, a_{j+1} + \sum_{i=1}^{j-1} b_i - a_j\right) = \sum_{i=1}^j b_i \\ b'_j &= b_{j+1} + S_j - S_{j+1} = b_{j+1} + \sum_{i=1}^{j-1} b_i - a_j - \sum_{i=1}^j b_i + a_{j+1} \\ &= a_{j+1} - a_j + b_{j+1} - b_j \\ a'_{n-2} &= P_{n-2} - \max(0, S_{n-2}) = \sum_{i=1}^{n-2} b_i - \max\left(0, \sum_{i=1}^{n-3} b_i - a_{n-2}\right) = a_{n-2} + b_{n-2} \\ b'_{n-2} &= S_{n-2} = \sum_{i=1}^{n-3} b_i - a_{n-2} \end{aligned}$$

To compute  $(a'', b'')$ , we refer to Theorem 3.35. Then we get  $a''_j = a_j$  and  $b''_j = b_j$  for  $1 \leq j \leq n-3$ , and

$$\begin{aligned}
a''_{n-2} &= a'_{n-2} - \max(a'_{n-2} + b'_{n-2}, 0, b'_{n-2}) \\
&= a_{n-2} + b_{n-2} - \max\left(a_{n-2} + b_{n-2} + \sum_{i=1}^{n-3} b_i - a_{n-2}, 0, \sum_{i=1}^{n-3} b_i - a_{n-2}\right) \\
&= a_{n-2} + b_{n-2} - \max\left(\sum_{i=1}^{n-3} b_i, 0, \sum_{i=1}^{n-3} b_i - a_{n-2}\right) = 2a_{n-2} + b_{n-2} - \sum_{i=1}^{n-3} b_i \\
b''_{n-2} &= a'_{n-2} + b'_{n-2} - \max(0, b'_{n-2}) \\
&= a_{n-2} + b_{n-2} + \sum_{i=1}^{n-3} b_i - a_{n-2} - \max\left(0, \sum_{i=1}^{n-3} b_i - a_{n-2}\right) \\
&= a_{n-2} + b_{n-2}
\end{aligned}$$

To summarize, the update rules in  $\mathcal{R}^{(n)}$  are given by

$$a''_j = \begin{cases} \sum_{i=1}^j b_i & 1 \leq j \leq n-3 \\ 2a_{n-2} + b_{n-2} - \sum_{i=1}^{n-3} b_i & j = n-2 \end{cases} \quad (4.2)$$

$$b''_j = \begin{cases} a_{j+1} - a_j + b_{j+1} - b_j & 1 \leq j \leq n-3 \\ a_{n-2} + b_{n-2} & j = n-2. \end{cases} \quad (4.3)$$

Write  $D^{(n)}$  for the update matrix in  $\mathcal{R}^{(n)}$ . Thus, for example  $D^{(5)}$  is given by

$$D^{(5)} = \begin{bmatrix} 0 & 0 & 0 & 1 & 0 & 0 \\ 0 & 0 & 0 & 1 & 1 & 0 \\ 0 & 0 & 2 & -1 & -1 & 1 \\ -1 & 1 & 0 & -1 & 1 & 0 \\ 0 & -1 & 1 & 0 & -1 & 1 \\ 0 & 0 & 1 & 0 & 0 & 1 \end{bmatrix}.$$

It is easy to check that  $D^{(5)}$  is a Dynnikov matrix since it has an eigenvalue  $r > 1$  and the corresponding eigenvector lies in  $\mathcal{R}^{(5)}$ . Our aim in the next step is to prove that for each  $n$ ,  $D^{(n)}$  is a Dynnikov matrix.

To do this we shall find a general form for the characteristic polynomial  $f_n(x)$  of  $D^{(n)}$  for each  $n$  and prove that  $f_n(x)$  has eigenvalue  $r > 1$  with

corresponding eigenvector  $(a^u, b^u)$  contained in  $\mathcal{R}^{(n)}$ , and hence conclude that  $\mathcal{R}^{(n)}$  is a Dynnikov region and  $D^{(n)}$  is a Dynnikov matrix.

3. **Step 3:** Let  $f_n(x)$  denote the characteristic polynomial of  $D^{(n)}$ . An inductive calculation using row and column expansion gives;

$$f_n(x) = (x+1)^{n-4}(x^n - 2x^{n-1} - 2x + 1). \quad (4.4)$$

Write  $\hat{f}_n(x)$  for the second factor of  $f_n(x)$ . Then,  $\hat{f}_n(1) = -2$  so that  $\hat{f}_n$  has a root  $r > 1$ . Next, we want to show that there is a unique eigenvector corresponding to  $r > 1$  in  $\mathcal{R}^{(n)}$  and hence show that  $\mathcal{R}^{(n)}$  is a Dynnikov region and  $D^{(n)}$  is the associated Dynnikov matrix.

Because  $a_j - a_k \leq \sum_{m=k}^{j-1} b_m$  for  $1 \leq k \leq j \leq n-2$  we have the following.

$$\begin{cases} a_2 &= a_1 + b_1 + c_0 \\ a_3 &= a_1 + b_1 + b_2 + c_0 + c_1 \\ a_4 &= a_1 + b_1 + b_2 + b_3 + c_0 + c_1 + c_2 \\ &\vdots \\ a_{n-2} &= a_1 + b_1 + \cdots + b_{n-3} + c_0 + c_1 + c_2 + \cdots + c_{n-4} \end{cases} \quad (4.5)$$

for  $c_j \geq 0$ . Solving the system  $D^{(n)}(a, b) = r(a, b)$  for  $(a, b)$  gives that,

$$a_j = \begin{cases} -r(r^j - 1); & 1 \leq j < n-2 \\ -(r^{n-1} - 1)(r-1) & j = n-2, \end{cases} \quad (4.6)$$

$$b_j = \begin{cases} -r^{j+1}(r-1) & 1 \leq j < n-2 \\ -(r^{n-1} - 1) & j = n-2. \end{cases} \quad (4.7)$$

Also observe that multiplying each of these coordinates with  $r+1$  gives the coordinates of  $(a^u, b^u)$  of the invariant unstable foliation of  $\beta_{m,n}$  for  $m = n-2$  and  $n = 1$  as given in Theorem 4.9.

Finally, we check that  $(a^u, b^u)$  given with Dynnikov coordinates as above is contained in  $\mathcal{R}^{(n)}$  for each braid  $\tau_n$  and hence corresponds to the Dynnikov coordinates of  $(\mathcal{F}^u, \mu^u)$ . We observe that for  $1 \leq j \leq n-4$ ,

$$a_j = -r(r^j - 1) \leq 0, \quad b_j = -r^{j+1}(r-1) \leq 0, \quad a_{j+1} = -r(r^{j+1} - 1) = a_j + b_j$$

and

$$a_{n-2} = (1 - r^{n-1})(r-1) \leq r - r^{n-1} = a_{n-3} + b_{n-3}$$

since  $r^n + 1 = 2(r^{n-1} + r) \geq 2r^{n-1}$  from (4.4). Our last note about this family of braids will regard its singularity structure. Namely, we shall see that the equation  $a_{j+1} = a_j + b_j$ ;  $1 \leq j \leq n - 4$  reveals the singularity structure of the invariant foliation  $[\mathcal{F}^u, \mu^u]$  of  $\beta$ .

Noting that  $a_j \leq 0$  and  $b_j \leq 0$  and using Theorem 3.19 we get

$$\alpha_{2j} = a_j + \frac{\beta_{j+1}}{2} \quad (4.8)$$

$$\alpha_{2j+2} = a_{j+1} + \frac{\beta_{j+2}}{2} \quad (4.9)$$

We have  $a_j + b_j = a_{j+1}$  for  $1 \leq j \leq n - 4$ . Adding  $b_{j+1}$  on both sides of the equation gives

$$a_j + b_{j+1} + b_j = a_{j+1} + b_{j+1}.$$

Since  $b_{j+1} = \frac{\beta_{j+1} - \beta_{j+2}}{2}$  we get

$$a_j + \frac{\beta_{j+1}}{2} + b_j = a_{j+1} + \frac{\beta_{j+2}}{2} + b_{j+1}$$

By (4.8) and using  $b_j \leq 0$ ,  $b_{j+1} \leq 0$  we have

$$\alpha_{2j} - |b_j| = \alpha_{2j+2} - |b_{j+1}|; \quad 1 \leq j \leq n - 4. \quad (4.10)$$

The equality in (4.10) implies that there exists a leaf which joins  $n - 3$  3-pronged singularities. A Whitehead move contracts this leaf and yields a  $n - 1$  pronged singularity. For an explicit example, consider the braid  $\tau_6 = \sigma_1 \sigma_2 \sigma_3 \sigma_4 \sigma_5^{-1} \in B_6$ . Then by (3.4),  $r \simeq 2.081$  and from (3.9) and (3.10),

$$\begin{array}{ll} a_1 \simeq -1 & b_1 \simeq -2.081 \\ a_2 \simeq -3.081 & b_2 \simeq -4.330 \\ a_3 \simeq -7.411 & b_3 \simeq -9.012 \\ a_4 \simeq -18.27 & b_4 \simeq -16.904 \end{array}$$

Thus, by Theorem 3.19 one can work out  $\alpha_j$  for all  $1 \leq j \leq 2n - 4$  and  $\beta_j$  for all  $1 \leq j \leq n - 1$  (Figure 4.3).

We observe that  $|\alpha_2| - b_1 = |\alpha_4| - b_2 = |\alpha_6| - b_3$  hence there exists a leaf which joins three 3-pronged singularities as depicted in Figure 4.3. A Whitehead move contracts this leaf and yields a 5 pronged singularity.

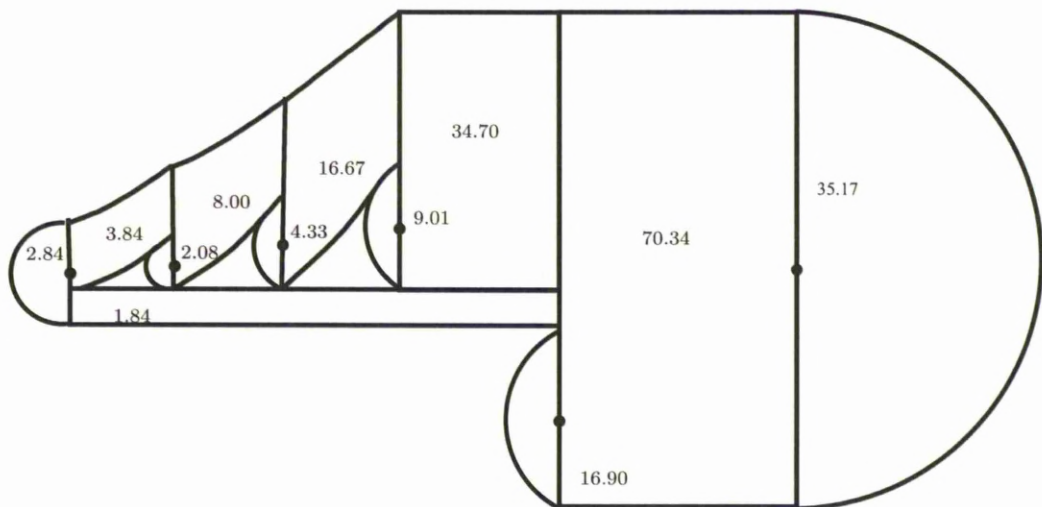


Figure 4.3: The unstable foliation  $(\mathcal{F}^u, \mu^u)$  for  $\beta_6$

## Part II

# On Dynnikov matrices and train track transition matrices of pseudo-Anosov braids

In the first part of the thesis, we showed that Dynnikov coordinates provide an explicit bijection between the space of measured foliations  $\mathcal{MF}_n$  (up to isotopy and Whitehead equivalence) on  $D_n$  and  $\mathcal{S}_n = \mathbb{R}^{2n-4} \setminus \{0\}$ . We described the action of a given braid  $\beta \in B_n$  on the projective space  $\mathcal{PS}_n = \mathcal{S}_n/\mathbb{R}^+$  using the update rules and proved that these rules induce a piecewise linear action on  $\mathcal{PS}_n$ . Then, we introduced the so-called *Dynnikov matrices* which describe the action of  $\beta$  near the invariant unstable foliation  $[\mathcal{F}^u, \mu^u] \in \mathcal{PS}_n$ . Often,  $[\mathcal{F}^u, \mu^u]$  lies on the boundary of several piecewise linear regions (as illustrated in Example 4.8): each region containing  $[\mathcal{F}^u, \mu^u]$  on its boundary is a *Dynnikov region* and the associated matrix is a *Dynnikov matrix*. The fact that each Dynnikov matrix has an eigenvalue  $\lambda > 1$  associated with the Dynnikov coordinates  $[a^u, b^u]$  of  $[\mathcal{F}^u, \mu^u]$ , and that  $\lambda$  gives the dilatation of  $\beta$ , yielded the method introduced in Chapter 4. That is, the topological entropy of each member of a given pseudo-Anosov braid family can be computed by finding a Dynnikov region with its associated Dynnikov matrix. This process was described in detail in Chapter 4.

The aim of this part of the thesis is to prove that any Dynnikov matrix  $D$  and any train track transition matrix  $T$  of a pseudo-Anosov braid  $\beta \in B_n$  are isospectral up to roots of unity and zeros. Chapter 5 provides the necessary background and Chapter 6 contains the results of this part of the thesis. To be more specific, Chapter 5 first describes train tracks and defines the space of transverse measures  $\mathcal{W}(\tau)$  on a given train track  $\tau$ . Section 5.1 then gives a description of the construction of measured foliations (and integral laminations) from a given train track and explains why train tracks can be used as coordinate systems, introducing the homeomorphism from the space of non-negative transverse measures  $\mathcal{W}^+(\tau)$  on a given train track  $\tau$  to the space of measured foliations  $\mathcal{MF}(\tau)$  carried by  $\tau$ . This background material can be found in [24, 26]. Section 5.2 contains some new material. It defines the measure  $\hat{p} : \mathcal{W}^+(\tau) \rightarrow \mathbb{R}^+$  of a *train path*  $p$  in a train track  $\tau$ , and shows that  $\hat{p}$  is piecewise linear. Section 5.3 summarizes some results from [5] regarding the dynamics of a given pseudo-Anosov isotopy class  $[f]$  on its invariant train track  $\tau$ . An important point here is that the associated train track transition matrix  $T$  describes the action of  $[f]$  on  $\mathcal{W}^+(\tau)$ .

Chapter 6 is divided into three sections. One essential tool is described in Section 6.1: the change of coordinate function from train track coordinates to Dynnikov coordinates. Then, the main results of this part of the thesis will be given in Section 6.2 and Section 6.3.

In Section 6.2 it is shown that when the unstable invariant measured foliation  $(\mathcal{F}^u, \mu^u)$  of a given pseudo-Anosov braid  $\beta \in B_n$  has only unpunctured 3-pronged and punctured 1-pronged singularities, then there is a unique Dyn-



Dynnikov matrix  $D$  which is isospectral to  $T$ . Section 6.3 studies the case when  $(\mathcal{F}^u, \mu^u)$  has singularities other than unpunctured 3-pronged and punctured 1-pronged singularities. In this case,  $(\mathcal{F}^u, \mu^u)$  is carried by a non-complete train track  $\tau$ , and the corresponding space  $\mathcal{MF}(\tau)$  does not define a chart in  $\mathcal{MF}_n$ . Two different ways of constructing a complete train track from  $\tau$  are described in Section 6.3.1. These complete train tracks are called *pinchings* and *diagonal extensions* of  $\tau$  [24, 26]. Our results are mainly based on the interplay between the charts constructed from these two different extensions. In particular, we shall introduce Lemma 6.18, which is new and plays a key role in our results: it explains how these charts fit together. In Section 6.3.2, we shall use this lemma and prove that if  $\beta$  fixes the prongs of  $(\mathcal{F}^u, \mu^u)$ , then every Dynnikov matrix is isospectral to  $T$  up to some eigenvalues 1. Then, we shall discuss the case in which  $\beta$  permutes the prongs of  $(\mathcal{F}^u, \mu^u)$  non-trivially in Section 6.3.3. In this case, we have not established that every Dynnikov matrix is isospectral to  $T$  up to roots of unity and zeros: this conjectured result has been observed in a wide range of examples, one of which is presented in detail in Section 6.3.3.

## Chapter 5

# Train Tracks

The purpose of this chapter is to explain some properties of train tracks which will be necessary for the results in Chapter 6. We shall start with some basic definitions and results all of which can be found in [5, 24, 26].

**Definitions 5.1.** A *train track*  $\tau$  on  $D_n$  is a one dimensional CW complex made up of vertices called *switches* and edges called *branches* smoothly embedded on  $D_n$  such that at each switch  $v$  there is a unique tangent vector  $T_v(\tau)$ . We require that every component of  $D_n - \tau$  is either a once-punctured  $p$ -gon with  $p \geq 1$  or an unpunctured  $k$ -gon with  $k \geq 3$  (see Figure 5.1). Fixing a direction in  $T_v(\tau)$  at each switch  $v$  we define *incoming* and *outgoing* branches as follows: a branch  $e$  of  $\tau$  incident to the switch  $v$  is called *incoming* at  $v$  if it agrees with the direction of  $T_v(\tau)$ , it is *outgoing* otherwise.

A train track  $\tau$  is called *complete* if each component of  $D_n - \tau$  is either a trigon or a once punctured monogon.

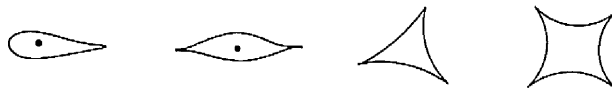


Figure 5.1: A punctured monogon, a punctured bigon, a trigon and a 4-gon

In Figure 5.2,  $D_n - \tau$  has 9 punctured monogons, a punctured 6-gon and a punctured trigon. Note that we treat  $\partial D_n$  as a puncture.

**Definitions 5.2.** A transverse measure  $\mu$  on  $\tau$  is a function which assigns a real number  $\mu(e) \in \mathbb{R}$  to each branch  $e$  of  $\tau$  called the *measure* on  $\tau$  such that:

- There is some  $e$  with  $\mu(e) \neq 0$

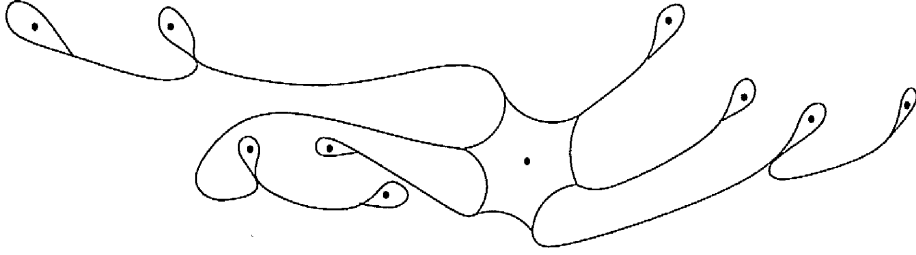


Figure 5.2: A train track on  $D_{10}$

- The *switch condition* holds at each switch  $v$ . That is,

$$\sum_{\text{incoming branches at } v} \mu(e) = \sum_{\text{outgoing branches at } v} \mu(e)$$

A *measured train track* is a train track equipped with a transverse measure  $\mu$ .

**Definitions 5.3.** Given a train track  $\tau$  on  $D_n$  with  $k$  branches,  $\mathcal{W}(\tau) \subset \mathbb{R}^k$  denotes the space of transverse measures on  $\tau$  and  $\mathcal{W}^+(\tau) \subset \mathcal{W}(\tau)$  denotes the set of non-negative transverse measures on  $\tau$ . Hence  $\mathcal{W}^+(\tau)$  is a polyhedral convex cone defined by the inequalities  $\mu(e_i) \geq 0$  for each branch  $e_i$ , some  $\mu(e_i) > 0$ , and the switch conditions (as linear equations) of  $\tau$ . The subspace  $\mathcal{W}_{\mathbb{Z}}^+(\tau)$  denotes the space of positive integer transverse measures on  $\tau$ . The dimension of  $\mathcal{W}(\tau)$  is denoted  $\text{rank}(\tau)$ .

Since  $\mathcal{W}^+(\tau)$  is a convex cone, for all  $w_1, w_2 \in \mathcal{W}^+(\tau)$  and  $k_1, k_2 \in \mathbb{R}^+$ , we have  $k_1 w_1 + k_2 w_2 \in \mathcal{W}^+(\tau)$ . In particular, there is a natural action of the positive reals  $\mathbb{R}^+$  on  $\mathcal{W}^+(\tau)$ .

**Definitions 5.4.** The space of projective transverse measures  $\mathcal{PW}^+(\tau)$  is the quotient space of  $\mathcal{W}^+(\tau)$  modulo  $w \sim kw$ ,  $k \in \mathbb{R}^+$ . That is,  $\mathcal{PW}^+(\tau)$  is the space of equivalence classes  $[w]$  where  $w$  is identified with  $kw$  for all  $k \in \mathbb{R}^+$ . An element of  $\mathcal{PW}^+(\tau)$  is called a projective measure on  $\tau$ .

**Definitions 5.5.** Endowing a regular neighborhood  $N_\tau$  of  $\tau$  with fibres of the retraction  $r : N_\tau \searrow \tau$  as depicted in Figure 5.3, we obtain a *fibred neighbourhood*  $N_\tau$  of  $\tau$ . Note that  $v$  is not a switch if and only if  $r^{-1}(v)$  is an interval: that is, for every switch  $v$  of  $\tau$ ,  $r^{-1}(v)$  is a singular fiber.

Given an integral lamination  $\mathcal{L} \in \mathcal{L}_n$ , we say that  $\mathcal{L}$  is carried by  $\tau$  if it has a representative  $L \subseteq N_\tau$  which is transverse to the fibres in  $N_\tau$  (Figure 5.4). Intuitively, the curves of  $\mathcal{L}$  can be realized by a train running along the track. The space of integral laminations carried by  $\tau$  is denoted  $\mathcal{L}(\tau)$ .

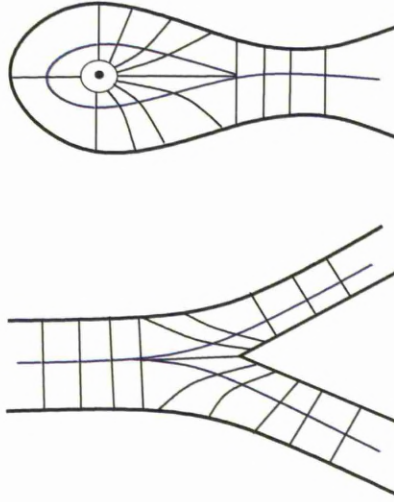


Figure 5.3: A fibred neighbourhood of a train track  $\tau$

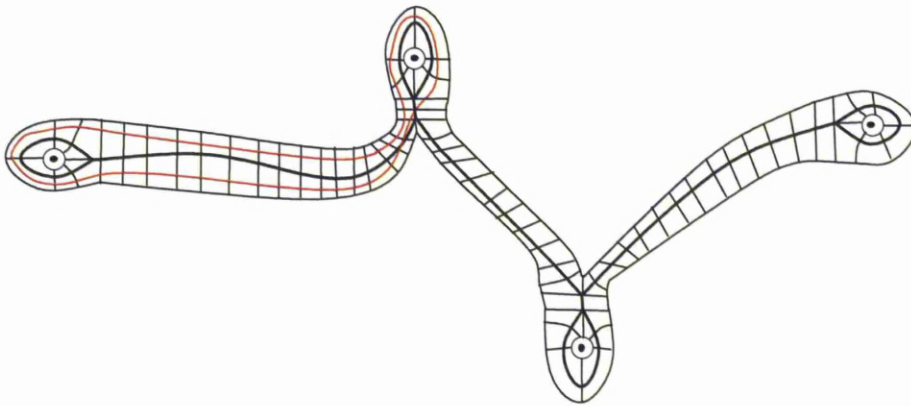


Figure 5.4: An integral lamination carried by a train track  $\tau$

## 5.1 Constructing integral laminations and measured foliations from a train track

Given a non-negative integer transverse measure  $\mu \in \mathcal{W}_{\mathbb{Z}}^+(\tau)$ , draw  $\mu(e_i)$  disjoint arcs in  $N_\tau$  parallel to the branch  $e_i$  for each  $i$ . At each switch  $v$  the number of arcs coming from the incoming branches is equal to the number of arcs going to the outgoing branches since  $\mu$  satisfies the switch conditions. Glue together the incoming arcs to the outgoing ones disjointly at each switch. This can be done uniquely (see Figure 5.5) and gives a collection of simple closed curves. Since there is no nullgon, monogon, bigon, once punctured nullgon or annulus in

$D_n - \tau$ , this collection of simple closed curves gives rise to an integral lamination. This defines a function  $\psi_\tau : \mathcal{W}_{\mathbb{Z}}^+(\tau) \rightarrow \mathcal{L}(\tau)$ . Conversely, if  $\mathcal{L}$  is carried by  $\tau$  then the measures  $\mu(e_1), \dots, \mu(e_k)$  assigned by  $\mathcal{L}$  on the branches  $e_1, \dots, e_k$  of  $\tau$  are given as the number of times a transverse representative  $L \subseteq N_\tau$  of  $\mathcal{L}$  passes over  $e_i$  and they satisfy the switch conditions. This gives the inverse function  $\psi_\tau^{-1} : \mathcal{L}(\tau) \rightarrow \mathcal{W}_{\mathbb{Z}}^+(\tau)$ . Therefore,  $\psi_\tau : \mathcal{W}_{\mathbb{Z}}^+(\tau) \rightarrow \mathcal{L}(\tau)$  is a bijection.

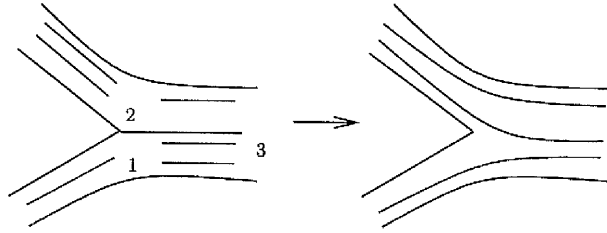


Figure 5.5: There is a unique way to join arcs at each vertex

Similarly, we can define a function  $\phi_\tau : \mathcal{W}^+(\tau) \rightarrow \mathcal{MF}_n$  as follows: Replace each branch  $e_i$  which has non-zero measure with a Euclidean rectangle  $R_i$  of length 1 and height  $\mu(e_i)$  and endow each  $R_i$  with a “horizontal” measured foliation where the transverse measure is induced from the Euclidean metrics on the rectangles. At each switch glue the vertical sides of the rectangles as depicted in Figure 5.6 and denote this union of glued rectangles  $\mathcal{R}^*$ . Since  $\tau$  satisfies the switch condition at each switch there is a unique measure preserving way to glue together the horizontal leaves, hence there is a well defined transverse measure on  $\mathcal{R}^*$ . A *pre-foliation*  $\mathcal{F}^*$  is the collection of leaves on  $\mathcal{R}^*$ . Collapsing each component of  $D_n - \mathcal{F}^*$  which doesn’t contain any branch of zero measure onto a spine as depicted in Figure 5.9 yields a full or partial measured foliation  $\phi_\tau(\mu) = (\mathcal{F}, \mu)$  [5].

**Definitions 5.6.** We say that  $(\mathcal{F}, \mu) \in \mathcal{MF}_n$  is *carried* by  $\tau$  if it arises from some transverse measure  $\mu$  on  $\tau$  in this way. We write  $\mathcal{MF}(\tau) = \phi_\tau(\mathcal{W}^+(\tau))$  for the set of measured foliations carried by  $\tau$  and  $\mathcal{PMF}(\tau)$  for the corresponding projective space.

Therefore, the measures on the branches of  $\tau$  provide (train track) coordinates for integral laminations and measured foliations carried by  $\tau$ .

**Remark 5.7.** We note that  $\tau$  is complete if and only if almost every foliation in  $\mathcal{MF}(\tau)$  is full and has only 1-pronged singularities at punctures and 3-pronged singularities elsewhere. Moreover, a foliation  $(\mathcal{F}, \mu)$  carried by a complete train track cannot be full if the measures on some branches are zero. Also a foliation

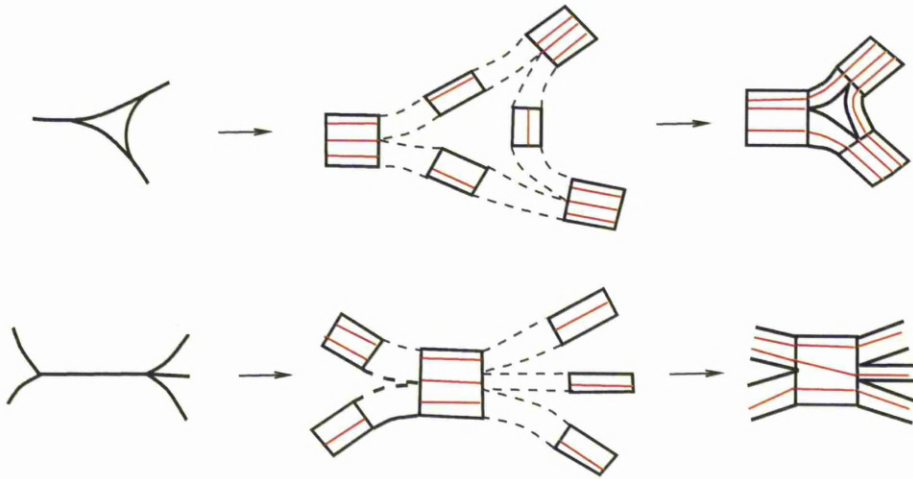


Figure 5.6: Gluing rectangles along vertical edges

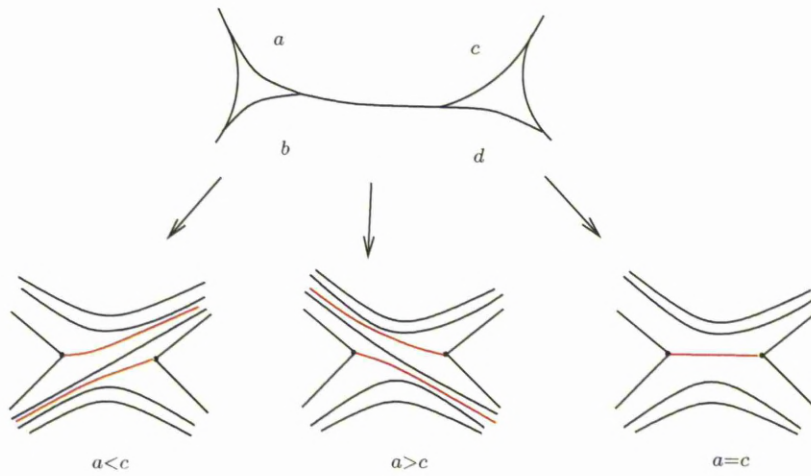


Figure 5.7: When  $a = c$  the two 3-pronged singularities join and give a 4-pronged singularity

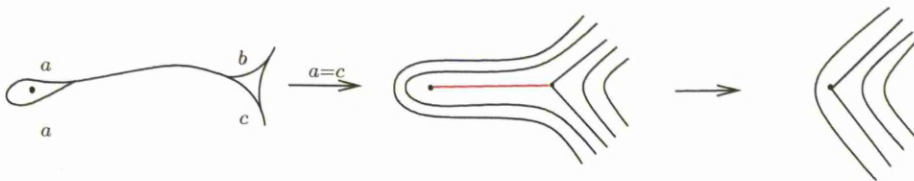


Figure 5.8: When  $a = c$  the 1-pronged singularity joins the 3-pronged singularity and gives a regular point

$(\mathcal{F}, \mu)$  Whitehead equivalent to a foliation with a  $k$ -pronged singularity  $k > 3$  can be carried by a complete train track. In Figure 5.7, when  $a = c$ , the singular leaves emanating from the 3-pronged singularities join and give a compact leaf. A Whitehead move collapses this leaf onto a point and yields a 4-pronged singularity. In Figure 5.8, when  $a = c$  a 1-pronged singularity joins a 3-pronged singularity and yields a regular point. Hence although the foliations in both cases are carried by complete train tracks, they have singularities other than 3-pronged and 1-pronged singularities.

**Lemma 5.8.** *The complete train tracks on  $D_n$  give an atlas for the piecewise integral linear structure of  $\mathcal{MF}_n$  and  $\mathcal{PMF}_n$ . That is, the transition functions between charts are piecewise linear with integer coefficients.*

*Proof.* See [26]. □

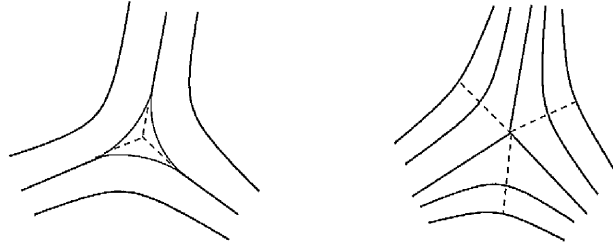


Figure 5.9: Collapsing complementary regions onto a spine

Noting that  $\mathcal{MF}_n$  and  $\mathcal{PMF}_n$  are homeomorphic to  $\mathbb{R}^{2n-4} \setminus \{0\}$  and  $\mathbb{S}^{2n-5}$  respectively,  $\mathcal{MF}(\tau)$  and  $\mathcal{PMF}(\tau)$  have the subspace topology and we have the following:

**Theorem 5.9.** *Given a train track  $\tau$  on  $D_n$ , the maps  $\phi_\tau : \mathcal{W}^+(\tau) \rightarrow \mathcal{MF}(\tau)$  and  $\hat{\phi}_\tau : \mathcal{PW}^+(\tau) \rightarrow \mathcal{PMF}(\tau)$  are homeomorphisms where  $\mathcal{W}^+(\tau)$  has the subspace and  $\mathcal{PW}^+(\tau)$  has the quotient topology.*

*Proof.* See [24]. □

**Lemma 5.10.** *Let  $\tau$  be a train track on  $D_n$  with  $k$  branches and  $s$  switches. The switch conditions on  $\tau$  are linearly independent and hence  $\mathcal{W}(\tau)$  has dimension  $\text{rank}(\tau) = k - s$ . Hence  $\mathcal{W}(\tau) \cong \mathbb{R}^{k-s} \setminus \{0\}$ .  $\tau$  is complete if and only if  $\text{rank}(\tau) = 2n - 4$ . That is,  $\tau$  is complete if and only if  $\text{rank}(\tau)$  is the same as the dimension of  $\mathcal{MF}_n$ .*

*Proof.* See [26]. □

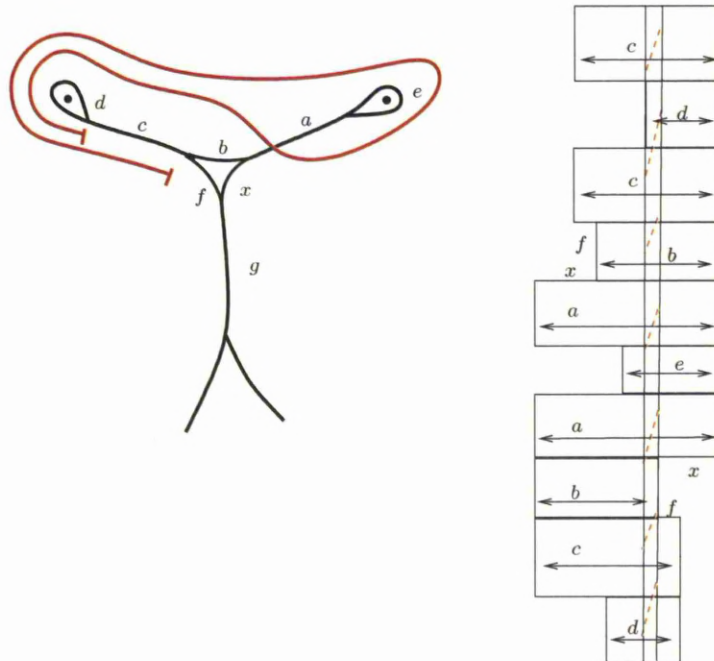


Figure 5.10: The space  $K$  for a train path  $p$

## 5.2 Train paths

**Definitions 5.11.** Suppose  $\tau$  is a train track with oriented branches  $e_1, \dots, e_k$ . A *train path*  $p = e_{i_1}^{\epsilon_1} e_{i_2}^{\epsilon_2} \dots e_{i_m}^{\epsilon_m}$ ,  $\epsilon_j = \pm 1$  is a smooth oriented edge-path in  $\tau$ . Given a train path  $p$  on  $\tau$  we define  $\hat{p} : \mathcal{W}^+(\tau) \rightarrow \mathbb{R}_{\geq 0}$  as follows: for each  $\mu \in \mathcal{W}^+(\tau)$ ,  $\hat{p}(\mu)$  is the total measure of leaves of  $\phi_\tau(\mu)$  following the train path  $p$ .

**Lemma 5.12.** For each train path  $p$  in  $\tau$ , the map  $\hat{p} : \mathcal{W}^+(\tau) \subseteq \mathbb{R}_+^k \rightarrow \mathbb{R}_{\geq 0}$  is piecewise linear.

*Proof.* Let  $R_1, \dots, R_k$  be the rectangles used in the construction of  $\phi_\tau(\mu)$  as described in Section 5.1. Associate a copy of  $R_{i_j}$  to each branch  $e_{i_j}^{\epsilon_j}$  in  $p$ , and glue  $R_{i_j}$  to  $R_{i_{j-1}}$  and  $R_{i_{j+1}}$  using the identifications described in Section 5.1. Denote the identification space  $K$ . Then  $\hat{p}(\mu)$  is the width of the largest rectangle which fits in  $K$  with edges parallel to the edges of each  $R_{i_j}$ . This is clearly a piecewise linear function of the widths of the rectangles (observe that  $\hat{p}(\mu)$  is the measure of leaves that pass along the shaded rectangle in Figure 5.10).

□

**Remark 5.13.** Note that Lemma 5.12 implies that  $\hat{p} : \mathcal{W}^+(\tau) \subseteq \mathbb{R}_+^k \rightarrow \mathbb{R}_{\geq 0}$  is linear in a neighbourhood of any measure for which the prongs of  $\mathcal{F}^*$  as described



in Section 5.1 are not connected.

### 5.3 Train tracks and pseudo-Anosov automorphisms

**Definitions 5.14.** Let  $\tau$  and  $\tau'$  be two train tracks on  $D_n$ . We say that  $\tau$  is *carried* by  $\tau'$  and write  $\tau < \tau'$  if there is a homeomorphism  $\psi : D_n \rightarrow D_n$  isotopic to the identity such that

- $\psi(\tau) \subseteq N_{\tau'}$ ,
- Each branch of  $\psi(\tau)$  is transverse to the fibers in  $N_{\tau'}$ ,
- for each branch  $e_i$  of  $\tau$  the end points of  $\psi(e_i)$  are contained in singular leaves of  $N_{\tau'}$ .

Let  $\{e_i\}_{1 \leq i \leq k}$  and  $\{f_i\}_{1 \leq i \leq k'}$  be the oriented branches of  $\tau$  and  $\tau'$  respectively. Let  $r' : N_{\tau'} \rightarrow \tau'$  be the retraction. For each  $1 \leq i \leq k$ ,  $r'(\psi(e_i))$  is an edge path in  $\tau'$ :  $r'(\psi(e_i)) = f_{i_1}^{\epsilon_1} f_{i_2}^{\epsilon_2} \dots f_{i_s}^{\epsilon_s}$ ,  $\epsilon_j = \pm 1$ . The *incidence matrix* associated to  $\tau$  and  $\tau'$  is the  $k' \times k$  matrix  $G : \mathcal{W}(\tau) \rightarrow \mathcal{W}(\tau')$  whose  $ij^{\text{th}}$  entry  $T_{ij}$  is given by the number of occurrences of  $f_i^{\pm 1}$  in  $r'(\psi(e_j))$ .

**Lemma 5.15.** *Let  $\tau < \tau'$ . Then  $\mathcal{MF}(\tau) \subset \mathcal{MF}(\tau')$  and the following diagram commutes:*

$$\begin{array}{ccc} \mathcal{W}^+(\tau) & \xrightarrow{G} & \mathcal{W}^+(\tau') \\ \downarrow \phi_\tau & & \downarrow \phi_{\tau'} \\ \mathcal{MF}(\tau) & \hookrightarrow & \mathcal{MF}(\tau'). \end{array}$$

*Proof.* See [24]. □

**Definition 5.16.** We say that a train track  $\tau$  is *invariant* under  $[f] \in \text{MCG}(D_n)$ , if  $f(\tau)$  is carried by  $\tau$ . Let  $\tau$  be an invariant train track of  $[f]$  and  $e_1, \dots, e_k$  be the oriented branches of  $\tau$ . Then, for each  $1 \leq i \leq k$ ,  $r(\psi(f(e_i)))$  is of the form  $r(\psi(f(e_i))) = e_{i_1}^{\epsilon_1} e_{i_2}^{\epsilon_2} \dots e_{i_k}^{\epsilon_k}$ ,  $\epsilon_j = \pm 1$ . The *transition matrix*  $T$  associated to  $\tau$  is the  $k \times k$  incidence matrix  $T : \mathcal{W}(f(\tau)) \rightarrow \mathcal{W}(\tau)$  described as in Definitions 5.14.

**Example 5.17.** An invariant train track  $\tau$  for the 5-braid  $\beta = \sigma_1 \sigma_2 \sigma_3^{-1} \sigma_4$  and its image under  $\beta$  are depicted in Figure 5.11. Hence the image edge paths are given by

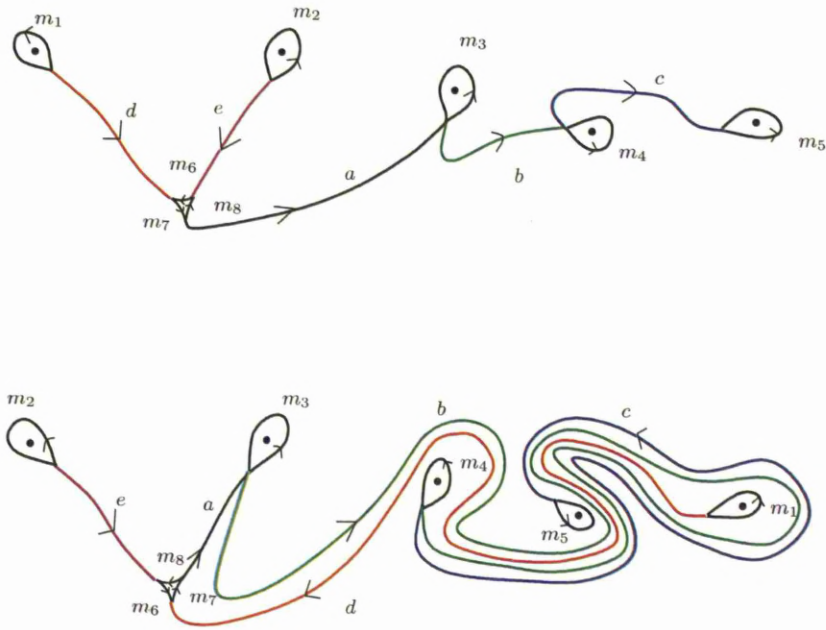


Figure 5.11: An invariant train track for the 5-braid  $\beta = \sigma_1 \sigma_2 \sigma_3^{-1} \sigma_4$  and its image under  $\beta$

$$a \rightarrow \bar{e}, \quad b \rightarrow em_8 a \bar{m}_3 b m_4 c \bar{m}_5 \bar{c} \bar{m}_4 \bar{b},$$

$$c \rightarrow b m_4 c m_5 \bar{c}, \quad d \rightarrow \bar{c} \bar{m}_4 \bar{b} m_3 \bar{a}, \quad e \rightarrow d$$

$$m_1 \rightarrow m_5, \quad m_5 \rightarrow m_4, \quad m_4 \rightarrow m_3, \quad m_3 \rightarrow m_2, \quad m_2 \rightarrow m_1$$

$$m_6 \rightarrow m_7, \quad m_7 \rightarrow m_8, \quad m_8 \rightarrow m_6.$$

Therefore the transition matrix  $T'$  associated to  $\tau$  is as given below.

$$T' = \begin{bmatrix} 0 & 1 & 0 & 1 & 0 & 0 & 0 & 0 & 0 & 0 & 0 & 0 & 0 \\ 0 & 2 & 1 & 1 & 0 & 0 & 0 & 0 & 0 & 0 & 0 & 0 & 0 \\ 0 & 2 & 2 & 1 & 0 & 0 & 0 & 0 & 0 & 0 & 0 & 0 & 0 \\ 0 & 0 & 0 & 0 & 1 & 0 & 0 & 0 & 0 & 0 & 0 & 0 & 0 \\ 1 & 1 & 0 & 0 & 0 & 0 & 0 & 0 & 0 & 0 & 0 & 0 & 0 \\ 0 & 0 & 0 & 0 & 0 & 0 & 1 & 0 & 0 & 0 & 0 & 0 & 0 \\ 0 & 0 & 0 & 0 & 0 & 0 & 0 & 1 & 0 & 0 & 0 & 0 & 0 \\ 0 & 1 & 0 & 1 & 0 & 0 & 0 & 0 & 1 & 0 & 0 & 0 & 0 \\ 0 & 2 & 1 & 1 & 0 & 0 & 0 & 0 & 0 & 1 & 0 & 0 & 0 \\ 0 & 1 & 1 & 0 & 0 & 1 & 0 & 0 & 0 & 0 & 0 & 0 & 0 \\ 0 & 0 & 0 & 0 & 0 & 0 & 0 & 0 & 0 & 0 & 0 & 0 & 1 \\ 0 & 0 & 0 & 0 & 0 & 0 & 0 & 0 & 0 & 0 & 1 & 0 & 0 \\ 0 & 1 & 0 & 0 & 0 & 0 & 0 & 0 & 0 & 0 & 0 & 1 & 0 \end{bmatrix}.$$

Notice that  $T'$  has the form

$$T' = \begin{pmatrix} T & 0 \\ A & P \end{pmatrix}$$

where  $T$  is a  $5 \times 5$  matrix giving the action on the edges  $a, b, c, d$  and  $e$ ; and  $P$  is a permutation matrix giving the action on the other edges.

**Theorem 5.18.** *Every pseudo-Anosov automorphism  $f \in \text{Aut}(D_n)$  has an invariant train track  $\tau$ . This train track  $\tau$  can be chosen so that*

- *The branches which bound interior  $p$ -gons (i.e. those which are disjoint from  $\partial D_n$ ) are permuted by  $f$ .*
- *The transition matrix is of the form*

$$T' = \begin{pmatrix} T & 0 \\ A & P \end{pmatrix}$$

*where  $P$  is a permutation matrix giving the action on the permuted branches and  $T$  is the matrix that gives the action on the other branches.*

- For each  $p$ , there are the same number of unpunctured (resp. punctured)  $p$ -gons in  $\tau$  as there are unpunctured (resp. punctured)  $p$ -pronged singularities in  $(\mathcal{F}^u, \mu^u)$  (this includes the “exterior” punctured  $p$ -gon and the singularity at infinity).

*Proof.* See [5]. □

The final point will be clarified in Lemma 5.20.

**Definition 5.19.** A train track  $\tau$  of the type in Theorem 5.18 is called a *regular train track*. A branch of a regular train track is called *infinitesimal* if it is permuted under the action of  $\beta$  (that is, if it bounds an interior  $p$ -gon), it is called *main* otherwise.

**Lemma 5.20.** Let  $f \in \text{Aut}(D_n)$  be a pseudo-Anosov automorphism with dilatation  $\lambda$ , unstable foliation  $(\mathcal{F}^u, \mu^u)$  and invariant regular train track  $\tau$  with associated transition matrix  $T'$ . The largest eigenvalue of  $T'$  equals  $\lambda$  and the entries of the unique associated column eigenvector  $v^u$  (up to scale) are strictly positive.  $v^u$  defines a transverse measure on  $\tau$  which yields a pre-foliation  $\mathcal{F}^*$  as described in page 110 whose prongs do not join and from which  $(\mathcal{F}^u, \mu^u)$  is constructed. That is,  $\phi_\tau(v^u) = (\mathcal{F}^u, \mu^u)$ .

*Proof.* See [5]. □

**Lemma 5.21.** Let  $\tau$  be an invariant train track for  $f \in \text{Aut}(D_n)$ . If all components of  $D_n - \tau$  are odd-gons (in particular, if  $\tau$  is complete), then there is a basis for  $\mathcal{W}(\tau)$  consisting of transverse measures  $\mu$  such that  $\mu(e) \neq 0$  for exactly one main branch  $e$ .

*Proof.* If  $D_n - \tau$  consists only of odd-gons, the switch conditions give a unique solution for the measures on the infinitesimal branches given measures on the main branches and a basis for  $\mathcal{W}(\tau)$  can be obtained by assigning 1 to one main branch and 0 to all other main branches of  $\tau$  since negative measures are allowed on the infinitesimal branches (Figure 5.12). See also [6]. □

**Remark 5.22.** Lemma 5.15 gives the following commutative diagram

$$\begin{array}{ccc}
 \mathcal{W}^+(\tau) & \xrightarrow{T'} & \mathcal{W}^+(\tau) \\
 \downarrow \phi_\tau & & \downarrow \phi_\tau \\
 \mathcal{MF}(\tau) & \xrightarrow{f} & \mathcal{MF}(\tau).
 \end{array}$$

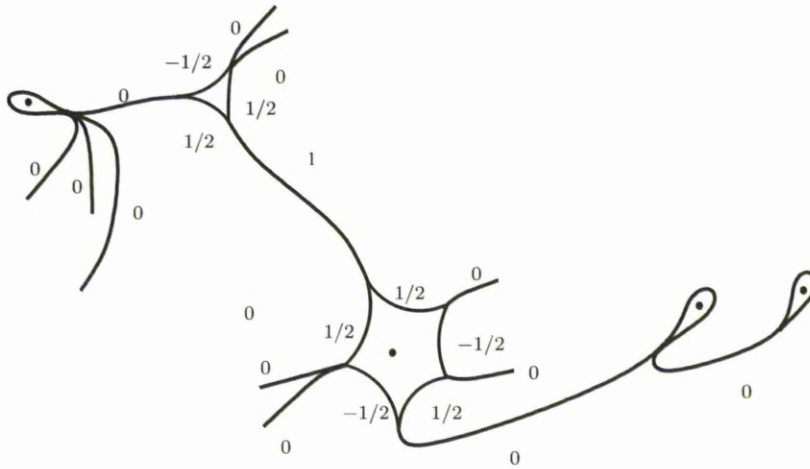


Figure 5.12: Constructing a basis for  $\mathcal{W}(\tau)$  when  $D_n - \tau$  consists of odd-gons

Hence the action on  $\mathcal{W}(\tau) \subseteq \mathbb{R}^k$  is given by the  $k \times k$  transition matrix

$$T' = \begin{pmatrix} T & 0 \\ A & P \end{pmatrix}$$

where  $T$  is the  $m \times m$  matrix which gives the action on the main branches of  $\tau$  by Lemma 5.18. When all components of  $D_n - \tau$  are odd-gons, a basis for  $\mathcal{W}(\tau) \cong \mathbb{R}^m$  can be constructed as described in Lemma 5.21 and hence the action on  $\mathcal{W}(\tau) \cong \mathbb{R}^m$  is given by the  $m \times m$  transition matrix  $T$ .

**Remark 5.23.** We note that such a basis can not be taken if  $D_n - \tau$  has an even-gon since the switch conditions are satisfied only when the alternating sum of the incoming measures on the switches of each even-gon is zero. However, there is still a basis consisting of weights on edges which may include infinitesimal ones, see [6].

## Chapter 6

# Transition matrices and Dybnikov matrices

The aim of Chapter 6 is to compare the spectra of Dybnikov matrices with the spectra of the train track transition matrices of a given pseudo-Anosov braid  $\beta \in B_n$ . Section 6.1 describes the change of coordinate function from train track coordinates to Dybnikov coordinates which is crucial for proving our results in Section 6.2 and Section 6.3.

In Section 6.2 it is shown that when the unstable invariant measured foliation  $(\mathcal{F}^u, \mu^u)$  of  $\beta \in B_n$  has only unpunctured 3-pronged and punctured 1-pronged singularities, then there is a unique Dybnikov matrix  $D$  which is isospectral to  $T$ . Section 6.3 studies the case when  $(\mathcal{F}^u, \mu^u)$  has singularities other than unpunctured 3-pronged and punctured 1-pronged singularities. First, two different ways of constructing a complete train track from  $\tau$  are described in Section 6.3.1 [24, 26]. Then, Lemma 6.18 is given: this new lemma plays a key role in our results since it explains how the charts constructed from these two different extensions fit together. In Section 6.3.2, it is shown that if  $\beta$  fixes the prongs of  $(\mathcal{F}^u, \mu^u)$ , then every Dybnikov matrix is isospectral to  $T$  up to some eigenvalues 1. The case in which  $\beta$  permutes the prongs of  $(\mathcal{F}^u, \mu^u)$  non-trivially is discussed in Section 6.3.3: a conjectured result, which has been observed in a wide range of examples, is illustrated with an example.

### 6.1 Train track coordinates and Dybnikov coordinates

In this section we will show that, for any train track  $\tau$  on  $D_n$ , the change of coordinate function  $L : \mathcal{W}^+(\tau) \rightarrow \mathcal{S}_n$  between train track coordinates and Dybnikov coordinates is piecewise linear.

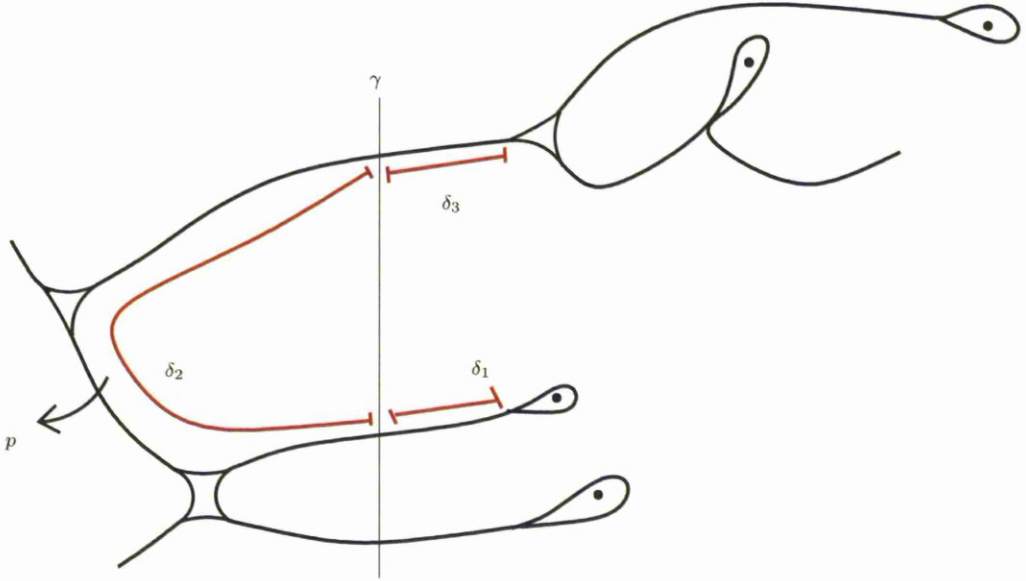


Figure 6.1: A minimal non-tight train path

**Definitions 6.1.** Let  $\tau$  be a train track on  $D_n$  and  $\mathcal{A}_n \subset D_n$  be the set of Dynnikov arcs  $\alpha_i$  ( $1 \leq i \leq 2n - 4$ ) and  $\beta_i$  ( $1 \leq i \leq n - 1$ ). A *standard embedding* of  $\tau$  in  $D_n$  with respect to  $\mathcal{A}_n$  satisfies the following:

- each branch  $e_i$  of  $\tau$  is tight (that is  $e_i$  doesn't bound any unpunctured disk with any Dynnikov arc)
- the arcs  $\alpha_i$  ( $1 \leq i \leq 2n - 4$ ) and  $\beta_i$  ( $1 \leq i \leq n - 1$ ) do not pass through the switches of  $\tau$ .

**Remark 6.2.** We shall always take a standard embedding of a given train track  $\tau$  as described in Definitions 6.1 throughout the text.

We say that a train path  $p$  in  $\tau$  is *non-tight* with respect to a Dynnikov arc  $\gamma$  if some subarc of  $p$  together with some subarc of  $\gamma$  bounds a disk containing no punctures. For each Dynnikov arc  $\gamma$  write  $\Pi_\gamma$  for the set of all train paths which are non-tight with respect to  $\gamma$ . There is a partial order  $\leq$  on  $\Pi_\gamma$  defined as follows:  $p_1 \leq p_2$  if  $p_1$  is a subpath of  $p_2$ . We define  $\Pi'_\gamma \subseteq \Pi_\gamma$  as the subset of minimal train paths with respect to the relation  $\leq$ . Then any minimal non-tight train path  $p \in \Pi'_\gamma$  is the concatenation  $p = \delta_1 \delta_2 \delta_3$  of three paths (not train paths) where  $\delta_2$  is the subarc bounding a disk with some subarc of  $\gamma$  and  $\delta_1$  and  $\delta_3$  are contained in single branches of  $\tau$  (Figure 6.1).

**Lemma 6.3.** *Let  $\tau$  be a train track. Then, the change of coordinate function  $L : \mathcal{W}^+(\tau) \rightarrow \mathcal{S}_n$  is piecewise linear.*

*Proof.* Given a Dynnikov arc  $\gamma$  and the branches  $\{e_1, \dots, e_k\}$  of  $\tau$  (standardly embedded) let  $n_i$  be the number of intersections of  $e_i$  with  $\gamma$ . To compute  $\mu(\gamma)$  we need to subtract the measure on all independent train paths which form a loop with  $\gamma$ . The only condition is that a train path should not be a subpath of another (two train paths neither of which is a subpath of the other define disjoint packets of leaves except perhaps their boundary leaves).

Thus the measure  $\mu(\gamma)$  of  $\gamma$  is given by

$$\mu(\gamma) = \sum_{i=1}^k n_i \mu(e_i) - 2 \sum_{p \in \Pi'_\gamma} \hat{p}(\mu). \quad (6.1)$$

We know that any  $p \in \Pi'_\gamma$  is of the form  $e_{i_1}^{\epsilon_1} \tilde{p} e_{i_2}^{\epsilon_2}$ , where  $e_{i_1}^{\epsilon_1}$  and  $e_{i_2}^{\epsilon_2}$  cross  $\gamma$  ( $e_{i_1}$  contains  $\delta_1$  and  $e_{i_2}$  contains  $\delta_3$ ). Note that  $\tilde{p}$  cannot contain the same branch with the same orientation twice since then it would contain a non-trivial loop which is impossible (a non-tight train path which contains a non-trivial loop is not minimal). Hence  $\mu(\gamma)$  is piecewise linear since  $\Pi'_\gamma$  is finite and for each of these train paths  $\hat{p}(\mu)$  is piecewise linear by Lemma 5.12. Therefore the map  $\mathcal{W}^+(\tau) \rightarrow \mathcal{S}_n$  is piecewise linear.  $\square$

Next, we shall illustrate Lemma 6.3 in the following example:

**Example 6.4.** Consider the 4-braid  $\beta = \sigma_1 \sigma_2 \sigma_3^{-1}$  on  $D_4$ . A standard embedding of the invariant train track  $\tau$  of  $\beta$  with respect to Dynnikov arcs is as depicted in Figure 6.2. Let  $a, b, c, d$  and  $m_1, m_2, m_3, m_4, m_5, m_6, m_7$  denote the measures on the main and infinitesimal branches of  $\tau$ . We first observe that the measures on the infinitesimal branches of  $\tau$  are determined by  $a, b, c, d$  since the switch conditions give

$$m_1 = a/2, \quad m_2 = b/2, \quad m_3 = (c + d)/2, \quad m_4 = d/2$$

$$m_5 = (a + b - c)/2, \quad m_6 = (b + c - a)/2, \quad m_7 = (a + c - b)/2.$$

Since  $D_n - \tau$  only has an unpunctured trigon and punctured monogons,  $\tau$  is complete and  $\text{rank}(\tau) = 4$ . We shall find the change of coordinate function  $(a, b, c, d) \mapsto (a_1, a_2, b_1, b_2)$  from train track coordinates to Dynnikov coordinates.

We have  $\beta_1 = a$ ,  $\beta_2 = c$  and  $\beta_3 = d$  since  $\Pi'_{\beta_i} = \emptyset$  for  $i = 1, 2, 3$ . Hence,

$$b_1 = \frac{a - c}{2} \quad \text{and} \quad b_2 = \frac{c - d}{2}.$$

We also have  $\Pi'_{\alpha_1} = \Pi'_{\alpha_3} = \emptyset$ , and  $\Pi'_{\alpha_2} = \{p_1\}$ ,  $\Pi'_{\alpha_4} = \{p_2\}$  where  $p_1$  and  $p_2$  are as depicted in Figure 6.2.



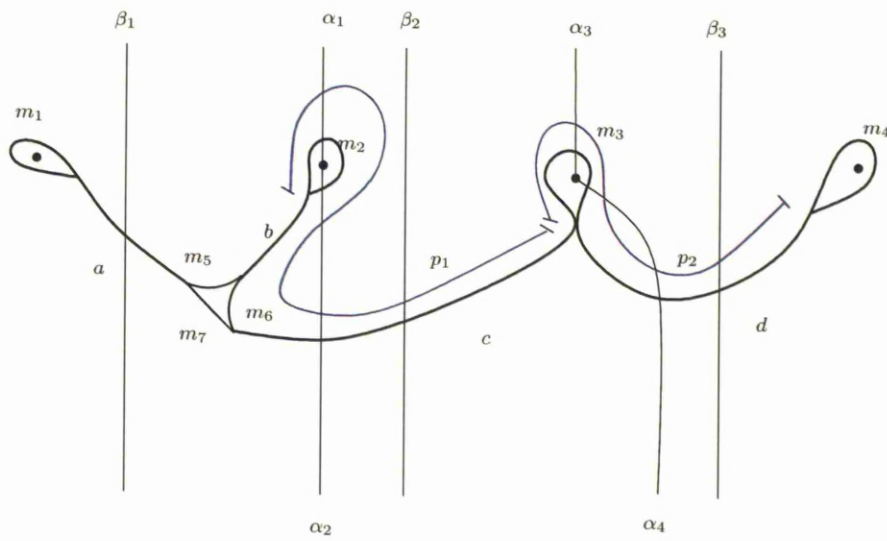


Figure 6.2: A standard embedding of  $\tau$  with respect to Dynnikov arcs

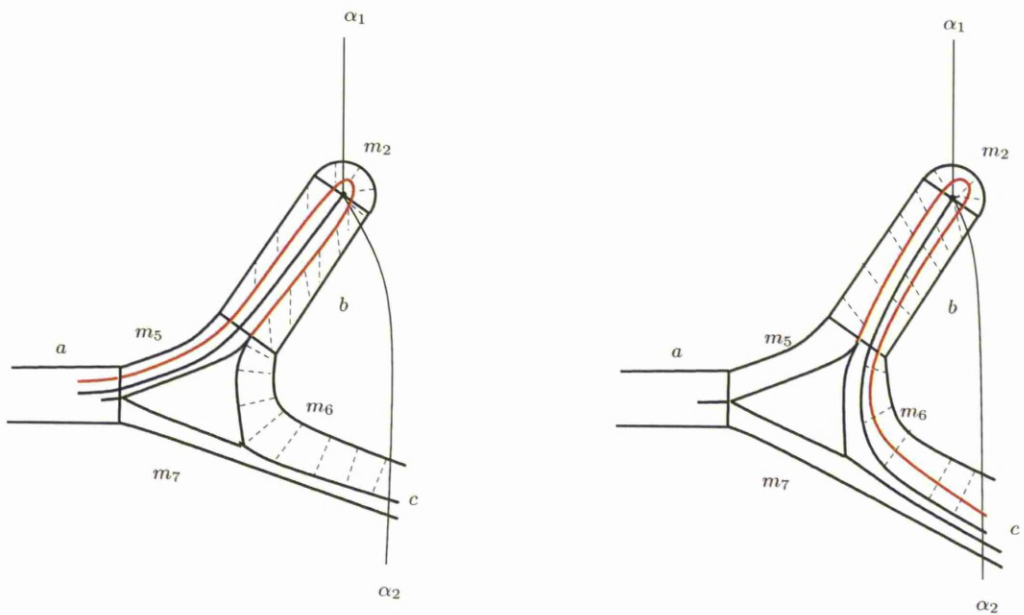


Figure 6.3:  $\hat{p}_1(\mu) = m_6$  on the left and  $\hat{p}_1(\mu) = b/2$  on the right

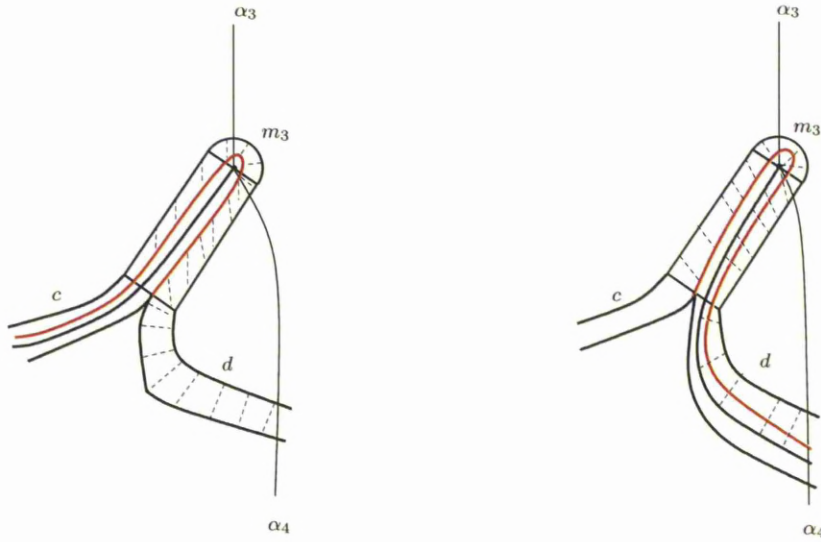


Figure 6.4:  $\hat{p}_2(\mu) = d$  on the left and  $\hat{p}_2(\mu) = m_3$  on the right

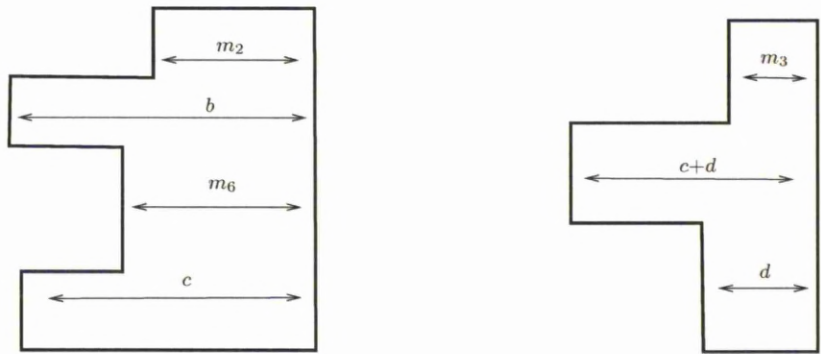


Figure 6.5:  $K_{p_1}$  and  $K_{p_2}$

We observe from Figure 6.3, Figure 6.4 and Figure 6.5 that

$$\hat{p}_1(\mu) = \min(m_2, m_6) \quad \text{and} \quad \hat{p}_2(\mu) = \min(d, m_3)$$

We have that

$$\alpha_1 = m_2 = b/2 \quad \text{and} \quad \alpha_2 = m_2 + c - 2\hat{p}_1(\mu).$$

Hence

$$\alpha_2 = \frac{b}{2} + c - \min(b, b + c - a) = \max(a, c) - \frac{b}{2},$$

and so,

$$a_1 = \frac{\alpha_2 - \alpha_1}{2} = \frac{\max(a, c) - b}{2}$$

We continue with  $\alpha_3$  and  $\alpha_4$ . Observe from Figure 6.2 that

$$\alpha_3 = m_3 = \frac{c + d}{2} \quad \text{and} \quad \alpha_4 = m_3 + d - 2\hat{p}_2(\mu).$$

Hence

$$\alpha_4 = \frac{c + d}{2} + d - \min(2d, c + d) = \max\left(\frac{c - d}{2}, \frac{d - c}{2}\right).$$

and so,  $\alpha_4 - \alpha_3 = \max(-c, -d)$  giving

$$a_2 = \frac{\alpha_4 - \alpha_3}{2} = \frac{\max(-c, -d)}{2}.$$

Hence,

$$(a_1, a_2, b_1, b_2) = \left( \frac{\max(a, c) - b}{2}, \frac{\max(-c, -d)}{2}, \frac{a - c}{2}, \frac{c - d}{2} \right).$$

## 6.2 The spectrum of a Dynnikov matrix when $\tau$ is complete

Let  $[f] \in \text{MCG}(D_n)$  be a pseudo-Anosov isotopy class with unstable invariant foliation  $(\mathcal{F}^u, \mu^u)$  and dilatation  $\lambda > 1$ . Let  $[a^u, b^u]$  denote the Dynnikov coordinates of  $(\mathcal{F}^u, \mu^u)$  on the projective space of Dynnikov coordinates  $\mathcal{PS}_n$ . Recall that the action of  $[f]$  on  $\mathcal{PS}_n$  is piecewise linear and each piece  $\mathcal{R}_i \subset \mathcal{PS}_n$  associated with a different matrix and containing  $[a^u, b^u]$  is called a *Dynnikov region*. Then a *Dynnikov matrix*  $\mathcal{D}_i : \mathcal{R}_i \rightarrow \mathcal{PS}_n$ , ( $1 \leq i \leq k$ ) is the  $(2n - 4) \times (2n - 4)$  integer matrix which describes the action of  $[f]$  in a Dynnikov region  $\mathcal{R}_i$ .

We also want to remark once more that finding Dynnikov matrices is much easier than finding train track transition matrices: given an infinite family of braids, train tracks are computed using, for example, the Bestvina-Handel algorithm [5] for enough examples to spot a general pattern. Then, we prove that the conjectured pattern holds for all isotopy classes in the family. The drawback in this method is that if the isotopy class is complicated that is, if its topological entropy is high, then it is far from straightforward to describe an infinite family of train tracks to verify that they are invariant under the relevant isotopy classes since the image edge paths will be too long to track. On the other hand, a Dynnikov region for  $[f]$  is easy to find since  $[a^u, b^u]$  is a globally attracting fixed point for the action of  $[f]$  on the boundary of  $\mathcal{PS}_n$  (see Chapter 4). We encourage the reader to take a random braid and try the two different methods using the train track and Dynnikov programs implemented in the C++ code by Toby Hall and both of which can be found at [18]. Take for example the 4-braid

$$\sigma_1^{-1}\sigma_2^{-3}\sigma_3^{-5}\sigma_1^4\sigma_2^{-2}\sigma_3^{-1}\sigma_1\sigma_2\sigma_3^{-2}(\sigma_2\sigma_3^{-2})^{19}\sigma_1^{-8}\sigma_3^{-1}\sigma_1^{-2}\sigma_2^2\sigma_3^{-1}\sigma_1^{-1}\sigma_2\sigma_3\sigma_1\sigma_2^{-1}\sigma_3^{-1}.$$

where the growth rate is approximately  $8.6 \times 10^{14}$  (entropy is  $\sim 34.38$ ). This means the initial image edge paths have length approximately  $8.6 \times 10^{14}$ . An edge path of this length occupies approximately  $10^5$  GB of memory and hence the train track program can not even start, whereas the Dynnikov matrix is found in less than a second (it is

$$\begin{bmatrix} -68900596045753 & 200002959211464 & 146825523685804 & -943752747512 \\ -181490417757959 & 526825930446403 & 386751743244292 & -2485930314639 \\ -188609831321041 & 547491989409364 & 401923043417627 & -2583447121425 \\ 76020009608848 & -220669018174468 & -161996823859176 & 1041269554295 \end{bmatrix},$$

with spectral radius  $215222411843143 + 4\sqrt{2895042909973767357229710094} + 2\sqrt{23160343279789934495527869988 + 430444823686286\sqrt{2895042909973767357229710094}}$ ).

This section focuses on the case where the invariant unstable foliation  $(\mathcal{F}^u, \mu^u)$  has only unpunctured 3-pronged and punctured 1-pronged singularities. In this case, we shall show that there is a unique Dynnikov region  $\mathcal{R}$  (and hence a unique Dynnikov matrix  $D$ ) and the transition matrix  $T$  associated with a (complete) invariant regular train track of  $[f]$  is isospectral to  $D$ . We shall then prove that the same result holds for any invariant train track of  $[f]$  up to roots of unity and zeros. This will follow from a result by Rykken [27] given in Theorem 6.6 below.

**Theorem 6.5.** *Let  $[f] \in \text{MCG}(D_n)$  be a pseudo-Anosov isotopy class with unstable invariant foliation  $(\mathcal{F}^u, \mu^u)$  and dilatation  $\lambda > 1$ . Let  $\tau$  be a regular invariant train track with associated transition matrix  $T$ . If  $(\mathcal{F}^u, \mu^u)$  has only unpunctured 3-pronged and punctured 1-pronged singularities, then  $\beta$  has a unique Dynnikov matrix  $D$ , and  $D$  and  $T$  are isospectral.*

*Proof.* Since  $(\mathcal{F}^u, \mu^u)$  has only unpunctured 3-pronged and punctured 1-pronged singularities,  $\tau$  is complete. That is,  $\mathcal{W}^+(\tau)$  has dimension  $2n - 4$ . Therefore,  $\mathcal{MF}(\tau)$  is a chart on  $\mathcal{MF}_n$  by Lemma 5.8. By Lemma 5.20, the eigenvector  $v$  associated with the dilatation  $\lambda > 1$  is a transverse measure on  $\tau$  with  $(\mathcal{F}^u, \mu^u) = \phi_\tau(v)$ . Furthermore, the entries of  $v$  are strictly positive. Therefore,  $\mathcal{W}^+(\tau)$  and  $\mathcal{MF}(\tau)$  are neighbourhoods of  $v$  and  $(\mathcal{F}^u, \mu^u)$  respectively. Construct the pre-foliation  $\mathcal{F}^*$  from  $\tau$  as described in Section 5.1. Because none of the prongs of  $\mathcal{F}^*$  are connected by Lemma 5.20, it follows from Remark 5.13 that there is a neighbourhood  $U$  of  $v \in \mathcal{W}^+(\tau)$  on which the change of coordinate function  $L = \rho \circ \phi_\tau$  from train track coordinates to Dynnikov coordinates is linear. Write  $\mathcal{R} = L(U) \subseteq \mathcal{S}_n$  which is a neighbourhood of  $L(v)$ . We have the following commutative diagram:

$$\begin{array}{ccc}
 \mathcal{W}^+(\tau) & \xrightarrow{T} & \mathcal{W}^+(\tau) \\
 \phi_\tau \downarrow & & \phi_\tau \downarrow \\
 \mathcal{MF}(\tau) & \xrightarrow{\beta} & \mathcal{MF}(\tau) \\
 \rho \downarrow & & \rho \downarrow \\
 \mathcal{R} \subseteq \mathcal{S}_n & \xrightarrow{F} & \mathcal{S}_n
 \end{array} \tag{6.2}$$

Then  $F|_{\mathcal{R}} = D = L \circ T \circ L^{-1}$  is linear and isospectral to  $T$ .

□

In the above we considered the transition matrix for a regular complete train track. A similar result follows for general train tracks from a result of Rykken [27]:

**Theorem 6.6** (Rykken). *Let  $f \in \text{Aut}(M)$  be a pseudo-Anosov automorphism on an orientable surface of genus  $g$  with oriented unstable manifolds. Let  $T$  be a train track transition matrix for  $f$ . If  $f$  preserves the orientation of unstable manifolds, then the eigenvalues of  $f_{1*} : H_1(M; \mathbb{R}) \rightarrow H_1(M; \mathbb{R})$  are the same as those of  $T$ , including multiplicity, up to roots of unity and zeros.*

**Lemma 6.7.** *Let  $\beta$  be a pseudo-Anosov isotopy class on  $D_n$  with invariant train track  $\tau$  and associated transition matrix  $T$ . Let  $\tilde{f}$  be the lift of  $f$  to the orientation*

double cover  $M$ . Let  $\tilde{\tau}$  and  $\tilde{T}$  be the lifted invariant train track and transition matrix associated to  $[\tilde{f}]$ . Then  $T$  and  $\tilde{T}$  are isospectral up to roots of unity.

*Proof.* Let  $\{e_i\}_{1 \leq i \leq N}$  be the oriented branches of  $\tau$ . Take a copy  $e'_i$  of each  $e_i$  and endow it with the opposite orientation. The lifted train track  $\tilde{\tau}$  is obtained by gluing together the branches  $e_i$  and  $e'_i$  following the pattern of the original train track  $\tau$ , but in such a way that the orientations of all of the branches at each switch are consistent. By construction, the edge path  $\tilde{f}(e_i)$  is obtained from the edge path  $f(e_i)$  by replacing each occurrence of  $\overline{e_j}$  with  $e'_j$ ; and similarly, the edge path  $\tilde{f}(e'_i)$  is obtained from the edge path  $\overline{f(e_i)}$  by replacing each occurrence of  $\overline{e_j}$  with  $e'_j$ .

Let  $A_{ij}$  be the number of occurrences of  $e_i$  in  $\tilde{f}(e_j)$  (that is, the number of occurrences of  $e_i$  in  $f(e_j)$ ), which by construction is equal to the number of occurrences of  $e'_i$  in  $\tilde{f}(e'_j)$ ; and let  $B_{ij}$  be the number of occurrences of  $e'_i$  in  $\tilde{f}(e_j)$  (that is, the number of occurrences of  $\overline{e_i}$  in  $f(e_j)$ ), which by construction is equal to the number of occurrences of  $e_i$  in  $\tilde{f}(e'_j)$ . Hence the lifted transition matrix  $\tilde{T}$  is of the form

$$\tilde{T} = \begin{pmatrix} A & B \\ B & A \end{pmatrix},$$

where  $A + B = T$  (and we have restricted to the main branches  $e_i$  ( $1 \leq i \leq k$ ) and their copies  $e'_i$ ). Hence we have

$$\begin{aligned} \chi(\tilde{T}) &= |xI_{2k} - \tilde{T}| = \begin{vmatrix} xI_k - A & -B \\ -B & xI_k - A \end{vmatrix} = \begin{vmatrix} xI_k - A & xI_k - T \\ -B & xI_k - T \end{vmatrix} \\ &= \begin{vmatrix} xI_k - A + B & 0_k \\ -B & xI_k - T \end{vmatrix} \\ &= |xI_k - A + B| |xI_k - T| \end{aligned}$$

That is, the set of eigenvalues of  $\tilde{T}$  is the union of the set of eigenvalues of  $T$  and the set of eigenvalues of  $A - B$ . It remains to show that the eigenvalues of  $A - B$  are roots of unity.

Now for each  $m \geq 1$ , let  $A_{ij}^{(m)}$  denote the number of occurrences of  $e_i$  in  $f^m(e_j)$ , and  $B_{ij}^{(m)}$  denote the number of occurrences of  $\overline{e_i}$  in  $f^m(e_j)$ . A straightforward induction shows that the matrix  $A^{(m)}$  is the sum of all products of  $m$  copies of  $A$  and  $B$  having an even number of  $B$ s, and  $B^{(m)}$  is the sum of all products of  $m$  copies of  $A$  and  $B$  having an odd number of  $B$ s: therefore  $A^{(m)} - B^{(m)} = (A - B)^m$ .

Let  $m$  be such that  $f^m$  fixes all of the prongs of  $\tau$ . Then for each  $e_i$ , the initial and terminal points of  $e_i$  and of  $f^m(e_i)$  are the same. Since each real branch

disconnects  $\tau$ , it follows that  $A_{ij}^{(m)} = B_{ij}^{(m)}$  for all  $i \neq j$ , and  $A_{ii}^{(m)} = B_{ii}^{(m)} + 1$  for all  $i$  (the number of times that  $f^m(e_i)$  crosses  $e_i$  in the positive direction is one more than the number of times it crosses in the negative direction). That is

$$(A - B)^m = A^{(m)} - B^{(m)} = Id,$$

so that all of the eigenvalues of  $A - B$  are roots of unity as required.  $\square$

**Corollary 6.8.** *Let  $[f] \in \text{MCG}(D_n)$  be a pseudo-Anosov isotopy class with unstable invariant foliation  $(\mathcal{F}^u, \mu^u)$  and dilatation  $\lambda > 1$ . Let  $\tau$  be any complete invariant train track with associated transition matrix  $T$ . Then  $T$  and  $D$  are isospectral up to roots of unity and zeros.*

*Proof.* If  $f \in \text{Aut}(D_n)$  is a pseudo-Anosov automorphism it lifts to a pseudo-Anosov automorphism  $\tilde{f} \in \text{Aut}(M)$  where  $M$  is the orientation double cover [27]. Pick a regular invariant train track  $\tau_r$  and an arbitrary invariant train track  $\tau$  of  $f \in \text{Aut}(D_n)$  with associated transition matrices  $T_r$  and  $T$ . Given two matrices  $A$  and  $B$ , write  $A \sim B$  if  $A$  and  $B$  are isospectral up to roots of unity and zeros. Then,  $D \sim T_r$  by Theorem 6.5,  $T_r \sim \tilde{T}_r$  by Lemma 6.7,  $\tilde{T}_r \sim \tilde{T}$  by Theorem 6.6 and  $\tilde{T} \sim T$  by Lemma 6.7. Therefore,  $D \sim T$ .  $\square$

**Example 6.9.** The 4-braid  $\beta = \sigma_1\sigma_2^{-1}\sigma_3^2\sigma_2\sigma_1\sigma_2^{-1}$  has an invariant train track as depicted in Figure 6.6 with associated transition matrix

$$T = \begin{bmatrix} 2 & 0 & 2 & 1 \\ 2 & 0 & 3 & 1 \\ 1 & 1 & 2 & 0 \\ 1 & 0 & 4 & 0 \end{bmatrix},$$

and the coordinates of the eigenvector of  $T$  corresponding to the Perron-Frobenius eigenvalue  $\lambda = 4.61158$  are given by

$$(0.50135, 0.59215, 0.41871, 0.47190).$$

$(\mathcal{F}^u, \mu^u)$  is in the interior of a Dynnikov region  $\mathcal{R}$  and the action on this region is given by the Dynnikov matrix

$$D = \begin{bmatrix} 5 & -2 & 3 & 1 \\ 3 & 0 & 1 & -2 \\ 1 & -1 & 1 & 1 \\ 1 & 1 & 0 & -2 \end{bmatrix}.$$

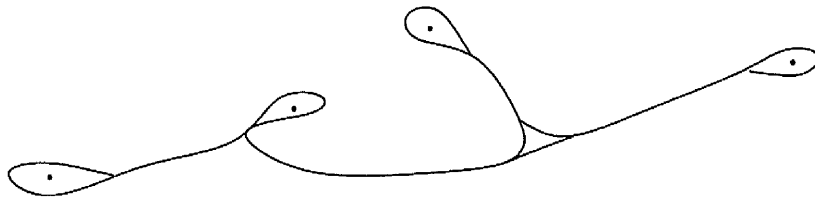


Figure 6.6: Invariant train track for  $\sigma_1 \sigma_2^{-1} \sigma_3^3 \sigma_2 \sigma_1 \sigma_2^{-1}$

Both  $D$  and  $T$  have spectrum

$$\{1 + \sqrt{2} \pm \sqrt{2 + 2\sqrt{2}}, 1 - \sqrt{2} \pm i\sqrt{2\sqrt{2} - 2}\}.$$

### 6.3 The spectrum of a Dynnikov matrix when $\tau$ is not complete

Let  $\beta \in B_n$  be a pseudo-Anosov braid with unstable invariant foliation  $(\mathcal{F}^u, \mu^u)$ , dilatation  $\lambda > 1$  and regular invariant train track  $\tau$  with transition matrix  $T$ . This section studies the case where the invariant unstable measured foliation  $(\mathcal{F}^u, \mu^u)$  has other than punctured 1-pronged and unpunctured 3-pronged singularities. In this case  $\tau$  is not complete and since  $\text{rank}(\tau) < 2n - 4$ ,  $\mathcal{MF}(\tau)$  does not define a chart on  $\mathcal{MF}_n$ . We shall study this case considering the two possibilities: first, where the prongs of the invariant foliations (the cusps of  $\tau$ ) are fixed by  $\beta$ ; and second, where they are permuted non-trivially.

If  $\beta$  fixes the prongs, we shall see that every Dynnikov matrix is isospectral to  $T$  up to some eigenvalues 1. If  $\beta$  permutes the prongs non-trivially, then for some power  $m$ ,  $\beta^m$  fixes the prongs and it follows that every Dynnikov matrix for  $\beta^m$  is isospectral to  $T^m$  up to some eigenvalues 1 and zeros.

However, since the induced action of  $\beta^m$  on  $\mathcal{PS}_n$  is a product of several Dynnikov matrices, we can not conclude in the permuted prongs case that a Dynnikov matrix  $D_i$  and  $T$  are isospectral up to roots of unity. This point will be clarified in Section 6.3.3.

The main tool to prove our results will be to extend non-complete train tracks to those which are complete. We shall use two basic moves: pinching and diagonal extension [24, 26]. The moves will be described in Section 6.3.1.

#### 6.3.1 Pinching and diagonal extension

In this section, we shall describe the two moves *pinching* and *diagonal extension* to construct a complete train track from a non-complete one [24, 26]. We shall



begin with the pinching move.

**Definition 6.10 (Pinching unpunctured t-gons).** Let  $\tau$  be a train track with an unpunctured  $t$ -gon  $P$ , where  $t \geq 4$ . Let  $e_1, \dots, e_t$  denote the (infinitesimal) edges of  $P$ . *Pinching* across  $e_i$  is a move which constructs a new train track  $\tau' > \tau$  by pinching together the two edges  $e_{i-1}$  and  $e_{i+1}$  adjacent to  $e_i$ <sup>1</sup>. See Figure 6.7. The train track  $\tau'$  has three additional edges denoted  $e'_{i-1}$ ,  $e'_{i+1}$  and  $\epsilon$ : in place of the  $t$ -gon  $P$  it has a  $(t-1)$ -gon and a trigon. The function  $\psi_{e_i} : \mathcal{W}(\tau) \rightarrow \mathcal{W}(\tau')$  is defined as follows.

If  $w = (w_1, \dots, w_t, w_{t+1}, \dots, w_k) \in \mathcal{W}(\tau)$ , then  $\psi_{e_i}(w)$  gives weights  $w_{i-1}$  to  $e'_{i-1}$ ,  $w_{i+1}$  to  $e'_{i+1}$ ,  $w_{i-1} + w_{i+1}$  to  $\epsilon$  and  $w_j$  to  $e_j$  for  $1 \leq j \leq k$ . We remark that if every component of  $w$  is positive, then the same is true for  $\psi_{e_i}(w)$ .

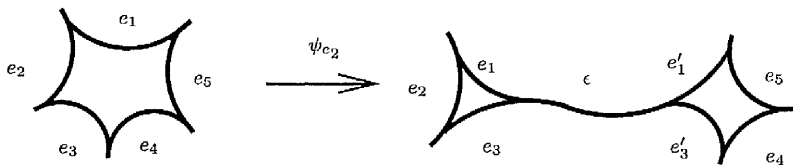


Figure 6.7: Pinching move (across  $e_2$ ) on an unpunctured 5-gon

**Definition 6.11 (Pinching punctured t-gons).** Let  $\tau$  be a train track with a punctured  $t$ -gon  $P$  where  $t \geq 2$ . Let  $e_1, \dots, e_t$  denote the (infinitesimal) edges of  $P$ . *Pinching* of  $e_i$  is a move which constructs a new train track  $\tau' > \tau$  by pinching  $e_i$  to itself around the puncture as depicted in Figure 6.8. The train track  $\tau'$  has three additional edges denoted  $\epsilon, e'_i, e''_i$ : in place of the punctured  $t$ -gon, it has an unpunctured  $(t+1)$ -gon and a punctured monogon.

The function  $\psi_{e_i} : \mathcal{W}(\tau) \rightarrow \mathcal{W}(\tau')$  is given as follows.

If  $w = (w_1, \dots, w_t, w_{t+1}, \dots, w_k) \in \mathcal{W}(\tau)$ ,  $\psi_{e_i}(w)$  gives weights  $2w_i$  to  $\epsilon$ ,  $w_i$  to  $e'_i$  and  $e''_i$ , and  $w_j$  to  $e_j$  for  $1 \leq j \leq k$ . We remark again that if every component of  $w$  is positive, then the same is true for  $\psi_{e_i}(w)$ .

**Definition 6.12.** We say that a complete train track  $\tau_p$  on  $D_n$  is a *pinching* of  $\tau$  if it is constructed from  $\tau$  by a sequence of pinching moves.

**Remark 6.13.** Given a train track  $\tau$ , pinching each punctured  $t$ -gon with  $t \geq 2$  yields a train track with only punctured monogons and unpunctured  $t$ -gons for  $t \geq 3$ . Pinching each unpunctured  $t$ -gon  $t-3$  times then yields a pinching of  $\tau$ . Observe that there are many different pinchings of  $\tau$  (Figure 6.9). The main

<sup>1</sup>Here and in what follows, indices are taken modulo  $t$

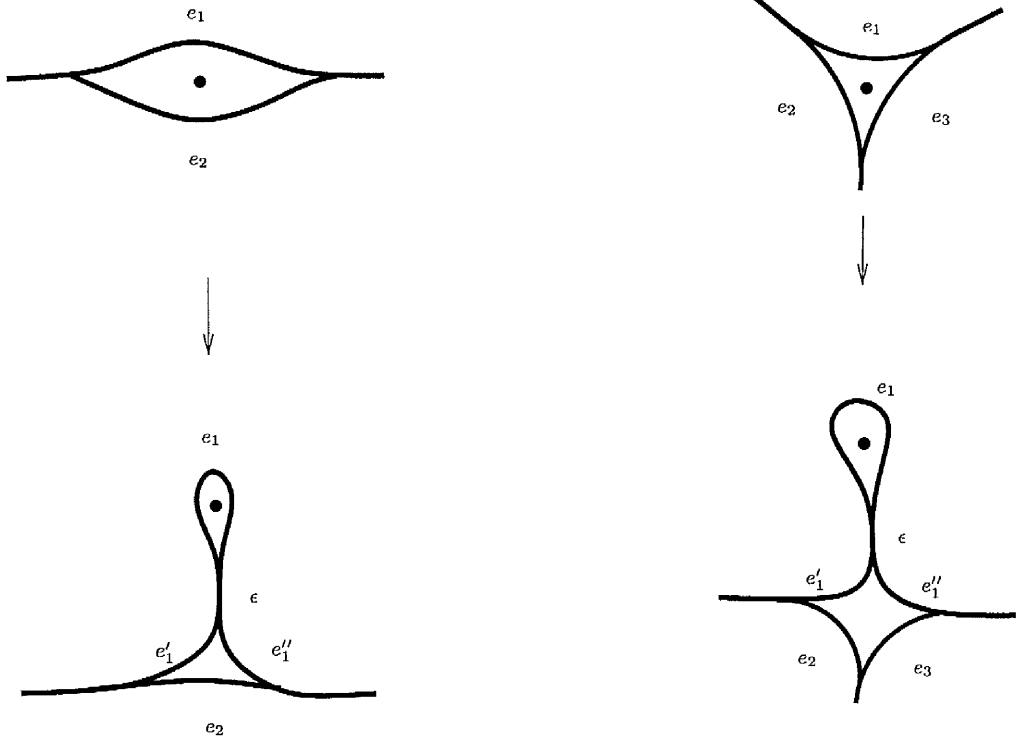


Figure 6.8: Pinching move (of  $e_1$ ) on a punctured bigon and a punctured trigon

result about pinched train tracks in Lemma 6.18 doesn't depend on the choice of pinching.

Therefore, pinching constructs a complete train track  $\tau_p$  from a non-complete one  $\tau$  in such a way that  $\tau < \tau_p$ , with the important feature that a strictly positive measure on  $\tau$  induces a strictly positive measure on  $\tau_p$ . Hence,  $\mathcal{MF}(\tau_p)$  defines a chart on  $\mathcal{MF}_n$  which contains  $(\mathcal{F}^u, \mu^u)$  in its interior. However, it should be noted that if  $\tau$  is an invariant train track for  $\beta$ ,  $\tau_p$  will not be invariant unless relevant prongs of  $(\mathcal{F}^u, \mu^u)$  are fixed by  $\beta$ . Therefore, we need a set of charts that fit nicely in  $\mathcal{MF}(\tau_p)$  with the property that the action in each of them is described explicitly.

We shall use the *diagonal extension* move to describe such charts. Diagonal extension gives a collection of *diagonally extended* train tracks  $\tau_i$  in such a way that  $\tau < \tau_i$ . The disadvantage of diagonal extension is that a strictly positive measure on  $\tau$  induces zero measure on the additional branches of  $\tau_i$  and hence  $(\mathcal{F}^u, \mu^u)$  is on the boundary of each  $\mathcal{MF}(\tau_i)$ . However, Lemma 6.18 gives that the charts  $\mathcal{MF}(\tau_i)$  fit together nicely and have union  $\mathcal{MF}(\tau_p)$ : moreover for each  $i$  there is some  $j$  such that  $\beta(\mathcal{MF}(\tau_i)) = \mathcal{MF}(\tau_j)$ , and this action can be simply described with respect to appropriate bases.

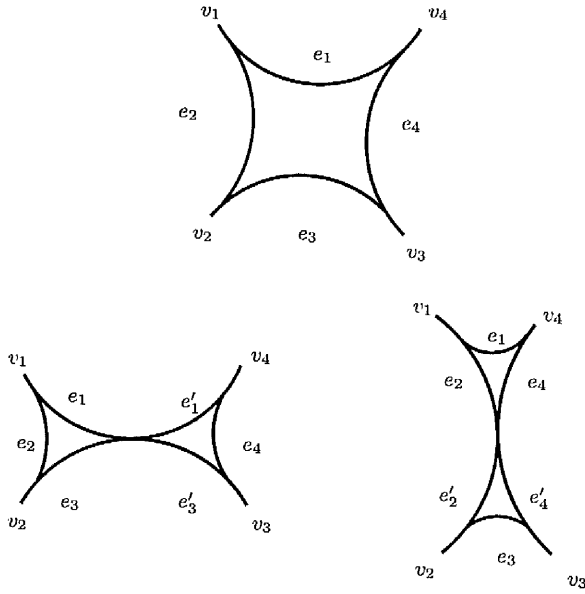


Figure 6.9: Two different pinchings of an unpunctured 4-gon

**Definition 6.14 (Diagonal extension on unpunctured t-gons).** Let  $\tau$  be a train track with an unpunctured  $t$ -gon  $P$  where  $t \geq 4$ . Let  $v_1, \dots, v_t$  denote the vertices of  $P$ . *Diagonal extension* of  $P$  is a move which constructs a new train track  $\tau' > \tau$  by adding  $t - 3$  branches (with disjoint interiors) inside  $P$  such that each additional branch joins two non-consecutive vertices  $v_i$  and  $v_j$  and is tangent to the (infinitesimal) edges of  $P$  at these vertices. See Figure 6.10. The train track  $\tau'$  has  $t - 3$  additional edges denoted  $\epsilon_{ij}$  for appropriate choices of  $i$  and  $j$  with  $|i - j| > 1$ : in place of the  $t$ -gon, it has  $t - 2$  unpunctured trigons. The function  $\psi : \mathcal{W}(\tau) \rightarrow \mathcal{W}(\tau')$  is given as follows.

If  $w = (w_1, \dots, w_k) \in \mathcal{W}(\tau)$ ,  $\psi(w)$  gives zero weights to each  $\epsilon_{ij}$ , and weight  $w_i$  to  $e_i$  for  $1 \leq i \leq k$ .

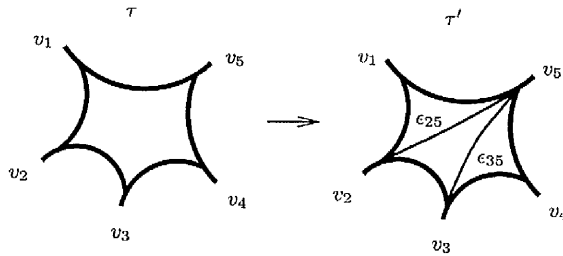


Figure 6.10: Diagonal extension on an unpunctured 5-gon

**Definition 6.15 (Diagonal extension on punctured t-gons).** Let  $\tau$  be a

train track with a punctured  $t$ -gon  $P$  where  $t \geq 2$ . Let  $v_1, \dots, v_t$  denote the vertices of  $P$ . *Diagonal extension* of  $P$  is a move which constructs a new train track  $\tau' > \tau$  by first adding a branch  $\epsilon_{ii}$  which encircles the puncture with both end points at a single vertex  $v_i$  (so that  $P$  is divided into a punctured monogon and an unpunctured  $(t+1)$ -gon); and then adding  $t-2$  additional branches to divide the  $(t+1)$ -gon into  $t-1$  trigons as in the unpunctured case. See Figure 6.11. The train track  $\tau'$  therefore has a punctured monogon and  $t-1$  unpunctured trigons in place of the punctured  $t$ -gon  $P$ . The function  $\psi : \mathcal{W}(\tau) \rightarrow \mathcal{W}(\tau')$  is given as follows.

If  $w = (w_1, \dots, w_k) \in \mathcal{W}(\tau)$ ,  $\psi(w)$  gives weight  $w_j$  to  $e_j$  for  $1 \leq j \leq k$ , and weight zero to the other edges.

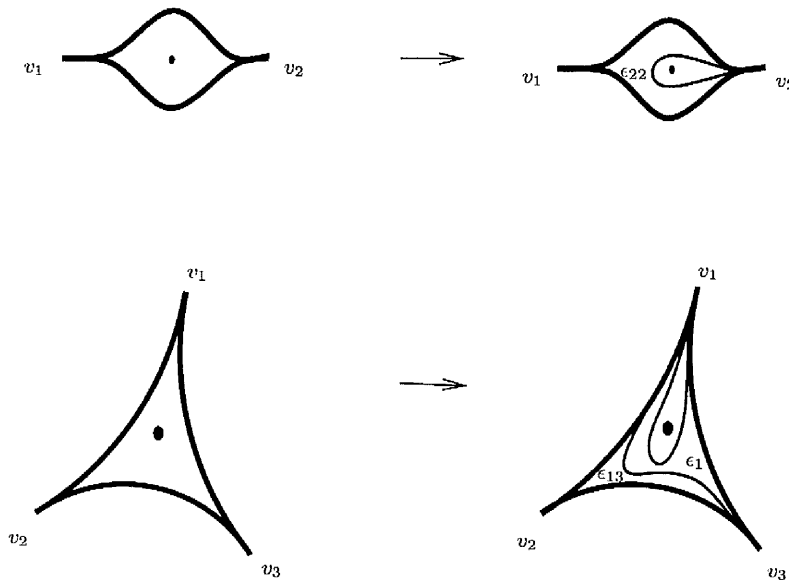


Figure 6.11: Diagonal extension on a punctured bigon and a punctured trigon

**Definition 6.16.** We say that a complete train track  $\tau'$  on  $D_n$  is a *diagonal extension* of  $\tau$  if it is constructed from  $\tau$  by a sequence of diagonal extensions. We write  $\tau_1, \tau_2, \dots, \tau_\xi$  to denote the different diagonal extensions of  $\tau$ .

**Remark 6.17.** Note that the number of diagonal extensions of an unpunctured  $t$ -gon is  $\xi = c_{t-2}$  where

$$c_t = \binom{2t}{t} - \binom{2t}{t-1}$$

is the  $t^{\text{th}}$  Catalan number, since the Catalan number gives the number of different ways to divide a polygon into triangles by joining its vertices with additional edges. See Figure 6.12.

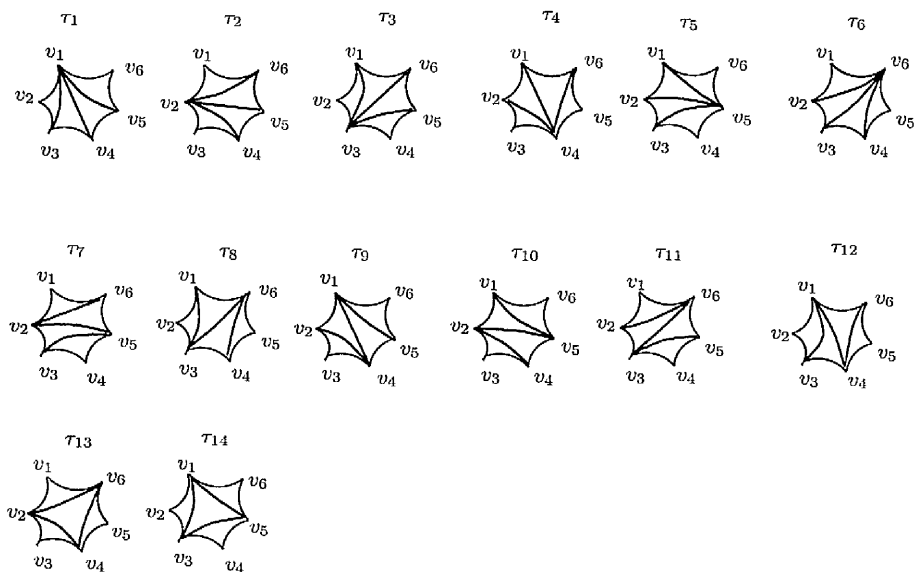


Figure 6.12: There are  $c_4 = 14$  different ways to diagonalize an unpunctured 6-gon.

Similarly, the number of diagonal extensions of a punctured  $t$ -gon is  $\xi = t \cdot c_{t-1}$ : after adding the encircling branch  $\epsilon_{ii}$  at vertex  $v_i$  ( $t$  choices),  $P$  is divided into an unpunctured  $(t+1)$ -gon and a punctured monogon. Since there are  $c_{t-1}$  different ways to divide an unpunctured  $(t+1)$ -gon into triangles the result follows.

Given a train track  $\tau$ , let  $G$  denote the set of unpunctured polygons of  $\tau$ , and given  $P \in G$  write  $n_P$  for the number of vertices of  $P$ . Similarly, let  $G'$  denote the set of punctured polygons of  $\tau$ , and given  $P \in G'$  write  $n_P$  for the number of vertices of  $P$ . Then the number of diagonal extensions of  $\tau$  is given by

$$\xi = \left( \prod_{P \in G} c_{n_P-2} \right) \cdot \left( \prod_{P \in G'} n_P \cdot c_{n_P-1} \right).$$

The fact that  $\xi$  can be large for relatively simple train tracks explains why there can be many Dynnikov regions for braids on relatively few strings (recall from Section 4.5 that there are  $2^{n-4}$  Dynnikov regions for  $\sigma_1 \dots \sigma_{n-2} \sigma_{n-1}^{-1} \in B_n$ ). It will be seen in Remark 6.24 that the number of Dynnikov regions is bounded above by the number of diagonal extensions of  $\tau$ .

Since each pinching  $\tau_p$  and diagonal extension  $\tau_i$  of  $\tau$  is complete, they define charts on  $\mathcal{MF}_n$  by Lemma 5.8. The following key lemma describes how these charts fit together.

**Lemma 6.18.** *Let  $\tau$  be a regular invariant train track for  $\beta$  with associated matrix  $T : \mathcal{W}(\tau) \rightarrow \mathcal{W}(\tau)$ . Let  $\tau_p$  be a pinching of  $\tau$ , and let  $\tau_1, \dots, \tau_\xi$  denote the diagonal extensions of  $\tau$ . Then,*

$$i. \bigcup_{1 \leq i \leq \xi} \mathcal{MF}(\tau_i) = \mathcal{MF}(\tau_p).$$

ii. *If  $i \neq j$ , then  $\mathcal{MF}(\tau_i)$  and  $\mathcal{MF}(\tau_j)$  intersect only on their boundaries.*

iii. *For each  $i$  there is some  $j$  such that  $\beta(\mathcal{MF}(\tau_i)) = \mathcal{MF}(\tau_j)$ , and the induced action of  $\beta : \mathcal{W}(\tau_i) \rightarrow \mathcal{W}(\tau_j)$  is given by a matrix of the form*

$$\tilde{T} = \begin{bmatrix} T & X \\ 0 & Id \end{bmatrix}$$

*with respect to an appropriate choice of bases of  $\mathcal{W}(\tau_i)$  and  $\mathcal{W}(\tau_j)$ .*

iv. *For each  $i$ , the change of coordinate function  $\rho \circ \phi_{\tau_i} : \mathcal{W}^+(\tau_i) \rightarrow \mathcal{S}_n$  is linear in a neighbourhood in  $\mathcal{W}^+(\tau_i)$  of  $v^u = \phi_{\tau_i}^{-1}(\mathcal{F}^u, \mu^u)$ .*

*Proof.* Assume first that every component of  $D_n - \tau$  is a punctured monogon or unpunctured trigon, except for one unpunctured  $t$ -gon  $P$  ( $t \geq 4$ ). Let  $v_1, v_2, \dots, v_t$  denote the vertices of  $P$ . Let  $\tau_p$  be a pinching of  $\tau$  and  $N$  denote a regular neighbourhood of the pinched  $t$ -gon. Let  $a_1, \dots, a_t$  denote the *gates* of  $N$  (that is, the components of the subset of  $\partial N$  which is not comprised of leaves). See Figure 6.13.

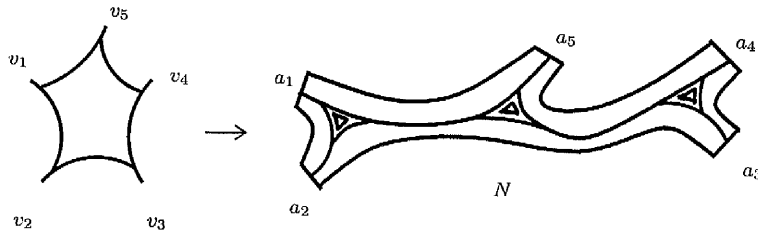


Figure 6.13: The regular neighbourhood  $N$  of a pinched unpunctured 5-gon

To each  $(\mathcal{F}, \mu) \in \mathcal{MF}(\tau_p)$  we associate the collection of two element sets  $\{j, k\}$  ( $|j - k| > 1$ ) such that  $(\mathcal{F}, \mu)$  has a leaf which enters  $N$  through  $a_j$  and exits through  $a_k$ . Denote this *label set*  $\Gamma(\mathcal{F}, \mu)$  and observe that the cardinality  $|\Gamma(\mathcal{F}, \mu)| \leq t - 3$  since leaves don't cross.

Similarly, to each diagonal extension  $\tau_i$  of  $\tau$ , we associate the set of pairs  $(j, k)$  such that  $\tau_i$  has a branch joining  $v_j$  to  $v_k$ . Denote this *label set*  $\Delta(\tau_i)$ . It is clear that  $(\mathcal{F}, \mu) \in \mathcal{MF}(\tau_i)$  if and only if  $\Gamma(\mathcal{F}, \mu) \subseteq \Delta(\tau_i)$ .

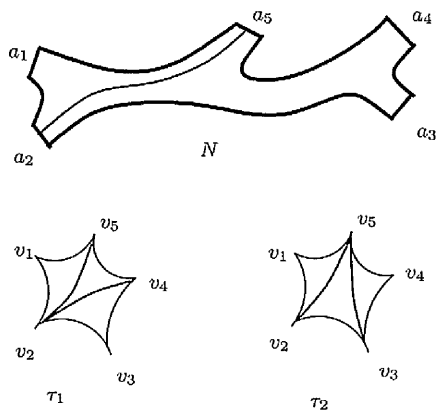


Figure 6.14: If  $\Gamma(\mathcal{F}, \mu) = \{\{2, 5\}\}$ , then  $(\mathcal{F}, \mu) \in \mathcal{MF}(\tau_1) \cap \mathcal{MF}(\tau_2)$ .

If  $|\Gamma(\mathcal{F}, \mu)| = t - 3$ , then there is a unique  $\tau_i$  with  $\Gamma(\mathcal{F}, \mu) = \Delta(\tau_i)$ ; while if  $|\Gamma(\mathcal{F}, \mu)| < t - 3$  then there are several  $\tau_i$  with  $\Gamma(\mathcal{F}, \mu) \subset \Delta(\tau_i)$  and for each of these  $\tau_i$ ,  $\phi_{\tau_i}^{-1}(\mathcal{F}, \mu)$  has some zero coordinates (see Figure 6.14). This establishes that

i.  $\mathcal{MF}(\tau_p) \subseteq \bigcup_{i=1}^{\xi} \mathcal{MF}(\tau_i)$ ; and

ii. If  $\tau_i \neq \tau_j$ , then  $\mathcal{MF}(\tau_i)$  and  $\mathcal{MF}(\tau_j)$  can only intersect along their boundary.

To show that  $\bigcup_{i=1}^{\xi} \mathcal{MF}(\tau_i) \subseteq \mathcal{MF}(\tau_p)$ , we observe that any two vertices of the pinched polygon of  $\tau_p$  can be connected by a smooth path in  $\tau_p$  and hence if  $(\mathcal{F}, \mu)$  is carried by any  $\tau_i$ , it is also carried by  $\tau_p$ .

Next assume that every component of  $D_n - \tau$  is a punctured monogon or unpunctured trigon, except for one punctured  $t$ -gon  $P$  ( $t \geq 2$ ). Let  $v_1, v_2, \dots, v_t$  denote the vertices of  $P$ . Let  $\tau_p$  be a pinching of  $\tau$  and  $N$  denote a regular neighbourhood of the pinched  $t$ -gon. Label the gates  $a_1, \dots, a_t$  of  $N$  in anticlockwise cyclic order and let  $l_i$  ( $1 \leq i \leq t$ ) denote the leaf of  $(\mathcal{F}, \mu)$  in  $\partial N$  which joins  $a_{i-1}$  to  $a_i$ . See Figure 6.15.

The label set  $\Gamma(\mathcal{F}, \mu)$  of a measured foliation  $(\mathcal{F}, \mu) \in \mathcal{MF}(\tau_p)$  will consist of pairs  $(j, k) \in \{1, \dots, t\} \times \{1, \dots, t\}$ . This contrasts with the case for unpunctured  $t$ -gons, since there are two possible paths for leaves joining the gates  $a_j$  and  $a_k$ , one on each side of the puncture. To describe this label set, first orient each gate  $a_i$  and each leaf  $l_i$  anticlockwise around  $\partial N$ . Then  $(j, k) \in \Gamma(\mathcal{F}, \mu)$  if and only if

- there is a leaf segment  $L$  of  $(\mathcal{F}, \mu)$  in  $N$  which joins  $a_j$  to  $a_k$ ;

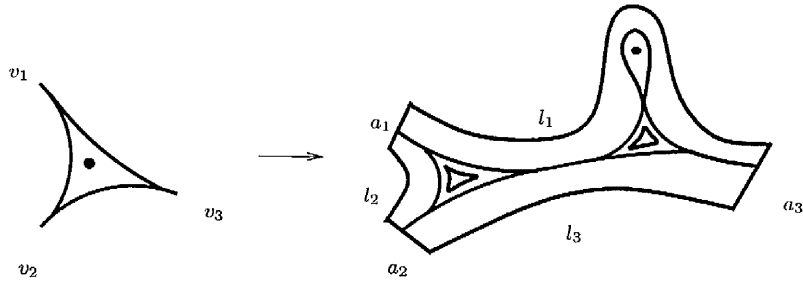


Figure 6.15: The regular neighbourhood  $N$  of a pinched punctured trigon

- when  $L$  is oriented from  $a_j$  to  $a_k$ , the oriented loop consisting of  $L$  and a subset of  $\partial N$  bounds a disk containing the puncture in its interior; and
- $k \neq j + 1$  (we don't include leaves which must necessarily be part of  $N$ ).

See Figure 6.16. Notice that  $(j, j) \in \Gamma(\mathcal{F}, \mu)$  if and only if the leaf from the 1-pronged singularity exits  $N$  through  $a_j$ . Of course, it is possible that this leaf doesn't exit  $N$  (e.g. if  $(\mathcal{F}, \mu) = (\mathcal{F}^u, \mu^u)$ ). Also, observe that the cardinality  $|\Gamma(\mathcal{F}, \mu)| \leq t - 1$  since leaves don't cross.

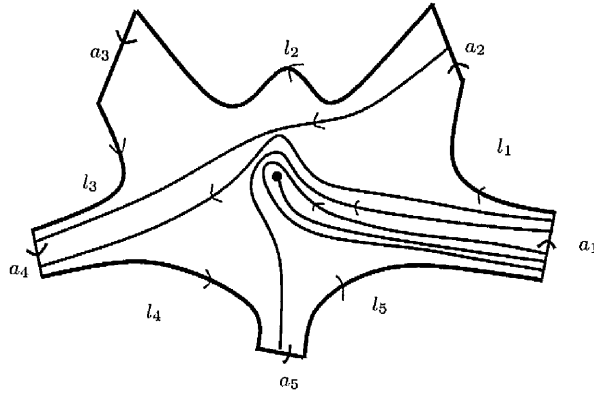


Figure 6.16: The label set  $\Gamma(\mathcal{F}, \mu)$  is given by  $\{(1, 1), (1, 5), (1, 4), (2, 4)\}$ .

To describe the label set  $\Delta(\tau_i)$  for a diagonal extension  $\tau_i$  of  $\tau$ , we label the vertices  $v_1, \dots, v_t$  of  $P$  in the anticlockwise cyclic order and put arrows on the edges of  $P$  pointing from  $v_j$  to  $v_{j+1}$ . For each additional branch, we place an arrow on the branch so that the loop composed of the branch and of edges of  $P$  which encloses the puncture is oriented consistently. Then  $\Delta(\tau_i)$  is the set of pairs  $(j, k)$  such that there is an additional branch from  $v_j$  to  $v_k$ . See Figure 6.17. It is clear that  $(\mathcal{F}, \mu) \in \mathcal{MF}(\tau_i)$  if and only if  $\Gamma(\mathcal{F}, \mu) \subseteq \Delta(\tau_i)$ .

If  $|\Gamma(\mathcal{F}, \mu)| = t - 1$ , then there is a unique  $\tau_i$  with  $\Gamma(\mathcal{F}, \mu) = \Delta(\tau_i)$ , while if  $|\Gamma(\mathcal{F}, \mu)| < t - 1$  then there are several  $\tau_i$  with  $\Gamma(\mathcal{F}, \mu) \subset \Delta(\tau_i)$  and for each of



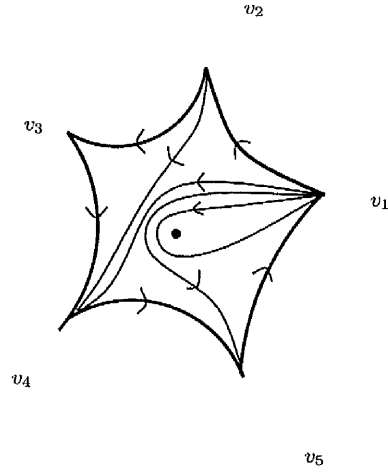


Figure 6.17: The label set  $\Delta(\tau_i)$  is given by  $\{(1, 1), (1, 5), (1, 4), (2, 4)\}$

these  $\tau_i$ ,  $\phi_{\tau_i}^{-1}(\mathcal{F}, \mu)$  has some zero coordinates. See Figure 6.18.

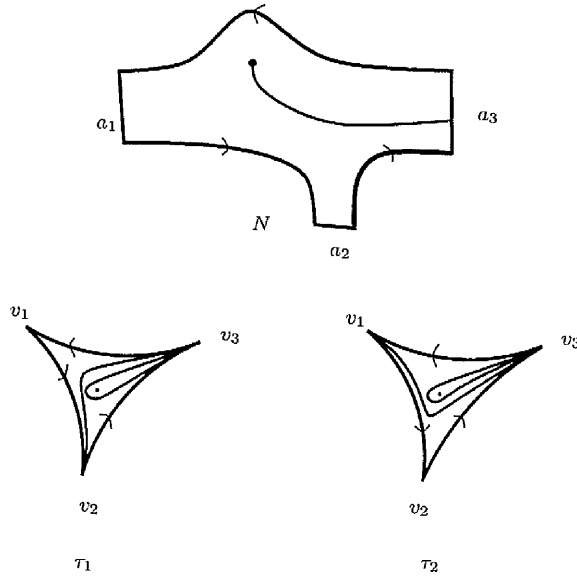


Figure 6.18: If  $\Gamma(\mathcal{F}, \mu) = \{(3, 3)\}$ , then  $(\mathcal{F}, \mu) \in \mathcal{MF}(\tau_1) \cap \mathcal{MF}(\tau_2)$ .

This establishes that

i.  $\mathcal{MF}(\tau_p) \subseteq \bigcup_{i=1}^{\xi} \mathcal{MF}(\tau_i)$ ; and

ii. If  $\tau_i \neq \tau_j$ , then  $\mathcal{MF}(\tau_i)$  and  $\mathcal{MF}(\tau_j)$  can only intersect along their boundary.

To show that  $\bigcup_{i=1}^{\xi} \mathcal{MF}(\tau_i) \subseteq \mathcal{MF}(\tau_p)$ , we observe that any two vertices of the pinched polygon of  $\tau_p$  can be connected by a smooth path in  $\tau_p$  and hence if  $(\mathcal{F}, \mu)$  is carried by any  $\tau_i$ , it is also carried by  $\tau_p$ .

Therefore, we have proved the first two statements of the lemma in the case where  $\tau$  has only one polygon which is not a punctured monogon or an unpunctured trigon. For the general case, we argue for each punctured and unpunctured polygon of  $\tau$  in the same way as above and observe that if  $(\mathcal{F}, \mu) \in \mathcal{MF}(\tau_p)$ , then there is a diagonal extension  $\tau_i$  of  $\tau$  so that  $(\mathcal{F}, \mu) \in \mathcal{MF}(\tau_i)$ . Conversely, if  $(\mathcal{F}, \mu) \in \mathcal{MF}(\tau_i)$  for some diagonal extension  $\tau_i$  of  $\tau$ , then  $(\mathcal{F}, \mu) \in \mathcal{MF}(\tau_p)$  since any two vertices of each pinched polygon of  $\tau_p$  can be connected by a smooth path. Also, if  $(\mathcal{F}, \mu)$  is carried by two diagonal extensions  $\tau_i$  and  $\tau_j$ , then  $\phi_{\tau_i}^{-1}(\mathcal{F}, \mu)$  has some zero coordinates from the argument above and hence  $\mathcal{MF}(\tau_i)$  and  $\mathcal{MF}(\tau_j)$  can only intersect along their boundary.

For the proof of the third statement, we first note that  $\beta$  permutes the vertices of  $\tau$ . Hence, given a diagonal extension  $\tau_i$  of  $\tau$ , the permutation on the vertices of  $\tau$  sends each additional branch of  $\tau_i$  onto another additional branch, and so gives another diagonal extension  $\tau_j$  of  $\tau$ . Therefore, we have  $\beta(\mathcal{MF}(\tau_i)) = \mathcal{MF}(\tau_j)$ . Then,  $\beta : \mathcal{W}^+(\tau_i) \rightarrow \mathcal{W}^+(\tau_j)$  is described by the matrix

$$\tilde{T} = \begin{bmatrix} T & X \\ 0 & Id \end{bmatrix}$$

with respect to the natural coherent choice of bases of  $\mathcal{W}^+(\tau_i)$  and  $\mathcal{W}^+(\tau_j)$ . We remark that if all components of  $D_n - \tau$  are odd-gons then  $\mathcal{W}^+(\tau_i)$  and  $\mathcal{W}^+(\tau_j)$  have bases consisting of weights on the main branches of  $\tau$  and the additional branches and hence  $X$  is zero. If  $D_n - \tau$  has an even-gon then  $X$  can be non-zero since the bases of  $\mathcal{W}^+(\tau_i)$  and  $\mathcal{W}^+(\tau_j)$  consists of weights on edges which includes infinitesimal and additional ones. For some main branch  $e_k$  of  $\tau_i$ , the corresponding weight  $w_k$  is the sum of weights on some infinitesimal and additional branches and  $f(e_k)$  may cover some basis elements. See Example 6.23.

For the fourth statement, we recall from (the proof of) Lemma 6.3, that the fact that each change of coordinates from train track coordinates  $\mathcal{W}^+(\tau_i)$  to Dynnikov coordinates is only piecewise linear is a consequence of the piecewise linearity of the function  $\hat{p} : \mathcal{W}^+(\tau_i) \rightarrow \mathbb{R}^+$ , where  $\hat{p}$  is a minimal non-tight train path with respect to some Dynnikov arc. The function  $\hat{p}$  makes a transition from one linear region to another at measures for which some leaf which follows the train path  $p$  connects two singularities (see the proof of Lemma 5.12).

At  $v^u = \phi_{\tau_i}^{-1}(\mathcal{F}^u, \mu^u) \in \mathcal{MF}(\tau_i)$  there are several such leaves connecting singularities but the choice of diagonal extension  $\tau_i$  is precisely a choice of the relative configurations of these leaves when the connection between singularities are broken, and therefore  $L : \mathcal{W}^+(\tau_i) \rightarrow \mathcal{S}_n$  is linear near  $v^u$ .  $\square$

### 6.3.2 The spectrum of the Dynnikov matrices when $\beta$ fixes the prongs of $\tau$

Let  $\beta \in B_n$  be a pseudo-Anosov braid with unstable invariant foliation  $(\mathcal{F}^u, \mu^u)$ , dilatation  $\lambda > 1$  and regular invariant train track  $\tau$ . In this section we shall prove that when  $\beta$  fixes the prongs of  $\tau$ , then every Dynnikov matrix is isospectral to  $T$  up to some eigenvalues 1.

**Theorem 6.19.** *Let  $\beta \in B_n$  be a pseudo-Anosov braid with unstable invariant measured foliation  $(\mathcal{F}^u, \mu^u)$  and dilatation  $\lambda > 1$ . Let  $\tau$  be a regular invariant train track of  $\beta$  with associated transition matrix  $T$ . If  $\beta$  fixes the prongs at all singularities other than unpunctured 3-pronged and punctured 1-pronged singularities, then any Dynnikov matrix  $D_i$  is isospectral to  $T$  up to some eigenvalues 1.*

*Proof.* Let  $\tau_p$  be a pinching of  $\tau$  and  $\tau_i$  ( $1 \leq i \leq \xi$ ) be the diagonal extensions of  $\tau$ . Since each strictly positive measure on  $\tau$  induces a strictly positive measure on  $\tau_p$ ,  $\mathcal{W}^+(\tau_p)$  and  $\mathcal{MF}(\tau_p)$  are neighbourhoods of  $v^u$  and  $(\mathcal{F}^u, \mu^u)$  respectively. Furthermore, by Lemma 6.18,  $\bigcup_{1 \leq i \leq \xi} \mathcal{MF}(\tau_i) = \mathcal{MF}(\tau_p)$  and for  $i \neq j$ ,  $\mathcal{MF}(\tau_i)$  and  $\mathcal{MF}(\tau_j)$  intersect only on their boundaries. Since  $\beta$  fixes the prongs at all singularities other than unpunctured 3-pronged and punctured 1-pronged singularities, for each  $\tau_i$  we have  $\beta(\mathcal{MF}(\tau_i)) = \mathcal{MF}(\tau_i)$  and the induced action  $\beta : \mathcal{W}^+(\tau_i) \rightarrow \mathcal{W}^+(\tau_i)$  is given by the matrix

$$\tilde{T} = \begin{bmatrix} T & X \\ 0 & Id \end{bmatrix}.$$

Using the fourth statement of Lemma 6.18, the change of coordinate function  $\rho \circ \phi_{\tau_i} : \mathcal{W}^+(\tau_i) \rightarrow \mathcal{S}_n$  is linear in a neighbourhood in  $\mathcal{W}^+(\tau_i)$  of  $v^u = \phi_{\tau_i}^{-1}(\mathcal{F}, \mu)$ . Therefore, for each  $\tau_i$  we have the following commutative diagram:

$$\begin{array}{ccc}
\mathcal{W}^+(\tau_i) & \xrightarrow{\tilde{T}} & \mathcal{W}^+(\tau_i) \\
\phi_{\tau_i} \downarrow & & \phi_{\tau_i} \downarrow \\
\mathcal{MF}(\tau_i) & \xrightarrow{\beta} & \mathcal{MF}(\tau_i) \\
\rho \downarrow & & \rho \downarrow \\
\mathcal{S}_n & \xrightarrow{F} & \mathcal{S}_n
\end{array} \tag{6.3}$$

where  $L_i = \rho \circ \phi_{\tau_i}$  is linear in a neighbourhood  $U_i \subseteq \mathcal{W}^+(\tau_i)$  of  $v^u$ . Let  $(a^u, b^u)$  denote the Dynnikov coordinates of  $(\mathcal{F}^u, \mu^u)$ . For each  $1 \leq i \leq \xi$ , we write  $\mathcal{R}_i = L_i(U_i)$ : by the above,  $\bigcup_{1 \leq i \leq \xi} \mathcal{R}_i$  is a neighbourhood of  $(a^u, b^u)$ . Then in  $\mathcal{R}_i$ ,

$D_i = F|_{\mathcal{R}_i} = L_i \circ \tilde{T} \circ L_i^{-1}$  is linear and isospectral to  $T$  up to some eigenvalues 1. These matrices  $D_i$  ( $1 \leq i \leq \xi$ ) are precisely the Dynnikov matrices for  $\beta \in B_n$ .  $\square$

In fact, if  $D_n - \tau$  has only odd-gons all of the Dynnikov matrices are equal and hence there is only one Dynnikov region in the fixed-pronged case.

**Theorem 6.20.** *Let  $\beta \in B_n$  be a pseudo-Anosov braid with unstable invariant measured foliation  $(\mathcal{F}^u, \mu^u)$  and dilatation  $\lambda > 1$ . Let  $\tau$  be a regular invariant train track of  $\beta$  with associated transition matrix  $T$ . If all components of  $D_n - \tau$  are odd-gons and  $\beta$  fixes the prongs at all singularities other than unpunctured 3-pronged and punctured 1-pronged singularities, then there is a unique Dynnikov region.*

*Proof.* We use the notation in the proof of Theorem 6.19. Let  $k = \text{rank}(\tau)$  and  $N = 2n - 4$  be the dimension of  $\mathcal{S}_n$ . We first note that each  $L_i$  is of the form  $(L|X_i)$  for some fixed  $N \times k$  matrix  $L$ , where  $L$  is the change of coordinates from  $\mathcal{W}^+(\tau)$  to  $\mathcal{S}_n$  on the hyperplane  $\mathcal{MF}(\tau)$ . Then each  $L_i^{-1}$  is of the form  $\begin{pmatrix} A \\ Y_i \end{pmatrix}$  for some fixed  $k \times N$  matrix  $A$  which gives the change of coordinates from the  $k$ -dimensional subspace of  $\mathcal{S}_n$  corresponding to  $\mathcal{MF}(\tau)$  to  $\mathcal{W}^+(\tau)$ . Therefore we have,

$$L_i^{-1}L_i = \begin{pmatrix} A \\ Y_i \end{pmatrix} (L|X_i)$$

Since  $L_i^{-1}L_i = Id$ ,  $AX_i$  and  $Y_iL$  are zero matrices for all  $i$ . It follows that for any  $i, j$  we have

$$L_j^{-1}L_i = \begin{bmatrix} Id_k & 0 \\ 0 & P_{ij} \end{bmatrix}.$$

for some  $(N - k) \times (N - k)$  matrix  $P_{ij}$ . In particular,  $L_j^{-1}L_i$  commutes with

$$\tilde{T} = \begin{bmatrix} T & 0 \\ 0 & Id \end{bmatrix}.$$

Hence,  $D_i = L_i\tilde{T}L_i^{-1} = L_j\tilde{T}L_j^{-1} = D_j$  for all  $i$  and  $j$ . □

In the above we considered the transition matrix for a *regular* non-complete train track. A similar result follows for general train tracks from Rykken's result Theorem 6.6 and Lemma 6.7.

**Corollary 6.21.** *Let  $\beta \in \text{MCG}(D_n)$  be a pseudo-Anosov braid with unstable invariant foliation  $(\mathcal{F}^u, \mu^u)$  and dilatation  $\lambda > 1$ . Let  $\tau$  be any invariant train track with associated transition matrix  $T$ . If  $\beta$  fixes the prongs at all singularities other than unpunctured 3-pronged and punctured 1-pronged singularities, then any Dynnikov matrix is isospectral to  $T$  up to roots of unity and zeros. Furthermore, if  $D_n - \tau$  consists of only odd-gons then there is a unique Dynnikov matrix.*

**Example 6.22.** Consider the 4-braid  $\gamma = \sigma_1^2\sigma_2^2\sigma_1\sigma_2\sigma_3^2\sigma_2\sigma_1^4\sigma_2\sigma_1^2\sigma_3^2\sigma_2\sigma_1$ .  $\gamma$  has Dynnikov matrix (as given by the Dynn.exe program [18])

$$D = \begin{bmatrix} 17 & 0 & 12 & 4 \\ 28 & 1 & 20 & 6 \\ 24 & 0 & 17 & 4 \\ 0 & 0 & 0 & 1 \end{bmatrix}$$

and transition matrix

$$T = \begin{bmatrix} 5 & 8 & 4 \\ 12 & 21 & 8 \\ 12 & 20 & 9 \end{bmatrix}$$

associated to the invariant train track  $\tau$  depicted in Figure 6.19.  $T$  has spectrum  $\{1, 17 \pm 12\sqrt{2}\}$  and the eigenvector  $v^u$  corresponding to the largest

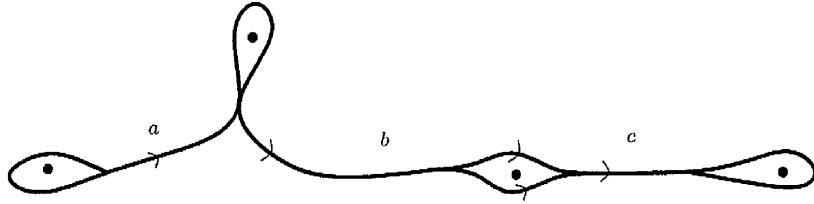


Figure 6.19: Invariant train track for  $\gamma$

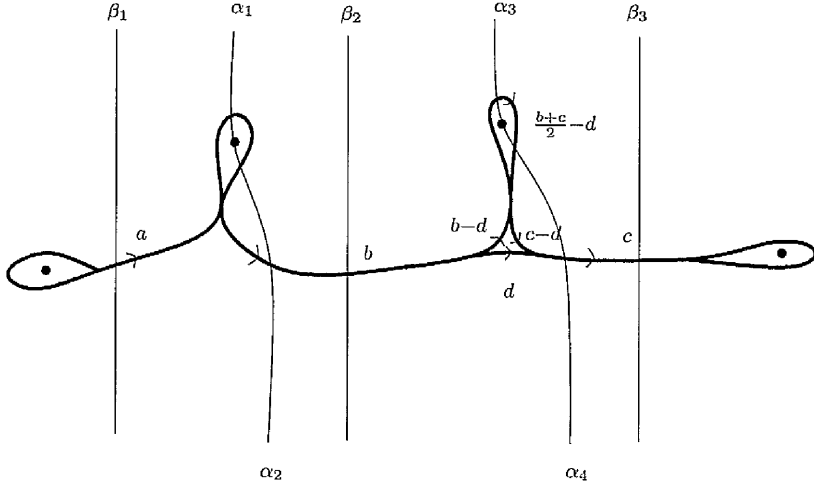


Figure 6.20: A standard embedding of the pinched train track  $\tau_p$

eigenvalue  $\lambda = 17 + 12\sqrt{2}$  is  $(1, 1 + \sqrt{2}, 1 + \sqrt{2})$ . That is,

$$v^u = \phi_\tau^{-1}(\mathcal{F}^u, \mu^u) = (1, 1 + \sqrt{2}, 1 + \sqrt{2}).$$

Since  $D_n - \tau$  contains a punctured bigon,  $\tau$  is not complete and we have  $\text{rank}(\tau) = 3$ . Pinching across an edge of the punctured bigon gives a complete pinched train track  $\tau_p$ . We depict a standard embedding of  $\tau_p$  with respect to the Dynnikov arcs in Figure 6.20. Since  $\gamma$  fixes the prongs of  $\tau$ , the transition matrix associated to  $\tau_p$  is given by

$$T_p = \begin{bmatrix} 5 & 8 & 4 & 0 \\ 12 & 21 & 8 & 0 \\ 12 & 20 & 9 & 0 \\ x & y & z & 1 \end{bmatrix}$$

for some  $x, y, z$  which will be determined later as  $x = 2, y = 3, z = 1$ .

We now compute the change of coordinate function  $L : \mathcal{W}^+(\tau_p) \rightarrow \mathcal{S}_4$  in a

neighbourhood of  $v^u$ . First observe that  $\beta_1 = a$ ,  $\beta_2 = b$ ,  $\beta_3 = c$ . Therefore,

$$b_1 = \frac{a-b}{2} \quad \text{and} \quad b_2 = \frac{b-c}{2}.$$

We have  $\alpha_1 = \frac{a+b}{2}$ ,  $\alpha_3 = \frac{b+c}{2} - d$ . Since  $\alpha_{2i-1} + \alpha_{2i} = \max(\beta_i, \beta_{i+1})$  we have,

$$\alpha_2 = \max(a, b) - \frac{a+b}{2} \quad \text{and} \quad \alpha_4 = \max(b, c) - \frac{b+c}{2} + d.$$

Since  $b > a$  at  $v^u$ ,  $\alpha_2 = \frac{b-a}{2}$  and

$$\alpha_4 = \begin{cases} \frac{b-c}{2} + d & b \geq c \\ \frac{c-b}{2} + d & b \leq c \end{cases}$$

so  $a_1 = -\frac{a}{2}$  and

$$a_2 = \frac{\alpha_4 - \alpha_3}{2} = \frac{\max(b, c)}{2} - \frac{b+c}{2} + d = \begin{cases} d - \frac{c}{2} & b \geq c \\ d - \frac{b}{2} & b \leq c \end{cases}$$

Therefore, when  $b \geq c$ ,  $L : \mathcal{W}^+(\tau_p) \rightarrow \mathcal{S}_n$  is given by

$$L_1 = \begin{bmatrix} -1/2 & 0 & 0 & 0 \\ 0 & -1/2 & 0 & 1 \\ 1/2 & -1/2 & 0 & 0 \\ 0 & 1/2 & -1/2 & 0 \end{bmatrix},$$

and when  $b \leq c$ ,  $L : \mathcal{W}^+(\tau_p) \rightarrow \mathcal{S}_n$  is given by

$$L_2 = \begin{bmatrix} -1/2 & 0 & 0 & 0 \\ 0 & 0 & -1/2 & 1 \\ 1/2 & -1/2 & 0 & 0 \\ 0 & 1/2 & -1/2 & 0 \end{bmatrix}.$$

The Dynnikov matrices of  $\beta$  are therefore  $D_1 = L_1 T_p L_1^{-1}$  and  $D_2 = L_2 T_p L_2^{-1}$ .

Using

$$T_p = \begin{bmatrix} 5 & 8 & 4 & 0 \\ 12 & 21 & 8 & 0 \\ 12 & 20 & 9 & 0 \\ x & y & z & 1 \end{bmatrix},$$

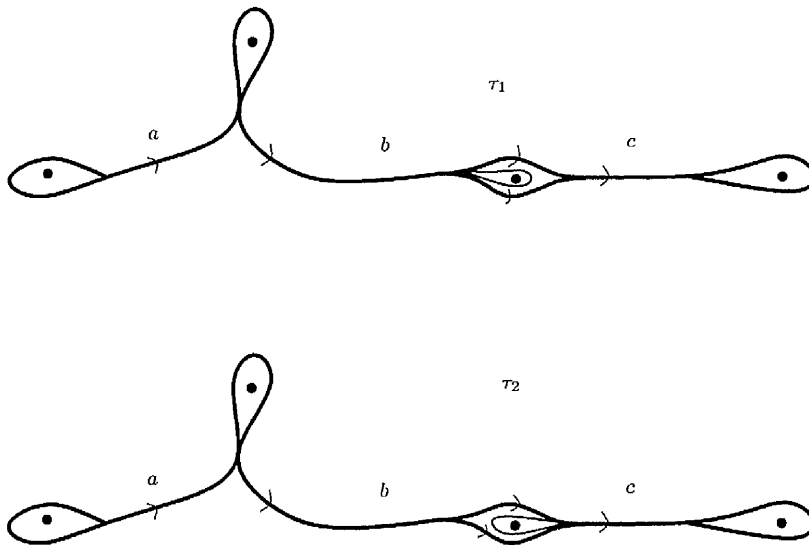


Figure 6.21: Diagonal extensions of  $\tau$

we compute that, for both  $i = 1$  and  $i = 2$ ,  $D_i$  is given by

$$D_i = \begin{bmatrix} 17 & 0 & 12 & 4 \\ 40 - 2x - 2y - 2z & 1 & 28 - 2y - 2z & 8 - 2z \\ 24 & 0 & 17 & 4 \\ 0 & 0 & 0 & 1 \end{bmatrix}.$$

Therefore, there is a unique Dynnikov matrix  $D$  as expected by Theorem 6.20. Comparing the second row of  $D_i$  with the known Dynnikov matrix  $D$  gives  $x = 2$ ,  $y = 3$ ,  $z = 1$  as claimed above. The spectrum of  $T_p$  and  $D$  is

$$\{1, 1, 17 \pm 12\sqrt{2}\}.$$

Figure 6.21 depicts the two possible diagonal extensions  $\tau_1$  and  $\tau_2$  of  $\tau$ . Observe that, given  $(\mathcal{F}, \mu) \in \mathcal{MF}(\tau_p)$ ,  $(\mathcal{F}, \mu) \in \mathcal{MF}(\tau_1)$  if and only if  $b \geq c$ , and  $(\mathcal{F}, \mu) \in \mathcal{MF}(\tau_2)$  if and only if  $c \geq b$ , corresponding to the two linear regions in the above coordinate change.

**Example 6.23.** Consider the 5-braid  $\beta_5 = \sigma_1\sigma_2\sigma_3\sigma_4^{-1}$  on  $D_5$ . A regular invariant train track  $\tau$  and its image under  $\beta_5$  are depicted in Figure 6.22.

Let  $a, b, c, d$  and  $e$  denote the measures on the main branches of  $\tau$  and  $x_1, x_2, x_3$  and  $x_4$  the measures on the branches of the 4-gon, as in Figure 6.22. We first observe that the measures on the branches of  $\tau$  are determined by



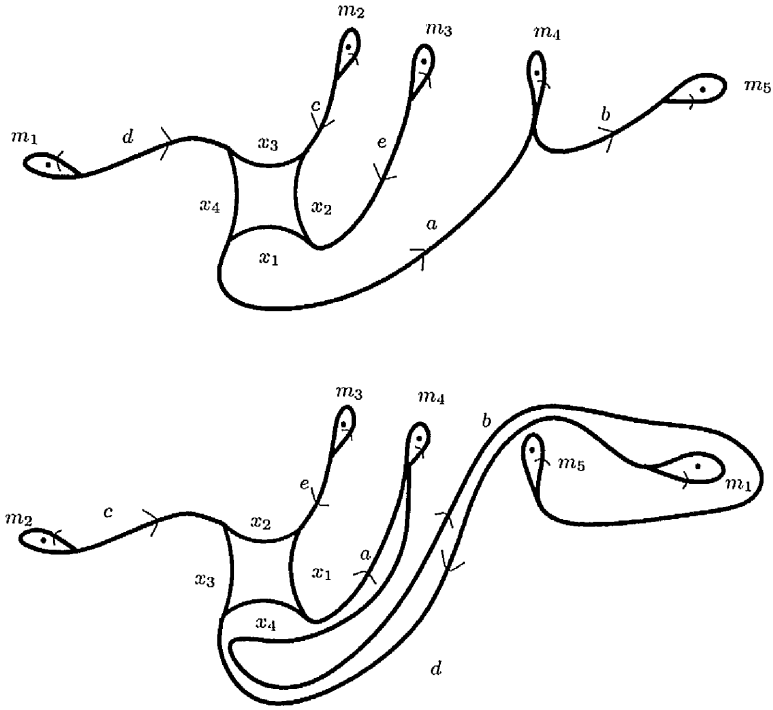


Figure 6.22: Invariant train track of  $\beta_5 = \sigma_1 \sigma_2 \sigma_3 \sigma_4^{-1}$  and its image

$x_1, x_2, x_3, x_4, b$  since the switch conditions give

$$a = x_1 + x_4, \quad c = x_2 + x_3, \quad d = x_3 + x_4, \quad e = x_1 + x_2.$$

Hence the set of measures  $(x_1, x_2, x_3, x_4, b)$  forms a basis for the 5-dimensional space  $\mathcal{W}^+(\tau)$ . We note that the vectors in  $\mathcal{W}^+(\tau)$  corresponding to  $a, b, c, d$  and  $e$  do not form a basis since  $a + c = b + d$  for every element of  $\mathcal{W}^+(\tau)$ . We also observe from Figure 6.22 that in the image  $\beta_5(\tau)$ ,  $x_1$  is covered by  $x_4$  and  $b$ ,  $x_2$  is covered by  $x_1$ ,  $x_3$  is covered by  $x_2$ ,  $x_4$  is covered by  $x_3$  and  $b$  is covered by  $b$  twice and  $d$ . Since  $d = x_3 + x_4$ , the matrix which describes the action of  $\beta$  on  $\mathcal{W}^+(\tau)$  with respect to the chosen basis is given by

$$T = \begin{bmatrix} 0 & 0 & 0 & 1 & 1 \\ 1 & 0 & 0 & 0 & 0 \\ 0 & 1 & 0 & 0 & 0 \\ 0 & 0 & 1 & 0 & 0 \\ 0 & 0 & 1 & 1 & 2 \end{bmatrix}$$

We note that  $T$  doesn't give the images of the branches, but how a set of measures  $(x_1, x_2, x_3, x_4, b)$  is transformed by  $\beta$  to new measures. Working to three decimal places, the largest eigenvalue of  $T$  is  $\lambda = 2.154$  and the associated eigenvector  $v^u$  corresponding to  $(\mathcal{F}^u, \mu^u)$  is given by

$$v^u = (x_1, x_2, x_3, x_4, b) \simeq (0.487, 0.226, 0.105, 0.049, 1).$$

In order to find the change of coordinate function  $L : \mathcal{W}^+(\tau) \rightarrow \mathbb{R}^6$  in a neighbourhood of  $v^u$  we use a standard embedding of  $\tau$  with respect to the Dynnikov arcs as depicted in Figure 6.23.

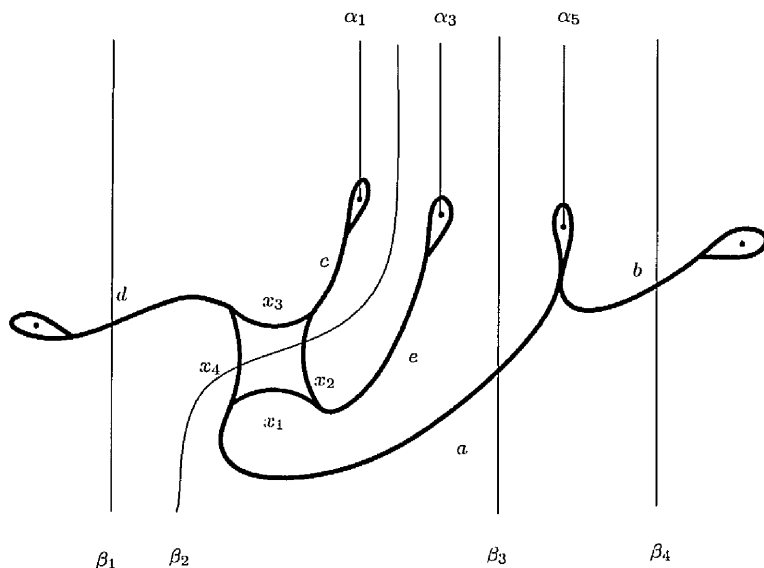


Figure 6.23: A standard embedding of  $\tau$  with respect to some of the Dynnikov arcs

Then we get,

$$\beta_1 = x_3 + x_4, \quad \beta_2 = x_2 + x_4, \quad \beta_3 = x_1 + x_4, \quad \beta_4 = b$$

$$\alpha_1 = \frac{x_2 + x_3}{2}, \quad \alpha_3 = \frac{x_1 + x_2}{2}, \quad \alpha_5 = \frac{x_1 + x_4 + b}{2}.$$

Since  $\alpha_{2i} = \max(\beta_i, \beta_{i+1}) - \alpha_{2i-1}$  we obtain,

$$\alpha_2 = \max(x_3 + x_4, x_2 + x_4) - \frac{x_2 + x_3}{2}, \quad \alpha_4 = \max(x_2 + x_4, x_1 + x_4) - \frac{x_1 + x_2}{2}$$

$$\alpha_6 = \max(x_1 + x_4, b) - \frac{x_1 + x_4 + b}{2}.$$

Since  $x_1 > x_2 > x_3 > x_4$  and  $b > x_1 + x_4$  at  $v^u$  we have,

$$\alpha_2 = x_2 + x_4 - \frac{x_2 + x_3}{2}, \quad \alpha_4 = x_1 + x_4 - \frac{x_1 + x_2}{2}, \quad \alpha_6 = b - \frac{x_1 + x_4 + b}{2}.$$

Therefore,

$$\begin{aligned} a_1 &= \frac{1}{2}(x_4 - x_3), & a_2 &= \frac{1}{2}(x_4 - x_2), & a_3 &= \frac{1}{2}(-x_1 - x_4), \\ b_1 &= \frac{1}{2}(x_3 - x_2), & b_2 &= \frac{1}{2}(x_2 - x_1), & b_3 &= \frac{1}{2}(x_1 + x_4 - b). \end{aligned}$$

That is, the change of coordinate function  $L : \mathcal{W}^+(\tau) \rightarrow \mathcal{S}_6$  is given by

$$L = \frac{1}{2} \begin{bmatrix} 0 & 0 & -1 & 1 & 0 \\ 0 & -1 & 0 & 1 & 0 \\ -1 & 0 & 0 & -1 & 0 \\ 0 & -1 & 1 & 0 & 0 \\ -1 & 1 & 0 & 0 & 0 \\ 1 & 0 & 0 & 1 & -1 \end{bmatrix}$$

in a neighbourhood of  $v^u$ . Now we shall construct the diagonal extensions of  $\tau$  and observe the connection between the associated change of coordinate functions and  $L$ . Figure 6.24 depicts the two different ways of diagonalizing an unpunctured 4-gon.

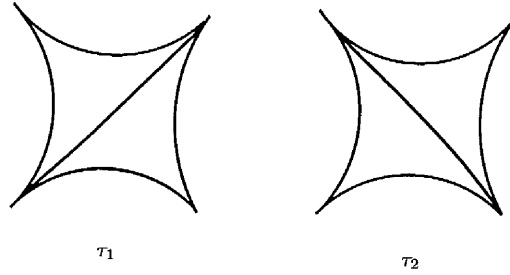


Figure 6.24: There are 2 different ways to diagonalize an unpunctured 4-gon

Hence, there are two diagonal extensions of  $\tau$  and we shall compute the change of coordinate functions for each of these. We begin with  $\tau_1$  as depicted in Figure 6.25. We observe that the measures on the branches of  $\tau_1$  are determined by  $x_1, x_2, x_3, x_4, b, \epsilon$  since the switch conditions give

$$a = x_1 + x_4, \quad c = x_2 + x_3 + \epsilon, \quad d = x_3 + x_4 + \epsilon, \quad e = x_1 + x_2.$$

We compute that,

$$\beta_1 = x_3 + x_4, \quad \beta_2 = x_2 + x_4 + \epsilon, \quad \beta_3 = x_1 + x_4 + \epsilon, \quad \beta_4 = b,$$

$$\alpha_1 = \frac{x_2 + x_3 + \epsilon}{2}, \quad \alpha_3 = \frac{x_1 + x_2}{2}, \quad \alpha_5 = \frac{x_1 + x_4 + b + \epsilon}{2}.$$

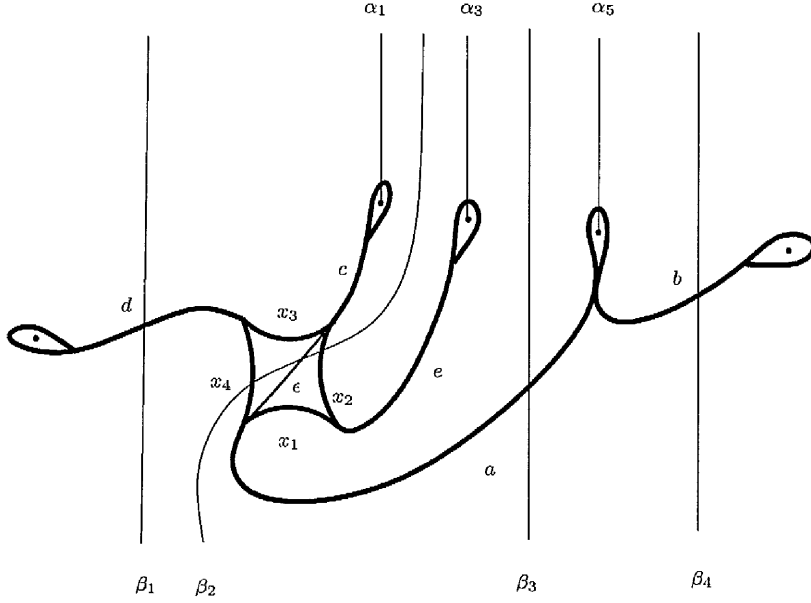


Figure 6.25: A standard embedding of the diagonal extension  $\tau_1$  with respect to some of the Dynnikov arcs

Since  $\alpha_{2i} = \max(\beta_i, \beta_{i+1}) - \alpha_{2i-1}$  we obtain,

$$\alpha_2 = \max(x_3 + x_4, x_2 + x_4 + \epsilon) - \frac{x_2 + x_3 + \epsilon}{2}, \quad \alpha_4 = \max(x_2 + x_4 + \epsilon, x_1 + x_4 + \epsilon) - \frac{x_1 + x_2}{2}$$

$$\alpha_6 = \max(x_1 + x_4 + \epsilon, b) - \frac{x_1 + x_4 + b + \epsilon}{2}.$$

Therefore,

$$a_1 = \frac{1}{2}(x_4 - x_3), \quad a_2 = \frac{1}{2}(x_4 - x_2 + \epsilon), \quad a_3 = \frac{1}{2}(-x_1 - x_4 - \epsilon),$$

$$b_1 = \frac{1}{2}(x_3 - x_2 - \epsilon), \quad b_2 = \frac{1}{2}(x_2 - x_1), \quad b_3 = \frac{1}{2}(x_1 + x_4 - b + \epsilon).$$

That is, the change of coordinate function  $L_1 : \mathcal{W}^+(\tau_1) \rightarrow \mathcal{S}_6$  is given by

$$L_1 = \frac{1}{2} \begin{bmatrix} 0 & 0 & -1 & 1 & 0 & 0 \\ 0 & -1 & 0 & 1 & 0 & 1 \\ -1 & 0 & 0 & -1 & 0 & -1 \\ 0 & -1 & 1 & 0 & 0 & -1 \\ -1 & 1 & 0 & 0 & 0 & 0 \\ 1 & 0 & 0 & 1 & -1 & 1 \end{bmatrix}$$

in a neighbourhood of  $v^u$  in  $\mathcal{W}^+(\tau_1)$ . Similar computations for the change of coordinate function  $L_2 : \mathcal{W}^+(\tau_2) \rightarrow \mathcal{S}_6$  associated to the other diagonal extension  $\tau_2$  give

$$L_2 = \frac{1}{2} \begin{bmatrix} 0 & 0 & -1 & 1 & 0 & 1 \\ 0 & -1 & 0 & 1 & 0 & -1 \\ -1 & 0 & 0 & -1 & 0 & 0 \\ 0 & -1 & 1 & 0 & 0 & 0 \\ -1 & 1 & 0 & 0 & 0 & 1 \\ 1 & 0 & 0 & 1 & -1 & 0 \end{bmatrix}$$

In this example, we have  $\beta(\mathcal{MF}(\tau_1)) = \mathcal{MF}(\tau_2)$  and  $\beta(\mathcal{MF}(\tau_2)) = \mathcal{MF}(\tau_1)$ . The induced action  $T_1 : \mathcal{W}^+(\tau_1) \rightarrow \mathcal{W}^+(\tau_2)$  and  $T_2 : \mathcal{W}^+(\tau_2) \rightarrow \mathcal{W}^+(\tau_1)$  are given by the matrices

$$T_1 = \begin{bmatrix} 0 & 0 & 0 & 1 & 1 & 0 \\ 1 & 0 & 0 & 0 & 0 & 0 \\ 0 & 1 & 0 & 0 & 0 & 0 \\ 0 & 0 & 1 & 0 & 0 & 0 \\ 0 & 0 & 1 & 1 & 2 & 0 \\ 0 & 0 & 0 & 0 & 0 & 1 \end{bmatrix}$$

and

$$T_2 = \begin{bmatrix} 0 & 0 & 0 & 1 & 1 & 0 \\ 1 & 0 & 0 & 0 & 0 & 0 \\ 0 & 1 & 0 & 0 & 0 & 0 \\ 0 & 0 & 1 & 0 & 0 & 0 \\ 0 & 0 & 1 & 1 & 2 & 1 \\ 0 & 0 & 0 & 0 & 0 & 1 \end{bmatrix}$$

with respect to the above choice of bases of  $\mathcal{W}(\tau_1)$  and  $\mathcal{W}(\tau_2)$ . We remark that  $T_1$  and  $T_2$  are different matrices. The reason for this is the following: Since  $b$  is covered by  $b$  twice and  $d$ , and that in  $\tau_2$ ,  $d = x_3 + x_4 + \epsilon$ , while in  $\tau_1$ ,  $d = x_3 + x_4$ , the  $(5, 6)^{\text{th}}$  entries of  $T_1$  and  $T_2$  are 0 and 1 respectively. We therefore have the commutative diagram

$$\begin{array}{ccc} \mathcal{W}^+(\tau_i) & \xrightarrow{T_i} & \mathcal{W}^+(\tau_{i+1}) \\ \phi_{\tau_i} \downarrow & & \phi_{\tau_{i+1}} \downarrow \\ \mathcal{MF}(\tau_i) & \xrightarrow{\beta} & \mathcal{MF}(\tau_{i+1}) \\ \rho \downarrow & & \rho \downarrow \\ \mathcal{S}_n & \xrightarrow{F} & \mathcal{S}_n \end{array} \quad (6.4)$$

where  $L_i = \rho \circ \phi_{\tau_i}$  is linear in a neighbourhood  $U_i$  of  $v^u$  in  $\mathcal{W}^+(\tau_i)$ . For each  $i$  ( $1 \leq i \leq 2$ ) write  $\mathcal{R}_i = L_i(U_i)$ . Let  $(a^u, b^u)$  be the Dynnikov coordinates of  $(\mathcal{F}^u, \mu^u)$ . Then,  $\bigcup_{1 \leq i \leq 2} \mathcal{R}_i$  is a neighbourhood of  $(a^u, b^u)$ , and in each  $R_i$ ,

$D_i = F|_{\mathcal{R}_i} = L_{i+1} \circ T_i \circ L_i^{-1}$  is linear. These matrices  $D_i$  ( $1 \leq i \leq 2$ ) are precisely the Dynnikov matrices for  $\beta \in B_5$ .

**Remark 6.24.** Since there is a unique Dynnikov region that corresponds to a diagonal extension  $\tau_i$  of  $\tau$ , the number of Dynnikov regions is bounded above by the number of diagonal extensions of  $\tau$  (which is given by the formula in Remark 6.17).

Let us calculate the Dynnikov matrices in our example and see how it is possible to determine the corresponding Dynnikov regions. In  $\mathcal{MF}(\tau_1)$ , the Dynnikov

matrix is given by

$$D_1 = L_2 T_1 L_1^{-1} = \begin{bmatrix} -1 & 1 & 0 & 0 & 0 & 0 \\ 0 & 0 & 0 & 1 & 1 & 0 \\ 0 & 0 & 2 & -1 & -1 & 1 \\ 0 & 0 & 0 & 0 & 1 & 0 \\ -1 & 0 & 1 & -1 & -1 & 1 \\ 0 & 0 & 1 & 0 & 0 & 1 \end{bmatrix}$$

Observe that

$$L_1^{-1} = \begin{bmatrix} 0 & -1 & -1 & 0 & -1 & 0 \\ 0 & -1 & -1 & 0 & 1 & 0 \\ -1 & 0 & -1 & 1 & 1 & 0 \\ 1 & 0 & -1 & 1 & 1 & 0 \\ 0 & 0 & -2 & 0 & 0 & -2 \\ -1 & 1 & 0 & -1 & 0 & 0 \end{bmatrix}$$

and from the bottom row of this matrix we can see that the relevant Dynnikov region is determined by the inequality  $\epsilon = -a_1 + a_2 - b_1 \geq 0$ .

Similarly, we compute the other Dynnikov matrix for  $\beta$ , and have that

$$D_2 = L_1 T_2 L_2^{-1} = \begin{bmatrix} 0 & 0 & 0 & 1 & 0 & 0 \\ 0 & 0 & 0 & 1 & 1 & 0 \\ 0 & 0 & 2 & -1 & -1 & 1 \\ -1 & 1 & 0 & -1 & 1 & 0 \\ 0 & -1 & 1 & 0 & -1 & 1 \\ 0 & 0 & 1 & 0 & 0 & 1 \end{bmatrix}$$

is the Dynnikov matrix in the region  $a_1 - a_2 + b_1 \geq 0$ .

### 6.3.3 Future work: The spectrum of Dynnikov matrices when $\beta$ permutes the prongs of $\tau$ non-trivially

Let  $\beta \in B_n$  be a pseudo-Anosov braid with unstable invariant foliation  $(\mathcal{F}^u, \mu^u)$ , dilatation  $\lambda > 1$  and regular invariant train track  $\tau$  with associated transition

matrix  $T$ . In this section we shall discuss the case when  $\beta$  permutes the prongs of  $(\mathcal{F}^u, \mu^u)$  non-trivially. We would like to prove that any Dynnikov matrix  $D_i$  is isospectral to  $T$  up to roots of unity: this has been confirmed with a wide range of examples. The problems which arise in this case, and some approaches to their solutions are illustrated in the following example.

**Example 6.25.** Consider the 6-braid  $\beta_6 = \sigma_1\sigma_2\sigma_3\sigma_4\sigma_5^{-1}$  on  $D_6$ . A regular invariant train track  $\tau$  and its image under  $\beta_6$  are depicted in Figure 6.26 and Figure 6.27. The image edge paths of the main edges are therefore:

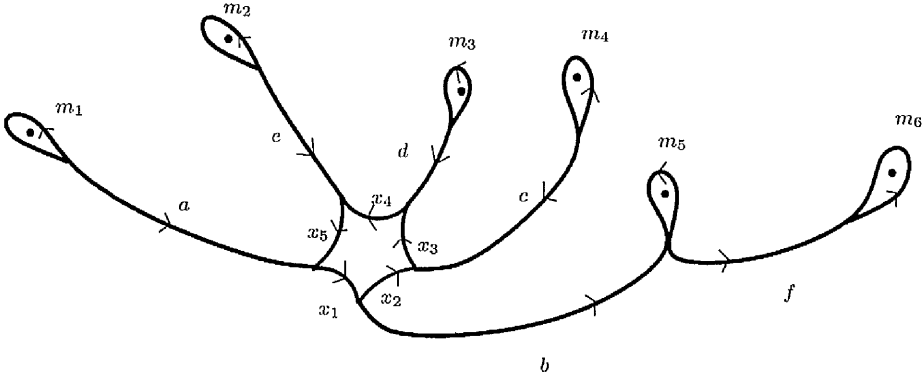


Figure 6.26: Invariant train track of  $\beta_6 = \sigma_1\sigma_2\sigma_3\sigma_4\sigma_5^{-1}$

$$a \rightarrow \bar{f}m_5\bar{b}, \quad b \rightarrow \bar{c}, \quad c \rightarrow d, \quad d \rightarrow e, \quad e \rightarrow a, \quad f \rightarrow cx_2b\bar{m}_5f\bar{m}_6\bar{f}$$

Therefore the transition matrix  $T$  associated to  $\tau$  is given by

$$T = \begin{bmatrix} 0 & 0 & 0 & 0 & 1 & 0 \\ 1 & 0 & 0 & 0 & 0 & 1 \\ 0 & 1 & 0 & 0 & 0 & 1 \\ 0 & 0 & 1 & 0 & 0 & 0 \\ 0 & 0 & 0 & 1 & 0 & 0 \\ 1 & 0 & 0 & 0 & 0 & 2 \end{bmatrix}$$

Let  $a, b, c, d, e, f$  and  $x_1, x_2, x_3, x_4, x_5, m_1, m_2, m_3, m_4, m_5, m_6$  denote the measures on the main and infinitesimal branches of  $\tau$ . Working to three decimal places, the largest eigenvalue of  $T$  is  $\lambda = 2.081$  and the associated eigenvector  $v^u$  corresponding to  $(\mathcal{F}^u, \mu^u)$  is given by

$$v^u = (a, b, c, d, e, f) \simeq (0.057, 0.370, 0.521, 0.250, 0.120, 0.714).$$



We observe that the weights  $x_1, x_2, x_3, x_4, x_5, m_1, m_2, m_3, m_4, m_5, m_6$  on the infinitesimal branches are determined by  $a, b, c, d, e, f$  since the switch conditions give

$$\begin{aligned} x_1 &= \frac{a+b+d-c-e}{2}, & x_2 &= \frac{b+c+e-a-d}{2}, & x_3 &= \frac{a+c+d-b-e}{2}, \\ x_4 &= \frac{b+d+e-a-c}{2}, & x_5 &= \frac{a+c+e-b-d}{2}, & m_1 &= \frac{a}{2}, & m_2 &= \frac{e}{2}, \\ m_3 &= \frac{d}{2}, & m_4 &= \frac{c}{2}, & m_5 &= \frac{b+f}{2}, & m_6 &= \frac{f}{2}. \end{aligned}$$

At  $v^u$ ,  $(a, b, c, d, e, f) \simeq (0.057, 0.370, 0.521, 0.250, 0.120, 0.714)$  and so,

$$\begin{aligned} x_1 &= 0.018, & x_2 &= 0.352, & x_3 &= 0.169, \\ x_4 &= 0.081, & x_5 &= 0.039, & m_1 &= 0.028, & m_2 &= 0.06, \\ m_3 &= 0.125, & m_4 &= 0.260, & m_5 &= 0.542, & m_6 &= 0.357. \end{aligned}$$

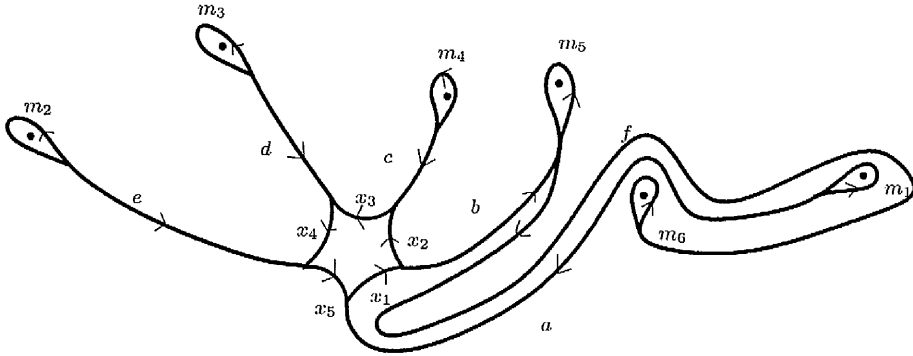


Figure 6.27: The image train track of  $\tau$  under  $\beta$

In order to find the change of coordinate function  $L : \mathcal{W}^+(\tau) \rightarrow \mathbb{R}^8$  in a neighbourhood of  $v^u$  we use a standard embedding of  $\tau$  with respect to the Dynnikov arcs as depicted in Figure 6.28.

Observe that  $\hat{p}_1(\mu) = \min(x_3, d/2)$  and  $\hat{p}_2(\mu) = \min(x_2, b/2)$  where  $p_1$  and  $p_2$  denote the minimal non-tight train paths depicted in Figure 6.28. Since  $x_3 \leq d/2$  and  $x_2 \leq b/2$  at  $v^u$ , we have in some neighbourhood of  $v^u$  that  $\hat{p}_1(\mu) = x_3$  and  $\hat{p}_2(\mu) = x_2$ . We compute that,

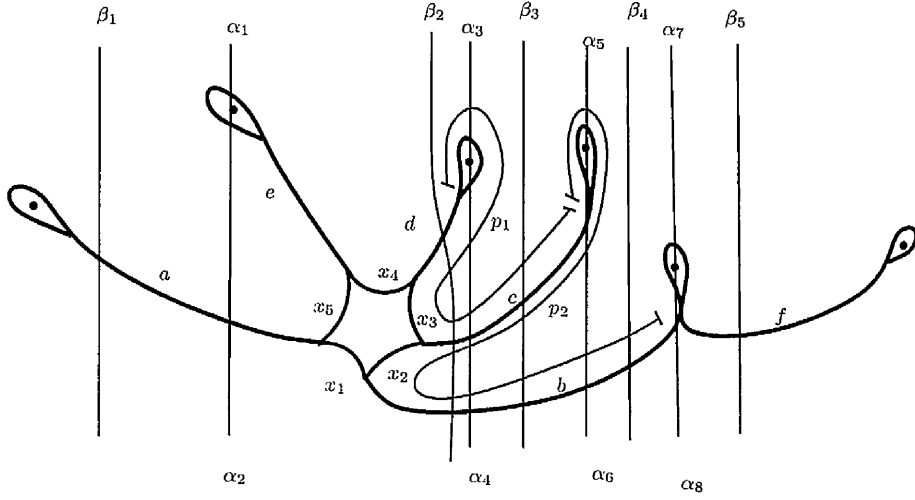


Figure 6.28: A standard embedding of  $\tau$  with respect to Dynnikov arcs

$$\beta_1 = a, \quad \beta_2 = b + c + d - 2\hat{p}_1(\mu) - 2\hat{p}_2(\mu)$$

$$\beta_3 = b + c - 2\hat{p}_2(\mu), \quad \beta_4 = b, \quad \beta_5 = f$$

$$\alpha_1 = m_2, \quad \alpha_3 = m_3, \quad \alpha_5 = m_4, \quad \alpha_7 = m_5.$$

That is,

$$\beta_1 = a, \quad \beta_2 = b + d - c, \quad \beta_3 = a + d - e, \quad \beta_4 = b, \quad \beta_5 = f$$

$$\alpha_1 = \frac{e}{2}, \quad \alpha_3 = \frac{d}{2}, \quad \alpha_5 = \frac{c}{2}, \quad \alpha_7 = \frac{b+f}{2}.$$

Since  $\alpha_{2i} = \max(\beta_i, \beta_{i+1}) - \alpha_{2i-1}$  we obtain,

$$\alpha_2 = \max(a, b + d - c) - \frac{e}{2}, \quad \alpha_4 = \max(b + d - c, a + d - e) - \frac{d}{2}$$

$$\alpha_6 = \max(a + d - e, b) - \frac{c}{2}, \quad \alpha_8 = \max(b, f) - \frac{b+f}{2}.$$

Since  $b + d - c > a$ ,  $a + d - e > b + d - c$ ,  $b > a + d - e$ , and  $f > b$  at  $v^u \simeq (0.057, 0.370, 0.521, 0.250, 0.120, 0.714)$  we have,

$$\alpha_2 = b + d - c - \frac{e}{2}, \quad \alpha_4 = a + d - e - \frac{d}{2}, \quad \alpha_6 = b - \frac{c}{2}, \quad \alpha_8 = f - \frac{b+f}{2}.$$

Therefore,

$$\begin{aligned}
a_1 &= \frac{1}{2}(b - c + d - e), & a_2 &= \frac{1}{2}(a - e), & a_3 &= \frac{1}{2}(b - c), & a_4 &= \frac{-b}{2}, \\
b_1 &= \frac{1}{2}(a - b + c - d), & b_2 &= \frac{1}{2}(-a + b - c + e), \\
b_3 &= \frac{1}{2}(a - b + d - e), & b_4 &= \frac{1}{2}(b - f).
\end{aligned}$$

That is, the change of coordinate function  $L : \mathcal{W}^+(\tau) \rightarrow \mathcal{S}_8$  is given by

$$L = \frac{1}{2} \begin{bmatrix} 0 & 1 & -1 & 1 & -1 & 0 \\ 1 & 0 & 0 & 0 & -1 & 0 \\ 0 & 1 & -1 & 0 & 0 & 0 \\ 0 & -1 & 0 & 0 & 0 & 0 \\ 1 & -1 & 1 & -1 & 0 & 0 \\ -1 & 1 & -1 & 0 & 1 & 0 \\ 1 & -1 & 0 & 1 & -1 & 0 \\ 0 & 1 & 0 & 0 & 0 & -1 \end{bmatrix}$$

in a neighbourhood of  $v^u$ . Now we shall construct the diagonal extensions of  $\tau$  and observe the connection between the associated change of coordinate functions and  $L$ .

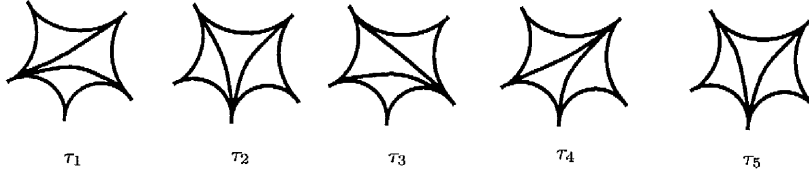


Figure 6.29: There are 5 different ways to diagonalize an unpunctured 5-gon

Figure 6.29 depicts the five different ways of diagonalizing an unpunctured 5-gon. Hence, there are five diagonal extensions of  $\tau$  and we shall compute the change of coordinate functions for each of these. We begin with  $\tau_1$  as depicted in Figure 6.30. The measures on the infinitesimal branches of  $\tau_1$  are determined by  $a, b, c, d, e, f, \epsilon_1, \epsilon_2$  since the switch conditions give,

$$\begin{aligned}
x_1 &= \frac{a + b + d - c - e}{2} - \epsilon_2, & x_2 &= \frac{b + c + e - a - d}{2} + \epsilon_2, & x_3 &= \frac{a + c + d - b - e}{2} - \epsilon_1 - \epsilon_2, \\
x_4 &= \frac{b + d + e - a - c}{2} + \epsilon_1, & x_5 &= \frac{a + c + e - b - d}{2} - \epsilon_1.
\end{aligned}$$

We observe that,

$$\beta_1 = a, \quad \beta_2 = b + d - c + 2\epsilon_1, \quad \beta_3 = a + d - e - 2\epsilon_2, \quad \beta_4 = b, \quad \beta_5 = f$$

$$\alpha_1 = \frac{e}{2}, \quad \alpha_3 = \frac{d}{2}, \quad \alpha_5 = \frac{c}{2}, \quad \alpha_7 = \frac{b+f}{2}.$$

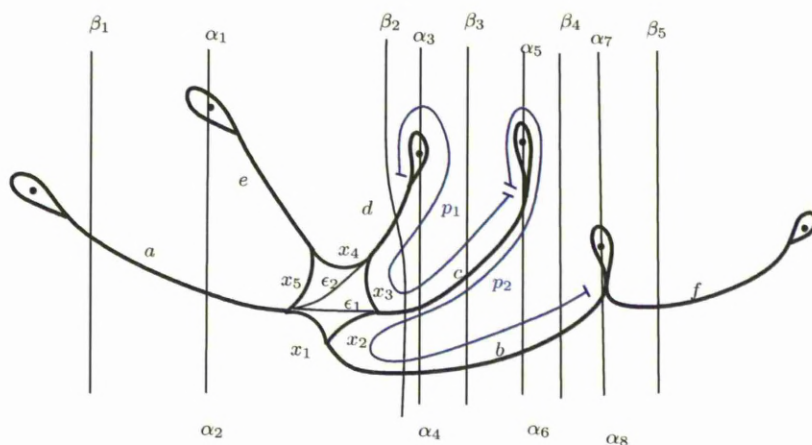


Figure 6.30: A standard embedding of the diagonal extension  $\tau_1$  with respect to the Dynnikov arcs

Since  $\alpha_{2i} = \max(\beta_i, \beta_{i+1}) - \alpha_{2i-1}$  we have,

$$\alpha_2 = \max(a, b + d - c + 2\epsilon_1) - \frac{e}{2}, \quad \alpha_4 = \max(b + d - c + 2\epsilon_1, a + d - e - 2\epsilon_2) - \frac{d}{2}$$

$$\alpha_6 = \max(a + d - e - 2\epsilon_2, b) - \frac{c}{2}, \quad \alpha_8 = \max(b, f) - \frac{b+f}{2}.$$

Therefore,

$$a_1 = \frac{1}{2}(b - c + d - e) + \epsilon_1, \quad a_2 = \frac{1}{2}(a - e) - \epsilon_2, \quad a_3 = \frac{1}{2}(b - c), \quad a_4 = \frac{-b}{2},$$

$$b_1 = \frac{1}{2}(a - b + c - d) - \epsilon_1, \quad b_2 = \frac{1}{2}(-a + b - c + e) + \epsilon_1 + \epsilon_2,$$

$$b_3 = \frac{1}{2}(a - b + d - e) - \epsilon_2, \quad b_4 = \frac{1}{2}(b - f).$$

That is, the change of coordinate function  $L_1 : \mathcal{W}^+(\tau_1) \rightarrow \mathcal{S}_8$  is given by

$$L_1 = \frac{1}{2} \begin{bmatrix} 0 & 1 & -1 & 1 & -1 & 0 & 2 & 0 \\ 1 & 0 & 0 & 0 & -1 & 0 & 0 & -2 \\ 0 & 1 & -1 & 0 & 0 & 0 & 0 & 0 \\ 0 & -1 & 0 & 0 & 0 & 0 & 0 & 0 \\ 1 & -1 & 1 & -1 & 0 & 0 & -2 & 0 \\ -1 & 1 & -1 & 0 & 1 & 0 & 2 & 2 \\ 1 & -1 & 0 & 1 & -1 & 0 & 0 & -2 \\ 0 & 1 & 0 & 0 & 0 & -1 & 0 & 0 \end{bmatrix}$$

in a neighbourhood of  $v^u$  in  $\mathcal{W}^+(\tau_1)$ .

We continue with  $\tau_2$  as depicted in Figure 6.31. The measures on the infinitesimal branches of  $\tau_2$  are given by

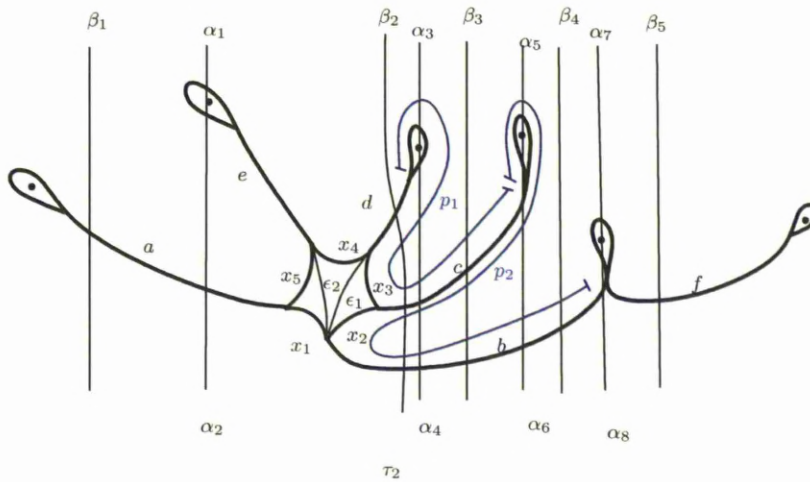


Figure 6.31: A standard embedding of the diagonal extension  $\tau_2$  with respect to the Dynnikov arcs

$$x_1 = \frac{a + b + d - c - e}{2} - \epsilon_1, \quad x_2 = \frac{b + c + e - a - d}{2} - \epsilon_2, \quad x_3 = \frac{a + c + d - b - e}{2} + \epsilon_2,$$

$$x_4 = \frac{b + d + e - a - c}{2} - \epsilon_1 - \epsilon_2, \quad x_5 = \frac{a + c + e - b - d}{2} + \epsilon_1.$$

We observe that,

$$\beta_1 = a, \quad \beta_2 = b + d - c - 2\epsilon_1, \quad \beta_3 = a + d - e + 2\epsilon_2, \quad \beta_4 = b, \quad \beta_5 = f$$

$$\alpha_1 = \frac{e}{2}, \quad \alpha_3 = \frac{d}{2}, \quad \alpha_5 = \frac{c}{2}, \quad \alpha_7 = \frac{b+f}{2}.$$

And,

$$\alpha_2 = \max(a, b + d - c - 2\epsilon_1) - \frac{e}{2}, \quad \alpha_4 = \max(b + d - c - 2\epsilon_1, a + d - e + 2\epsilon_2) - \frac{d}{2}$$

$$\alpha_6 = \max(a + d - e + 2\epsilon_2, b) - \frac{c}{2}, \quad \alpha_8 = \max(b, f) - \frac{b+f}{2}.$$

Therefore,

$$a_1 = \frac{1}{2}(b - c + d - e) - \epsilon_1, \quad a_2 = \frac{1}{2}(a - e) + \epsilon_2, \quad a_3 = \frac{1}{2}(b - c), \quad a_4 = \frac{-b}{2},$$

$$b_1 = \frac{1}{2}(a - b + c - d) + \epsilon_1, \quad b_2 = \frac{1}{2}(-a + b - c + e) - \epsilon_1 - \epsilon_2,$$

$$b_3 = \frac{1}{2}(a - b + d - e) + \epsilon_2, \quad b_4 = \frac{1}{2}(b - f).$$

That is, the change of coordinate function  $L_2 : \mathcal{W}^+(\tau_2) \rightarrow \mathcal{S}_8$  is given by,

$$L_2 = \frac{1}{2} \begin{bmatrix} 0 & 1 & -1 & 1 & -1 & 0 & -2 & 0 \\ 1 & 0 & 0 & 0 & -1 & 0 & 0 & 2 \\ 0 & 1 & -1 & 0 & 0 & 0 & 0 & 0 \\ 0 & -1 & 0 & 0 & 0 & 0 & 0 & 0 \\ 1 & -1 & 1 & -1 & 0 & 0 & 2 & 0 \\ -1 & 1 & -1 & 0 & 1 & 0 & -2 & -2 \\ 1 & -1 & 0 & 1 & -1 & 0 & 0 & 2 \\ 0 & 1 & 0 & 0 & 0 & -1 & 0 & 0 \end{bmatrix}$$

in a neighbourhood of  $v^u$  in  $\mathcal{W}^+(\tau_2)$ . Similar computations for the change of coordinate matrices associated to the other three diagonal extensions  $\tau_3$ ,  $\tau_4$  and  $\tau_5$  give:

$$L_3 = \frac{1}{2} \begin{bmatrix} 0 & 1 & -1 & 1 & -1 & 0 & 2 & 2 \\ 1 & 0 & 0 & 0 & -1 & 0 & 2 & 0 \\ 0 & 1 & -1 & 0 & 0 & 0 & 0 & 0 \\ 0 & -1 & 0 & 0 & 0 & 0 & 0 & 0 \\ 1 & -1 & 1 & -1 & 0 & 0 & -2 & -2 \\ -1 & 1 & -1 & 0 & 1 & 0 & 0 & 2 \\ 1 & -1 & 0 & 1 & -1 & 0 & 2 & 0 \\ 0 & 1 & 0 & 0 & 0 & -1 & 0 & 0 \end{bmatrix}$$

$$L_4 = \frac{1}{2} \begin{bmatrix} 0 & 1 & -1 & 1 & -1 & 0 & 0 & -2 \\ 1 & 0 & 0 & 0 & -1 & 0 & -2 & 0 \\ 0 & 1 & -1 & 0 & 0 & 0 & 0 & 0 \\ 0 & -1 & 0 & 0 & 0 & 0 & 0 & 0 \\ 1 & -1 & 1 & -1 & 0 & 0 & 0 & 2 \\ -1 & 1 & -1 & 0 & 1 & 0 & 2 & -2 \\ 1 & -1 & 0 & 1 & -1 & 0 & -2 & 0 \\ 0 & 1 & 0 & 0 & 0 & -1 & 0 & 0 \end{bmatrix}$$

and

$$L_5 = \frac{1}{2} \begin{bmatrix} 0 & 1 & -1 & 1 & -1 & 0 & 0 & 2 \\ 1 & 0 & 0 & 0 & -1 & 0 & 2 & 2 \\ 0 & 1 & -1 & 0 & 0 & 0 & 0 & 0 \\ 0 & -1 & 0 & 0 & 0 & 0 & 0 & 0 \\ 1 & -1 & 1 & -1 & 0 & 0 & 0 & -2 \\ -1 & 1 & -1 & 0 & 1 & 0 & -2 & 0 \\ 1 & -1 & 0 & 1 & -1 & 0 & 2 & 2 \\ 0 & 1 & 0 & 0 & 0 & -1 & 0 & 0 \end{bmatrix}$$

In this example, we have  $\beta(\mathcal{MF}(\tau_i)) = \mathcal{MF}(\tau_{i+1})$  and the induced action  $\beta : \mathcal{W}(\tau_i) \rightarrow \mathcal{W}(\tau_{i+1})$  is given by the matrix

$$\tilde{T} = \begin{bmatrix} T & 0 \\ 0 & Id \end{bmatrix}$$

with respect to the above choice of bases of  $\mathcal{W}(\tau_i)$  and  $\mathcal{W}(\tau_{i+1})$ . We therefore have the commutative diagram for each  $i$ :

$$\begin{array}{ccc} \mathcal{W}^+(\tau_i) & \xrightarrow{\tilde{T}} & \mathcal{W}^+(\tau_{i+1}) \\ \phi_{\tau_i} \downarrow & & \phi_{\tau_{i+1}} \downarrow \\ \mathcal{MF}(\tau_i) & \xrightarrow{\beta} & \mathcal{MF}(\tau_{i+1}) \\ \rho \downarrow & & \rho \downarrow \\ \mathcal{S}_n & \xrightarrow{F} & \mathcal{S}_n \end{array} \quad (6.5)$$

where  $L_i = \rho \circ \phi_{\tau_i}$  is linear in a neighbourhood  $U_i$  of  $v^u$  in  $\mathcal{W}^+(\tau_i)$ . For  $1 \leq i \leq 5$ , write  $\mathcal{R}_i = L_i(U_i)$ . Let  $(a^u, b^u)$  be the Dynnikov coordinates of  $(\mathcal{F}^u, \mu^u)$ . Then,  $\bigcup_{1 \leq i \leq 5} \mathcal{R}_i$  is a neighbourhood of  $(a^u, b^u)$ , and in  $\mathcal{R}_i$ ,  $D_i = F|_{\mathcal{R}_i} = L_{i+1} \circ \tilde{T} \circ L_i^{-1}$  is linear. These matrices  $D_i$  ( $1 \leq i \leq 5$ ) are precisely the Dynnikov matrices for  $\beta \in B_6$ .

Let us calculate the Dynnikov matrices in our example and see how it is possible to determine the corresponding Dynnikov regions. In  $\mathcal{MF}(\tau_1)$ , the Dynnikov matrix is given by

$$L_2 \tilde{T} L_1^{-1} = D_1 = \begin{bmatrix} 0 & 0 & 0 & 0 & 1 & 0 & 0 & 0 \\ 0 & 0 & 0 & 0 & 1 & 1 & 0 & 0 \\ 0 & 0 & 0 & 0 & 1 & 1 & 1 & 0 \\ 0 & 0 & 0 & 2 & -1 & -1 & -1 & 1 \\ -1 & 1 & 0 & 0 & -1 & 1 & 0 & 0 \\ 0 & -1 & 1 & 0 & 0 & -1 & 1 & 0 \\ 0 & 0 & -1 & 1 & 0 & 0 & -1 & 1 \\ 0 & 0 & 0 & 1 & 0 & 0 & 0 & 1 \end{bmatrix}$$

Observe that



$$L_1^{-1} = \frac{1}{2} \begin{bmatrix} 0 & 0 & 0 & -2 & 2 & 2 & 2 & 0 \\ 0 & 0 & 0 & -2 & 0 & 0 & 0 & 0 \\ 0 & 0 & -2 & -2 & 0 & 0 & 0 & 0 \\ 0 & -2 & 0 & -2 & 0 & 0 & 2 & 0 \\ -2 & 0 & 0 & -2 & 0 & 2 & 2 & 0 \\ 0 & 0 & 0 & -2 & 0 & 0 & 0 & -2 \\ 0 & 1 & -1 & 0 & 0 & 1 & 0 & 0 \\ 1 & -1 & 0 & 0 & 1 & 0 & 0 & 0 \end{bmatrix},$$

and from the bottom two rows of this matrix we can see that the relevant Dynnikov region is determined by the inequalities  $\epsilon_1 = a_2 - a_3 + b_2 \geq 0$  and  $\epsilon_2 = a_1 - a_2 + b_1 \geq 0$ . Similarly, we compute the other Dynnikov matrices for  $\beta$ , and have that

$$L_3 \tilde{T} L_2^{-1} = D_2 = \begin{bmatrix} -1 & 1 & 0 & 0 & 0 & 0 & 0 & 0 \\ -1 & 0 & 1 & 0 & 0 & 0 & 0 & 0 \\ 0 & 0 & 0 & 0 & 1 & 1 & 1 & 0 \\ 0 & 0 & 0 & 2 & -1 & -1 & -1 & 1 \\ 0 & 0 & 0 & 0 & 0 & 1 & 0 & 0 \\ 0 & 0 & 0 & 0 & 0 & 0 & 1 & 0 \\ -1 & 0 & 0 & 1 & -1 & -1 & -1 & 1 \\ 0 & 0 & 0 & 1 & 0 & 0 & 0 & 1 \end{bmatrix}$$

is the Dynnikov matrix in the region  $-a_1 + a_2 - b_1 \geq 0$  and  $-a_2 + a_3 - b_2 \geq 0$ .

$$L_4 \tilde{T} L_3^{-1} = D_3 = \begin{bmatrix} -1 & 1 & 0 & 0 & 0 & 0 & 0 & 0 \\ 0 & 0 & 0 & 0 & 1 & 1 & 0 & 0 \\ 0 & 0 & 0 & 0 & 1 & 1 & 1 & 0 \\ 0 & 0 & 0 & 2 & -1 & -1 & -1 & 1 \\ 0 & 0 & 0 & 0 & 0 & 1 & 0 & 0 \\ -1 & 0 & 1 & 0 & -1 & -1 & 1 & 0 \\ 0 & 0 & -1 & 1 & 0 & 0 & -1 & 1 \\ 0 & 0 & 0 & 1 & 0 & 0 & 0 & 1 \end{bmatrix}$$

is the Dynnikov matrix in the region  $-a_1 + a_2 - b_1 \geq 0$  and  $a_1 - a_3 + b_1 + b_2 \geq 0$ .

$$L_5 \tilde{T} L_4^{-1} = D_4 = \begin{bmatrix} 0 & 0 & 0 & 0 & 1 & 0 & 0 & 0 \\ 0 & -1 & 1 & 0 & 1 & 0 & 0 & 0 \\ 0 & 0 & 0 & 0 & 1 & 1 & 1 & 0 \\ 0 & 0 & 0 & 2 & -1 & -1 & -1 & 1 \\ -1 & 1 & 0 & 0 & -1 & 1 & 0 & 0 \\ 0 & 0 & 0 & 0 & 0 & 0 & 1 & 0 \\ 0 & -1 & 0 & 1 & 0 & -1 & -1 & 1 \\ 0 & 0 & 0 & 1 & 0 & 0 & 0 & 1 \end{bmatrix}$$

is the Dynnikov matrix in the region  $a_1 - a_2 + b_1 \geq 0$  and  $-a_2 + a_3 - b_2 \geq 0$ .

And,

$$L_1 \tilde{T} L_5^{-1} = D_5 = \begin{bmatrix} -1 & 1 & 0 & 0 & 0 & 0 & 0 & 0 \\ -1 & 0 & 1 & 0 & 0 & 0 & 0 & 0 \\ 0 & 0 & 0 & 0 & 1 & 1 & 1 & 0 \\ 0 & 0 & 0 & 2 & -1 & -1 & -1 & 1 \\ 0 & 0 & 1 & -1 & 0 & 0 & -1 & 0 \\ 0 & 0 & 1 & -1 & 1 & 0 & -1 & 0 \\ 0 & 0 & 1 & -1 & 0 & 1 & -1 & 0 \\ 0 & 0 & 0 & 1 & 0 & 0 & 0 & 1 \end{bmatrix}$$

is the Dynnikov matrix in the region  $-a_1 + a_3 - b_1 - b_2 \geq 0$  and  $a_2 - a_3 + b_2 \geq 0$ .

We observe that  $D_2 = L_3 \tilde{T} L_2^{-1}$  and  $D_5 = L_1 \tilde{T} L_5^{-1}$  are the same and hence there are four Dynnikov matrices, and all these Dynnikov matrices are isospectral to  $T$  up to roots of unity.

**Question 6.26.** *Let  $\beta \in B_n$  be a pseudo-Anosov braid with unstable invariant foliation  $(\mathcal{F}^u, \mu^u)$ , dilatation  $\lambda > 1$  and regular invariant train track  $\tau$  having transition matrix  $T$ . If  $\beta$  permutes the prongs of  $(\mathcal{F}^u, \mu^u)$  non-trivially, is every Dynnikov matrix  $D_i$  isospectral to  $T$  up to roots of unity?*

**Remark 6.27.** Note that when  $\beta$  permutes the prongs of  $(\mathcal{F}^u, \mu^u)$  non-trivially, then for some  $m \in \mathbb{Z}^+$ ,  $\beta^m$  fixes the prongs. The transition matrix for  $\beta^m$  on a diagonal extension of  $\tau$  is of the form

$$T' = \begin{bmatrix} T^m & 0 \\ 0 & Id \end{bmatrix}.$$

By Theorems 6.19 and 6.20 every Dynnikov matrix for  $\beta^m$  is isospectral to  $T^m$  up to some eigenvalues 1. In the above example we have

$$\mathcal{MF}(\tau_1) \rightarrow \mathcal{MF}(\tau_2) \rightarrow \mathcal{MF}(\tau_3) \rightarrow \mathcal{MF}(\tau_4) \rightarrow \mathcal{MF}(\tau_5) \rightarrow \mathcal{MF}(\tau_1)$$

and  $D_i = L_{i+1} \tilde{T} L_i^{-1}$ . Hence, for  $i = 1, 2, 3, 4, 5$  the Dynnikov matrix for  $\beta^5$  on  $\mathcal{MF}(\tau_i)$  is given by

$$D_{i+4} D_{i+3} D_{i+2} D_{i+1} D_i = L_i \tilde{T}^5 L_i^{-1}$$

which is clearly isospectral to  $T^5$  up to two eigenvalues 1. By Theorem 6.20, the five Dynnikov matrices  $D_i = L_i \tilde{T}^5 L_i^{-1}$  are all equal, and given by

$$D = \begin{bmatrix} 1 & 1 & 2 & 4 & 1 & 1 & 2 & 4 \\ 0 & 1 & 1 & 2 & 0 & 1 & 1 & 2 \\ 0 & 0 & 1 & 1 & 0 & 0 & 1 & 1 \\ 2 & 6 & 14 & 33 & 4 & 8 & 16 & 31 \\ -1 & -2 & -4 & -8 & 0 & -2 & -4 & -8 \\ -1 & -3 & -6 & -12 & -2 & -2 & -6 & -12 \\ -1 & -3 & -7 & -14 & -2 & -4 & -6 & -14 \\ 1 & 3 & 7 & 17 & 2 & 4 & 8 & 16 \end{bmatrix}.$$

# Bibliography

- [1] R. L. Adler, A. G. Konheim, and M. H. McAndrew. Topological entropy. *Trans. Amer. Math. Soc.*, 114:309–319, 1965.
- [2] V. M. Alekseev and M. V. Yakobson. Symbolic dynamics and hyperbolic dynamic systems. *Phys. Rep.*, 75(5):287–325, 1981.
- [3] E. Artin. Theorie der Zöpfe. *Abh. Math. Sem. Univ. Hamburg (4)*, pages 47–72, 1925.
- [4] E. Artin. Theory of braids. *Ann. of Math. (2)*, 48:101–126, 1947.
- [5] M. Bestvina and M. Handel. Train-tracks for surface homeomorphisms. *Topology*, 34(1):109–140, 1995.
- [6] J. Birman, P. Brinkmann, and K. Kawamuro. A polynomial invariant of pseudo-Anosov maps. *arXiv: 1001.5094*, 2010.
- [7] J. S. Birman. *Braids, links, and mapping class groups*. Princeton University Press, Princeton, N.J., 1974. Annals of Mathematics Studies, No. 82.
- [8] R. Bowen. Entropy for group endomorphisms and homogeneous spaces. *Trans. Amer. Math. Soc.*, 153:401–414, 1970.
- [9] R. Bowen. Entropy and the fundamental group. In *The structure of attractors in dynamical systems (Proc. Conf., North Dakota State Univ., Fargo, N.D., 1977)*, volume 668 of *Lecture Notes in Math.*, pages 21–29. Springer, Berlin, 1978.
- [10] W-L. Chow. On the algebraical braid group. *Ann. of Math. (2)*, 49:654–658, 1948.
- [11] P. Dehornoy. Efficient solutions to the braid isotopy problem. *Discrete Appl. Math.*, 156(16):3091–3112, 2008.

- [12] P. Dehornoy, I. Dynnikov, D. Rolfsen, and B. Wiest. *Why are braids orderable?*, volume 14 of *Panoramas et Synthèses [Panoramas and Syntheses]*. Société Mathématique de France, Paris, 2002.
- [13] I. Dynnikov. On a Yang-Baxter mapping and the Dehornoy ordering. *Uspekhi Mat. Nauk*, 57(3(345)):151–152, 2002.
- [14] I. Dynnikov and B. Wiest. On the complexity of braids. *J. Eur. Math. Soc. (JEMS)*, 9(4):801–840, 2007.
- [15] D. B. A. Epstein. Curves on 2-manifolds and isotopies. *Acta Math.*, 115:83–107, 1966.
- [16] A. Fathi, F. Laudenbach, and V. Poenaru. *Travaux de Thurston sur les surfaces*, volume 66 of *Astérisque*. Société Mathématique de France, Paris, 1979. Séminaire Orsay.
- [17] J. Franks and M. Misiurewicz. Cycles for disk homeomorphisms and thick trees. In *Nielsen theory and dynamical systems (South Hadley, MA, 1992)*, volume 152 of *Contemp. Math.*, pages 69–139. Amer. Math. Soc., Providence, RI, 1993.
- [18] T. Hall. Software available for download from <http://www.maths.liv.ac.uk/~tobyhall/software/>.
- [19] T. Hall and S. Ö. Yurttaş. On the topological entropy of families of braids. *Topology Appl.*, 156(8):1554–1564, 2009.
- [20] E. Hironaka and E. Kin. A family of pseudo-Anosov braids with small dilatation. *Algebr. Geom. Topol.*, 6:699–738 (electronic), 2006.
- [21] B. P. Kitchens. *Symbolic dynamics*. Universitext. Springer-Verlag, Berlin, 1998.
- [22] J. E. Los. Pseudo-Anosov maps and invariant train tracks in the disc: a finite algorithm. *Proc. London Math. Soc. (3)*, 66(2):400–430, 1993.
- [23] A. Manning. Topological entropy and the first homology group. In *Dynamical systems—Warwick 1974 (Proc. Sympos. Appl. Topology and Dynamical Systems, Univ. Warwick, Coventry, 1973/1974; presented to E. C. Zeeman on his fiftieth birthday)*, pages 185–190. Lecture Notes in Math., Vol. 468. Springer, Berlin, 1975.

- [24] L. Mosher. Train track expansions of measured foliations. Preprint available from <http://andromeda.rutgers.edu/~mosher/>, 2003.
- [25] J-O. Moussafr. On computing the entropy of braids. *Funct. Anal. Other Math.*, 1(1):37–46, 2006.
- [26] R. C. Penner and J. L. Harer. *Combinatorics of train tracks*, volume 125 of *Annals of Mathematics Studies*. Princeton University Press, Princeton, NJ, 1992.
- [27] E. Rykken. Expanding factors for pseudo-anosov homeomorphisms. *Rocky Mountain J. Math.*, 28(3):1103–1124, 1998.
- [28] D. Thurston. Geometric intersection of curves on surfaces. Preprint available from <http://www.math.columbia.edu/~dpt/>.
- [29] W. P. Thurston. On the geometry and dynamics of diffeomorphisms of surfaces. *Bull. Amer. Math. Soc. (N.S.)*, 19(2):417–431, 1988.